UNIVERSITY OF CALIFORNIA, SAN DIEGO

Expanding circadian input, output, and the clock through genomic screens

A dissertation submitted in partial satisfaction of the requirements for the degree
Doctor of Philosophy

in

Biology

by

Ann Margaret Atwood

Committee in charge:

Professor Steve A. Kay, Chair
Professor Steven Briggs
Professor Christopher Glass
Professor Susan Golden
Professor Marc Montminy
Professor Steven Wasserman

2011

The Dissertation of Ann Margaret Atwood is approved and of acceptable quality and form for publication on microfilm and electronically:

_____

_____

_____

_____

_____

_____

Chair

University of California, San Diego

2011

Table of Contents

List of Abbreviations and Symbols

The following list contains abbreviation and gene symbols—both human and mouse—used within the dissertation. Human gene symbols are italicized and in all capital letters (i.e. *BMAL1*). Mouse gene symbols are italicized with the first letter capitalized (i.e. *Bmal1*). The mouse format is used in this list when the gene is discussed in both human and mouse studies and the gene symbol is the same.

***ACSF3*:** acyl-CoA synthetase family member 3

***Alb*:** albumin

***Aldoa*:** aldolase A, fructose-bisphosphate

***AldoB* :** aldolase B,

APKC: atypical protein kinase C

***ApoCIII* (Official symbol: *ApoCIII*):** apolipoprotein C-III

***B4GALT2*:** UDP-Gal:betaGlcNAc beta 1,4- galactosyltransferase, polypeptide 2

***BLNK*:** B-cell linker

***Bmal1* (Official symbol: *Arntl)*:** aryl hydrocarbon receptor nuclear translocator-like

Bmal1:dLuc: reporter construct where destabilized fire-fly luciferase is under the control of the mouse Bmal1 promoter

***C/EBPα*:** CCAAT/enhancer binding protein (C/EBP), alpha

***C/EBPβ*:** CCAAT/enhancer binding protein (C/EBP), beta

***C/EBPγ*:** CCAAT/enhancer binding protein (C/EBP), gamma

cAMP: cyclic AMP (adenosine-monophosphate)

CCG: clock controlled gene. These genes are regulated by the clock and involved in circadian output networks.

***CEACAM21*:** carcinoembryonic antigen-related cell adhesion molecule 21

ChIP: chromatin-immunoprecipitation

ChIP-chip: technique that combines chromatin-immunoprecipitation with microarray technology to identify DNA binding sites of a specific protein throughout the genome. However, unlike ChIP-Seq, the sequences able to be identified in ChIP-chip are limited to those represented by probes on the microarray.

ChIP-Seq: technique to identify physical protein:DNA interactions at the genome-wide level which combines chromatin-immunoprecipitation with next generation sequencing to identify DNA sequences bound by a specific protein throughout the genome. Unlike ChIP-chip which is limited to identifying only sequences represented in the array probes, ChIP-Seq utilizes sequencing and can detect any DNA sequence in the genome.

Clock: circadian locomotor rhythms kaput

***COX4N*:** COX4 neighbor

***Creb*:** cAMP responsive element binding protein 1

***Cry*:** *Cryptochrome* genes of which there are 2 in mammals: *Cry1* and *Cry2*

CNSK1D: casein kinase 1, delta

CT: circadian time

D-box: transcription factor binding site bound by DBP or E4BP4 to activate or repress transcription, respectively

***Dbp*:** D-box binding protein

DMSO: dimethyl sulfoxide

***E4PB4* (Official symbol: *Nfil3*):** nuclear factor, interleukin 3, regulated

E-box: transcription factor binding site bound by BMAL1/CLOCK dimers to activate transcription

EDTA: ethylenediaminetetraacetic acid

ENU: N-ethyl-N-nitrosourea, a potent mutagen used for random mutagenesis screens

***FBXL3*:** F-box and leucine-rich repeat protein 3

FDR: false discovery rate

FEO: food entrainable oscillator

FFT NLLS: fast fourier transform non-linear least squares (in BRASS software)

***FHIT*:** fragile histidine triad gene

FibB (Official symbol: *Fgb*): fibrinogen beta-chain

***Fus*:** fusion, derived from t(12;16) malignant liposarcoma (human)

***Gapdh*:** glyceraldehyde-3-phosphate dehydrogenase

GEO: gene expression omnibus (http://www.ncbi.nlm.nih.gov/geo/)

GO: gene ontology

GPCR: G-protein coupled receptor.

***HCF1*:** host cell factor C1 (VP16-accessory protein)

***HDAC3*:** histone deacetylase 3

***Heca*:** headcase homolog (Drosophila)

HGF: hepatocyte growth factor

***HIST1H1B*:** histone cluster 1, H1b

***Hmgr* (Official symbol: *Hmgcr*):** 3-hydroxy-3-methylglutaryl-CoA reductase

HNF1: hepatocyte nuclear factor 1

HNF3: hepatocyte nuclear factor 3

HNF4: hepatocyte nuclear factor 4

***Hspa1b*:** heat shock protein 1B

***Hspa8*:** heat shock protein 8

HTS: high throughput screening

***Ikbkg*:** inhibitor of kappaB kinase gamma

***IKBKB*:** inhibitor of kappa light polypeptide gene enhancer in B-cells, kinase beta

IKK: IκB kinase

JNK: c-Jun N-terminal kinase

KD: knockdown

***MAPK8*:** mitogen-activated protein kinase 8

MMH-D3: Met murine hepatocyte cell line derived from 3-day old liver

***MPG*:** N-methylpurine-DNA glycosylase

***MTOR* (Alias symbol: *FRAP1*):** mechanistic target of rapamycin (serine/threonine kinase)

NFKB: nuclear factor kappa-light-chain-enhancer of activated B cells

***Nfkb1*:** nuclear factor of kappa light polypeptide gene enhancer in B-cells 1, p105

***Nfkb2*:** nuclear factor of kappa light polypeptide gene enhancer in B-cells 2, p49/p100

NIH3T3: immortalized mouse fibroblast cell line

***Odc1*:** ornithine decarboxylase, structural 1

PBS: phosphate buffered saline

***PDE1B*:** phosphodiesterase 1B, calmodulin-dependent

***Per*:** *Period* gene, of which there are three: *Per1*, *Per2*, *Per3*.

***Per2:dLuc*:** reporter construct in which destabilized fire-fly luciferase is under the control of the mouse *Per2* promoter

PFK: phosphofructokinase (involved in glycolysis)

***PFKP*:** phosphofructokinase, platelet

PI3K: phosphatidylinositol 3-kinase

***PIK3R5*:** phosphoinositide-3-kinase, regulatory subunit 5

***PKLR*:** pyruvate kinase, liver and RBC

***POLR3F*:** polymerase (RNA) III (DNA directed) polypeptide F, 39 kDa

***Ppara*:** peroxisome proliferator activated receptor alpha

PPI: protein-protein interaction

***PRKCI*:** protein kinase C, iota

***PRPF4*:** PRP4 pre-mRNA processing factor 4 homolog (yeast)

PYK: pyruvate kinase

qPCR: quantitative real time pcr

QTL: quantitative trait locus

Rev-erb **(Official family symbol: *NR1D*):** nuclear receptor subfamily 1, group D (NR1D group), there are two group members Rev-erbα (NR1D1) and Rev-erbβ (NR1D2), both are transcriptional repressors and members of the RRE loop of the clock.

RNAi: RNA interference

***Ror*:** retinoic acid related orphan receptor. This group of nuclear receptors has three family members Rora, Rorb, and Rorc. RORs are transcriptional activators and components of the RRE loop of the clock.

RORE: ROR/REV-ERB transcription factor binding site; synonymous with RRE

RRE: ROR/REV-ERB transcription factor binding site; synonymous with RORE

***RRP12*:** ribosomal RNA processing 12 homolog (S. cerevisiae)

SCN: suprachiasmatic nucleus of the hypothalamus

±SD: plus or minus the standard deviation

***SEC13*:** SEC13 homolog (S. cerevisiae)

***SELO*:** selenoprotein O

siRNA: small interfering RNA

***Sirt1*:** sirtuin 1

***Sms*:** spermine synthase

***Srm*:** spermidine synthase

***TBCB*:** tubulin folding cofactor B

TFBS: transcription factor binding site

***TP53*:** tumor protein p53

***Ttr*:** transthyretin

U2-OS: an immortalized human osteosarcoma cell line

***Ugt1a1*:** UDP glucuronosyltransferase 1 family, polypeptide A1

***UNC119*:** unc-119 homolog (C. elegans)

***Vldlr*:** very low density lipoprotein receptor

***Wee1*:** WEE 1 homolog 1 (S. pombe)

WT: wildtype.

***ZMAT3*:** zinc finger, matrin-type 3

***Zo-1* (Official symbol: *Tjp1*):** tight junction protein 1

List of Figures

Chapter 1:

Chapter 2:

Chapter 3:

List of Tables

Chapter 2:

Acknowledgements

I would like to thank my advisor Steve A. Kay, my committee members, collaborators, and members of the Kay lab for their help and support throughout my graduate education. In particular, I would like to thank Robert DeConde, Susanna Wang, Tsuyoshi Hirota, Pagakpol "Yhew" Pongsawakul, Colleen Doherty, and Andrew C. Liu.

The study presented in Chapter 2 and the presented figures were published in *Cell* in the research article:

Zhang EE, Liu AC, Hirota T, Miraglia LJ, Welch G, Pongsawakul PY, Liu X, Atwood A, Huss, Jon W., III, Janes J, Su AI, Hogenesch JB & Kay SA (2009) A genome-wide RNAi screen for modifiers of the circadian clock in human cells. *Cell* 139: 199-210.

The dissertation author was an author on this paper.

Chapter 3, in full, is a reprint of the article published in the journal *Proceedings of the National Academy of Sciences, USA* with the combining of captions with respective supplementary tables (Tables S1, Table S2, and Table S3) in the Chapter 3 appendices:

Atwood A, DeConde R, Wang SS, Mockler TC, Ideker T & SA Kay (2011) Cell-autonomous circadian clock of hepatocytes drives rhythms in transcription and polyamine synthesis. *Proc Natl Acad Sci U S A* 108:18560-18565.

The dissertation author was the primary investigator and author of this paper.

Vita

2002-2004	Internship, Baylor College of Medicine
2005	Internship, New England Primate Research Center
2005-2006	Undergraduate researcher, Brown University
2006	Bachelor of Science, Brown University
2006-2007	Graduate researcher, The Scripps Research Institute
2007-2011	Graduate researcher, University of California, San Diego
2011	Doctor of Philosophy, University of California, San Diego

Fields of Study

Major Field: Biology

Circadian Biology
Professor Steven A. Kay, University of California, San Diego

Biomechanics of Maneuvering Bat Flight
Professor Sharon Swartz, Brown University

Evolution of Human Immunodeficiency Virus
Professor Welkin Johnson, New England Primate Research Center

Extracellular matrix in inflammation and infection
Professor Pyong Woo Park, Baylor College of Medicine

Abstract of the Dissertation

Expanding circadian input, output, and the clock through genomic screens

by

Ann Margaret Atwood

Doctor of Philosophy in Biology

University of California, San Diego

Professor Steve A. Kay, Chair

Many aspects of mammalian physiology display circadian—or once daily—rhythms, such as heart rate, blood pressure, activity levels, metabolism, and liver regeneration. These rhythms are regulated by an entrainable, self-sustaining, cell-autonomous mechanism found in nearly every cell of the body: the circadian clock. The circadian clock itself represents a regulatory network, composed of interlocking negative feedback loops, that in turn is influenced by two other types of regulatory networks: it is impinged upon by input networks to synchronize the clock to the

external environment and coordinate the timing of clocks throughout the body; and output networks by which the circadian clock governs overt rhythms in behavior and physiology. To expand our understanding of the composition of input network and gears of the clock, a genome-wide siRNA screen was performed, and identified hundreds of novel genes that can alter clock function, which represent input and novel clock gene candidates. These clock modifier genes not only display knockdown effects similar to known clock components, they also revealed a high degree of interconnectedness between the circadian clock and other functional pathways, suggesting intertwinement between the circadian system and overall cellular biology. To address the composition and nature of circadian output regulation, the respective roles of local, cell-autonomous regulation in peripheral tissues and systemic circadian regulation emanating from the central nervous system needed to be assessed. Using the MMH-D3 hepatocyte cell line, gene expression profiling revealed that cell-autonomous circadian regulation can drive rhythms in over 1,000 transcripts, indicating that cell-autonomous clock does contribute to circadian rhythms in gene expression and establishing MMH-D3 as a valid circadian cell-based model system. The protein-protein interactions of these circadian genes display organization based on co- and anti-phasic relationships, suggesting that competitive relationships may represent an organizing theme for circadian regulation, extending beyond the clock itself. Finally, circadian oscillations in polyamine synthesis were revealed at both the transcriptional and enzymatic level in MMH-D3. As polyamines are closely associated

with cell proliferation and required for initiation of liver regeneration, this may represent a role for the cell-autonomous clock in circadian gating of liver regeneration.

Chapter 1: Introduction

Section 1.1: Circadian rhythms and clockwork:

The rotation of the earth produces 24 hour cycles of light and dark (day and night). Many organisms on Earth, including bacteria, plants, animals, and mammals, have evolved internal timing mechanisms by which to coordinate and consolidate aspects of their behavior and physiology to specific times during this 24 hour cycle, producing circadian—about 24 hour—rhythms (1, 2).

Many aspects of mammalian behavior and physiology exhibit circadian rhythms. For example, humans display circadian oscillations in their activity level and sleep/wake cycle. As diurnal animals, humans are awake and active during daylight hours, and inactive at night while sleeping. Circadian rhythms display a high degree of coordination, whereby the one physiological oscillation actually primes the body for the next change, such as is seen in the circadian rhythms in heart rate and blood pressure. In the late night/early morning while still asleep, both heart rate and blood pressure display a steep increase in preparation for the onset of wakefulness. Thus, upon waking up, the body is prepared to meet the requirements of the active phase (2).

Other examples of mammalian circadian rhythms include oscillations in overall metabolic rate, xenobiotic metabolism, release of some hormones, cell proliferation, liver regeneration, and glucose homeostasis (2-4). These rhythms are the products of gene regulatory networks through which gene expression and protein activity are regulated by an internal timing mechanism. These rhythms are important

to human health. Disruption of circadian rhythms or their timing mechanisms can result in jetlag, shift work syndrome, and sleep disorders. Circadian disruption is associated with increased risk of cancer, dysregulation of the innate immune system, mood disorders, and metabolic syndrome which predisposes one to heart disease, Type 2 diabetes, and obesity (5-7).

Circadian rhythms are regulated by the internal molecular timing mechanism, the circadian clock (Figure 1) (8), which is an endogenous, self-sustaining network composed of three interlocking negative feedback transcription-translation loops. Each loop displays cyclic expression of component transcription activator and repressor genes and is defined by the transcription factor binding site through which its components act: the E-box, RRE, and D-box loop. The E-box loop is also known as the core loop and is required for cycling of the clock. It is composed of the transcription factors, BMAL1 (official name: ARNTL) and CLOCK, which dimerize and activate transcription of target genes through E-boxes (CACGTG). Among these target genes are the loop's other components, the *Period*—or *Per*—genes (*Per1*, *Per2*, *Per3*) and *Cryptochrome*—or *Cry*—genes (*Cry1*, *Cry2*). PER and CRY proteins dimerize and feedback to repress transcription of Bmal1 and Clock. The RRE and D-box loop are interlocked with the core loop, and, while they are not required for the circadian clock to run, they are believed to play important roles in phase resetting (conferring input information to synchronize the clock to the external environment), stabilizing the core loop, and in regulating some clock outputs. The RRE consists of ROR (RORa, RORb, RORc) transcriptional activators and REV-ERB transcriptional

repressors (REV-ERBα, REV-ERBβ, whose official names are NR1D1 and NR1D2). BMAL1/CLOCK activates transcription of *Ror* and *Rev-erb* genes through E-boxes in their promoter sequences. RORs and REV-ERBs competitively bind and act through the RRE sequence ([A/T]A[A/T]NT[A/G]GGTCA), allowing them to feedback on the core loop through the RRE in the *Bmal1* and *Clock* promoters. The D-box loop consists of the transcription activator DBP and the repressor E4BP4 (official name: NFIL3). BMAL1/CLOCK activates transcription of Dbp; while *E4bp4* transcription is controlled by an RRE in its promoter. DBP and E4BP4 act as transcription activator and repressor, respectively, through binding to D-boxes (TTA[T/C]GTAA) in target genes, including the *Per* genes, closing the D-box loop (4, 9, 10).

Section 1.2: The multi-oscillator circadian system

Circadian regulation at the organismal level is complex since the body contains multiple clocks. Nearly every mammalian cell type contains a circadian, giving rise to a multi-oscillator system *in vivo* (2). These oscillators can be divided into two classes: the central pacemaker and peripheral oscillators.

The central pacemaker, located in the suprachiasmatic nucleus (SCN) of the hypothalamus, directly receives light input from the retina, allowing direct entrainment to the day/night cycle. The SCN acts as a conductor to synchronize the circadian clocks in peripheral tissues, allowing for coordination of physiology across multiple tissues. This orchestration is believed to occur through systemic cues, including neuro-endocrine signaling, hormones, and metabolites. These systemic cues

may act upon the circadian clock to entrain the phase of circadian gene expression or to directly drive gene expression in the target tissue (11).

Peripheral oscillators are the cell-autonomous clocks found in peripheral tissues, such as the liver, lung, aorta, and skeletal muscle. Peripheral clocks are entrained differently than the SCN as they do not receive direct light input (2). Instead, they respond to other stimuli, such as feeding, hormones, or metabolites, which have yet to be fully characterized as well as the mechanisms by which these clocks communicate with one another (2, 4). In addition, approximately 10% of the genome exhibits circadian cycles in any tissue, but in a tissue-specific manner, such that very few transcripts that cycle in the liver also cycle in the SCN (3, 12, 13). The respective roles of the central pacemaker and local, peripheral oscillators in governing these gene expression rhythms in gene expression and rhythms in physiology remain unknown. As the liver represents a physiologically relevant tissue for human health, we will focus on it as an example of a peripheral oscillator.

Section 1.3: Circadian regulatory networks: input, output, and the clock

These transcriptional-translational negative feedback loops form the backbone of our understanding of the circadian clock, yet much remains unclear about the circadian clock, its regulation, and how it governs overt rhythms in physiology. These areas represent the three types of regulatory networks whose composition and architecture are areas of active research: (a) the clockwork—gears of the clock—

(b) input—by which environmental signals impinge upon the clock—and (c) output—by which the clock to governs physiology (Figure 2).

For the clockwork, we know that the E-box, D-box, and RRE transcription-translation negative feedback loops are gears of the clock (Section 1.1), but experts hypothesize that additional clock genes remain to be discovered based on quantitative trait loci (QTL) studies, that mouse mutagenesis screens have not reached saturation, and the large number of genes with circadian cycles in microarray studies (14).

Input networks convey external signals to align—entrain—the circadian clock to its environment. While the circadian clock is a self-sustaining mechanism, it also must respond to changes in its environment, such as seasonal changes in dawn, dusk, and day length, in order to maintain alignment of internal circadian time with the external environment. For the SCN, light represents that major entrainment signal. Light input is conveyed to SCN neurons through direct connections with retinal ganglion cells (2). However, peripheral clocks do not receive direct light input, but are entrained and synchronized by other signals, such as behavior—like feeding—neuronal impulses, hormones, and metabolites (2, 4). For example, feeding plays a key role in entrainment of the liver clock. Restricting food access to a few hours of the normal rest period, inverts the timing of the liver clock in accordance to food access while the SCN remains entrained to the light/dark cycle (11, 15, 16). However, the specific input molecules and networks by which these signals impinge upon the clock in peripheral tissues, like the liver, have yet to be defined. We can begin characterizing these networks at a cell-autonomous level by defining which genes impinge upon

clock function since conveying input information to the clock will require the ability to alter clock function. This will provide a starting point for characterizing the intracellular cell-autonomous input networks by analyzing these genes' interactions and functions.

Finally, through output regulatory networks of gene expression, the circadian clock governs overt rhythms in behavior and physiology. Genes, whose expression is regulated by the clock, display 24-hour rhythms of gene expression and are known as clock controlled genes (CCGs) which are organized in regulatory networks to govern behavior and physiology (2, 3). The composition and architecture of these networks remain to be elucidated. Characterizing output networks in peripheral tissues has proven a challenge due to the complexity of circadian regulation at an organismal level as both systemic regulation driven by the central pacemaker in the SCN and local cell-autonomous circadian regulation may contribute to output regulation (4). In any specific tissue, CCGS represent approximately 10% of the genome (3, 12, 13, 17). However, rhythmic gene expression displays tissue-specificity, such that little overlap exists between the transcripts that cycle in the liver and those that cycle in the SCN (3, 12, 13). This tissue specificity implies that physiological rhythms may be under local, tissue-specific regulation. However, the role of the cell-autonomous clock or the extent of its contribution to the regulation of gene expression remains unclear. In Chapter 3, we begin to address these questions in the liver.

Section 1.4: The liver—a case study for peripheral circadian output regulation

The liver forms an important tissue in terms of metabolism for the body, and exhibits a number of circadian rhythms, such as rhythms in glucose and lipid homeostasis, regeneration, and xenobiotic metabolism. *In vivo* with both a central pacemaker and local liver clock intact, over 3,000 transcripts cycle with a circadian period, including rate-limiting enzymes key liver functions (3, 17). Mice with dysfunctional clocks display problems related to liver function. *Clock* mutant mice display an obese phenotype as well as symptoms of metabolic syndrome (18). *Bmal1 -/-* mice have impaired gluconeogenesis (19). The liver is essential to maintaining glucose homeostasis. It acts as a buffer, performing both taking up glucose from the blood for storage and consumption when glucose levels are high, but also generating glucose by gluconeogenesis pathway when blood glucose levels are low (3). Rhythms in hepatic gluconeogenesis were identified as being circadian gated by the core loop of the circadian clock (20). During the rest phase, CRY repressors block GPCR mediated rises in cAMP in response to glucagon. cAMP and phosphorylated CREB (mediated by cAMP) induce the expression of gluconeogenic gene expression program (20). By blocking cAMP rise, the clock effectively gates the gluconeogenic response (20). Furthermore, *Cry1 -/-* mice exhibit impaired liver regeneration (21). At 72 hours after partial hepatectomy, *Cry1 -/-* liver remnants displayed fewer cells undergoing cell division and less mass than that of wild-type (WT) controls (21). Wee1, a kinase involved in the cell cycle, displays robust rhythms in WT liver, and gates circadian regulation of cell proliferation (21). These defects

indicate the significance of the circadian regulation in hepatic function and overall health.

Much effort is going into uncovering the networks and molecular mechanisms by which the circadian clock regulates liver function; however, it has become increasingly apparent the complexity of circadian regulation in peripheral tissues. Since the body contains multiple clocks which all may influence circadian regulation, rhythms in physiology and gene expression may be influenced by multiple levels of circadian regulation, such as systemic regulation from circulating systemic cues under control of the circadian clock in the SCN or cell-autonomous circadian regulation exerted by the intracellular hepatic clock. Recent studies have suggested both levels of regulation likely exist, but their individual contributions to liver physiology remain unclear. In 2007, Kornmann et al. reported that if the liver clock was stopped but all other body clocks allowed persist, few rhythms in gene expression can be detected in the liver (22), suggesting that the local liver clock is required for many rhythms in hepatic gene expression and physiology. However, in 2009, Vollmers et al. reported that feeding alone can drive many rhythms of hepatic gene expression, even in the absence of a functional circadian clock (23). This finding suggests that systemic cues, such as feeding behavior and hormones, can drive rhythms in liver gene expression. Since feeding behavior and the sleep/wake cycle are governed by the SCN, this finding implies that the central pacemaker may drive rhythms in peripheral tissues.

Taken together, these findings indicate that complex relationships may govern peripheral circadian rhythms and the definitive role of the systemic and cell-

autonomous circadian regulation remains unclear. Yet, both studies addressed peripheral rhythms *in vivo*, where systemic regulation may be exerted by other tissues. It remains to directly examine the role of cell-autonomous circadian regulation and elucidate the cell-autonomous clock controlled gene regulatory networks.

Section 1.5: Investigating cell-autonomous circadian regulatory networks

Our primary interest is in characterizing the role and components of the cell-autonomous circadian networks involved in input, output, and novel components of the clockwork, itself. While both systemic and cell-autonomous circadian regulatory networks remain to be elucidated, we focused on the cell-autonomous regulation because this level of regulation represents a more accessible system, representing fewer variables than systemic networks. Cell-autonomous regulation occurs at an intracellular level, and can be addressed in cell culture where potentially confounding variables of behavior and systemic regulation applied by other tissues of the body are eliminated. The circadian clock not only exists in nearly all cell types *in vivo*; it continues to run *ex vivo* in tissue explants and even persists in individual cells, including SCN neurons (24), fibroblasts (25, 26), primary hepatocytes (17), embryonic fibroblasts (27), Rat-1 fibroblasts (28), NIH-3T3 fibroblasts (29), the U2-OS human osteosarcoma cell line (8, 30-32), and the MMH-D3 mouse hepatocyte cell line (Chapter 3).

Peripheral tissue explants and cultured dissociated or peripheral cells contain functional clocks that cycle robustly on a cell-autonomous level. But they require

synchronization treatments, such as medium changes, forskolin, dexamethasone, or serum shock, to consolidate the phases of individual clocks. Coherent rhythms persist for multiple days after synchronization, but, over time, population recordings of these cultures display "dampening" of rhythms due to the individual clocks drifting out of phase with one another in the absence of external entraining signals. This occurs because, while the cell-autonomous clocks continue to cycle robustly, they differ slightly in period length from one another which results in gradual loss of coherence of rhythms at the population level. Thus, experiments performed in cell culture are performed following synchronization treatments (2, 24).

Specifically, we chose to work in immortalized cell lines, which provided a homogeneous population, enabling greater precision in data gathered and providing systems that are experimentally tractable. They are amenable to transfection and/or infection with expression constructs, allowing one to test hypotheses regarding molecular interactions. Transient transfection assays and the generation of stable cell lines requires less time than the generation of a transgenic mouse, allowing one to test multiple hypotheses in a shorter period of time. In fact, some cell lines, such as U2-OS, can be utilized in high throughput screening (HTS), enabling one to examine gene expression or circadian effects at a genome-wide level in addition to more focused follow-up experiments (8, 30, 32).

Thus, we elected to investigate cell-autonomous circadian regulation in immortalized cell lines. Yet, each cell line has different characteristics, which make it better suited for some experiments than others. To identify input and additional clock

genes, we selected the human osteosarcoma cell line U2-OS (Chapter 2). To begin characterizing the role of the cell-autonomous clock in hepatic output, we established the mouse hepatocytes MMH-D3 cell line as a circadian model system (Chapter 3). The following sections explain our rationale for utilizing U2-OS (Section 1.6) and MMH-D3 (Section 1.7), respectively.

Section 1.6: U2-OS—a model system for clockwork and input studies

U2-OS is an immortalized cell line derived from a tibular osteosarcoma of a 15-year old female (33). The tumor was characterized as moderately differentiated, and the cell line is transformed in nature. A high degree of chromosomal rearrangements exist, with few normal chromosomes observed, and, although Ponten et al. originally reported that most cells were hypodiploid, a preponderance of hypertriploid cells have been reported by ATCC (33, 34). Thus, this cell line is transformed and more closely reflects the biology of that cancer rather than healthy osteoid (33, 34).

Although not exhibiting a highly differentiated state, the U2-OS cell line is widely used in many areas of biology due to its experimental tractability. The U2-OS cell line grows at a rapid rate with a doubling time of ~25 hours (35) and is able to be transfected at high efficiency—an essential factor for siRNA studies. Furthermore, it is amenable to over-expression of cDNA constructs and been successfully used to perform RNAi (30, 32). Furthermore, U2-OS contains a functional circadian clock as indicated by stable circadian luciferase reporter U2-OS cell lines (Figure 3) (8, 30,

31). These cell lines express firefly luciferase under the control of a clock gene promoter and enable kinetic assessment of clock function through measurement of luminescence. Thus, rhythmic luciferase expression results in rhythms in luciferase enzymatic activity, producing rhythms of light emission, which indicates a functional cell-autonomous clock (Figure 3) (8, 30, 31). In U2-OS, robust rhythms are observed for multiple days after synchronization with a period of roughly 24 hours, indicating circadian regulation of that clock gene promoter and, therefore, cycling of the circadian clock.

Moreover, U2-OS has already been successfully employed in circadian studies. In 2008, Hirota et al. performed a chemical screen in U2-OS to identify chemicals that alter circadian period (i.e. the running speed of the clock) (8). In 2009, Baggs et al. dissected the network connections of the clock genes in detail, revealing the dose dependent effects of individual clock genes on the others (31). Moreover, in 2009, Maier et al. performed a limited-scale RNAi screen for circadian modifiers in U2-OS (32). Finally, in 2009, Hughes et al. characterized at high resolution and statistical stringency transcripts displaying circadian oscillations in U2-OS (17). Hughes et al. revealed that very few transcripts cycle—in fact, less than one dozen ($q<0.1$) (17)—introducing a caveat to circadian usage of U2-OS. Cyclers consisted of almost exclusively known clock genes and CCGs which directly interact with the clock (17). While expression of clock genes and clock function (period) recapitulates that found in healthy, normal mammalian cells, the scarcity of cycling transcripts indicates that rhythms in output are maintained in U2-OS, making it inappropriate for the study of

circadian output networks. Yet, U2-OS does contain a robust clock mechanism, making it sufficiently suited for examining the inner workings of the clock and its input networks since U2-OS clocks are still capable of being synchronized using conventional chemical treatments, such as dexamethasone and serum shock (8, 17). Combined with their high transfection efficiency, U2-OS provides an appropriate environment for our siRNA screen to identify novel clock components and input genes (Chapter 2).

Section 1.7: MMH-D3—a model system for hepatic cell-autonomous circadian output

Since little overlap exists between cycling transcripts of different tissues, it is believed that circadian output regulation is tissue- or cell-type specific. To investigate circadian output regulation, we chose to use the liver, a tissue that contains many circadian expressed transcripts and plays an important role in many aspects of physiology, including glucose homeostasis, detoxification of xenobiotics, lipid homeostasis, production of circulating proteins, vitamin A (retinoid) metabolism, as well as some aspects of immune function (3, 36, 37). However, role of the cell-autonomous hepatic clock in governing circadian oscillations in these transcripts and resultant physiology remains to be elucidated. We begin to address these questions through the use of a cell-based model system which is new for circadian applications: the Met Murine Hepatocytes Day 3 (MMH-D3) hepatocyte cell line, an immortalized

cell line derived from the livers of 3-day old transgenic mouse livers expressing a constitutively active cytoplasmic form of Met (38).

MMH-D3 is a homogenous cell line that is immortalized, but not transformed that displays many characteristics of a mature hepatocyte. This cell line is homogenous as it was derived from a single focus of dissociated liver cells in continuous culture, representing the progeny of a single spontaneously immortalized hepatocyte, and MMH-D3 gives rise to a single morphological type of differentiated cell: a mature hepatocyte (38, 39).

Unlike hepatoma cell lines, MMH-D3 is immortalized but not transformed. It fails to form colonies in soft agar (38, 39) and does not form tumors in nude mice (39). In fact, MMH-D3 maintains contact inhibition (Figure 4) (40), meaning that the proportion of cells undergoing active cell division is inversely correlated with confluence. However, the MMH-D3 cell line displays a rapid rate of generation with a doubling time of ~24-hours during expansion and an ability to recover from low density seeding (38, 39).

MMH-D3 displays many characteristics of mature hepatocytes in morphology, gene expression, and functionality, especially upon induction of differentiation (39, 40). At confluence, MMH-D3 up-regulates hepatic gene markers and proteins associated with hepatocyte functions (40). This differentiation program can be reinforced, and induction maintained by adding DMSO as a differentiation agent to the culture medium (36, 39).

First, MMH-D3 is hypotetraploid (39), similar to hepatocytes, which also display increased ploidy. Moreover, MMH-D3 displays hepatocyte morphology. MMH-D3 cells are polygonal in shape, similar to hepatocytes.

Next, MMH-D3 displays epithelial characteristics. It contains tight, adherens, and gap junctions based gene expression and staining. These junctions found in hepatocytes are important for these epithelial cells to anchor themselves together in sheets or plates and communicate with one another. ZO-1 (official symbol: Tpj1), a protein in tight junctions, is expressed and localized to only surfaces of cell-cell contact, indicating tight junctions that are restricted to surfaces of intercellular contact (38, 39). The ZO-1 network at the cell interaction surfaces establishes the simple epithelial polarity of MMH-D3 (38). MMH-D3's epithelial nature is further supported by their extensive intracellular network of intermediate filaments and expression of intermediate filament components: cytokeratin 8 (type I keratin) and cytokeratin 18 (type II keratin), which indicates their epithelial growth pattern (38, 39). E-cadherin (epithelial cadherin), a component of aherens junctions, is also expressed in MMH-D3 (39). Adherens junctions are required in MMH-D3 to induce differentiation into mature hepatocytes (40). Lastly, like the liver, MMH-D3 highly expresses connexin 32 (Figure 5A), a component of gap junctions (38).

Furthermore, MMH-D3 expresses liver enriched transcription factors (HNF1, HNF4, C/EBPα, C/EBPβ, and C/EBPγ) (Figure 5A) (38) as well as genes important to hepatic functions, including cholesterol metabolism (Hmgr), lipid homeostasis (Pparα, ApoCIII, and Vldlr), glucose homoestasis (AldoB), and secreted protein products

(albumin: Alb, β-fibrinogen: FibB (official symbol: Fgb), transthyretin: TTR) (Figure 5) (38, 40). This pattern of gene expression supports MMH-D3 maintains characteristics of highly differentiated hepatocytes. Furthermore, after DMSO differentiation, MMH-D3 cells not only express RNA for albumin, β-fibrinogen, and transthyretin, but also secrete them into the medium, characteristic of a mature hepatocyte (36-38, 40).

Moreover, in addition to its maintenance of hepatocyte traits, MMH-D3 provides other characteristics suited to development as a circadian cell-based model system: it is experimentally tractable and contains a functional circadian clock. Whereas, primary hepatocytes display very low transfection rates, MMH-D3 is experimentally tractable, being amenable to lenti-viral infection during the sub-confluent, growth stage (40). Furthermore, MMH-D3 contains a robust circadian clock—an essential trait for use as a circadian cell-based model system (Figure 6). The Kay lab has generated stable MMH-D3 lines containing circadian luciferase reporters using *Bmal1* and *Per2* promoters as described for U2-OS circadian reporter lines (Section 1.6). In synchronized, differentiated MMH-D3 cultures, robust oscillations in fire-fly luciferase activity are observed for multiple days, indicating the MMH-D3 contains a functional clock (Figure 6).

Through these combined characteristics, MMH-D3 provides a tractable system in which to investigate the cell-autonomous regulation in hepatocytes.

Section 1.8: Dissertation objectives and summary

We set out to expand our understanding of cell-autonomous circadian regulation. We separated this into two main studies: (a) investigating genes involved in modifying clock function, which may represent novel clock genes or components of input networks, and (b) characterizing the role of the cell-autonomous hepatic circadian clock in output regulation (Figure 7).

In the first study (Chapter 2), we want to identify genes that can alter the running of the clock, such as changing the speed or amplitude of clock cycles. These genes will be involved in either transmitting input information to the circadian clock so entrain its phase to external, or these genes may represent novel clock genes. Novel clock genes may be part of feedback loops like known clock genes, in which these genes are both regulated by the clock (rhythmic gene expression) and affect clock function. In a high throughput, genome-wide siRNA screen in the human osteosarcoma U2-OS cell line, we addressed the following questions:

1. Which genes can influence clock function, such as the speed or amplitude of clock cycling?
2. Are these clock modifiers novel genes to circadian biology?
3. Do the clock modifiers have known protein-protein or genetic interactions with the clock?
4. What type of genes and pathways are clock modifiers? Are specific molecular functions and/or pathways enriched for clock modifiers?

We hypothesized that many genes would be clock modifiers, including not only transcription factors, but other genes with many different molecular functions. In our siRNA screen, we identified over 300 genes whose knock-down (KD) significantly altered clock function, as detailed in Chapter 2.

In the second study (Chapter 3), we investigated the role of the cell-autonomous hepatic clock regulation of output. Since gene expression and output physiology rhythms appear to be tissue specific, we chose a well-studied tissue that exhibits circadian rhythms of gene expression and physiology *in vivo*: the liver. Since we are interested in the cell-autonomous circadian regulation, we employed a cell-based model system: the MMH-D3 mouse hepatocyte cell line. Using this cell line eliminates systemic circadian regulation while maintaining a level of differentiation, allowing us to characterize which rhythms of gene expression can be driven by the intracellular hepatic circadian clock. In this study we posed the following questions:

1. Can the cell-autonomous clock drive rhythms of gene expression in hepatocytes?
2. Which transcripts display circadian expression patterns in the absence of systemic circadian regulation in hepatocytes?
3. In the broader, mouse protein-protein interaction network, are circadian genes centrally located in the network? Do these genes display phasic relationships with regards to proximity of one circadian gene to another in the network?

4. Of this list, what molecular functions and functional pathways are represented? Is the circadian list enriched for any pathways?
5. Does the activity of the gene products reflect the circadian rhythms observed in their transcripts?
6. What is there a role for the cell-autonomous clock?

We hypothesized that many genes of various molecular functions would display circadian rhythms in MMH-D3 hepatocytes, suggesting a significant role for the cell-autonomous circadian regulation. As described in Chapter 3, we identified 1,130 transcripts displaying circadian rhythms. In the mouse protein-protein interaction network, these circadian genes are both central and display phasic relationships, such that co- and anti-phasic genes are in closest proximity to one another. Finally, we reveal cell-autonomous circadian oscillations of in polyamine synthesis, whose products are essential for the initiation of liver regeneration and may represent a novel mechanism for regeneration's circadian gating.

Section 1.9: Chapter 1 references

1. Panda S, Hogenesch JB & Kay SA (2002) Circadian rhythms from flies to human. *Nature* 417: 329-335.

2. Hastings MH, Reddy AB & Maywood ES (2003) A clockwork web: Circadian timing in brain and periphery, in health and disease. *Nature Reviews Neuroscience* 4: 649-661.

3. Panda S, Antoch MP, Miller BH, Su AI, Schook AB, Straume M, Schultz PG, Kay SA, Takahashi JS & Hogenesch JB (2002) Coordinated transcription of key pathways in the mouse by the circadian clock. *Cell* 109: 307-320.

4. Zhang EE & Kay SA (2010) Clocks not winding down: Unravelling circadian networks. *Nat Rev Mol Cell Biol* 11: 764-776.

5. Staels B (2006) When the clock stops ticking, metabolic syndrome explodes. *Nat Med* 12: 54-55.

6. Hastings M, O'Neill JS & Maywood ES (2007) Circadian clocks: Regulators of endocrine and metabolic rhythms. *J Endocrinol* 195: 187-198.

7. Castanon-Cervantes O, Wu M, Ehlen JC, Paul K, Gamble KL, Johnson RL, Besing RC, Menaker M, Gewirtz AT & Davidson AJ (2010) Dysregulation of inflammatory responses by chronic circadian disruption. *Journal of Immunology* 185: 5796-5805.

8. Hirota T, Lewis WG, Liu AC, Lee JW, Schultz PG & Kay SA (2008) A chemical biology approach reveals period shortening of the mammalian circadian clock by specific inhibition of GSK-3 beta. *Proc Natl Acad Sci U S A* 105: 20746-20751.

9. Ukai-Tadenuma M, Kasukawa T & Ueda HR (2008) Proof-by-synthesis of the transcriptional logic of mammalian circadian clocks. *Nat Cell Biol* 10: 1154-1163.

10. Kumaki Y, Ukai-Tadenuma M, Uno KD, Nishio J, Masumoto K, Nagano M, Komori T, Shigeyoshi Y, Hogenesch JB & Ueda HR (2008) Analysis and synthesis of high-amplitude cis-elements in the mammalian circadian clock. *Proc Natl Acad Sci U S A* 105: 14946-14951.

11. Green CB, Takahashi JS & Bass J (2008) The meter of metabolism. *Cell* 134: 728-742.

12. Storch KF, Lipan O, Leykin I, Viswanathan N, Davis FC, Wong WH & Weitz CJ (2002) Extensive and divergent circadian gene expression in liver and heart. *Nature* 417: 78-83.

13. Rudic RD, McNamara P, Reilly D, Grosser T, Curtis AM, Price TS, Panda S, Hogenesch JB & FitzGerald GA (2005) Bioinformatic analysis of circadian gene oscillation in mouse aorta. *Circulation* 112: 2716-2724.

14. Takahashi JS (2004) Finding new clock components: Past and future. *J Biol Rhythms* 19: 339-347.

15. Damiola F, Le Minh N, Preitner N, Kornmann B, Fleury-Olela F & Schibler U (2000) Restricted feeding uncouples circadian oscillators in peripheral tissues from the central pacemaker in the suprachiasmatic nucleus. *Genes Dev* 14: 2950-2961.

16. Hara R, Wan K, Wakamatsu H, Aida R, Moriya T, Akiyama M & Shibata S (2001) Restricted feeding entrains liver clock without participation of the suprachiasmatic nucleus. *Genes Cells* 6: 269-278.

17. Hughes ME, DiTacchio L, Hayes KR, Vollmers C, Pulivarthy S, Baggs JE, Panda S & Hogenesch JB (2009) Harmonics of circadian gene transcription in mammals. *PLoS Genet* 5: e1000442.

18. Turek FW, Joshu C, Kohsaka A, Lin E, Ivanova G, McDearmon E, Laposky A, Losee-Olson S, Easton A, Jensen DR, Eckel RH, Takahashi JS & Bass J (2005) Obesity and metabolic syndrome in circadian clock mutant mice. *Science* 308: 1043-1045.

19. Rudic RD, McNamara P, Curtis AM, Boston RC, Panda S, Hogenesch JB & FitzGerald GA (2004) BMAL1 and CLOCK, two essential components of the circadian clock, are involved in glucose homeostasis. *Plos Biology* 2: 1893-1899.

20. Zhang EE, Liu Y, Dentin R, Pongsawakul PY, Liu AC, Hirota T, Nusinow DA, Sun X, Landais S, Kodama Y, Brenner DA, Montminy M & Kay SA (2010) Cryptochrome mediates circadian regulation of cAMP signaling and hepatic gluconeogenesis. *Nat Med* 16: 1152-U133.

21. Matsuo T, Yamaguchi S, Mitsui S, Emi A, Shimoda F & Okamura H (2003) Control mechanism of the circadian clock for timing of cell division in vivo. *Science* 302: 255-259.

22. Kornmann B, Schaad O, Bujard H, Takahashi JS & Schibler U (2007) System-driven and oscillator-dependent circadian transcription in mice with a conditionally active liver clock. *Plos Biology* 5: 179-189.

23. Vollmers C, Gill S, DiTacchio L, Pulivarthy SR, Le HD & Panda S (2009) Time of feeding and the intrinsic circadian clock drive rhythms in hepatic gene expression. *Proc Natl Acad Sci U S A* 106: 21453-21458.

24. Welsh DK, Yoo SH, Liu AC, Takahashi JS & Kay SA (2004) Bioluminescence imaging of individual fibroblasts reveals persistent, independently phased circadian rhythms of clock gene expression. *Current Biology* 14: 2289-2295.

25. Liu AC, Tran HG, Zhang EE, Priest AA, Welsh DK & Kay SA (2008) Redundant function of REV-ERB alpha and beta and non-essential role for BMAL1 cycling in transcriptional regulation of intracellular circadian rhythms. *Plos Genetics* 4: e1000023.

26. Balsalobre A, Damiola F & Schibler U (1998) A serum shock induces circadian gene expression in mammalian tissue culture cells. *Cell* 93: 929-937.

27. Grundschober C, Delaunay F, Puhlhofer A, Triqueneaux G, Laudet V, Bartfai T & Nef P (2001) Circadian regulation of diverse gene products revealed by mRNA expression profiling of synchronized fibroblasts. *J Biol Chem* 276: 46751-46758.

28. Duffield GE, Best JD, Meurers BH, Bittner A, Loros JJ & Dunlap JC (2002) Circadian programs of transcriptional activation, signaling, and protein turnover revealed by microarray analysis of mammalian cells. *Current Biology* 12: 551-557.

29. Menger GJ, Allen GC, Neuendorff N, Nahm S, Thomas TL, Cassone VM & Earnest DJ (2007) Circadian profiling of the transcriptome in NIH/3T3 fibroblasts: Comparison with rhythmic gene expression in SCN2.2 cells and the rat SCN. *Physiological Genomics* 29: 280-289.

30. Zhang EE, Liu AC, Hirota T, Miraglia LJ, Welch G, Pongsawakul PY, Liu X, Atwood A, Huss,Jon W.,,III, Janes J, Su AI, Hogenesch JB & Kay SA (2009) A genome-wide RNAi screen for modifiers of the circadian clock in human cells. *Cell* 139: 199-210.

31. Baggs JE, Price TS, DiTacchio L, Panda S, FitzGerald GA & Hogenesch JB (2009) Network features of the mammalian circadian clock. *Plos Biology* 7: 563-575.

32. Maier B, Wendt S, Vanselow JT, Wallach T, Reischl S, Oehmke S, Schlosser A & Kramer A (2009) A large-scale functional RNAi screen reveals a role for CK2 in the mammalian circadian clock. *Genes Dev* 23: 708-718.

33. Ponten J (1967) Spontaneous lymphoblastoid transformation of long-term cell cultures from human milignant lymphoma. *International Journal of Cancer* 2: 311-&.

34. ATCC *Homo sapiens* U-2 OS (ATCC HTB-96™) August 4 2011: http://www.atcc.org/ATCCAdvancedCatalogSearch/ProductDetails/tabid/452/Default.aspx?ATCCNum=HTB-96&Template=cellBiology

35. Perego P, Capranico G, Supino R & Zunino F (1994) Topoisomerase-i gene-expression and cell sensitivity to camptothecin in human cell-lines of different tumor types. *Anticancer Drugs* 5: 645-649.

36. Bordoni V, Alonzi T, Agrati C, Poccia F, Borsellino G, Mancino G, Fimia GM, Piacentini M, Fantoni A & Tripodi M (2004) Murine hepatocyte cell lines promote expansion and differentiation of NK cells from stem cell precursors. *Hepatology* 39: 1508-1516.

37. Bellovino D, Lanyau Y, Garacuso I, Amicone L, Cavallari C, Tripodi M & Gaetani S (1999) MMH cells: An in vitro model for the study of retinol-binding protein secretion regulated by retinol. *J Cell Physiol* 181: 24-32.

38. Amicone L, Spagnoli FM, Spath G, Giordano S, Tommasini C, Bernardini S, DeLuca V, DellaRocca C, Weiss MC, Comoglio PM & Tripodi M (1997) Transgenic expression in the liver of truncated met blocks apoptosis and permits immortalization of hepatocytes. *EMBO J* 16: 495-503.

39. Spagnoli FM, Amicone L, Tripodi M & Weiss MC (1998) Identification of a bipotential precursor cell in hepatic cell lines derived from transgenic mice expressing cyto-met in the liver. *J Cell Biol* 143: 1101-1112.

40. Mancone C, Conti B, Amicone L, Bordoni V, Cicchini C, Calvo L, Perdomo AB, Fimia GM, Tripodi M & Alonzi T (2010) Proteomic analysis reveals a major role for contact inhibition in the terminal differentiation of hepatocytes. *J Hepatol* 52: 234-243.

Section 1.10: Chapter 1 figures

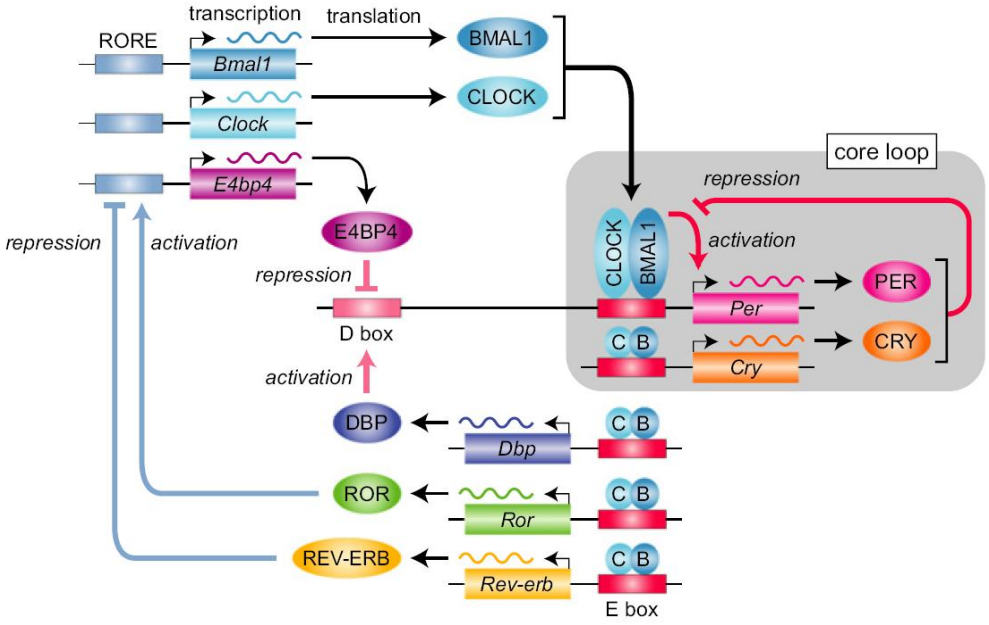

Figure 1: The mammalian circadian clock consists of three interlocked negative feedback loops: the E-box or core loop (*Bmal1*, *Clock*, *Per*, and *Cry*), the D-box loop (*Dbp* and *E4bp4)*, and the RRE loop (*Rev-erb* and *Ror*). RORE (ROR/REV-ERB element) is synonymous with RRE . This figure is from Hirota et al. (8).

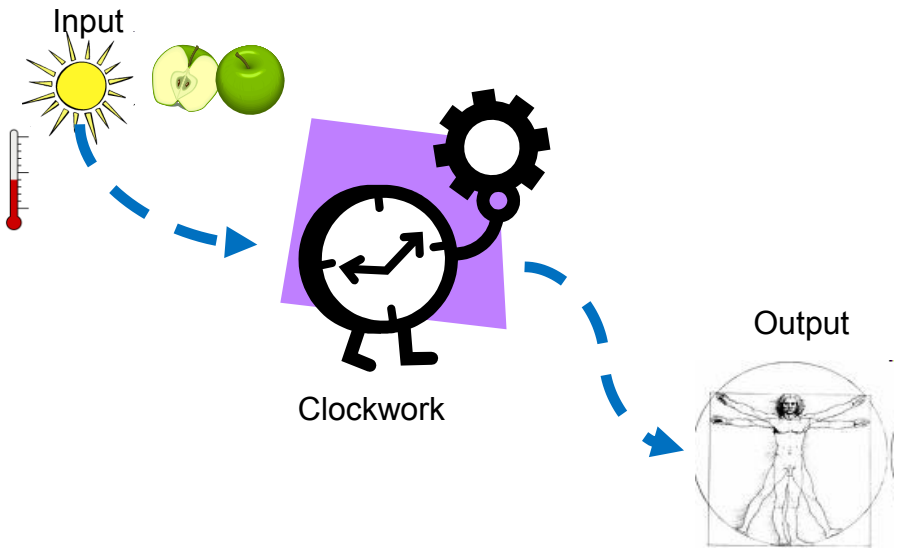

Figure 2: Circadian regulation consists of three types of regulatory networks: input networks, which convey external timing information to the clock; the clockwork—or gears of the clock—which keeps internal circadian time; and output networks through which the clock regulates physiology and behavior.

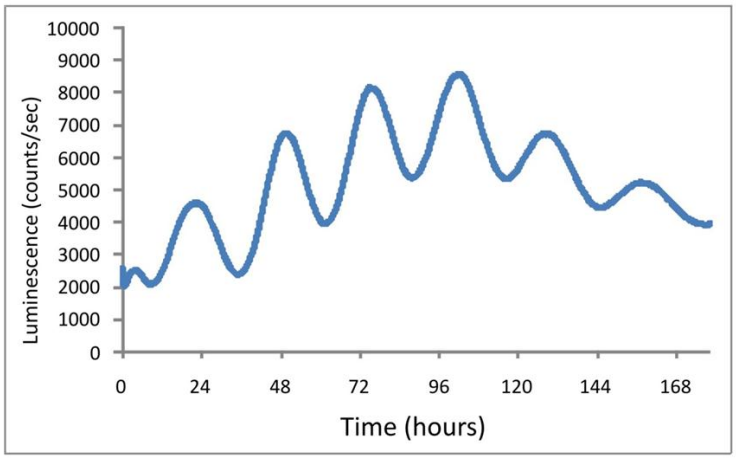

Figure 3: U2-OS contains a functional circadian clock based on rhythms of luciferase activity in Bmal1-dluc U2-OS circadian reporter cell line. Graph from Baggs et al. (31).

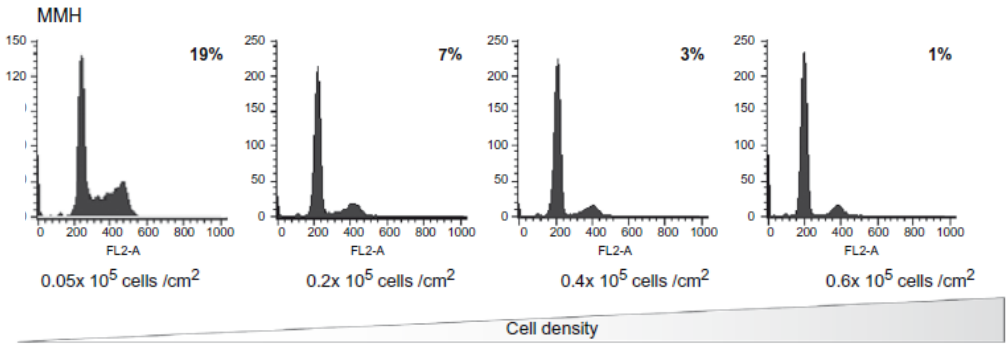

Figure 4: MMH-D3 displays contact inhibition. As cell density increases, the proportion of cell actively undergoing cell division decreases. Charts display propidium iodide stained cultures of increasing density whose DNA content was determined by flow cytometry. Charts are from Mancone et al. (40).

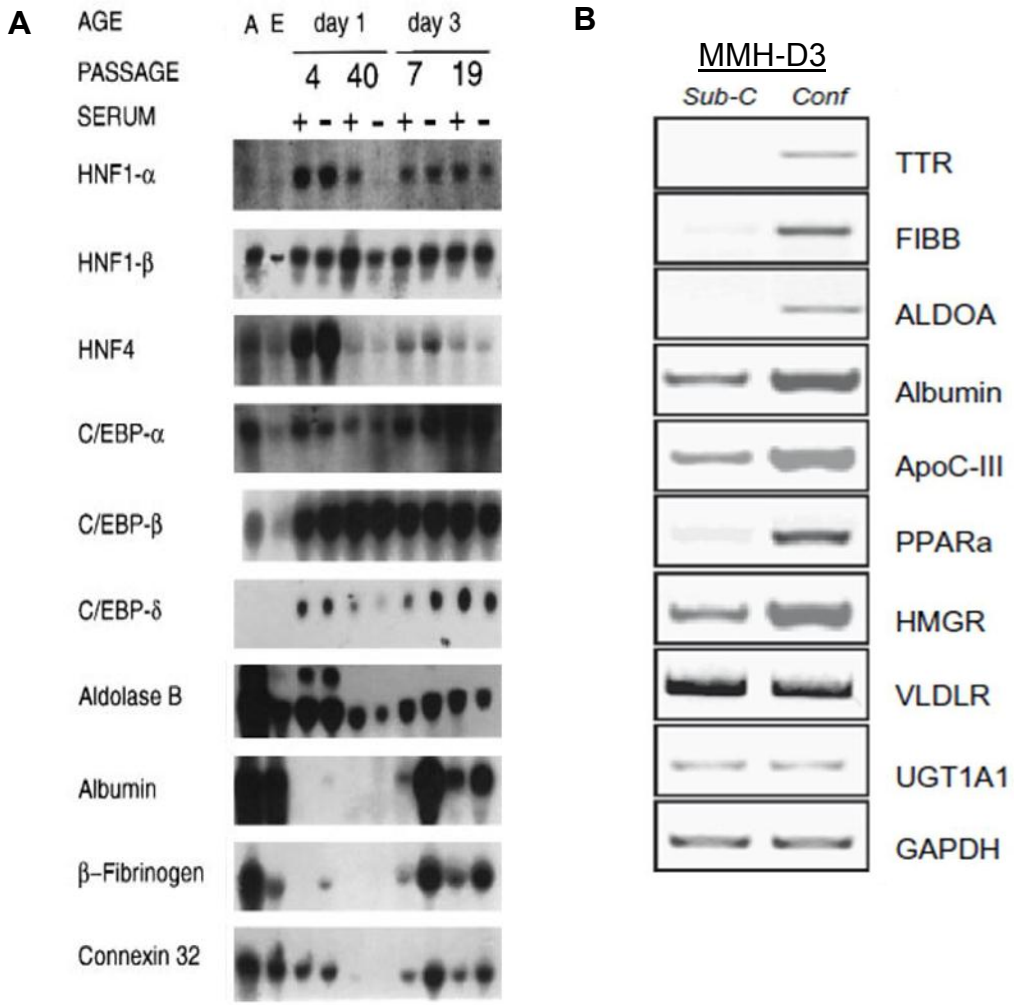

Figure 5: MMH-D3 expresses characteristic hepatocyte genes. **A:** Northern blot of mRNA expression with (+) and without (-) serum in adult liver (A), embryonic liver (E), MMH-D3 (day 3), and another MMH cell line from 1-day old mouse liver (day 1). **B:** Northern blot of MMH-D3 mRNA expression in sub-confluent (sub-C) and confluent (Conf) cultures. Northern blot in **A** is from Amicone et al. (38), and Northern blot in **B** is from Mancone et al. (40).

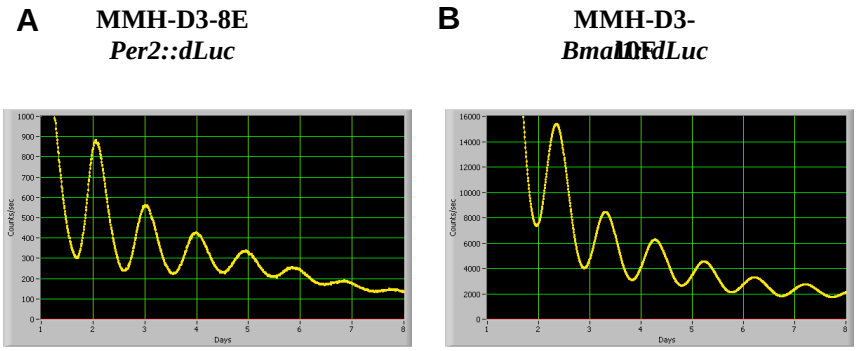

Figure 6: MMH-D3 contains a functional circadian clock. Robust circadian rhythms are observed in MMH-D3 circadian reporter lines with luciferase expression under the control of the *Per2* **(A)** and the *Bmal1* **(B)** promoters. X-axis units are days of kinetic luminescence recording. Data courtesy of Andrew C. Liu (personal communication).

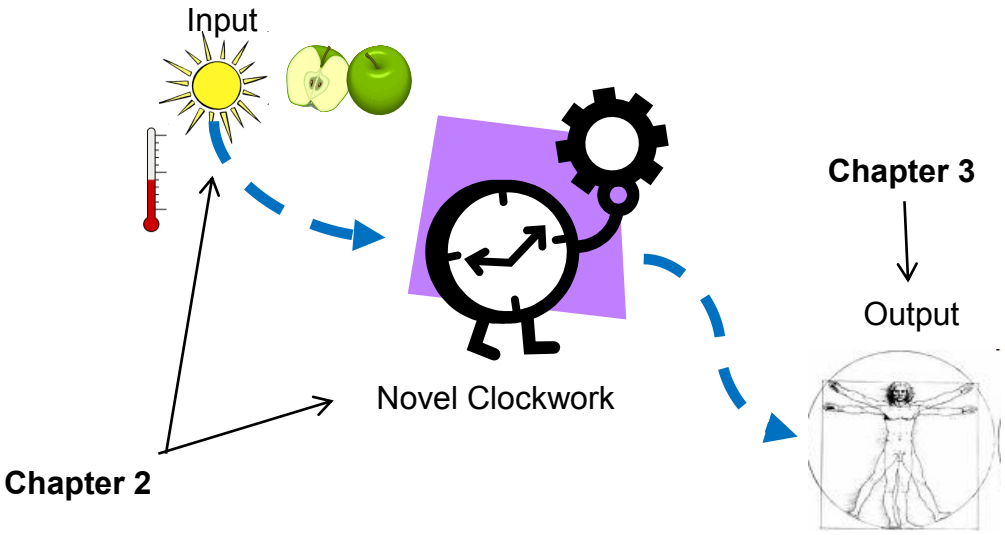

Figure 7: Summary aims for subsequent chapters. In Chapter 2, we identify clock modifier genes which may represent novel components of the clockwork and input networks. In Chapter 3, we assess the role of the cell-autonomous hepatic clock to begin characterizing hepatic circadian output networks.

Chapter 2: Genome-wide siRNA screen reveals novel clock modifying genes

Section 2.1: Introduction

Recent decades revealed many molecular components of the circadian clock, such as the core loop composed of the activators BMAL1/CLOCK and PER/CRY repressors. This negative feedback loop is required for clock function and loss of its individual components can significantly alter or abolish circadian rhythms *in vivo* (1). Two associated clock loops were then discovered: the RRE and D-box loops (1), and are thought to be involved in phase resetting, stabilizing the clock, and output regulation (2-4). Recent studies have also revealed that other mechanisms in addition to transcriptional regulation play roles in regulating clock speed and stability, such as post-translational modifications involved in protein activity and degradation and chromatin modifications. For example, ENU mutagenesis screening in mice revealed F-box and leucine rich protein 3 (FBXL3), an E3 ubiquitin ligase, mediates the degradation of CRY proteins (5). Likewise, casein kinase 1 delta (CSK1D) phosphorylation mediates PER degradation (6). In addition, clock genes can regulate transcription through sequence-specific, DNA-binding transcription factors and chromatin modification. Histone modifying enzymes, such as the histone deacetylase Sirtuin 1 (SIRT1) was revealed to associate with PER and play a role in repressing BMAL1/CLOCK mediated transcription (1, 7, 8). Similarly, REV-ERBα (NR1D1) associates with Histone Deacetylase 3 (HDAC3) to repress RRE mediated transcription (9). These new mechanisms have expanded our view of the clock and its

complexity. But, is this the whole picture of the clock? Are more clock components still to be discovered?

Evidence, including quantitative trait loci (QTL) studies, continued mutagenesis screens, and microarray studies, suggests that novel clock components as well as genes that can modify the clock remain to be uncovered. For example, inbred strains of mice exhibit distinct differences in circadian phenotype and behavior, but few QTLs have been mapped to known clock genes. Moreover, forward genetic screens have yet to reach saturation because mutagenesis screens continue to uncover new loci. Recessive mutagenesis screens promise additional loci. Furthermore, microarrays have identified thousands of transcripts with circadian expression patterns. We still do not know the how these genes are regulated or what they in turn regulate—some may be novel clock loops. Taken together, this evidence suggests that more exists than the currently known clock genes, novel clock components await discovery (10).

In addition, while the manner in which lighting information is conveyed to SCN neurons has been elucidated, other entrainment signals, such as metabolic and hormonal cues, and cell-autonomous input networks are not well understood (1, 3, 4). We can begin characterizing these networks at a cell autonomous level by defining which genes impinge upon clock function since conveying input information to the clock will require the ability to alter clock function in order to synchronize the clock to its environment. This will provide a candidate gene list with which to start characterizing the intracellular cell-autonomous input networks.

To identify novel clock and input gene candidates, a genome-wide siRNA screen was performed in a robust, cell-autonomous circadian system. HTS was employed during to enable the efficient assessment of the effects of ~90,000 siRNAs on circadian function. Hundreds of genes were found to significant alter period length or increase amplitude of circadian rhythms in a manner consistent with the knockdown (KD) of known clock components. These siRNA hits or clock modifiers not only expand our understanding of the circadian clock but also widen our perspective of what other cellular pathways may be involved in circadian regulation.

Section 2.2: Results

Section 2.2.1: U2-OS as a circadian HTS system

U2-OS has become a conventional system for studying the cell-autonomous circadian clock (11-15). This cell line, while transformed and expressing few cyclic transcripts, does exhibit robust cycles of the known clock genes (Figure 1A, Figure 2) (11, 12) and is amenable to high efficiency transfection and high expression of exogenous constructs. Our lab established stable U2-OS circadian reporter lines, where a luciferase reporter is expressed under the control of mouse core clock loop (E-box loop) gene promoters for either an activator (*Bmal1*) or repressor (*Per2*) These reporters display circadian rhythms of expression in U2-OS with high amplitude oscillations and reproducible periods (Figure 1C, Figure 2). These characteristics allow for assessment of whether a given condition—in our case, KD of a specific

gene—can affect the speed at which the clock runs (period length) or the robustness of the rhythms (amplitude).

siRNA requires high transfection efficiencies in order to produce significant KD of the target gene product. U2-OS has been successfully used for RNAi studies and can be transfected at high efficiencies. Plus, KD of clock genes *CRY1*, *CRY2*, and *BMAL1* resulted in circadian phenotypes consistent with previous knockout mouse and KD cell-based assays (Figure 1C, Figure 2) (11-13, 16). KD of *CRY1* shortens period length, while KD of *CRY2* lengthens period length. KD of either *BMAL1* or both *CRY1* and *CRY2* results in arrhythmicity. Moreover, members of the Kay lab were able to optimize the siRNA and luminescent recording procedures so that they can be scaled from 35-mm^2 cultures down to 96-well and 384-well plates. This scaling allows for siRNA assays to be performed as a HTS enabling investigation of which genes can alter clock function on a genome-wide scale, expanding the amount of information gathered beyond smaller scale screens (14).

Section 2.2.2: The siRNA screen

The siRNA screen consisted of a primary screen, data analysis to characterize the siRNAs that produced significant period length and amplitude phenotypes, two independent secondary screens of these siRNAs, and validation studies (Figure 1A).

The primary screen was performed in *Bmal1-dLuc* U2-OS since this reporter line produced more robust (higher amplitude) luminescent rhythms than *Per2-dLuc* U2-OS. These cultures were screened in 384-well format where 2 siRNAs were

pooled for each well and 2 wells were allocated per targeted gene. Each plate contained wells with *CRY2* siRNAs as a positive control. Kinetic bioluminescence recordings were made following siRNA transfection every 2 hours for 4 days, for a total of 48 time-points per assay. For the entire primary screen, over 4.3 million data points were recorded. The bioluminescence recording for each well was analyzed for period length and rhythm amplitude using the MultiCycle Analysis program (Actimetrics) Plate-to-plate variation was low (Figure 3), indicating limited variability in transfection and recording between plates and that the phenotypes for individual wells likely stem from the effects of those specific siRNAs. Hits were defined as siRNA pools that produced significant changes to period length or amplitude of the rhythm (Figure 1B).

For period length, the average of duplicate wells was divided by the mean period length for the entire screen. This value was then plotted in log2 space (Figure 1B), and a hit was defined as $\pm$0.1, which corresponds to a $\leq$ 23.55 hours (short period) or $\geq$26.85 hours (long period). Arrhythmic traces were discarded from analysis since arrhythmicity could not be distinguished from overall poor cell health. Arrhythmic traces usually returned a period value of 48-hours, and, thus, wells with 48-hour period calls were considered arrhythmic. In addition, period lengths over 38-hours (log2 value >0.4) displayed poor curve-fitting and were considered arrhythmic as well. In total, 1,028 short period hits and 4,230 long period hits were identified.

For amplitude, hits were defined as those KDs that significantly increased rhythm amplitude. Low amplitude rhythms displayed poor curve-fitting, producing

variable period length calls from one period to the next. Thus, low amplitude rhythms (representing <4.5% of all wells) were omitted from analysis. Extremely high amplitude rhythms are of interest since they may suggest mechanisms by which to stabilize or enhance circadian rhythms. To define high amplitude hits, the average was taken of amplitude for duplicate wells and then divided by the mean amplitude for the entire screen (Figure 1B). This value for a high amplitude hit was ≥2.2 (corresponding to a raw amplitude value of 7,390) (Figure 1B). 493 high amplitude hits were identified.

A further consistency filter was applied to narrow the hit list before proceeding to the secondary screen. Since siRNAs can have "off target" effects, efforts were focused on identifying those genes that produced a similar phenotype with at least 2 independent siRNAs (17). Traces for each of these period and high amplitude hits were individually plotted and visually inspected to eliminate false positives due to poor curve fitting. 254 genes were selected whose KD by independent siRNAs resulted in consistent, strong circadian phenotypes (Figure 4). An additional 89 siRNA pairs were chosen that produced strong circadian phenotypes across duplicate wells. In total, 343 genes—including known clock components—were selected as primary screen hits to be confirmed in the secondary screen.

The raw analyzed data from the primary screen was deposited in BioGPS (see Section 2.2.5), an open access online database that integrates siRNA screen data with additional bioinformatics sources of information so that the scientific community can continue to mine this data set for insights into circadian biology. .

Two independent secondary screens were performed: one in *Bmal1-dLuc* U2-OS and the other in *Per2-dLuc* U2-OS. Each was carried out in 384-well plate format as in the primary screen except each well contained an individual siRNA and at least 4 wells were assessed per gene. If the KD of a gene displayed a consistent phenotype in both reporters, then the effect on the clock is neither reporter nor response element specific, and represented a confirmed hit. The *Bmal1-dLuc* secondary screen confirmed the vast majority of hits from the primary screen. Of the 238 double hits from the primary screen, 222 were confirmed, and, of the 83 single hits, 47 were confirmed (Figure 5A, Table 1). 219 genes were independently confirmed in the *Per2-dLuc* secondary screen (Figure 4, Figure 5B). The other genes either did not have multiple siRNAs that produced a consistent phenotype or did not produce the same phenotype in *Bmal1-dLuc* and *Per2-dLuc* reporters. Yet, the secondary screens did identify hundreds of confirmed hits for genes whose KD affect clock function.

Section 2.2.3: Validation studies

To validate hits from the siRNA screen, further investigation was performed to assess the sensitivity of their impact on clock function (circadian phenotype) and clock gene expression. Based on a previous study, it was known that altering the dosage of a clock gene can result in dynamic changes in clock function and clock gene expression (12). But, can the clock modifier genes identified in our siRNA screen produce similar effects?

First, the sensitivity of impact for a handful of clock modifiers (siRNA screen hits) on clock phenotype was assessed using gene dosage analysis based on varying degree of KD of individual clock modifier genes. 17 genes that displayed severe phenotypes in the primary screen were chosen for this experiment, representing all three categories of siRNA hits. The long period genes chosen were *HCF1*, *POLR3F*, *PRPF4*, *SEC13*, *UNC119*, and *ZMAT3*. The short period genes selected were *ACSF3*, *B4GALT2*, *CEACAM21*, *TBCB*, *MPG*, and *SELO*. Lastly, the high amplitude hits examined were *COX4NB*, *FHIT*, *HIST1H1B*, and *PDE1B*. To determine whether the clock phenotypes observed in the siRNA screen display a dose-dependent relationship to the level of clock modifier gene expression, an 8-point dose-response curve was achieved by using a 2-fold dilution series of siRNA transfected into *Bmal1-dLuc* U2-OS, followed by bioluminescent recording (Figure 6A). qPCR was used to assess efficacy of target gene KD in the highest siRNA dosage (Figure 6B). 16 of the 17 genes tested (all but *SELO*) displayed a dose-dependent effect on clock function, such that, with increasing levels of siRNA administered, increasingly severe clock phenotypes were observed (Figure 6). This result not only confirms the results of the screen (that KD of these genes affect clock function to an equivalent or greater extent than the KD of known clock components) but also indicates that the impact these genes can have on clock phenotype can be dependent on dosage of clock modifier expression similar to known clock genes.

To address the clock modifier KD effects on clock gene expression, additional validation studies were performed. Due to the complexity of interactions within the

clock, KD or dosage manipulation of one component can produce dynamic changes in many other clock gene components resulting from interactions within the network (known as "network effects") (12). Therefore, it was asked, "Can clock modifiers change the gene expression of clock gene in a similar manner?"

Dose-dependent effects on clock gene expression were assessed for 6 of the clock modifier gene found to have dose-dependent effects on clock phenotype. These genes were in three categories: long period (*POLR3F*, *PRPF4*, and *SEC13*), short period (*ACSF3* and *MPG*), and high amplitude (*COX4NB*) genes. Several clock genes (*BMAL1*, *CLOCK*, *PER1*, *PER2*, *CRY1*, *CRY2*, *DBP*, *FBXL3*, and *NR1D1*—also known as *REV-ERBα*) were also included as controls based on known their known effects on the clock network (12). KD of *CRY2* or *FBXL3* produces a long period phenotype, while, KD of *CRY1* produces a short period phenotype. Lastly, *BMAL1* and *NR1D1* (*REV-ERBα*) are involved in amplitude modulation. An 8-point dosage response was determined using a 2-fold dilution series of siRNA KD of individual clock modifiers in *Bmal1-dLuc* U2-OS. Bioluminescent rhythms (Figure 7A) were recorded as well as qPCR performed to determine the efficacy of KD (Figure 7B) and clock gene levels (Figure 7C). The effects on clock gene expression are summarized in (Figure 7D). The phenotypes and effects on clock gene expression resulting from KD of known clock components (*BMAL1*, *CLOCK*, *PER1*, *PER2*, *CRY1*, *CRY2*, *DBP*, *FBXL3*, and *NR1D1*) were consistent with previously published work (12). Many of the clock modifiers tested also produced potent effects on not only circadian phenotype but clock gene expression. KD of most clock modifiers resulted in a dose-

dependent reduction of *NR1D1* and *DBP* transcript levels. Both of these transcripts are E-box regulated. E-box regulation not only contributes to the expression pattern of many clock genes (including the *PER*s, the *CRY*s, *DBP, NR1D1, NR1D2*—also known as *REV-ERBβ*—and *RORc*) but has also been suggested to play a significant role in output regulation (18, 19) and liver circadian regulation when a cell-autonomous liver clock is present (20). The down-regulation of E-box driven genes *NR1D1* and *DBP* in a dose dependent manner in this assay supports the idea that regulation of E-box mediated transcription is a vulnerability of the mammalian clock. *NR1D1* is thought to impact clock gene expression through network effects, KD of *SEC13*, similarly, produced an increase in *BMAL1* transcript, suggesting that *SEC13* may also impact the clock through network effects. *POLR3F* and *ACSF3* produced few or no effect on clock gene expression, but their KD does result in dose-dependent circadian phenotypes. They may function similarly to *CRY2*—whose KD produces a significant clock phenotype without effecting clock gene expression. These genes may impact other clock components not at the transcriptional level but through post-translational modifications, regulation of protein stability, function, or localization.

In sum, not only can many of the siRNA hits tested produce potent circadian phenotypes on par with or more severe than those observed with the KD of clock genes, but, for many of the genes tested, these phenotypes are dose-dependent, similar to the effects observed with the KD of known clock genes (Figure 6) (12). Moreover, KD of some of these clock modifiers can result in dose-dependent effects on expression of clock genes (Figure 7). KD of many of these clock modifiers resulted in

down-regulation of *NR1D1* and *DBP*—two E-box regulated clock genes, implying that E-box regulation should be investigated further in terms of input regulation and an access point by which to modulate clock function.

Section 2.2.4: Expansion of the clock network

Having validated that that siRNA hits can modify clock function and gene expression in a manner consistent with those induced by the KD of known clock components, the following questions remained, "How do these siRNA hits relate to the known circadian clock components? How do they function in the cell?" Bioinformatic analyses can suggest answers to these questions by identifying protein-protein interactions (PPIs) to reveal possible network connections between siRNA hits and known clock components as well as examining the siRNA hit list for enriched functional pathways to suggest cellular processes involved in the regulation of circadian function.

To determine if the siRNA hits interact with known clock components either directly or indirectly, the Entrez Gene and Prolexys PPI databases were utilized to identify a comprehensive list of interactions with the siRNA hits and the known clock components (Table 2). These were used to construct a gene interaction network (Figure 8). Most of the siRNA hits were in a cluster centered on the core clock components: BMAL1, CLOCK, the PERs (PER1, PER2, PER3), and the CRYs (CRY1, CRY2). Some siRNA hits (ZMAT3, BLNK, RRP12) connect directly to known clock components, but most connect indirectly through a common interactor—

or bridging molecule. Many of these bridging molecules produced circadian phenotypes in the siRNA screen—although not to the extent to meet all the criteria to be a named a hit—suggesting that they may be involved in the siRNA hits' effects on circadian function. This interaction network expands the view of the circadian clock and taken with the dose-dependent phenotype and clock gene expression results emphasizes that the circadian clock represents a genetic network including not only the handful of known clock components but many other genes as well.

Thus, we progressed to the question of function. What roles do these siRNA hit genes play in cellular pathways? Specifically, are any pathways over-represented in the siRNA hit list? Enrichment in a particular pathway would provide evidence that this pathway impinges on the clock and, therefore, may be involved in input regulation or maintenance of the circadian clock. NIH DAVID functional analysis (21) identified a number of cellular pathways enriched in the siRNA list, including folate metabolism ($P<0.014$), hedgehog signaling ($P<0.0088$), cell cycle ($P<0.054$), and insulin signaling ($P<0.013$) (Figure 9, Figure 10A). Hedgehog signaling, cell cycle, and insulin signaling contain mostly long period siRNA hits, while folate metabolism components include long period, short period, and high amplitude hits. In addition to clock modifiers, these pathways contain multiple components identified as circadian regulated at the transcriptional level (transcripts cycle) or implicated in the clock (11, 22) (Figure 9, Figure 10), which indicates that these cellular processes and the circadian clock are functionally intertwined.

As an example, we looked more closely at interconnections between insulin signaling and the clock. Insulin signaling is enriched for clock modifiers identified by the siRNA screen. KD of multiple individual genes in this pathway results in alteration of clock function. KD of genes for JNK (*MAPK8*), IKK (*IKBKB*), PI3K (*PIK3R5*), MTOR (*FRAP1*), APKC (*PRKCI*), or PYK (*PKLR*) lengthens the period of the clock, while, KD of PFK (*PFKP*) shortens its period (Figure 10B). Plus, 19 components of this cellular pathway are under transcriptional regulation by the circadian clock (i.e. transcripts cycle) (Figure 10A). Moreover, application of chemical inhibitors or activators against specific components of the insulin signaling pathway results in alteration of clock period or phase (Figure 10C). Application of JNK inhibitor (SP600125) or PKC inhibitor (Dequalinium analog C14 linker) lengthens its period; whereas, PKC activator (PMA) shortens period. PI3K inhibitor (wortmannin or LY294002) produces a phase delay. These alterations of clock function are consistent with the siRNA phenotypes observed and provide independent validation that the insulin signaling pathway and the clock are functionally interconnected.

Section 2.2.5: Distribution of siRNA screen data through BioGPS

To facilitate the use of the siRNA primary screen data, we have created an online database, BioGPS (http://biogps.gnf.org). BioGPS is an open access database that aggregates many online annotation sources as plug-ins for convenient use and visualization. A custom circadian layout has been created within BioGPS (Figure 11), which for a queried gene (*PER2* in this example) displays the siRNA screen data as

well as high resolution microarray results for liver and pituitary (from the CIRCA database, http://bioinf.itmat.upenn.edu/circa) (11), the UCSC Genome Browser (http://genome.ucsc.edu/), reference gene expression data for multiple tissues and cell lines (23, 24), and the gene's Wikipedia article. Thus, researchers can search their own genes of interest in a single location to visualize annotation information regarding both its circadian and general features, as opposed to individually searching multiple scattered databases across the web for this information. Moreover, BioGPS provides a flexible platform in which you can customize your own layouts from the over 100 additional datasets and resources in the plug-in library, including plug-ins for KEGG, Pubmed, MGI, and reagent retailers. Due to its flexibility and breadth of information sources, BioGPS provides a portal for circadian and all biologists to access our screen data and place it in context with many other annotation sources in order to design new experiments and ultimately uncover the regulatory relationships of the mammalian circadian system.

Section 2.3: Discussion

To identify novel genes that can modify clock function, a genome-wide siRNA screen was performed in a robust cell-autonomous circadian system: the U2-OS cell line. Hundreds of genes were identified that can alter the running of the clock either by shortening its period, lengthening its period, or increasing the amplitude of its rhythms. These siRNA screen hits therefore represent clock modifier genes. The circadian phenotypes resulting from clock modifier KD are, in many cases, dose-

dependent, consistent with the effects of knocking down known clock components (12). A handful of clock modifiers were selected to assess the sensitivity of their effects on known clock gene expression. Nearly all the clock modifiers tested displayed dose-dependent transcriptional effects of the expression of at least some of the clock genes, suggesting that many clock modifiers impinge upon clock function through transcriptional regulation. Transcriptional regulation of clock genes implies that these clock modifiers may represent novel clock genes to be added to the circadian clockwork, especially if they display rhythms of gene expression, as well. Comparison of the siRNA hit list with circadian microarray studies will determine which clock modifiers are under circadian transcriptional regulation and tissue-specificity, thus, focusing the novel clock gene candidate list. Additional experiments will characterize which clock modifiers represent novel clock components and the regulatory mechanisms by which these genes affect the clock. In particular, chromatin immune-precipitation (ChIP) information must be assessed for the clock modifiers to determine if direct transcriptional regulation exists.

PPIs for the clock modifiers and clock genes were used to construct an expanded gene interaction network that displays a high degree of connectivity between the clock modifiers and the clock. Some clock modifiers physically interact with clock genes, while most interact with a bridging molecule that directly interacts with clock genes. Pathway analysis revealed an over-representation of siRNA hits in many functional pathways, including folate metabolism, hedgehog signaling, cell cycle, and insulin signaling. Components of these pathways have previously been found to be

under circadian transcriptional regulation, suggesting that these pathways are interconnected with the clock and possibly involved in feedback circadian networks.

Both the expanded clock gene interaction network and the enrichment in functional pathways emphasize the interconnectedness between the circadian clock and what had been considered other areas of biological study. Perturbation of one area can lead to effects throughout the network. Movement forward needs to cross these traditional field boundaries so that we can avoid the adverse effects and unintended consequences based ignorance that two pathways affect one another. Likewise, we can leverage the knowledge and existing tools from both fields for future studies. For example, specific inhibitors exist for the above pathways that may prove useful for dissecting circadian phenotypes. This awareness not only expands our view of the clock and its relationship with other areas of biology but emphasizes the necessity of resources that aggregate knowledge across many fields, like BioGPS.

Section 2.4: Methods

Methods used are as stated in Zhang et al. (25).

Section 2.5: Contributions

Coauthors from the Kay lab and GNF performed the siRNA screen and validation experiments described above. John Hogenesch constructed the PPI network. Andrew Su's group at GNF created BioGPS. My role in this study pertained to data manipulation, annotation, and compilation of raw data and screen measurements

within and between primary and secondary screens. This included automating the compilation and cross-referencing of raw data in primary and secondary screens for individual and replicate wells. Due to the volume of data amassed in the screen (>4.3 million data-points for the primary screen), the ability to automate the compilation and indexing of the data was non-trivial. Automation of these processes using Visual Basic scripts and formulae increased both the efficiency and systematic accuracy of this analysis. Annotation and compilation of screen data analysis measurements required both automation and generation of a searchable key to map siRNA identification numbers to plate and well identifiers within the secondary screens. Screen measurements were catalogued and then mapped to corresponding annotations, including gene symbol, gene description, and GenBank ID. These roles were significant for maintaining the integrity of data analysis and reporting.

This paper made significant contributions to circadian biology. It identified hundreds of novel clock modifying genes that can modify clock function and, thus, may represent either novel clock genes themselves or genes involved in transmitting input to the clock. Thus, we have increased our understanding of the composition of circadian networks as well as expanded the significance of the clock to broader biology. A high level of interconnectedness was revealed between the novel clock modifier genes, genes known to be under circadian regulation, and important cellular pathways, such as insulin signaling, cell cycle, folate metabolism, and hedgehog signaling. Interconnectedness between these pathways and the clock reveals that the circadian clock is intertwined with many cellular functions, and characterizing these

connections is essential to understanding both the cellular pathways and circadian biology. Lastly, BioGPS was created to present the siRNA screen data for continued use as well as to compile many scattered annotation sources into one visualization platform. This makes BioGPS an important resource not only for circadian biologists, but also for those in a diverse array of fields. Through the impact of this paper, my contribution to its progress and publication can contribute to both the circadian field and general biology.

Section 2.6: Acknowledgements

The study presented in Chapter 2 and the presented figures were published in *Cell* in the research article:

Zhang EE, Liu AC, Hirota T, Miraglia LJ, Welch G, Pongsawakul PY, Liu X, Atwood A, Huss, Jon W., III, Janes J, Su AI, Hogenesch JB & Kay SA (2009) A genome-wide RNAi screen for modifiers of the circadian clock in human cells. *Cell* 139: 199-210.

The dissertation author was an author on this paper.

Section 2.7: Chapter 2 references

1. Zhang EE & Kay SA (2010) Clocks not winding down: Unravelling circadian networks. *Nat Rev Mol Cell Biol* 11: 764-776.

2. Staels B (2006) When the clock stops ticking, metabolic syndrome explodes. *Nat Med* 12: 54-55.

3. Hastings MH, Reddy AB & Maywood ES (2003) A clockwork web: Circadian timing in brain and periphery, in health and disease. *Nature Reviews Neuroscience* 4: 649-661.

4. Hastings M, O'Neill JS & Maywood ES (2007) Circadian clocks: Regulators of endocrine and metabolic rhythms. *J Endocrinol* 195: 187-198.

5. Siepka SM, Yoo S, Park J, Song W, Kumar V, Hu Y, Lee C & Takahashi JS (2007) Circadian mutant overtime reveals F-box protein FBXL3 regulation of cryptochrome and period gene expression. *Cell* 129: 1011-1023.

6. Zhang EE, Liu Y, Dentin R, Pongsawakul PY, Liu AC, Hirota T, Nusinow DA, Sun X, Landais S, Kodama Y, Brenner DA, Montminy M & Kay SA (2010) Cryptochrome mediates circadian regulation of cAMP signaling and hepatic gluconeogenesis. *Nat Med* 16: 1152-U133.

7. Asher G, Gatfield D, Stratmann M, Reinke H, Dibner C, Kreppel F, Mostoslavsky R, Alt FW & Schibler U (2008) SIRT1 regulates circadian clock gene expression through PER2 deacetylation. *Cell* 134: 317-328.

8. Nakahata Y, Kaluzova M, Grimaldi B, Sahar S, Hirayama J, Chen D, Guarente LP & Sassone-Corsi P (2008) The NAD(+)-dependent deacetylase SIRT1 modulates CLOCK-mediated chromatin remodeling and circadian control. *Cell* 134: 329-340.

9. Feng D, Liu T, Sun Z, Bugge A, Mullican SE, Alenghat T, Liu XS & Lazar MA (2011) A circadian rhythm orchestrated by histone deacetylase 3 controls hepatic lipid metabolism. *Science* 331: 1315-1319.

10. Takahashi JS (2004) Finding new clock components: Past and future. *J Biol Rhythms* 19: 339-347.

11. Hughes ME, DiTacchio L, Hayes KR, Vollmers C, Pulivarthy S, Baggs JE, Panda S & Hogenesch JB (2009) Harmonics of circadian gene transcription in mammals. *PLoS Genet* 5: e1000442.

12. Baggs JE, Price TS, DiTacchio L, Panda S, FitzGerald GA & Hogenesch JB (2009) Network features of the mammalian circadian clock. *Plos Biology* 7: 563-575.

13. Liu AC, Tran HG, Zhang EE, Priest AA, Welsh DK & Kay SA (2008) Redundant function of REV-ERB alpha and beta and non-essential role for BMAL1 cycling in transcriptional regulation of intracellular circadian rhythms. *Plos Genetics* 4: e1000023.

14. Maier B, Wendt S, Vanselow JT, Wallach T, Reischl S, Oehmke S, Schlosser A & Kramer A (2009) A large-scale functional RNAi screen reveals a role for CK2 in the mammalian circadian clock. *Genes Dev* 23: 708-718.

15. Hirota T, Lewis WG, Liu AC, Lee JW, Schultz PG & Kay SA (2008) A chemical biology approach reveals period shortening of the mammalian circadian clock by specific inhibition of GSK-3 beta. *Proc Natl Acad Sci U S A* 105: 20746-20751.

16. Liu AC, Welsh DK, Ko CH, Tran HG, Zhang EE, Priest AA, Buhr ED, Singer O, Meeker K, Verma IM, Doyle,Francis J.,,III, Takahashi JS & Kay SA (2007) Intercellular coupling confers robustness against mutations in the SCN circadian clock network. *Cell* 129: 605-616.

17. Echeverri CJ, Beachy PA, Baum B, Boutros M, Buchholz F, Chanda SK, Downward J, Ellenberg J, Fraser AG, Hacohen N, Hahn WC, Jackson AL, Kiger A, Linsley PS, Lum L, Ma Y, Mathey-Prevot B, Root DE, Sabatini DM, Taipale J, Perrimon N & Bernards R (2006) Minimizing the risk of reporting false positives in large-scale RNAi screens. *Nature Methods* 3: 777-779.

18. Green CB, Takahashi JS & Bass J (2008) The meter of metabolism. *Cell* 134: 728-742.

19. Ueda HR, Hayashi S, Chen WB, Sano M, Machida M, Shigeyoshi Y, Iino M & Hashimoto S (2005) System-level identification of transcriptional circuits underlying mammalian circadian clocks. *Nat Genet* 37: 187-192.

20. Bozek K, Rosahl AL, Gaub S, Lorenzen S & Herzel H (2010) Circadian transcription in liver. *BioSystems* 102: 61-69.

21. Huang DW, Sherman BT & Lempicki RA (2009) Systematic and integrative analysis of large gene lists using DAVID bioinformatics resources. *Nat Protoc* 4: 44-57.

22. Panda S, Antoch MP, Miller BH, Su AI, Schook AB, Straume M, Schultz PG, Kay SA, Takahashi JS & Hogenesch JB (2002) Coordinated transcription of key pathways in the mouse by the circadian clock. *Cell* 109: 307-320.

23. Su AI, Cooke MP, Ching KA, Hakak Y, Walker JR, Wiltshire T, Orth AP, Vega RG, Sapinoso LM, Moqrich A, Patapoutian A, Hampton GM, Schultz PG & Hogenesch JB (2002) Large-scale analysis of the human and mouse transcriptomes. *Proc Natl Acad Sci U S A* 99: 4465-4470.

24. Su AI, Wiltshire T, Batalov S, Lapp H, Ching KA, Block D, Zhang J, Soden R, Hayakawa M, Kreiman G, Cooke MP, Walker JR & Hogenesch JB (2004) A gene

atlas of the mouse and human protein-encoding transcriptomes. *Proc Natl Acad Sci U S A* 101: 6062-6067.

25. Zhang EE, Liu AC, Hirota T, Miraglia LJ, Welch G, Pongsawakul PY, Liu X, Atwood A, Huss,Jon W.,,III, Janes J, Su AI, Hogenesch JB & Kay SA (2009) A genome-wide RNAi screen for modifiers of the circadian clock in human cells. *Cell* 139: 199-210.

Section 2.8: Chapter 2 figures and tables

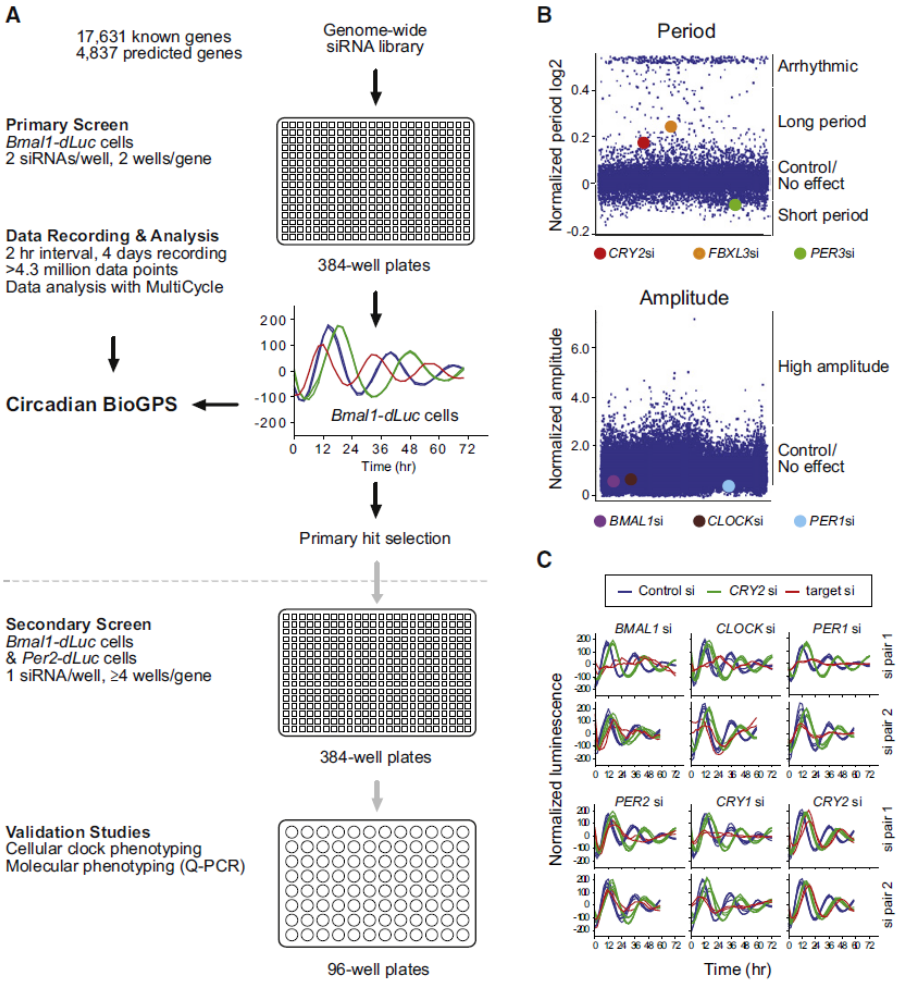

Figure 1: The siRNA screen. **A:** Overview of the genome-wide siRNA screen, including the primary screen, data mining, hit selection, secondary screen, validation studies, and deposit of primary screen data in online database: BioGPS. B: Distribution of primary screen data. The dots represent normalized period lengths (upper) and amplitude (lower). To obtain normalized period length, the average of duplicate wells is divided by the mean period length of the entire screen and then shown in log2 space. The cutoff for period length hits are ±0.1, corresponding to periods <23.55 hours or >26.85 hours). Arrhythmic traces generally returned a period length value of 48-hours; therefore, period lengths of 48-hours were considered arrhythmic and excluded from further analysis. Likewise, Log2 values >0.4 displayed poor curve fitting and were also considered arrhythmic. Amplitude measurements were normalized by averaging duplicate wells and then dividing by the mean amplitude of the entire screen. The high amplitude hit cutoff was 2.20 (raw data value of 7,390). Measurements for KD of known clock genes are shown in these plots by colored dots. C: Bioluminescent profiles for KD of the known clock genes *BMAL1*, *CLOCK*, *PER1*, *PER2*, *CRY1*, and *CRY2* are shown for 2 independent pairs of siRNA for each gene in the primary screen in *Bmal1-dLuc* U2-OS. Bioluminescence spikes in the initial 10-hours of recording result from media change and were removed from plot for analysis.

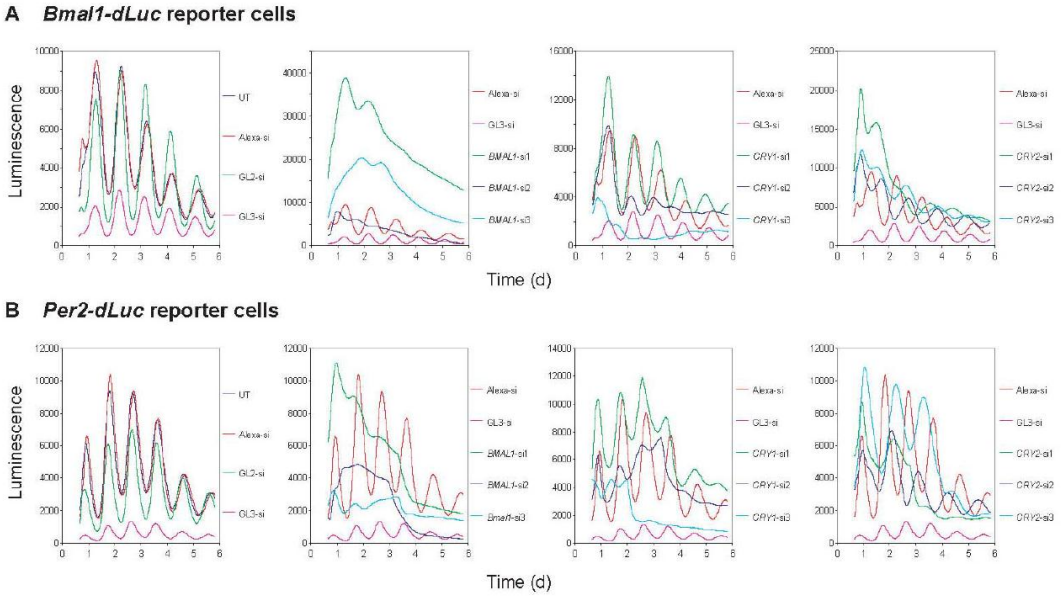

Figure 2: Two clonal U2-OS circadian reporter lines were used: *Bmal1-dLuc* **(A)** and *Per2-dLuc* **(B)**. These lines display robust bioluminescence rhythms for multiple days and have nearly anti-phasic oscillations. Transfection with siRNAs to KD the known clock genes *BMAL1*, *CRY1*, *CRY2*, or both *CRY1* and *CRY2* produced circadian phenotypes consistent with previous studies. Results from 35mm^2 dishes, but the methods have been adapted to 96-well and 384-well plate format for HTS. UT: samples untreated with siRNA. Alexa fluo labeled siRNAs were used as a control and to assess transfection efficiency. GL2 and GL3 siRNAs represent negative and positive controls, respectively, targeting the firefly luciferase in the pGL3 vector series used to generate these reporter cell lines.

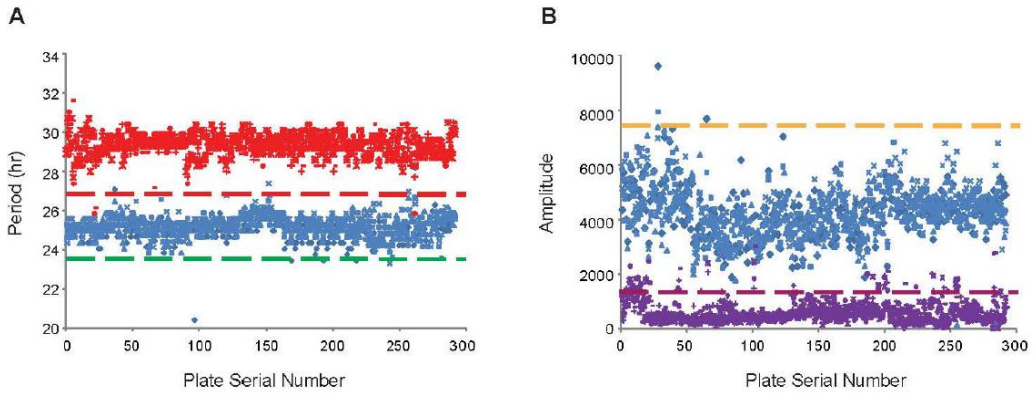

Figure 3: Low plate-to-plate variation was observed period length **(A)** and amplitude **(B)** for control siRNAs in the entire primary screen (4 wells/each control per 384-well plate and a total of 292 plates). **A:** The cutoffs for short and long period hits were determined based on the positive and negative controls: *CRY2* and GL2 siRNAs, respectively. Negative control wells (GL2, blue) display a period of 25.20 hours $\pm$ 0.55 (n=1176) while the positive control (*CRY2* siRNA, red) has a period length of 29.43 hours $\pm$ 0.65 (n=1176). The red and green dashed lines denoted upper and lower period limits and represent 3 SD from control. **B:** Negative control wells (blue) displayed a mean amplitude of 4380 $\pm$ 1010 while *BMAL1* siRNA (positive control, purple) have an amplitude of 692 $\pm$ 626 (n=1176). The high amplitude cutoff was set at the upper limit of 3 SDs from the control population (yellow dashed line). The purple dashed line is 1 SD from the *BMAL1 s*iRNA control population and serves as the cutoff for arrhythmic wells.

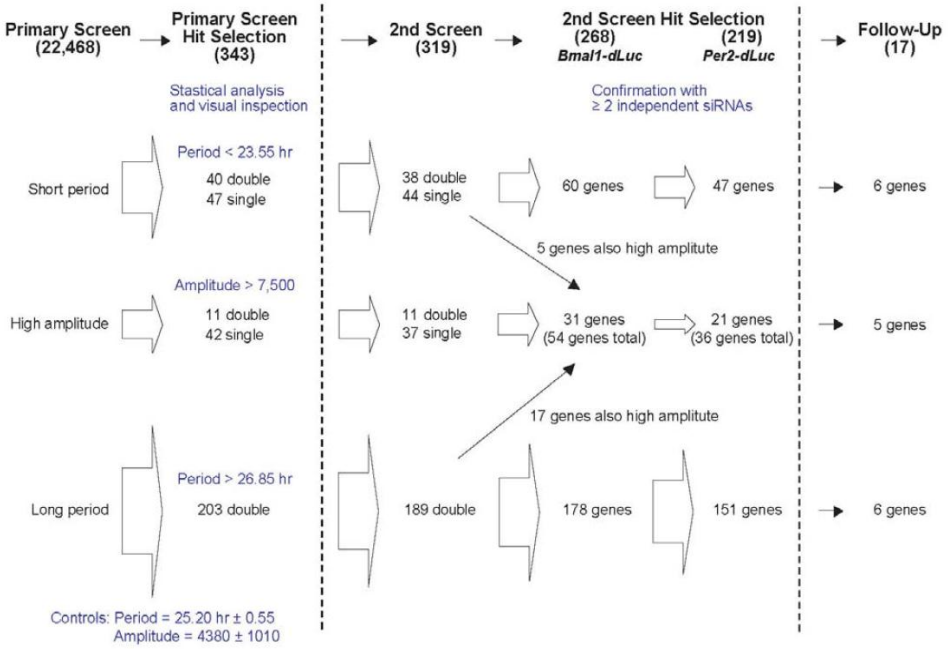

Figure 4: Summary of genome-wide siRNA screen results. The primary screen in *Bmal1-dLuc* U2-OS identified 343 hits, including 319 primary screen hits which proceeded to the secondary screen and 24 hits which were not further tested for technical issues. In the secondary screen, 222 of 238 double hits and 47 of 83 single hits were reconfirmed in *Bmal1-dLuc* U2-OS. 17 genes representing the 3 circadian phenotypes (short period, long period, and high amplitude) were chosen for use in validations studies.

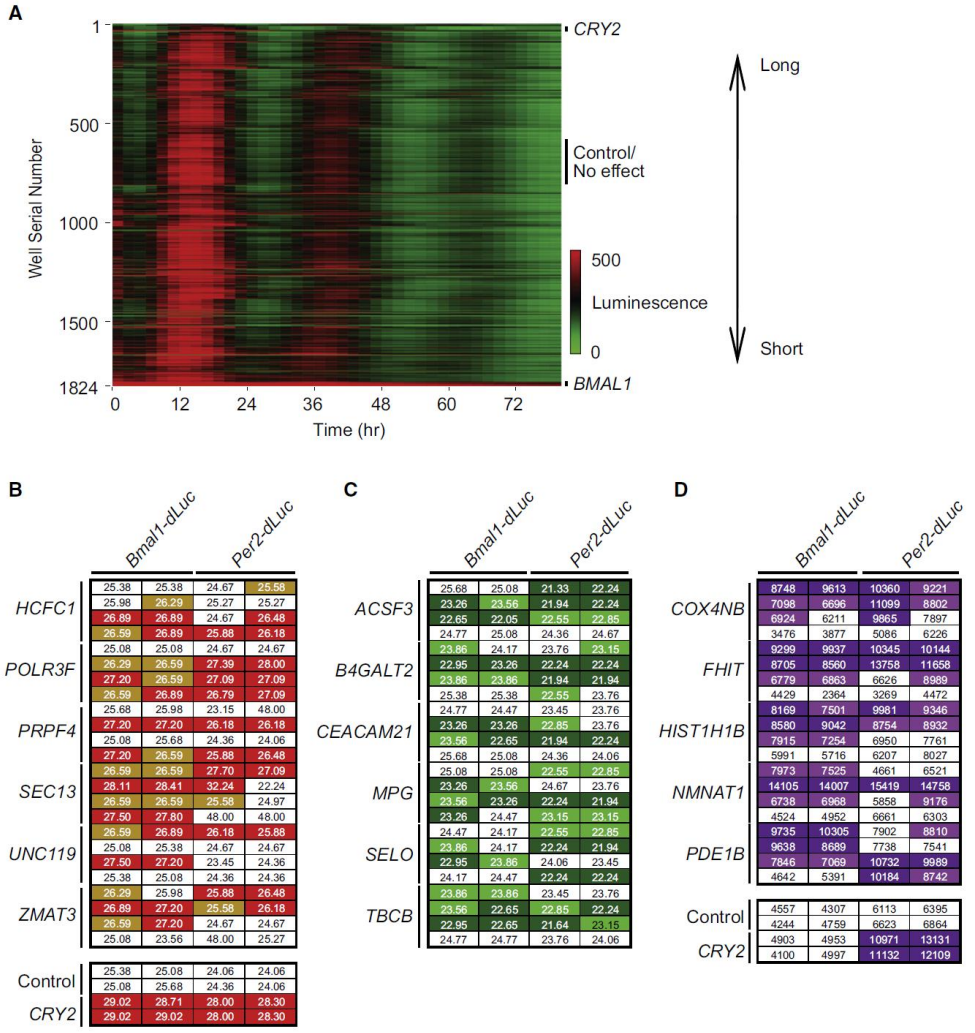

Figure 5: Secondary siRNA screen results. **A:** Heat map of secondary screen results in *Bmal1-dLuc* U2-OS. 872 independent pairs of siRNA against 154 genes in duplicate along with 20 wells for each of the controls (GL2, *CRY2*, *BMAL1*, and GL3 siRNAs) for a total of 1824 wells. Each horizontal line represents the bioluminescence profile for a single well plotted versus time (hours). Circadian profiles from each well were classified by hierarchical clustering (clustering method: maximum complete linkage; similarity measure: correlation; ordering function: average value). **B-D:** Circadian parameters in both *Bmal1-dLuc* and *Per2-dLuc* U2-OS for the KD of 17 genes, representing each of the three classes of hits: long period **(B)**, short period **(C)**, and high amplitude **(D)**. Circadian phenotypes are shaded based on the strength of parameter alteration. Darker colors correspond to stronger alteration of parameters (mean $\pm$ 3 x SD) than lighter colors (mean $\pm$ 2 x SD). 4 different siRNAs (y-axis) were tested for each gene, and assay was performed in duplicates (x-axis) in each reporter line (*Bmal1-dLuc* and *Per2-dLuc*). *CRY2* siRNA was used as a positive control. In *Bmal1-dLuc* cells, control wells displayed a period of 25.07 hours $\pm$ 0.59 with an amplitude of 4120 $\pm$ 1285 (mean $\pm$ SD, n=768). In *Per2-dLuc* cells, control wells displayed a period of 24.18 hours $\pm$ 0.55 with an amplitude of 6,438 $\pm$ 1,140 (n=768).

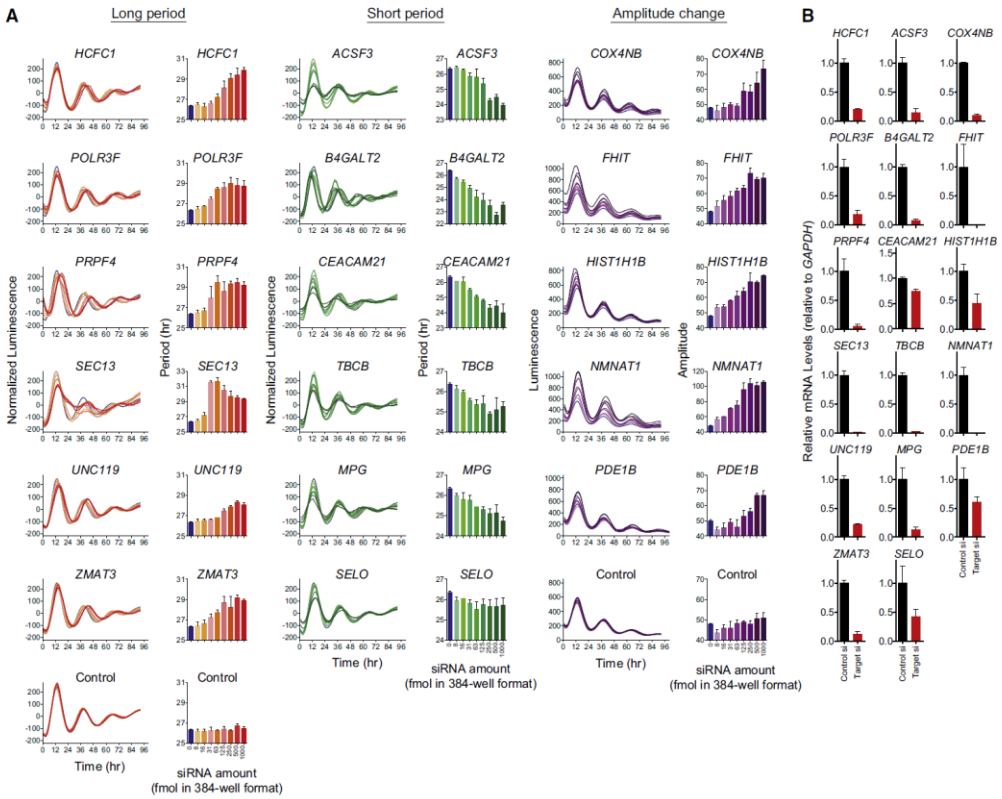

Figure 6: Clock modifiers display dose-dependent effect on circadian phenotype. **A:** Dose dependent effects on circadian phenotype. *Bmal1-dLuc* U2-OS cells were transfected with the indicated amounts of siRNA in 384-well format (an 8-point, 2 fold dilution series with final concentrations 8-1,000 fmol/well) for 17 genes. Bioluminescence profiles (left) were recorded and analyzed for circadian parameters (right), revealing dose dependent effects of many of the genes tested on circadian phenotype. **B:** Extent of KD assessed by qPCR analysis of *Bmal1-dLuc* U2-OS transfected with 3,000 fmol/well siRNA in 96-well format (corresponds to 1,000 fmol/well in 384-well format) under unsynchronized conditions. mRNA levels are relative to GAPDH and represent mean $\pm$ SD (n=2). Parallel experiments recorded bioluminescence profiles and confirmed circadian phenotype.

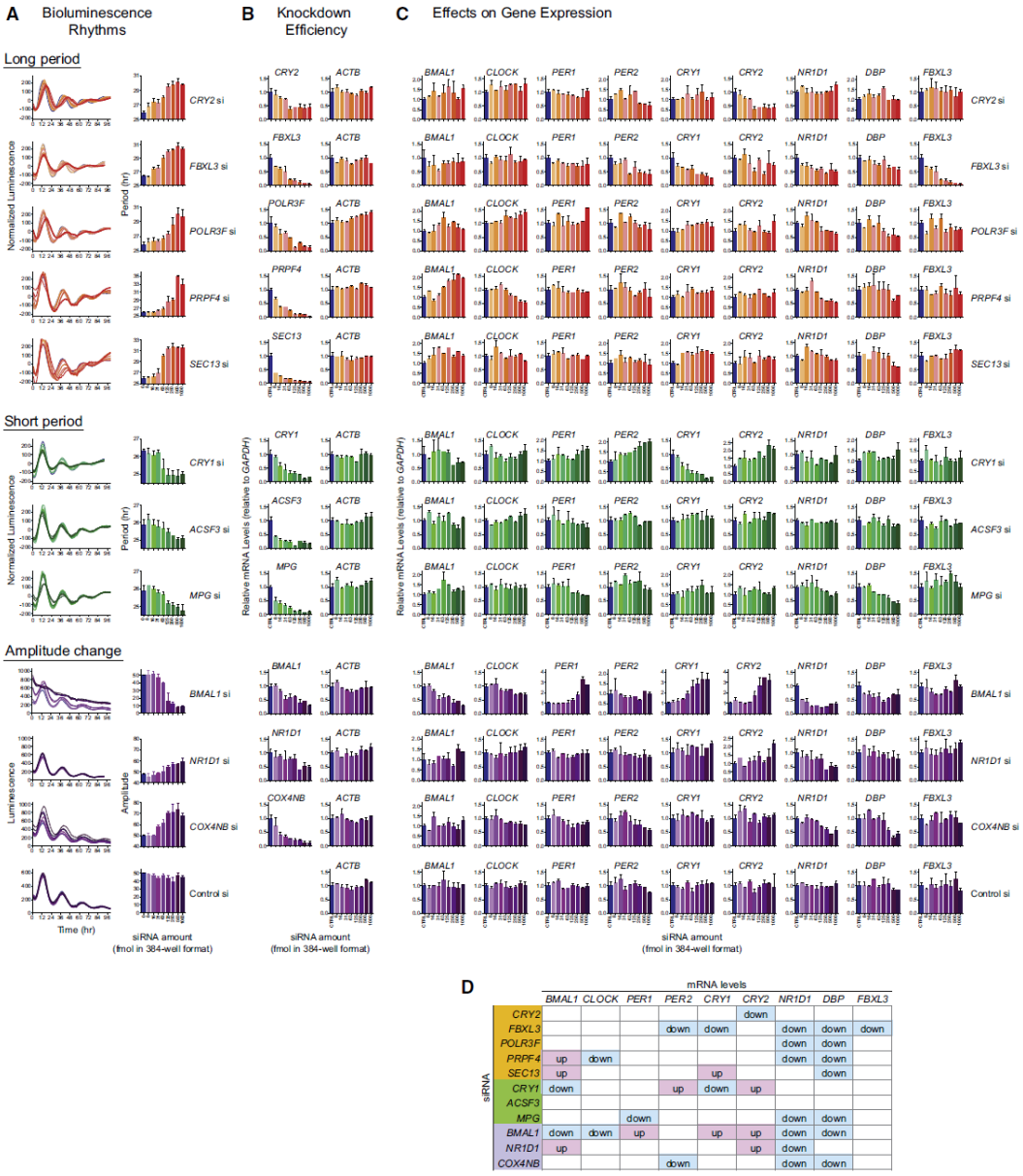

siRNA	BMAL1	CLOCK	PER1	PER2	CRY1	CRY2	NR1D1	DBP	FBXL3
CRY2						down			
FBXL3				down	down		down	down	down
POLR3F							down	down	
PRPF4	up	down					down	down	
SEC13	up				up			down	
CRY1	down			up	down	up			
ACSF3									
MPG			down				down	down	
BMAL1	down	down	up		up	up	down	down	
NR1D1	up					up	down		
COX4NB				down			down	down	

Figure 7: Clock modifiers display dose-dependent effects on clock gene expression. **A:** The circadian phenotype in *Bmal1-dLuc* U2-OS transfected with indicated amount of siRNA (an 8-point, 2-fold dilution series of 8-1,000 fmol/well) against 11 genes, including clock gene controls. Representative bioluminescence profiles displayed at left and circadian parameters to right. Data represents ± SD (n=3). **B-C:** Dose dependent effects of KD on siRNA target gene **(B)** and known clock gene expression **(C)**. *Bmal1-dLuc* U2-OS were transfected with the indicated amount of siRNA (8-point, 2-fold dilution series of 24-3,000 fmol/well) and qPCR performed under unsynchronized conditions. mRNA of target gene (left) and ACTB (right) are relative to GAPDH. Data represents the mean ± SD (n=2). Parallel experiments confirmed bioluminescence phenotypes. **D:** Summary of dose-dependent effects of clock modifier KD on the expression of known clock genes.

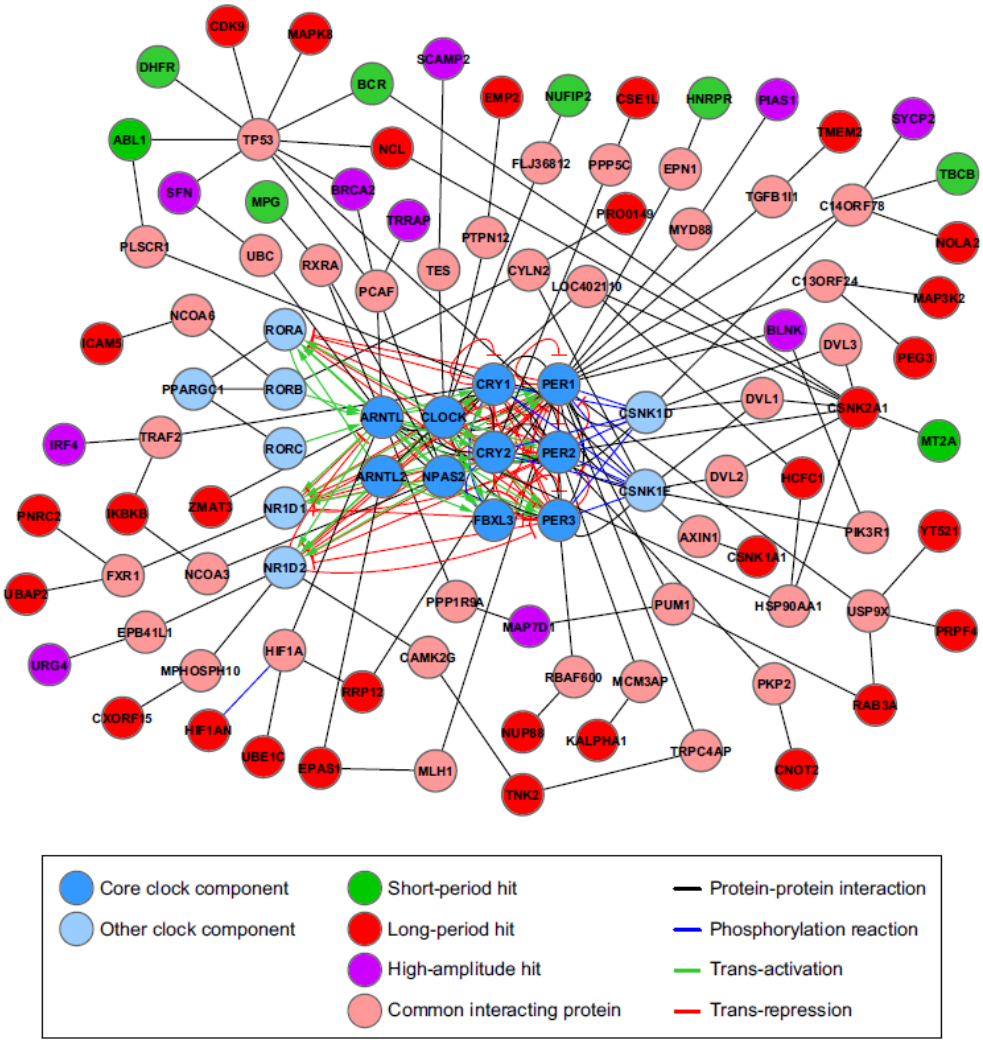

Figure 8: Expanded clock PPI network. Core clock loop components (blue) and additional known clock components (light blue) were used to identify interactions (Table 2) with the primary screen hits (short period: green; long period: red; high amplitude: purple). Common interacting proteins that were not hits in the primary screen are represented as pink nodes. Edges are colored based on the type of interaction: protein-protein interaction (black), phosphorylation reaction (blue), trans-activation (green), and trans-repression (red). Visualization was prepared in Cytoscape (http://www.cytoscape.org).

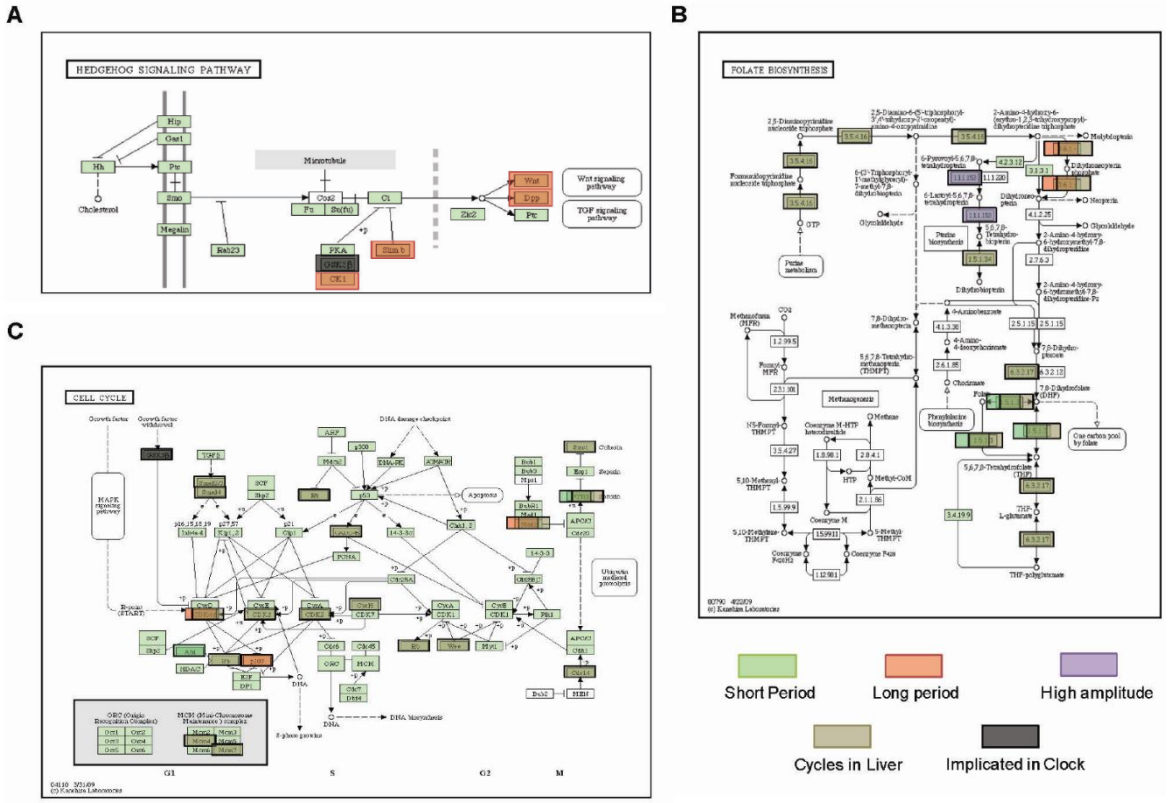

Figure 9: NIH DAVID Pathway Analysis revealed enrichment of clock modifiers in hedgehog signaling **(A)**, folate biosynthesis **(B)**, and cell cycle **(C)**. Primary screen hits are highlighted in these pathways based on the circadian phenotype observed: short period (green), long period (orange), and high amplitude (purple). Previous studies have identified that components of these pathways display circadian regulation ("Cycle in Liver", taupe) or have been implicated in the clock mechanism (grey). This evidence supports a high degree of interconnectedness between the clock and these pathways.

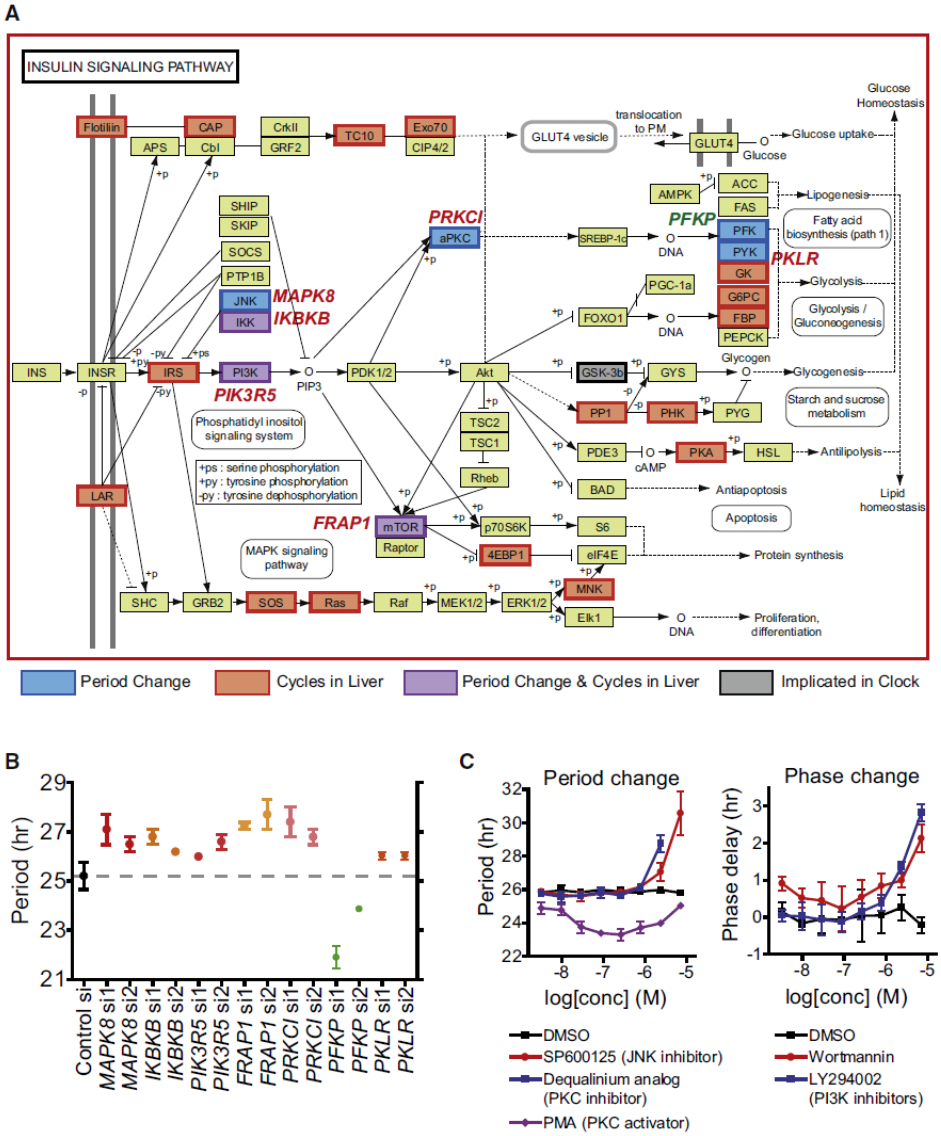

Figure 10: Insulin signaling displays a high degree of interconnectedness with the circadian clock. **A:** Clock modifiers and components regulated by the clock are highlighted: siRNA hits (blue), cycles in the liver (red), siRNA hits that cycle in the liver (purple), and implicated in the clock (grey). **B:** Representative results on circadian period length are shown for individual siRNAs from secondary screen. Data represents the mean ± SD (n=2). **C:** Effects of chemical inhibitors of protein kinases in insulin signaling supports connections between this pathway and the clock. Bioluminescence rhythms in the presence of various concentrations of compounds (8-points in a 3-fold dilution series with final concentrations of 3nM-7μM) were recorded, analyzed for circadian parameters, and results plotted versus final concentration of compound. Data represents the mean ± SD (n=4). Results for SP6002 and PMA are consistent with Hirota et al. (15).

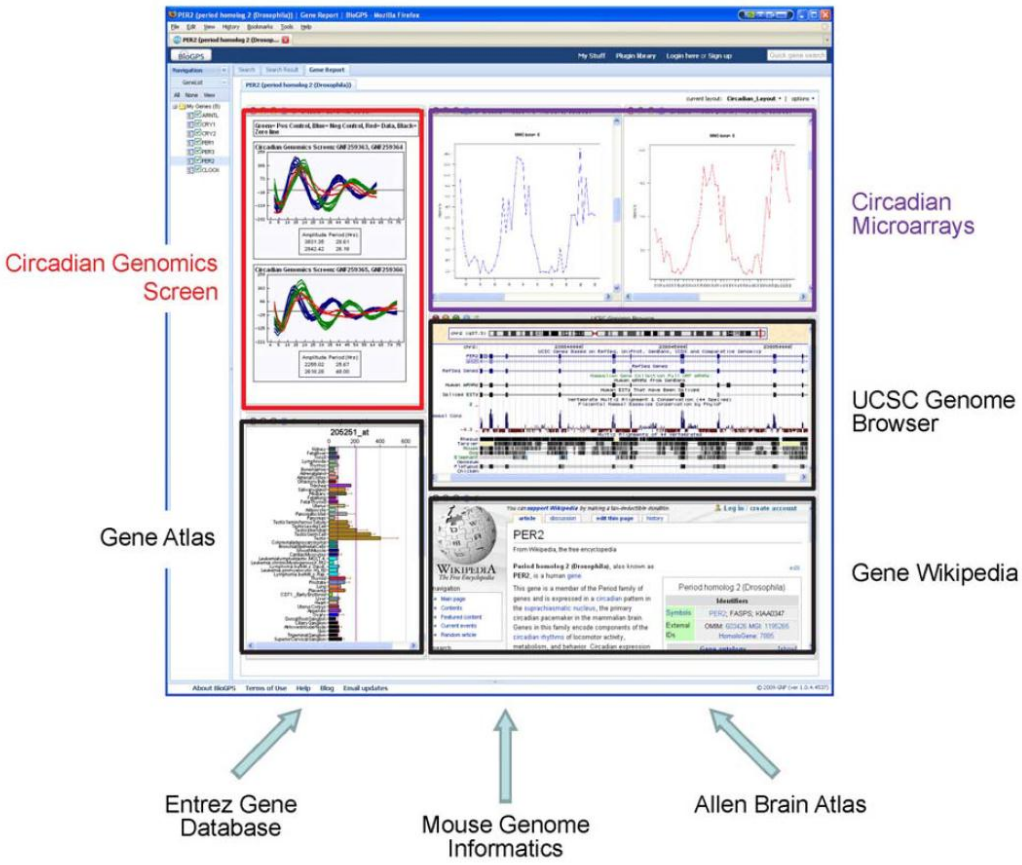

Figure 11: BioGPS (http://biogps.gnf.org/circadian) is an online database that aggregates multiple annotation resources and datasets, including the primary siRNA screen data. The circadian layout in BioGPS the primary screen data and circadian parameters ("Circadian Genomics Screen", red) as well as circadian microarrays (purple) and additional biological annotations (black): UCSC Genome Browser, Gene Atlas database to assess expression across many tissues and cell lines, and Gene Wikipedia. BioGPS also provides a flexible platform within which to customize the information presented to the user's specific interests via plug-in library.

Table 1: siRNA primary screen hits. Hits are color coded by consistency and phenotype: double hits for high amplitude (purple), double hits for short period (teal), double hits for long period (red), single hits for high amplitude (light purple), single hits for short period (green). Double and single hit refer to how many siRNA pairs produced the specified circadian phenotype for that gene. Asterisk notes that one or two traces for this gene are not visible in BioGPS.

Phenotype color coding

double hits for high amplitude
double hits for short period
double hits for long period
single hits for high amplitude
single hits for short period

Confirmed by individual siRNA in *Bmal1-dLuc*	Symbol	GenbankID	Description
yes	**BRCA2**	NM_000059	breast cancer 2, early onset
yes	**C1orf85**	NM_144580	kidney predominant protein NCU-G1, chromosome 1 open reading frame 85
no	**C22orf30**	NM_173566	hypothetical protein MGC50372; chromosome 22 open reading frame 30
yes	**CCDC108**	NM_194302	coiled-coil domain containing 108
yes	**DDB1**	NM_001923	damage-specific DNA binding protein 1, 127kDa
yes	**DMAP1**	NM_019100	DNA methyltransferase 1 associated protein 1
yes	**DUSP8**	NM_004420	dual specificity phosphatase 8
yes	**LOXL3**	NM_032603	lysyl oxidase-like 3
yes	**PEA15**	NM_003768	phosphoprotein enriched in astrocytes 15
yes	**PIAS1**	NM_016166	protein inhibitor of activated STAT, 1
yes	**SKIV2L2**	NM_015360	superkiller viralicidic activity 2-like 2 (S. cerevisiae)
yes	**ABL1**	NM_005157	v-abl Abelson murine leukemia viral oncogene homolog 1
yes	**ACSF3**	NM_174917	acyl-CoA synthetase family member 3
yes	**ATF6**	NM_007348	activating transcription factor 6
yes	**B4GALT2**	NM_001005417	UDP-Gal:betaGlcNAc beta 1,4- galactosyltransferase, polypeptide 2
yes	**BCR**	NM_004327	breakpoint cluster region
yes	**C1orf109**	NM_017850	hypothetical protein FLJ20508, chromosome 1 open reading frame 109
no	**C20orf160**	NM_080625	chromosome 20 open reading frame 160
yes	**C6orf89**	NM_152734	chromosome 6 open reading frame 89
yes	**CASC1**	NM_018272	cancer susceptibility candidate 1
yes	**CCT5**	NM_012073	chaperonin containing TCP1, subunit 5 (epsilon)
yes	**CEACAM21**	NM_033543	carcinoembryonic antigen-related cell adhesion molecule
no	**CENPM**	NM_024053	centromere protein M
no	**CLPX**	NM_006660	ClpX caseinolytic protease X homolog (E. coli)
yes	**CNNM4**	NM_020184	cyclin M4
yes	**COPE**	NM_007263	coatomer protein complex, subunit epsilon
not tested	**DHX29**	NM_019030	DEAH (Asp-Glu-Ala-His) box polypeptide 29
yes	**GPR78**	NM_080819	G protein-coupled receptor 78
yes	**HEATR5B**	NM_019024	HEAT repeat containing 5B
yes	**HNRPR**	NM_005826	heterogeneous nuclear ribonucleoprotein R
Yes	**LBX1**	NM_006562	transcription factor similar to D. melanogaster homeodomain protein lady bird late

Table 1: siRNA primary screen hits (continued)

Confirmed by	Symbol	GenbankID	Description

individual siRNA in *Bmal1-dLuc*			
Yes	**LILRB1**	NM_006669	leukocyte immunoglobulin-like receptor, subfamily B (with TM and ITIM domains), member 1
Yes	**LYG1**	NM_174898	lysozyme G-like 1
Yes	**MMP3**	NM_002422	matrix metalloproteinase 3 (stromelysin 1, progelatinase)
Yes	**MOSC2**	NM_017898	MOCO sulphurase C-terminal domain containing 2
Yes	**MPND**	NM_032868	MPN domain containing
Yes	**NUFIP2**	NM_020772	82-kD nuclear fragile X mental retardation protein Interacting Protein
Yes	**OR51B2**	NM_033180	olfactory receptor, family 51, subfamily B, member 2
Yes	**PLEKHJ1**	NM_018049	pleckstrin homology domain containing, family J member 1
Yes	**PPM1B**	NM_002706	protein phosphatase 1B (formerly 2C); magnesium-dependent; beta isoform
not tested	**PPP1R2P9**	NM_025210	protein phosphatase 1, regulatory (inhibitor) subunit 2 pseudogene 9
Yes	**RCV1**	NM_002903	Recoverin
Yes	**SCARA3**	NM_016240	scavenger receptor class A, member 3
Yes	**SCHIP1**	NM_014575	schwannomin interacting protein 1
Yes	**SELO**	NM_031454	selenoprotein O
Yes	**tAKR**	XM_372302	aldo-keto reductase, truncated
Yes	**TMEM130**	NM_152913	transmembrane protein 130
No	**TMSNB**	NM_021992	thymosin, beta, identified in neuroblastoma cells
Yes	**UBQLN4**	NM_020131	ubiquilin 4
Yes	**ZNF273**	NM_021148	zinc finger protein 273
Yes	**ZNF358**	NM_018083	zinc finger protein 358
Yes	**ABCC3**	NM_003786	ATP-binding cassette, sub-family C (CFTR/MRP), member 3
Yes	**ACTL6A**	NM_004301	actin-like 6A
Yes	**ANKLE1**	NM_152363	ankyrin repeat and LEM domain containing 1
Yes	**ANTXR1**	NM_018153	anthrax toxin receptor 1
Yes	**APPBP1**	NM_003905	amyloid beta precursor protein binding protein 1, 59kDa
Yes	**ASB5**	NM_080874	ankyrin repeat and SOCS box-containing 5
Yes	**ASCC3**	NM_022091	activating signal cointegrator 1 complex subunit 3
Yes	**BDP1**	NM_018429	B double prime 1, subunit of RNA polymerase III transcription initiation factor IIIB
Yes	**BMP4**	NM_001202	bone morphogenetic protein 4
No	**BOLA3**	NM_212552	bolA homolog 3 (E. coli)
Yes	**BSCL2**	NM_032667	Bernardinelli-Seip congenital lipodystrophy 2 (seipin)
Yes	**BTN2A2**	NM_006995	butyrophilin; subfamily 2; member A2
not tested	**BTNL8**	NM_024850	butyrophilin-like 8
Yes	**C10orf137**	NM_015608	chromosome 10 open reading frame 137
Yes	**C1ORF131**	NM_152379	hypothetical protein DKFZp547B1713, C1orf131
not tested	**C9orf86**	NM_024718	chromosome 9 open reading frame 86
No	**CBLN1**	NM_004352	cerebellin 1 precursor
Yes	**CCDC81**	NM_021827	coiled-coil domain containing 81
yes	**CCDC87**	NM_018219	coiled-coil domain containing 87
yes	**CDC2L1**	NM_033487	cell division cycle 2-like 1 (PITSLRE proteins)
yes	**CDK3**	NM_001258	cyclin-dependent kinase 3

Table 1: siRNA primary screen hits (continued)

Confirmed by individual siRNA	Symbol	GenbankID	Description

in *Bmal1-dLuc*			
yes	**CDK6**	NM_001259	cyclin-dependent kinase 6
yes	**CDK9**	NM_001261	cyclin-dependent kinase 9 (CDC2-related kinase)
yes	**CMYA4**	NM_173167	cardiomyopathy associated 4
yes	**CNOT2**	NM_014515	CCR4-NOT transcription complex, subunit 2
yes	**COX7B**	NM_001866	cytochrome c oxidase subunit VIIb
yes	**Cry2**	NM_021117	cryptochrome 2
yes	**CSE1L**	NM_001316	CSE1 chromosome segregation 1-like (yeast)
yes	**CSNK1A1**	NM_001892	casein kinase 1; alpha 1
yes	**CSNK1E**	NM_001894	casein kinase 1, epsilon
yes	**CSNK2A1**	NM_001895	casein kinase 2, alpha 1 polypeptide
yes	**CTDP1**	NM_004715	CTD (carboxy-terminal domain; RNA polymerase II; polypeptide A) phosphatase; subunit 1
yes	**CX3CL1**	NM_002996	chemokine (C-X3-C motif) ligand 1
yes	**CXorf15**	NM_018360	chromosome X open reading frame 15
yes	**DCLRE1A**	NM_014881	DNA cross-link repair 1A (PSO2 homolog; S. cerevisiae)
yes	**DDX3X**	NM_001356	DEAD (Asp-Glu-Ala-Asp) box polypeptide 3, X-linked
yes	**DGKQ**	NM_001347	diacylglycerol kinase; theta 110kDa
yes	**e(y)2**	NM_020189	e(y)2 protein
not tested	**EEIG1**	NM_203305	early estrogen-induced gene 1 protein
yes	**EMP2**	NM_001424	epithelial membrane protein 2
yes	**EMR2**	NM_013447	egf-like module containing; mucin-like; hormone receptor-like 2
no	**EPAS1**	NM_001430	EPAS1 endothelial PAS domain protein 1/HIF2A
no	**EXOSC4**	NM_019037	exosome component 4
yes	**FAM55D**	NM_017678	family with sequence similarity 55, member D, transcript variant 2
yes	**FBXL3**	NM_012158	F-box and leucine-rich repeat protein 3
yes	**FBXO45**	XM_117294	F-box protein 45
yes	**FBXW11**	NM_012300	F-box and WD-40 domain protein 11
yes	**FGF10**	NM_004465	fibroblast growth factor 10
yes	**FGF19**	NM_005117	fibroblast growth factor 19
yes	**FKSG2**	NM_021631	apoptosis inhibitor
yes	**FOXA3**	NM_004497	forkhead box A3
yes	**FRAP1**	NM_004958	FK506 binding protein 12-rapamycin associated protein 1
no	**FUT5**	NM_002034	fucosyltransferase 5 (alpha (1,3) fucosyltransferase)
yes	**GFAP**	NM_002055	glial fibrillary acidic protein
yes	**GIPC2**	NM_017655	PDZ domain protein GIPC2
yes	**GJB7**	NM_198568	gap junction protein, beta 7
yes	**GPR124**	NM_032777	G protein-coupled receptor 124
yes	***GPR135**	NM_022571	G protein-coupled receptor 135
yes	**GPR137**	NM_020155	G protein-coupled receptor 137
yes	**GPR158**	NM_020752	G protein-coupled receptor 158
yes	**GPR17**	NM_005291	G protein-coupled receptor 17
yes	**GPR37L1**	NM_004767	G-protein coupled receptor 37 like 1
yes	**GPR45**	NM_007227	G protein-coupled receptor 45
yes	**GRM5**	NM_000842	glutamate receptor; metabotropic 5

Table 1: siRNA primary screen hits (continued)

Confirmed by individual siRNA in *Bmal1-dLuc*	Symbol	GenbankID	Description
yes	**GRPR**	NM_005314	gastrin-releasing peptide receptor
no	**HAS3**	NM_005329	hyaluronan synthase 3
yes	**HCFC1**	NM_005334	host cell factor C1 (VP16-accessory protein)
yes	**HIF1AN**	NM_017902	HIF1AN hypoxia-inducible factor 1; alpha subunit inhibitor
yes	**HOMER3**	NM_004838	homer homolog 3 (Drosophila)
not tested	**HRB2**	NM_007043	HIV-1 rev binding protein 2
yes	**HRPT2**	NM_024529	hyperparathyroidism 2 (with jaw tumor)
yes	**HSPC148**	NM_016403	hypothetical protein HSPC148
no	**ICAM5**	NM_003259	intercellular adhesion molecule 5, telencephalin
yes	**IF**	NM_000204	I factor (complement)
yes	**IFNK**	NM_020124	interferon; kappa
yes	**IGSF4C**	NM_145296	immunoglobulin superfamily, member 4C
yes	**IKBKB**	NM_001556	inhibitor of kappa light polypeptide gene enhancer in B-cells; kinase beta
yes	**INTS2**	NM_020748	integrator complex subunit 2
not tested	**INTS4**	NM_033547	integrator complex subunit 4
yes	**ITGA2B**	NM_000419	integrin; alpha 2b (platelet glycoprotein IIb of IIb/IIIa complex; antigen CD41B)
yes	**JAZF1**	NM_175061	juxtaposed with another zinc finger gene 1
yes	**JUND**	NM_005354	jun D proto-oncogene
yes	***KALPHA1**	NM_006082	tubulin; alpha; ubiquitous
yes	**KCNG2**	NM_012283	potassium voltage-gated channel; subfamily G; member 2
yes	**KCNJ1**	NM_000220	potassium inwardly-rectifying channel; subfamily J; member 1
yes	**KIAA1797**	NM_017794	KIAA1797
yes	**KPNA4**	NM_002268	karyopherin alpha 4 (importin alpha 3)
yes	**LHCGR**	NM_000233	luteinizing hormone/choriogonadotropin receptor
yes	**LHX1**	NM_005568	LIM homeobox 1
yes	**LIMK1**	NM_002314	LIM domain kinase 1
yes	**LIPG**	NM_006033	lipase; endothelial
yes	**LPHN1**	NM_014921	latrophilin 1
yes	**LSM7**	NM_016199	LSM7 homolog, U6 small nuclear RNA associated (S. cerevisiae)
no	**MAD2L1**	NM_002358	MAD2 mitotic arrest deficient-like 1 (yeast)
yes	**MAP3K11**	NM_002419	mitogen-activated protein kinase kinase kinase 11
yes	**MAP3K2**	NM_006609	mitogen-activated protein kinase kinase kinase 2
yes	**MAPK8**	NM_002750	mitogen-activated protein kinase 8
yes	**MARCH4**	NM_020814	membrane-associated ring finger (C3HC4) 4
not tested	**MED10**	NM_032286	mediator complex subunit 10
yes	**MEPCE**	NM_019606	methylphosphate capping enzyme
yes	**METTL11B**	NM_001136107	methyltransferase like 11B
yes	**MFNG**	NM_002405	manic fringe homolog (Drosophila)
yes	**MKL1**	NM_020831	megakaryoblastic leukemia (translocation) 1
yes	**MPN2**	NM_183062	marapsin 2
yes	***MRGPRE**	XM_171536	MAS-related GPR; member E
no	**MRPL18**	NM_014161	mitochondrial ribosomal protein L18

Table 1: siRNA primary screen hits (continued)

Confirmed by individual siRNA in *Bmal1-dLuc*	Symbol	GenbankID	Description
not tested	**MSRB2**	NM_012228	methionine sulfoxide reductase B2
not tested	**MYL5**	NM_002477	myosin, light polypeptide 5, regulatory
yes	**MYOC**	NM_000261	myocilin; trabecular meshwork inducible glucocorticoid response
yes	**NAGLU**	NM_000263	N-acetylglucosaminidase; alpha- (Sanfilippo disease IIIB)
yes	**NCL**	NM_005381	Nucleolin
yes	**NFE2**	NM_006163	nuclear factor (erythroid-derived 2), 45kDa
yes	**NOB1P**	NM_014062	likely ortholog of mouse nin one binding protein
yes	**NOL6**	NM_022917	nucleolar protein family 6 (RNA-associated)
yes	**NOLA2**	NM_017838	nucleolar protein family A, member 2 (H/ACA small nucleolar RNPs)
yes	**NUP88**	NM_002532	nucleoporin 88kDa
yes	**NYX**	NM_022567	Nyctalopin
yes	**OPN1LW**	NM_020061	opsin 1 (cone pigments), long-wave-sensitive (color blindness, protan)
yes	**OPN1MW**	NM_000513	opsin 1 (cone pigments); medium-wave-sensitive (color blindness; deutan)
yes	**OPN5**	NM_181744	opsin 5
yes	**OR1E1**	NM_003553	olfactory receptor, family 1, subfamily E, member 1
not tested	**OXNAD1**	NM_138381	oxidoreductase NAD-binding domain containing 1
yes	**P2RY10**	NM_014499	purinergic receptor P2Y; G-protein coupled; 10
yes	**PANK2**	NM_024960	pantothenate kinase 2 (Hallervorden-Spatz syndrome)
yes	**PAPOLB**	NM_020144	poly(A) polymerase beta (testis specific)
yes	**PAQR4**	NM_152341	progestin and adipoQ receptor family member IV
yes	**PARD6A**	NM_016948	par-6 partitioning defective 6 homolog alpha (C.elegans)
yes	**PDGFC**	NM_016205	platelet derived growth factor C
yes	**PEF**	NM_012392	PEF protein with a long N-terminal hydrophobic domain (peflin)
yes	**PEG3**	NM_006210	paternally expressed 3
yes	***PHEX**	NM_000444	phosphate regulating endopeptidase homolog; X-linked (hypophosphatemia; vitamin D resistant rickets)
yes	**PHF23**	NM_024297	PHD finger protein 23
yes	**PIK3R5**	NM_014308	phosphoinositide-3-kinase, regulatory subunit 5, p101
yes	**PKLR**	NM_000298	pyruvate kinase; liver and RBC
yes	**PKP1**	NM_000299	plakophilin 1 (ectodermal dysplasia/skin fragility syndrome)
yes	**PNRC2**	NM_017761	proline-rich nuclear receptor coactivator 2
yes	**POLR2B**	NM_000938	polymerase (RNA) II (DNA directed) polypeptide B, 140kDa
yes	**POLR3F**	NM_006466	polymerase (RNA) III (DNA directed) polypeptide F
yes	**POP1**	NM_015029	processing of precursor 1, ribonuclease P/MRP subunit (S. cerevisiae)
yes	***PRKCI**	NM_002740	protein kinase C, iota
yes	**PRO0149**	NM_014117	PRO0149 protein
yes	**PRPF4**	NM_004697	PRP4 pre-mRNA processing factor 4 homolog (yeast)
yes	**PSMD13**	NM_002817	proteasome (prosome, macropain) 26S subunit, non-ATPase, 13
yes	**PTGER3**	NM_000957	prostaglandin E receptor 3 (subtype EP3)
yes	**PTK2**	NM_005607	PTK2 protein tyrosine kinase 2
yes	**PWP2H**	NM_005049	PWP2 periodic tryptophan protein homolog (yeast)

Table 1: siRNA primary screen hits (continued)

Confirmed by individual siRNA in *Bmal1-dLuc*	Symbol	GenbankID	Description
yes	**RAB20**	NM_017817	RAB20; member RAS oncogene family
yes	**RAB3A**	NM_002866	RAB3A; member RAS oncogene family
yes	**RABGEF1**	NM_014504	RAB guanine nucleotide exchange factor (GEF) 1
yes	**RAP1GA1**	NM_002885	RAP1, GTPase activating protein 1
yes	**RBL1**	NM_002895	retinoblastoma-like 1 (p107)
yes	**RBM43**	NM_198557	RNA binding motif protein 43
yes	**RBX1**	NM_014248	ring-box 1
yes	**RETN**	NM_020415	Resistin
yes	**RGPR**	NM_033127	regucalcin gene promotor region related protein
yes	**RING1**	NM_002931	ring finger protein 1
yes	**RLN3R2**	NM_181885	relaxin 3 receptor 2
yes	**RNF34**	NM_025126	ring finger protein 34
not tested	**RPS4X**	NM_001007	ribosomal protein S4, X-linked
yes	**RRH**	NM_006583	retinal pigment epithelium-derived rhodopsin homolog
yes	**RRP12**	NM_015179	ribosomal RNA processing 12 homolog (S. cerevisiae)
yes	**SART3**	NM_014706	squamous cell carcinoma antigen recognised by T cells 3
yes	**SEC13L1**	NM_030673	SEC13-like 1 (S. cerevisiae)
yes	**SERPINA12**	NM_173850	serine (or cysteine) proteinase inhibitor; clade A (alpha-1 antiproteinase; antitrypsin); member 12
yes	**SF1**	NM_004630	splicing factor 1
yes	**SLC22A8**	NM_004254	solute carrier family 22 (organic anion transporter), member 8
yes	**SLC24A3**	NM_020689	solute carrier family 24 (sodium/potassium/calcium exchanger); member 3
yes	**SLC32A1**	NM_080552	solute carrier family 32 (GABA vesicular transporter), member 1
yes	**SLC34A3**	NM_080877	solute carrier family 34 (sodium phosphate), member 3
yes	**SLC3A1**	NM_000341	solute carrier family 3 (cystine; dibasic and neutral amino acid transporters; activator of cystine; dibasic and neutral amino acid transport); member 1
not tested	**SLC7A13**	NM_138817	solute carrier family 7, (cationic amino acid transporter, y+ system) member 13
yes	**SLICK**	NM_198503	sodium- and chloride-activated ATP-sensitive potassium channel
not tested	**SNRPB2**	NM_003092	small nuclear ribonucleoprotein polypeptide B"
yes	**SOCS4**	NM_080867	suppressor of cytokine signaling 4
yes	**SPAG4L**	NM_080675	sperm associated antigen 4-like
yes	**SRPRB**	NM_021203	signal recognition particle receptor, B subunit
yes	**SSBP1**	NM_003143	single-stranded DNA binding protein 1
yes	**SUCNR1**	NM_033050	succinate receptor 1
yes	**TDE2**	NM_020755	tumor differentially expressed 2
yes	**TH**	NM_000360	tyrosine hydroxylase
yes	**THRAP6**	NM_080651	thyroid hormone receptor associated protein 6
yes	**TMEM2**	NM_013390	transmembrane protein 2
yes	**TNK2**	NM_005781	tyrosine kinase; non-receptor; 2
yes	**TPO**	NM_000547	thyroid peroxidase
yes	**TRIM59**	NM_173084	tripartite motif-containing 59
yes	**TRPM4**	NM_017636	transient receptor potential cation channel; subfamily M; member 4

Table 1: siRNA primary screen hits (continued)

Confirmed by individual siRNA in *Bmal1-dLuc*	Symbol	GenbankID	Description
yes	**TSHB**	NM_000549	thyroid stimulating hormone; beta
no	**TWIST2**	NM_057179	twist homolog 2 (Drosophila)
yes	**UBAP2**	NM_018449	ubiquitin associated protein 2
yes	**UBE1C**	NM_003968	ubiquitin-activating enzyme E1C (UBA3 homolog, yeast)
yes	**UBE2B**	NM_003337	ubiquitin-conjugating enzyme E2B (RAD6 homolog)
yes	**UNC119**	NM_005148	unc-119 homolog (C. elegans)
yes	**USP1**	NM_003368	ubiquitin specific protease 1
no	**VPS4A**	NM_013245	vacuolar protein sorting 4A (yeast)
not tested	**WBP11**	NM_016312	WW domain binding protein 11
yes	**WDR86**	NM_198285	WD repeat domain 86
yes	**WNT2**	NM_003391	wingless-type MMTV integration site family member 2
yes	**YT521**	NM_133370	splicing factor YT521-B
yes	**ZADH2**	NM_175907	zinc binding alcohol dehydrogenase; domain containing 2
yes	**ZMAT3**	NM_022470	zinc finger, matrin type 3, transcript variant 1
yes	***ZNF91**	NM_003430	zinc finger protein 91 (HPF7, HTF10)
yes	**ZNF261**	NM_005096	zinc finger protein 261
not tested	**ZSWIM3**	NM_080752	zinc finger, SWIM domain containing 3
no	**BAI3**	NM_001704	brain-specific angiogenesis inhibitor 3
yes	**BLNK**	NM_013314	B-cell linker
no	**BTC**	NM_001729	betacellulin
no	**BTNL2**	NM_019602	butyrophilin-like 2 (MHC class II associated)
yes	**CAD**	NM_004341	carbamoyl-phosphate synthetase 2, aspartate transcarbamylase, and dihydroorotase
no	**CIDEC**	NM_022094	cell death-inducing DFFA-like effector c
not tested	**CLCN6**	NM_001286	chloride channel 6
yes	**DENND2D**	NM_024901	DENN/MADD domain containing 2D
no	**DOK5**	NM_018431	docking protein 5
yes	**FHIT**	NM_002012	fragile histidine triad gene
yes	**FKBP11**	NM_016594	FK506 binding protein 11, 19 kDa
yes	**FOXL1**	NM_005250	forkhead box L1
no	**GMNN**	NM_015895	geminin, DNA replication inhibitor
no	**GRIA2**	NM_000826	glutamate receptor, ionotropic, AMPA 2
yes	**HIST1H1B**	NM_005322	histone 1, H1b
no	**INPP5D**	NM_005541	inositol polyphosphate-5-phosphatase, 145kDa
yes	**IRF4**	NM_002460	interferon regulatory factor 4
no	**KCNV1**	NM_014379	potassium channel, subfamily V, member 1
yes	**MAP7D1**	NM_018067	MAP7 domain containing 1
yes	**MT3**	NM_005954	metallothionein 3 (growth inhibitory factor (neurotrophic))
yes	**NMNAT1**	NM_022787	nicotinamide nucleotide adenylyltransferase 1
yes	**OR2W1**	NM_030903	olfactory receptor, family 2, subfamily W, member 1
yes	**PDE1B**	NM_000924	phosphodiesterase 1B, calmodulin-dependent
no	**RNF103**	NM_005667	ring finger protein 103
yes	**RNP**	NM_017619	U11/U12 snRNP 65K
yes	**SCAMP2**	NM_005697	secretory carrier membrane protein 2
no	**SFN**	NM_006142	stratifin

Table 1: siRNA primary screen hits (continued)

Confirmed by individual siRNA in *Bmal1-dLuc*	Symbol	GenbankID	Description
no	**SLC39A12**	NM_152725	solute carrier family 39 (zinc transporter), member 12
Yes	**SLC8A2**	NM_015063	solute carrier family 8 (sodium-calcium exchanger), member 2
not tested	**SPR**	NM_003124	sepiapterin reductase (7,8-dihydrobiopterin:NADP+ oxidoreductase)
No	**STX4A**	NM_004604	syntaxin 4A (placental)
Yes	**SUV420H1**	NM_016028	suppressor of variegation 4-20 homolog 1 (Drosophila), transcript variant 2
no	**SYCP2**	NM_014258	synaptonemal complex protein 2
yes	**TCTA**	NM_022171	T-cell leukemia translocation altered gene
not tested	**TNT**	NM_182831	TNT protein
no	**TREM2**	NM_018965	triggering receptor expressed on myeloid cells 2
yes	**TRRAP**	NM_003496	transformation/transcription domain-associated protein
yes	**URG4**	NM_017920	up-regulated gene 4
not tested	**VMD2**	NM_004183	vitelliform macular dystrophy (Best disease, bestrophin)
not tested	**WDR9**	NM_001007246	WD repeat domain 9
no	**ZNF211**	NM_006385	zinc finger protein 211
yes	**ZNF75**	NM_007131	zinc finger protein 75 (D8C6)
no	**ARFIP2**	NM_012402	ADP-ribosylation factor interacting protein 2 (arfaptin 2)
no	**CARD11**	NM_032415	caspase recruitment domain family, member 11
no	**CARD9**	NM_052813.1	caspase recruitment domain family, member 9
no	**CES1**	NM_001266	carboxylesterase 1 (monocyte/macrophage serine esterase 1)
yes	**CHID1**	NM_023947	chitinase domain containing 1, transcript variant 3
yes	**CKLF**	NM_016951	chemokine-like factor
yes	**CKLFSF7**	NM_138410	chemokine-like factor super family 7
no	**COPS2**	NM_004236	COP9 constitutive photomorphogenic homolog subunit 2 (Arabidopsis)
yes	**COX4NB**	NM_006067	neighbor of COX4
no	**CRYGD**	NM_006891	crystallin, gamma D
yes	**DDX56**	NM_019082	DEAD (Asp-Glu-Ala-Asp) box polypeptide 56
yes	**DHFR**	NM_000791	dihydrofolate reductase
yes	**ENG**	NM_000118	endoglin (Osler-Rendu-Weber syndrome 1)
no	**FBXO16**	NM_172366	F-box protein 16
no	**FOXF1**	NM_001451	forkhead box F1
yes	**FUCA1**	NM_000147	fucosidase, alpha-L- 1, tissue
yes	**FZD10**	NM_007197	frizzled homolog 10 (Drosophila)
no	**GLT25D2**	NM_015101	glycosyltransferase 25 domain containing 2
yes	**GMFG**	NM_004877	glia maturation factor, gamma
not tested	**GPR40**	NM_005303	G protein-coupled receptor 40
yes	**GPR89**	NM_016334	G protein-coupled receptor 89
yes	**GUCY2C**	NM_004963	guanylate cyclase 2C (heat stable enterotoxin receptor)
yes	**HGFAC**	NM_001528	HGF activator
no	**KIAA0020**	NM_014878	KIAA0020
no	**LYPD5**	NM_182573	LY6/PLAUR domain containing 5 (LYPD5), transcript variant B

Table 1: siRNA primary screen hits (continued)

Confirmed by individual siRNA in *Bmal1-dLuc*	Symbol	GenbankID	Description
yes	**MAGEA12**	NM_005367	melanoma antigen, family A, 12
no	**MAPRE2**	NM_014268	microtubule-associated protein, RP/EB family, member 2
not tested	**MCR**	NM_016011	nuclear receptor binding factor 1
yes	**MPG**	NM_002434	N-methylpurine-DNA glycosylase
yes	**MT2A**	NM_005953	metallothionein 2A
no	**NEIL1**	NM_024608	nei endonuclease VIII-like 1 (E. coli)
yes	**NPC1L1**	NM_013389	NPC1 (Niemann-Pick disease, type C1, gene)-like 1
yes	**NR0B2**	NM_021969	nuclear receptor subfamily 0, group B, member 2
yes	**PFKP**	NM_002627	phosphofructokinase, platelet
no	**PTTG2**	NM_006607	pituitary tumor-transforming 2
yes	**RANBP6**	NM_012416	RAN binding protein 6
not tested	**RRBP1**	NM_004587	ribosome binding protein 1 homolog 180kDa (dog)
yes	**SERPINC1**	NM_000488	serine (or cysteine) proteinase inhibitor, clade C (antithrombin), member 1
yes	**SH3GL2**	NM_003026	SH3-domain GRB2-like 2
no	**SLAMF7**	NM_021181	SLAM family member 7
no	**SLC25A27**	NM_004277	solute carrier family 25, member 27
yes	**SPRR1B**	NM_003125	small proline-rich protein 1B (cornifin)
yes	**TBC1D9**	NM_015130	TBC1 domain family, member 9
yes	**TBCB**	NM_001281	cytoskeleton associated protein 1
yes	**TD-60**	NM_018715	RCC1-like
no	**WDSOF1**	NM_015420	WD repeats and SOF domain containing 1
no	**ZBTB20**	NM_015642	zinc finger and BTB domain containing 20
	* One or two trace profiles of these genes are not shown on BioGPS		

Table 2: PPIs for between clock genes and clock modifiers by direct interaction **(A)** or indirect interactions intermediated a common interactor (bridging gene) **(B)**. Gene names are color coded: clock genes (blue), high amplitude hits (purple), short period hits (green), long period hits (red).

Color coding
clock genes
high amplitude
short period
long period

A. Direct Interaction

Clock Ref	Clock Symbol	Hit Ref	Hit Symbol
NM_001178	ARNTL	NM_022470	ZMAT3
NM_002616	PER1	NM_013314	BLNK
NM_002616	PER1	NM_015179	RRP12

B. "One-Molecule-Intermediated" Interaction

Clock Ref	Clock Symbol	Interactant Ref	Interactant Symbol	Hit Ref	Hit Symbol
NM_001178	ARNTL	XM_374491	PPP1R9A	NM_018067	MAP7D1
NM_001178	ARNTL	NM_021009	UBC	NM_006142	SFN
NM_001178	ARNTL	NM_003884	PCAF	NM_000059	BRCA2
NM_001178	ARNTL	NM_003884	PCAF	NM_003496	TRRAP
NM_001178	ARNTL	NM_002957	RXRA	NM_002434	MPG
NM_001178	ARNTL	NM_001530	HIF1A	NM_003968	UBE1C
NM_001178	ARNTL	NM_001530	HIF1A	NM_017902	HIF1AN
NM_001178	ARNTL	NM_001530	HIF1A	NM_015179	RRP12
NM_001178	ARNTL	NM_005348	HSP90AA1	NM_177559	CSNK2A1
NM_001178	ARNTL	NM_005348	HSP90AA1	NM_005334	HCFC1
NM_004898	CLOCK	NM_015641	TES	NM_005697	SCAMP2
NM_004898	CLOCK	NM_153260	FLJ36812	NM_020772	NUFIP2
NM_004898	CLOCK	XM_377778	LOC402110	NM_005334	HCFC1
NM_004898	CLOCK	NM_002835	PTPN12	NM_001424	EMP2
NM_004898	CLOCK	NM_020183	ARNTL2	NM_001430	EPAS1
NM_002518	NPAS2	NM_003884	PCAF	NM_000059	BRCA2
NM_002518	NPAS2	NM_003884	PCAF	NM_003496	TRRAP
NM_002518	NPAS2	NM_002957	RXRA	NM_002434	MPG
NM_002518	NPAS2	NM_181659	NCOA3	NM_001556	IKBKB
NM_002616	PER1	XM_290629	C14ORF78	NM_014258	SYCP2
NM_002616	PER1	NM_002468	MYD88	NM_016166	PIAS1
NM_002616	PER1	NM_014676	PUM1	NM_018067	MAP7D1
NM_002616	PER1	NM_013333	EPN1	NM_005826	HNRPR
NM_002616	PER1	XM_290629	C14ORF78	NM_001281	TBCB
NM_002616	PER1	NM_021906	USP9X	NM_004697	PRPF4
NM_002616	PER1	NM_006346	C13ORF24	NM_006609	MAP3K2
NM_002616	PER1	NM_015638	TRPC4AP	NM_005781	TNK2
NM_002616	PER1	NM_000249	MLH1	NM_001430	EPAS1
NM_002616	PER1	NM_021906	USP9X	NM_002866	RAB3A
NM_002616	PER1	XM_290629	C14ORF78	NM_017838	NOLA2
NM_002616	PER1	NM_014676	PUM1	NM_002866	RAB3A
NM_002616	PER1	NM_006346	C13ORF24	NM_006210	PEG3
NM_002616	PER1	NM_015927	TGFB1I1	NM_013390	TMEM2
NM_002616	PER1	NM_021906	USP9X	NM_133370	YT521
NM_022817	PER2	NM_001895	CSNK2A1	NM_005953	MT2A
NM_022817	PER2	NM_001895	CSNK2A1	NM_004327	BCR
NM_022817	PER2	NM_178552	MGC35206	NM_018449	UBAP2
NM_022817	PER2	NM_004572	PKP2	NM_014515	CNOT2
NM_022817	PER2	NM_003906	MCM3AP	NM_006082	KALPHA1
NM_016831	PER3	NM_002616	PER1	NM_013314	BLNK
NM_016831	PER3	NM_002616	PER1	NM_015179	RRP12
NM_016831	PER3	NM_020765	RBAF600	NM_002532	NUP88
NM_004075	CRY1	NM_021138	TRAF2	NM_002460	IRF4
NM_004075	CRY1	NM_021105	PLSCR1	NM_005157	ABL1
NM_004075	CRY1	NM_021138	TRAF2	NM_001556	IKBKB
NM_021117	CRY2	NM_006247	PPP5C	NM_001316	CSE1L
NM_005126	NR1D2	NM_177986	EPB41L1	NM_017920	URG4
NM_021724	NR1D1	NM_005087	FXR1	NM_018449	UBAP2
NM_021724	NR1D1	NM_005087	FXR1	NM_017761	PNRC2
NM_005126	NR1D2	NM_001222	CAMK2G	NM_005781	TNK2
NM_005126	NR1D2	NM_005791	MPHOSPH10	NM_018360	CXORF15
NM_006914	RORB	NM_014071	NCOA6	NM_003259	ICAM5
NM_006914	RORB	NM_003388	CYLN2	NM_001894	CSNK1E
NM_001893	CSNK1D	XM_290629	C14ORF78	NM_014258	SYCP2
NM_001893	CSNK1D	XM_290629	C14ORF78	NM_001281	TBCB
NM_001893	CSNK1D	NM_181870	DVL1	NM_001895	CSNK2A1
NM_001893	CSNK1D	NM_004423	DVL3	NM_001895	CSNK2A1
NM_001893	CSNK1D	XM_290629	C14ORF78	NM_017838	NOLA2
NM_001894	CSNK1E	NM_181523	PIK3R1	NM_013314	BLNK
NM_001894	CSNK1E	NM_000546	TP53	NM_000059	BRCA2
NM_001894	CSNK1E	NM_000546	TP53	NM_006142	SFN
NM_001894	CSNK1E	NM_000546	TP53	NM_005157	ABL1
NM_001894	CSNK1E	NM_000546	TP53	NM_004327	BCR
NM_001894	CSNK1E	NM_000546	TP53	NM_000791	DHFR
NM_001894	CSNK1E	NM_000546	TP53	NM_001261	CDK9
NM_001894	CSNK1E	NM_000546	TP53	NM_139046	MAPK8
NM_001894	CSNK1E	NM_000546	TP53	NM_005381	NCL
NM_001894	CSNK1E	NM_003502	AXIN1	NM_001892	CSNK1A1
NM_001894	CSNK1E	NM_032421	CYLN2	NM_014117	PRO0149
NM_001894	CSNK1E	NM_181870	DVL1	NM_001895	CSNK2A1
NM_001894	CSNK1E	NM_004422	DVL2	NM_001895	CSNK2A1

Chapter 3: Cell-autonomous circadian clock of hepatocytes drives rhythms in transcription and polyamine synthesis

PNAS PNAS PNAS PNAS

Cell-autonomous circadian clock of hepatocytes drives rhythms in transcription and polyamine synthesis

Ann Atwood[a,1], Robert DeConde[b,1], Susanna S. Wang[a], Todd C. Mockler[c], Jamal S. M. Sabir[d], Trey Ideker[b], and Steve A. Kay[a,2]

[a]Section of Cell and Developmental Biology, Division of Biological Sciences, and the Center for Chronobiology, University of California at San Diego, La Jolla, CA 92093-0130; [b]Departments of Medicine and Bioengineering, University of California at San Diego, La Jolla, CA 92093-0063; [c]The Donald Danforth Plant Science Center, St. Louis, MO 63132; and [d]Department of Biological Sciences, King Abdulaziz University, Jeddah, Kingdom of Saudi Arabia 21589

Contributed by Steve A. Kay, October 5, 2011 (sent for review August 3, 2011)

The circadian clock generates daily rhythms in mammalian liver processes, such as glucose and lipid homeostasis, xenobiotic metabolism, and regeneration. The mechanisms governing these rhythms are not well understood, particularly the distinct contributions of the cell-autonomous clock and central pacemaker to rhythmic liver physiology. Through microarray expression profiling in Met murine hepatocytes (MMH)-D3, we identified over 1,000 transcripts that exhibit circadian oscillations, demonstrating that the cell-autonomous clock can drive many rhythms, and that MMH-D3 is a valid circadian model system. The genes represented by these circadian transcripts displayed both cophasic and antiphasic organization within a protein–protein interaction network, suggesting the existence of competition for binding sites or partners by genes of disparate transcriptional phases. Multiple pathways displayed enrichment in MMH-D3 circadian transcripts, including the polyamine synthesis module of the glutathione metabolic pathway. The polyamine synthesis module, which is highly associated with cell proliferation and whose products are required for initiation of liver regeneration, includes enzymes whose transcripts exhibit circadian oscillations, such as ornithine decarboxylase and spermidine synthase. Metabolic profiling revealed that the enzymatic product of spermidine synthase, spermidine, cycles as well. Thus, the cell-autonomous hepatocyte clock can drive a significant amount of transcriptional rhythms and orchestrate physiologically relevant modules such as polyamine synthesis.

networks | chronobiology | resistance distance

Many aspects of mammalian physiology and behavior display circadian (~24-h) rhythms, including the sleep/wake cycle, blood pressure, heart rate, metabolism, and liver regeneration (1, 2). These rhythms are regulated by the circadian clock, which enables consolidation and coordination of physiological events to specific phases of the 24-h cycle in anticipation of daily environmental changes. Dysfunction of the clock is associated with serious human health conditions, including shift work syndrome, sleep disorders, increased risk of cancer, cardiovascular disease, and metabolic syndrome (1, 2).

The circadian clock is a self-sustaining, entrainable, cell-autonomous network of three interlocked transcriptional negative feedback loops (2). The primary loop consists of BMAL1/CLOCK transcriptional activators, which dimerize and turn on transcription of *Period* (*Per1*, *Per2*, and *Per3*) and *Crytochrome* (*Cry1* and *Cry2*) genes through E-box elements. PER and CRY proteins dimerize and feed back to inhibit BMAL1/CLOCK activation. Two associate loops interlock with the core loop: the ROR/REV-ERB element (RRE) loop composed of ROR activators (RORa, RORb, and RORc) and REV-ERB repressors (REV-ERBα and REV-ERBβ), which compete for RRE transcription factor binding sites (TFBS), and the D-box loop composed of the activator DBP and repressor E4BP4, which act through D-box TFBS (2).

In addition to internal regulation of clock genes, the clock also orchestrates circadian rhythms of output networks, which ultimately govern overt rhythms in physiology and behavior. Nearly all mammalian cell types contain a circadian clock, producing at the organismal level a multioscillator system in which systemic and local circadian signals may jointly regulate physiology. This system can be divided into two main classes of clocks: the central pacemaker and peripheral clocks. The central pacemaker resides in the suprachiasmatic nucleus (SCN) and receives light input directly from the retina, entraining it directly to the light/dark cycle (1). The SCN acts to synchronize peripheral clocks in other tissues through systemic signals, and orchestrates rhythms in physiology. In contrast, the role of peripheral clocks remains to be elucidated. Despite ~10% of the genome displaying circadian rhythms in gene expression in many tissues, little overlap of rhythmic genes exists across tissues, suggesting that tissue-specific regulatory networks generate rhythms in local physiology (3, 4). In mice, disrupting the local liver clock abolishes circadian rhythms in many liver genes, even in the presence of a functional central pacemaker, implying a significant role for the liver clock in hepatic gene expression (5).

Rhythmic feeding behavior also represents a major entrainment signal for the hepatic clock. Restricting food access to the middle of the light period induces phase inversion of the liver clock in wild-type (WT) mice (6), and rhythmic feeding alone can drive oscillations in hepatic gene expression (7). When food is plentiful, feeding behavior is synchronized with the light/dark SCN-driven activity cycle. However, in conditions of scarcity or restricted access to food, feeding rhythms can be driven by the food-entrainable oscillator (FEO), which is independent of SCN light entrainment and is believed to involve multiple regions of the central nervous system (8–10). It remains unclear how hepatocytes balance the respective roles of systemic circadian regulation applied by the SCN and FEO vs. cell-autonomous regulation from the hepatic clock to generate circadian rhythms in liver functions.

To address the role of the cell-autonomous circadian clock, systemic influences need to be removed while still maintaining the integrity of the circadian clock and its physiological outputs. We selected the immortalized mouse cell line Met murine hepatocytes (MMH)-D3 as a candidate model system. Derived from the 3-d-old liver of transgenic c-Met mice (11), MMH-D3 is immortalized but not transformed, and maintains a high level of differentiation upon induction (11, 12), providing a system that reflects to a significant extent an in vivo hepatocyte.

We combined multiple analytic methods for the identification of circadian rhythms in large datasets. Using this pipeline, we reveal that MMH-D3 hepatocytes contain a functional cell-autonomous

Author contributions: A.A., R.D., S.S.W., and S.A.K. designed research; A.A., R.D., and S.S.W. performed research; A.A., R.D., and T.C.M. contributed new reagents/analytic tools; A.A., R.D., S.S.W., T.C.M., J.S.M.S., T.I., and S.A.K. analyzed data; and A.A., R.D., T.I., and S.A.K. wrote the paper.

The authors declare no conflict of interest.

Freely available online through the PNAS open access option.

[1]A.A. and R.D. contributed equally to this work.

[2]To whom correspondence should be addressed. E-mail: skay@ucsd.edu.

This article contains supporting information online at www.pnas.org/lookup/suppl/doi:10.1073/pnas.1115753108/-/DCSupplemental.

clock that can drive rhythms in gene expression of 1,130 transcripts, suggesting a significant role for this peripheral clock in the production of circadian physiology. We use these transcripts to demonstrate co- and antiphasic organization of circadian genes within the mouse protein interaction network, implying a general strategy of combining both positive and negative signals in the control of circadian processes. Last, we uncover cell-autonomous circadian cycles in polyamine biosynthesis, whose products are integral to initiating liver regeneration, suggesting a role for the hepatic clock in gating the initiation of liver regeneration (1, 2).

Results

Bioinformatics Pipeline for Identifying Circadian Rhythms. Recent reports demonstrate that circadian rhythm identification algorithms call different transcripts as cycling, even in the same dataset (4, 13). Further, existing methods show a dramatic reduction in the number of identified transcripts as the sampling rate decreases. Consequently, single methods applied to lower-resolution datasets produce very sparse lists of circadian calls (4), which may limit the types of further analyses run on these lists.

To address this issue, we constructed a bioinformatics pipeline for the identification of circadian rhythms in large datasets by combining two major analytic methods used in the analysis of circadian datasets: signal decomposition and model-matching (Fig. 1*A*) (4, 13, 14). The signal decomposition arm uses two Fourier analysis algorithms to identify cosine-based rhythms in an amplitude insensitive manner: Fisher's *G* test (4, 15) and Biological Rhythms Analysis Software System (BRASS) Fast Fourier transform nonlinear least squares (FFT NLLS) (16). The model-matching arm employs one algorithm, HAYSTACK, which uses user-defined models of a variety of phases and waveforms that extend beyond simple cosines—including spikes, box waves, rigid waves, and asymmetric rigid waves (Fig. S1) (14). Transcripts identified by the model-matching and signal decomposition arms are combined to form the pipeline output.

To illustrate the effect of our pipeline on circadian transcript identification, we applied it to Hughes et al.'s (4) in vivo data from WT mouse liver (the Hughes WT liver dataset), which was collected at 1-h resolution over 48 h, and then to lower-resolution datasets created by subdividing the original at 2-, 3-, and 4-h intervals. Our pipeline identifies a greater number of transcripts than the 3,667 found by Hughes et al. (4) at 1-h resolution or either component analytic method individually (Fig. 1*B* and Fig. S2 *A*–*C*). This increase in called transcripts mitigates the decline of circadian calls at lower sampling resolutions without sacrificing consistency, as evidenced by the >98% of 2-h circadian transcripts represented in the 1-h results (Fig. S2 *D*–*F*).

Cell-Autonomous MMH-D3 Clock Drives Circadian Gene Expression. To characterize the role of the cell-autonomous clock in MMH-D3 hepatocytes, we conducted a 2-h resolution microarray time-course experiment spanning 48 h and applied our pipeline for data analysis. We identified 1,130 transcripts displaying circadian expression: 801 transcripts called by model matching and 427 called by signal decomposition (Fig. 2*A* and Table S1). Algorithmic calls were validated using quantitative PCR (qPCR) for five clock genes, including at least one from each of the three interlocking feedback loops. The qPCR results corroborated the microarray traces for each of these genes (Fig. 2 *B*–*F*) and the algorithm-predicted peak times of not only the first peak but also the second peak in the time course. Moreover, the phase differences between the clock genes representing each of the three negative feedback loops is consistent with the phase differences of the same genes in the Hughes WT liver dataset (Fig. S3 *A* and *B*), and the MMH-D3 circadian transcripts display a bimodal distribution across the 24-h day, characteristic of circadian expression data (3, 5), confirming that the cell-autonomous clock is intact and can drive many rhythms in gene expression.

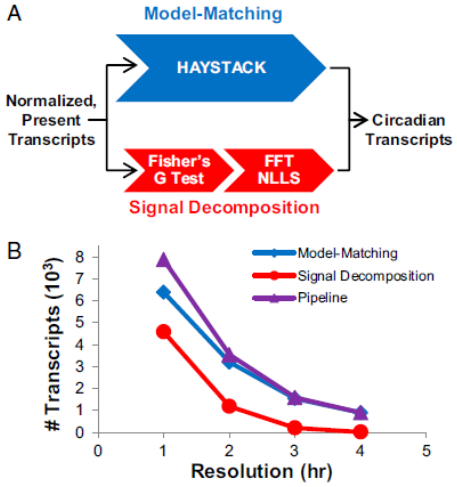

Fig. 1. Bioinformatics pipeline combines two analytic methods to increase circadian transcript yield. (*A*) Diagram depicting the pipeline component analytic methods: signal decomposition and model-matching algorithms. (*B*) Circadian transcripts identified by each analytic method (model-matching: blue, signal decomposition: red) and by the pipeline (purple) at decreasing resolution.

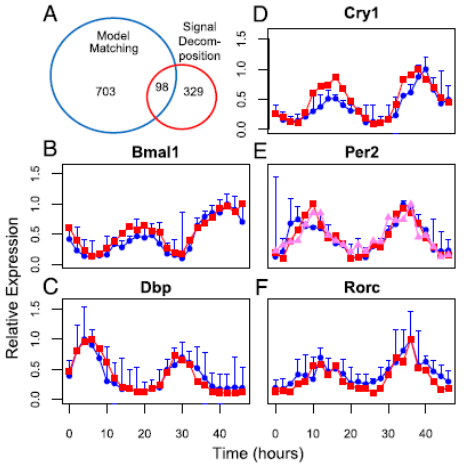

Fig. 2. MMH-D3 displays circadian rhythms of transcription. (*A*) MMH-D3 circadian transcript calls for each arm of pipeline. (*B*–*F*) qPCR (blue) and microarray transcript (red and pink) for indicated clock genes. Error bars on qPCR traces represent SD of replicates ($n = 3$).

SYSTEMS BIOLOGY

COMPUTER SCIENCES

These results contrast the findings of Hughes et al. (4), based on their studies of U2-OS and NIH 3T3 cell lines, that little circadian regulation is maintained in immortalized cell lines. For comparison with in vivo liver data, we applied our pipeline to the Hughes WT liver dataset subsampled at 2-h resolution. Because liver cell lines can exhibit increased glycolytic vs. oxidative profiles for energy metabolism (17), and glucose and lipid homeostasis are circadian regulated in liver (3), we assessed the degree of circadian regulation of glycolysis and oxidative respiration in MMH-D3 and the Hughes WT liver datasets using Gene Ontology (GO) annotation enrichment of the circadian transcript lists. Neither the liver nor MMH-D3 displayed over- or underrepresentation of cycling transcripts associated with glycolysis. Though the Hughes WT liver data displays enrichment in transcripts involved in regulation of fatty acid β-chain oxidation [$P = 0.01$ (even hours), $P = 0.05$ (odd hours)]—a process by which fatty acids are oxidized to enter the TCA cycle—MMH-D3 displays fewer transcripts involved in this process and displays neither over- nor underrepresentation. Despite these metabolic differences, we found 28% concordance of MMH-D3 circadian calls with those of the liver (Fig. S3 *C* and *D*) (4). This overlap is substantial ($P = 2.2 \times 10^{-16}$, one-tailed Fisher's exact test) given that circadian microarray sets can display as little as 11% overlap between datasets, with an average of 24%, and only 54% overlap between replicates from the same experiment (18, 19).

Phasic Localization of Circadian Genes in Protein–Protein Interaction Network. To study the organization of circadian genes within the broader mouse protein–protein interaction (PPI) network, we constructed a mouse PPI network using iRefIndex, a meta-database that combines interaction data from 10 primary databases (20). The constructed network of 7,052 genes contained 297 of the genes represented by the 1,130 MMH-D3 transcripts. In this

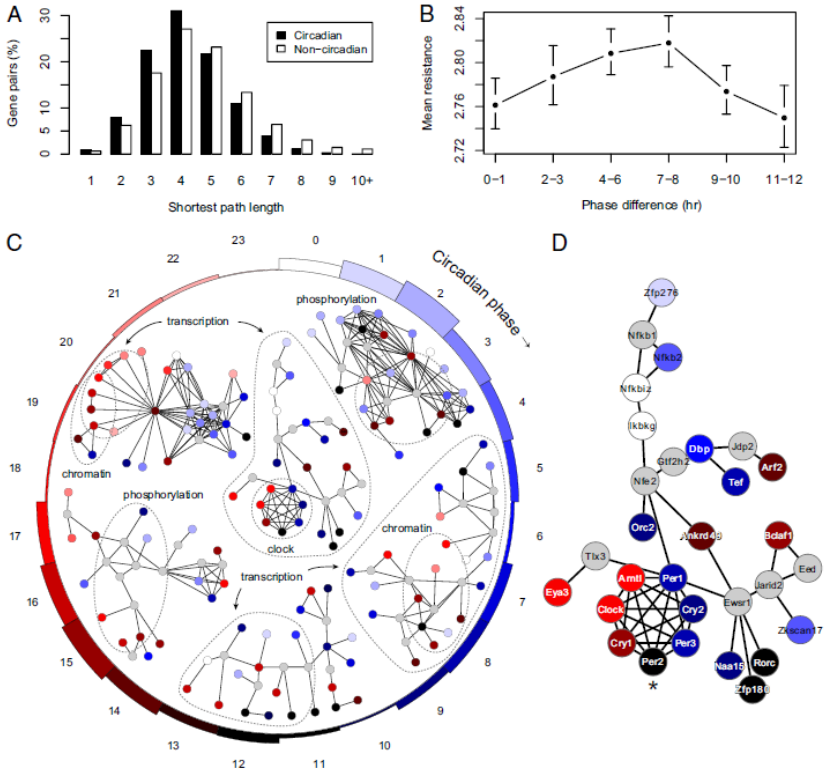

Fig. 3. Circadian genes display co- and antiphasic organization within the mouse PPI network. (*A*) Discreet distributions of shortest path lengths of circadian and noncircadian nodes. (*B*) Mean resistance distances for all pairs of circadian genes within the largest connected component of the mouse PPI network, binned by phase difference. Error bars represent the 95% confidence interval around the estimates of the mean resistance distance for each bin. (*C*) Modules identified by the MATISSE algorithm (inside circle), which finds modules enriched for cophasic pairs, generally exhibit a biphasic pattern, as does the general distribution of phases across all circadian genes in the network (outer star chart). Colors represent the 0–23 (h) circadian phases. Circled annotation groups reflect enriched DAVID functional annotation clusters identified for the 1,130 MMH-D3 circadian transcripts. A larger version of these modules can be found in Fig. S5. (*D*) Specific cophasic module exhibiting the general biphasic pattern. The starred gene (*) Per2 was also found to be cycling in Kornmann et al. (5), where only systemic circadian signals were present.

network, circadian gene pairs display reduced shortest-path lengths between one another compared with noncircadian genes (Fig. 3*A*; Wilcoxon rank-sum test, $P < 10^{-15}$). We also examined closeness centrality—a measure inversely proportional to the mean shortest path between a given gene and all other genes in the network (21). On average, closeness was greater for circadian genes than noncircadian ones (Wilcoxon rank-sum test, $P = 0.017$; Fig. S4*A*). These results indicate that circadian genes are closer to one another and more centrally located in the network than noncircadian genes.

To determine if similarly phased genes were closer than those of disparate phase, we analyzed the resistance distance between pairs of circadian genes based on their difference in phase. Also referred to as commute time, the resistance distance is proportional to the average number of steps required for a random walk to run from one node to the other and back, and represents the strength of the overall connectivity between two nodes in a graph (22). We define the phase difference as the number of hours spanned by the smaller distance between the two phases on a 24-h clock, thus ranging from 0 to 12 h. Our analysis revealed that co- and antiphasic gene pairs have significantly smaller mean resistance between them than those of intermediate phase differences (Fig. 3*B*). In addition, all phase differences showed significantly smaller mean resistance compared with permuted data (maximum $P < 0.05$ across the six bins), but to a greater extent for differences of 0–1 h and 9–12 h ($P < 0.01$ over 1,000 permutations; *Methods*). These results suggest a global organization of circadian genes by co- and antiphasic relationships. The same property at the local level—analyzed using the distribution of phase differences among all first neighbors of each gene in the network—revealed a similar enrichment for co- and antiphasic gene pairs (Fig. S4*B*).

To further examine the local circadian features of the network, we applied the MATISSE algorithm (23) to identify clusters of cophasic genes within the PPI network. The highest-scoring modules tended to be biphasic, consistent with the described proximity for co- and antiphasic genes in the network, making large, separable clusters uncommon (Fig. 3 *C* and *D* and Fig. S5). These modules reflect annotation clusters enriched in the MMH-D3 circadian transcript list identified by DAVID functional annotation clustering with GO and SwissProt keywords (Table S2), such as transcriptional regulators (transcriptional regulation: $P = 8.91 \times 10^{-6}$), chromatin-associated proteins (chromatin: $P = 2.08 \times 10^{-3}$), and regulators of phosphorylation (regulation of phosphorylation: $P = 6.72 \times 10^{-4}$; Fig. 3*C*) (24). These annotation clusters not only illustrate the breadth of the MMH-D3 circadian transcript list, but are consistent with our understanding of circadian regulation, because transcription, phosphorylation, and chromatin modification play key roles in regulating clock genes and clock function (2).

One module contained all of the clock genes in the core loop, and was dominated by transcriptional regulation (Fig. 3*D*) and illustrates the relationship of co- and antiphasic genes in the network. This module suggests specific interactions for future circadian studies. Not only are components of transcription factor NF-κB (NF-κB1, NF-κB2) represented, but also the regulator of its activating kinase (IKBKG) is also connected to clock genes through neighboring nodes. NF-κB has been tenuously associated with the clock, but its regulatory interactions with the circadian system remain unclear (25, 26).

We compared our results for autonomous cycling calls in the MMH-D3 cell line with the 29 genes that Kornmann et al. (5) identified as having rhythms driven by systemic circadian regulation alone. The two lists displayed a moderately significant overlap of five genes (Per2, Fus, Hspa1b, Hspa8, and Heca; $P = 0.036$, Fisher's exact test), whereas the overlap of these 29 genes with the Hughes WT liver data were a more significant 21 genes ($P = 3.5 \times 10^{-8}$). These results support the conclusion that the Kornmann et al. (5) genes represent a largely distinct subset of the wild-type circadian system (the systemic component) from those represented by the MMH-D3 cells (the cell-autonomous component). The five genes that do overlap—of which all but Heca appear in the PPI network and the MATISSE modules (Fig. 3*D* and Fig. S5)—display rhythms in both systemic and cell-autonomous conditions, and thus may represent interfaces between the two branches of circadian regulation.

Polyamine Synthesis Cycles in MMH-D3. DAVID pathway analysis (24) applied to the MMH-D3 circadian transcript list revealed enrichment in multiple pathways, including mammalian target of rapamycin (mTOR) signaling ($P = 3.2 \times 10^{-4}$), MAPK signaling ($P = 5.6 \times 10^{-3}$), and glutathione metabolism ($P = 5.6 \times 10^{-4}$)—specifically including the polyamine synthesis module (Fig. 4*A*, Table S3, and Fig. S6). The polyamines putrescine, spermidine, and spermine are small, aliphatic cations under physiological conditions that play key roles in cell proliferation and are essential for initiation of liver regeneration (27, 28). Our MMH-D3 hepatocyte time-course results displayed cell-autonomous circadian oscillations in the transcription of both the rate-limiting enzyme ornithine decarboxylase (Odc1) and the subsequent enzyme in the pathway, spermidine synthase (Srm; Fig. 4 *B* and *C*) (27–29). Odc1 and Srm are also rhythmically expressed in the Hughes WT liver dataset (Fig. S7 *A* and *B*) (4), but are not rhythmic in the livers of Vollmers et al.'s (7) *Cry1*/*Cry2* knockout or Miller et al.'s (30) *Clock* mutant mouse data (Fig. S7 *C*–*F*), indicating that these rhythms are controlled by the circadian clock. Using mass spectrometry, we found that spermidine (the enzymatic product of

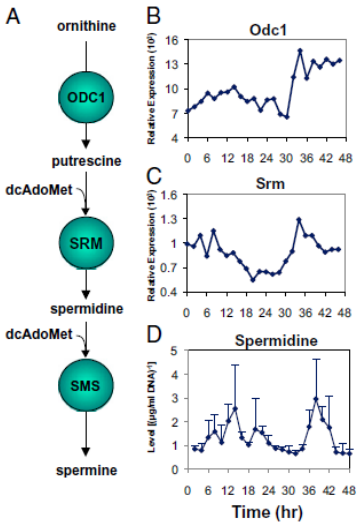

Fig. 4. Circadian rhythms of polyamine synthesis in both transcription and enzymatic activity. (*A*) Polyamine biosynthesis pathway. Ornithine is converted to putrescine (the first polyamine) by ornithine decarboxylase (ODC1). Putrescine is then converted to spermidine with the addition of decarboxylated S-adenosyl methionine (dcAdoMet) by spermidine synthase (SRM). Spermidine is then converted to spermine by spermine synthase (SMS). (*B* and *C*) Odc1 and Srm display circadian rhythms in MMH-D3 hepatocytes. (*D*) Spermidine displays circadian rhythmicity in MMH-D3 hepatocytes. Data points represent mean values for biological replicates ($n = 3$, except at hour 46, where $n = 2$) and error bars their SD.

SRM) exhibits circadian oscillations in MMH-D3 hepatocytes (Fig. 4*D*). Because the phases of Odc1 and Srm transcriptional rhythms are coordinated, and ODC1 is the rate-limiting enzyme, oscillations in spermidine reflect not only the activity of SRM but ODC1 as well.

Discussion

In this study, using a bioinformatics pipeline that combines multiple analytic methods, we identified 1,130 circadian transcripts in MMH-D3 hepatocytes, indicating that the cell-autonomous hepatic clock can drive a significant proportion of circadian rhythms, and validating MMH-D3 as a model system for circadian biology.

The distribution of these genes within a mouse PPI network was both more central and concentrated than expected at random, and further organized to bring together co- and antiphasic genes. The proximity of antiphasic genes resembles relationships we observe within the circadian clock. Positive and negative components of individual clock loops are expressed at disparate phases and compete for the same binding sites, such as ROR activators and REV-ERB repressors competing for RRE binding sites (2). The phasic organization may reflect a general strategy of coupling positive and negative signals in the control and maintenance of specific circadian processes.

Last, we revealed robust cell-autonomous cycles in the polyamine synthesis module at both the transcriptional level and in enzymatic activity in MMH-D3 hepatocytes. Polyamines are strongly associated with cell proliferation, up-regulated in many cancers, and essential for liver regeneration, so circadian regulation of this pathway may gate the hepatocyte's permissibility to initiate liver regeneration (27–29).

Liver regeneration is known to be under circadian regulation, such that disruption of the clock retards liver regeneration and desynchronizes cell proliferation (31). Cell proliferation in regenerating hepatocytes is circadian and is gated by the kinase Wee1 (31). Because polyamines are required for the initiation of liver regeneration, they may provide an upstream or additional mechanism for circadian regulation of the induction of the regeneration program. The mechanism by which polyamines initiate liver regeneration remains unclear, but they are essential to protein and DNA synthesis (32), and may play direct roles in stabilizing and transporting ribosomal RNA (32) as well as modulating protein–protein and protein–DNA interactions involved in transcription (28). Polyamines can also induce changes in DNA curvature to a more accessible conformation associated with transcription start sites (28). Thus, polyamines may act in the regulation of transcription in circadian output, including the induction of cell proliferation programs.

Cycling of Odc1 and Srm transcripts may result from direct transcriptional regulation by the core clock loop, composed of BMAL1/CLOCK activators and PER/CRY repressors. Both Odc1 and Srm are activated by c-Myc/MAX complexes binding to E-boxes in their regulatory regions (33, 34)—the same binding-site sequence used by BMAL1/CLOCK. It is known that BMAL1/CLOCK and c-Myc can regulate the same genes (35). Also, in MMH-D3 hepatocytes, Odc1 and Srm transcripts peak at a similar time to the known BMAL1/CLOCK targets: Dbp, Per2, and Rorc. Furthermore, E-box regulation is enriched in circadian liver transcripts, but only when the local liver clock is intact, suggesting that much E-box–mediated transcriptional regulation requires a cell-autonomous liver clock (36). Further investigation should test the regulatory relationship between the core clock loop and polyamine synthesis.

Though polyamine synthesis can be induced in the in vivo liver by some systemic signals, including glucocorticoids, insulin, growth hormone, and food intake, previous studies did not address the intrinsic regulatory relationships within hepatocytes over circadian time (32). We present evidence of circadian regulation of polyamine synthesis in MMH-D3 hepatocytes by the cell-autonomous clock, and, by extension, that the cell-autonomous clock may play a role in liver regeneration. In vivo, this cell-autonomous role likely integrates with systemic circadian regulatory signals to control polyamine synthesis and liver regeneration. Cell-autonomous circadian regulation may reflect the permissibility of hepatocytes to respond to systemic signals and liver injury at different times of the day, whereas systemic signals drive responses to changing external conditions.

Methods

MMH-D3 Culture. Cultures were maintained and differentiated before experiments in accordance with conditions in Amicone et al. (11). Cultures were synchronized via serum shock (37) and changed to serum-free medium for time-course collection. Cultures were incubated at 37 °C with 5% CO_2 for 12 h (microarrays) and 14 h (spermidine measurement) before the start of time-course collection.

MMH-D3 RNA and Microarray Preparation. Time-course collection began 12 h after synchronization of cultures. Every 2 h for 48-h duration, samples were collected in triplicate. Cell lysates were homogenized using Qiagen QIAshredder columns, and RNA was extracted using Qiagen RNeasy Miniprep Kit. Samples were normalized based on total RNA concentration, amplified, and applied to Affymetrix GeneChip Mouse 430 2.0 arrays per manufacturer specifications. This dataset is available at the Gene Expression Omnibus (GEO) database, www.ncbi.nlm.nih.gov/geo (accession no. GSE31049).

Microarray Analysis. The Hughes WT liver arrays were obtained from GEO accession no. GSE11923 (4) in vivo mouse liver dataset and processed using the methods described below. *Cry1*, *Cry2*$^{-/-}$ mouse liver with ad libitum feeding dataset from Vollmers et al. (7) was obtained from GEO accession no. GSE13093 as a GCRMA-normalized expression matrix. *Clock* mutant liver dataset from Miller et al. (30) was obtained from GEO accession no. GSE3748 as a GCRMA-normalized expression matrix; plotted values represent the mean of two replicate arrays at each time point. All arrays were normalized using GCRMA and present/absent calls made by MAS5 performed in R/BioConductor. For further processing, only those transcripts that surpass the present threshold for datasets being analyzed were used.

Pipeline Analysis. Present, normalized transcripts for each dataset were applied to the statistical analysis pipeline depicted in Fig. 1*A*. For signal decomposition analysis, present, normalized datasets were subjected to Fisher's *G* test implemented in the GeneCycle package and a post hoc q-value estimate performed in GeneTS according to the methods of Hughes et al. (4) to call rhythmic transcripts at distinct Fourier frequencies corresponding to periods of 48, 24, 16, 12, 8, 6, 4.6, and 4 h. BRASS FFT NLLS was applied to transcripts with a Fisher's *G* test, $q < 0.05$, to define period and phase with a confidence interval of 0.95 (16). Circadian transcripts were those with a period of 20–30 h.

For model-matching analysis, HAYSTACK (http://haystack.cgrb.oregonstate.edu/) was applied with user-defined models (Fig. S1), as described in Michael et al. (14). These models define cosine waveforms at 1-h increments from 20 to 28 h and alternate waveforms with 24-h periods (Fig. S1). Correlation cutoffs corresponding to a pseudo-FDR <0.05 were determined for the MMH-D3 dataset and the Hughes WT liver dataset using 500 and 1,000 permutations, respectively, for each resolution analyzed. The correlation cutoffs were: MMH-D3 0.6067, Hughes WT liver 1-h resolution 0.4549, Hughes WT liver 2-h resolution 0.6314, Hughes WT liver 3-h resolution 0.7639, and Hughes WT liver 4-h resolution 0.8520. When a transcript was called by both analytical arms of the pipeline, the signal decomposition phase value was used.

Functional Annotation. DAVID functional annotation clustering was performed using GO and SwissProt keywords with medium clustering stringency. Clusters with enrichment scores >1.3 (corresponding to mean $P < 0.05$) were significant (24). DAVID pathway analysis was performed using KEGG PATHWAY. Overrepresented pathways displayed a $P < 0.05$ and fold enrichment ≥1.5 (24). GO annotation for assessment of glycolysis and oxidative respiration performed in R/Biocoductor using the GOstats package (38).

qPCR. Quantitative real-time PCR was performed on the same RNA samples as used for MMH-D3 microarrays according to the methods of Liu et al. (37) using TaqMan assays and normalized based on GAPDH levels. Three replicates of each qPCR reaction were performed. Relative expression values are reported in percentage of maximum mean normalized values. Data points

reflect the percent expression mean of replicates (n = 3), and error bars represent SD of replicates.

Spermidine Measurement. Samples were collected starting 14 h after synchronization of differentiated MMH-D3 cultures. At 2-h intervals for a duration of 48 h, three live-cell pellets, each representing 10^6 cells, were collected, except for time point 23 (hour 46) in which two live-cell pellets were collected. To collect cell pellets, cultures were washed three times with cold (4 °C) PBS, trypsinized using 0.25% trypsin with EDTA, washed with PBS, flash-frozen in liquid nitrogen, and stored at −80 °C. Biochemical extraction, mass spectrometry, and metabolite quantification were performed by Metabolon (Metabolon, Inc.) as described previously (39, 40). Sample measurements were normalized by DNA concentration from each cell pellet sample. Spermidine levels represent the mean of DNA-normalized samples at each time point, and error bars are their SD.

Protein–Protein Interaction Network Construction and Analysis. Network visualization of protein–protein interactions and MMH-D3 circadian phases was performed using Cytoscape 2.8.1 (http://www.cytoscape.org/) (41). To construct the mouse PPI network, we pulled all mouse-specific interactions from iRefIndex (version 8.0), a metadatabase that combines interaction data from 10 primary databases (20) (*SI Methods*). To generate consistent network statistics regarding direct PPIs, redundant edges were collapsed into a single (undirected) edge, excluding edges representing "colocalization," and we replaced nodes for protein complexes with all pairwise edges, resulting in an undirected network of 7,052 genes and 91,457 edges. Of the 930 MMH-D3 circadian genes (1,130 transcripts), 297 mapped to nodes in the network by Entrez Gene IDs. This larger network was used for the enrichment analysis of first neighbors, which does not require a single connected component. The shortest path, closeness centrality, resistance distance, and MATISSE analyses were applied to the largest connected component—meaning all pairs of genes in the subnetwork were connected by at least one path—of this network, consisting of 5,302 genes, 230 of which were circadian.

Resistance distance was calculated using the Moore–Penrose inverse of the normalized Laplacian matrix of the largest connected component of the PPI network. The normalized Laplacian of a graph is defined as $L = I - D^{-1}A$, where I is the identity matrix, D is the degree matrix of the graph (a diagonal matrix where d_{ii} is the degree of node i), and A is the graph adjacency matrix. Mean values were calculated for all pairs of genes within each phase-difference bin, and permutation analysis was done using 1,000 permutations of the phase values across the network. P values for each bin were calculated as the proportion of the permuted bin means exceeding the mean value for that bin from the nonrandomized results.

For the analysis of first neighbors (Fig. S4B), the sets of first neighbors of every gene in the network were found, and the phase differences between all pairs of circadian genes within each neighborhood set were counted and summed across all neighborhoods. These sums were then normalized by the total number of circadian pairs in all of the neighborhoods, providing a distribution across the phase differences. This same analysis was performed on 1,000 permuted networks with the measured phase values randomly assigned to different nodes, and signed P values were calculated using the proportion of times the value in a given bin in the measured distribution was greater or less than the same value in the permuted distributions.

The MATISSE algorithm (http://acgt.cs.tau.ac.il/matisse/) (23) was applied to identify cophasic modules. We used the custom MATISSE algorithm from the program, which allowed us to specify a similarity matrix for the circadian nodes in the network, which we defined as the phase difference, normalized to the range 0–1, and raised to the fourth power. The exponent served to increase the relative similarity score of cophasic genes from those with phases differing by ≥3 h. Other chosen parameters were the minimum seed size (five nodes), the maximum seed size (five nodes), the seed strategy (all neighbors), the minimum module size (five nodes), and the maximum module size (30 nodes).

ACKNOWLEDGMENTS. This work was supported in part by National Institutes of Health Grants R01 GM074868, R01 MH051573, and P50GM085764 (to S.A.K.) and Cell and Molecular Genetics Training Program National Institutes of Health Grant GM07240 (to A.A.).

1. Hastings MH, Reddy AB, Maywood ES (2003) A clockwork web: Circadian timing in brain and periphery, in health and disease. *Nat Rev Neurosci* 4:649–661.
2. Zhang EE, Kay SA (2010) Clocks not winding down: Unravelling circadian networks. *Nat Rev Mol Cell Biol* 11:764–776.
3. Panda S, et al. (2002) Coordinated transcription of key pathways in the mouse by the circadian clock. *Cell* 109:307–320.
4. Hughes ME, et al. (2009) Harmonics of circadian gene transcription in mammals. *PLoS Genet* 5:e1000442.
5. Kornmann B, Schaad O, Bujard H, Takahashi JS, Schibler U (2007) System-driven and oscillator-dependent circadian transcription in mice with a conditionally active liver clock. *PLoS Biol* 5:e34.
6. Damiola F, et al. (2000) Restricted feeding uncouples circadian oscillators in peripheral tissues from the central pacemaker in the suprachiasmatic nucleus. *Genes Dev* 14:2950–2961.
7. Vollmers C, et al. (2009) Time of feeding and the intrinsic circadian clock drive rhythms in hepatic gene expression. *Proc Natl Acad Sci USA* 106:21453–21458.
8. Fuller PM, Lu J, Saper CB (2008) Differential rescue of light- and food-entrainable circadian rhythms. *Science* 320:1074–1077.
9. Storch KF, Weitz CJ (2009) Daily rhythms of food-anticipatory behavioral activity do not require the known circadian clock. *Proc Natl Acad Sci USA* 106:6808–6813.
10. Carneiro BT, Araujo JF (2009) The food-entrainable oscillator: A network of interconnected brain structures entrained by humoral signals? *Chronobiol Int* 26:1273–1289.
11. Amicone L, et al. (1997) Transgenic expression in the liver of truncated Met blocks apoptosis and permits immortalization of hepatocytes. *EMBO J* 16:495–503.
12. Mancone C, et al. (2010) Proteomic analysis reveals a major role for contact inhibition in the terminal differentiation of hepatocytes. *J Hepatol* 52:234–243.
13. Khan S, Rowe SC, Harmon FG (2010) Coordination of the maize transcriptome by a conserved circadian clock. *BMC Plant Biol* 10:126.
14. Michael TP, et al. (2008) Network discovery pipeline elucidates conserved time-of-day-specific cis-regulatory modules. *PLoS Genet* 4:e14.
15. Wichert S, Fokianos K, Strimmer K (2004) Identifying periodically expressed transcripts in microarray time series data. *Bioinformatics* 20:5–20.
16. Brown PE (2004) Biological Rhythms Analysis Software System. Available at: http://millar.bio.ed.ac.uk/Downloads.html.
17. Bissell DM, Levine GA, Bissell MJ (1978) Glucose metabolism by adult hepatocytes in primary culture and by cell lines from rat liver. *Am J Physiol* 234:C122–C130.
18. Covington MF, Maloof JN, Straume M, Kay SA, Harmer SL (2008) Global transcriptome analysis reveals circadian regulation of key pathways in plant growth and development. *Genome Biol* 9:R130.
19. Keegan KP, Pradhan S, Wang JP, Allada R (2007) Meta-analysis of *Drosophila* circadian microarray studies identifies a novel set of rhythmically expressed genes. *PLOS Comput Biol* 3:e208.
20. Razick S, Magklaras G, Donaldson IM (2008) iRefIndex: A consolidated protein interaction database with provenance. *BMC Bioinformatics* 9:405.
21. Newman MEJ (2005) A measure of betweenness centrality based on random walks. *Soc Networks* 27:39–54.
22. Klein DJ, Randic M (1993) Resistance distance. *J Math Chem* 12:81–95.
23. Ulitsky I, Shamir R (2007) Identification of functional modules using network topology and high-throughput data. *BMC Syst Biol* 1:8.
24. Huang W, Sherman BT, Lempicki RA (2009) Systematic and integrative analysis of large gene lists using DAVID bioinformatics resources. *Nat Protoc* 4:44–57.
25. Kuo TH, Pike DH, Beizaeipour Z, Williams JA (2010) Sleep triggered by an immune response in *Drosophila* is regulated by the circadian clock and requires the NFkappaB Relish. *BMC Neurosci* 11:17.
26. Cecon E, Fernandes PA, Pinato L, Ferreira ZS, Markus RP (2010) Daily variation of constitutively activated nuclear factor kappa B (NFKB) in rat pineal gland. *Chronobiol Int* 27:52–67.
27. Alhonen L, et al. (2002) Polyamines are required for the initiation of rat liver regeneration. *Biochem J* 362:149–153.
28. Thomas T, Thomas TJ (2003) Polyamine metabolism and cancer. *J Cell Mol Med* 7:113–126.
29. Jänne J, et al. (2005) Animal disease models generated by genetic engineering of polyamine metabolism. *J Cell Mol Med* 9:865–882.
30. Miller BH, et al. (2007) Circadian and CLOCK-controlled regulation of the mouse transcriptome and cell proliferation. *Proc Natl Acad Sci USA* 104:3342–3347.
31. Matsuo T, et al. (2003) Control mechanism of the circadian clock for timing of cell division in vivo. *Science* 302:255–259.
32. Russell DH, Byus CV, Manen CA (1976) Proposed model of major sequential biochemical events of a trophic response. *Life Sci* 19:1297–1305.
33. Forshell TP, Rimpi S, Nilsson JA (2010) Chemoprevention of B-cell lymphomas by inhibition of the Myc target spermidine synthase. *Cancer Prev Res (Phila)* 3:140–147.
34. Bello-Fernandez C, Packham G, Cleveland JL (1993) The ornithine decarboxylase gene is a transcriptional target of c-Myc. *Proc Natl Acad Sci USA* 90:7804–7808.
35. Sherman H, Froy O (2008) Expression of human beta-defensin 1 is regulated via c-Myc and the biological clock. *Mol Immunol* 45:3163–3167.
36. Bozek K, Rosahl AL, Gaub S, Lorenzen S, Herzel H (2010) Circadian transcription in liver. *Biosystems* 102:61–69.
37. Liu AC, et al. (2008) Redundant function of REV-ERBalpha and beta and non-essential role for Bmal1 cycling in transcriptional regulation of intracellular circadian rhythms. *PLoS Genet* 4:e1000023.
38. Falcon S, Gentleman R (2007) Using GOstats to test gene lists for GO term association. *Bioinformatics* 23:257–258.
39. Evans AM, DeHaven CD, Barrett T, Mitchell M, Milgram E (2009) Integrated, nontargeted ultrahigh performance liquid chromatography/electrospray ionization tandem mass spectrometry platform for the identification and relative quantification of the small-molecule complement of biological systems. *Anal Chem* 81:6656–6667.
40. Ryals J, Lawton K, Stevens D, Milburn M (2007) Metabolon, Inc. *Pharmacogenomics* 8:863–866.
41. Smoot ME, Ono K, Ruscheinski J, Wang PL, Ideker T (2011) Cytoscape 2.8: New features for data integration and network visualization. *Bioinformatics* 27:431–432.

Supporting Information

Atwood et al. 10.1073/pnas.1115753108

SI Methods

The mouse protein–protein interaction network was downloaded from the iRefIndex metadatabase, which combines 10 primary PPI databases: BIND (1, 2), BioGRID (3), CORUM (4), DIP (5), HPRD (6, 7), IntAct (8, 9), MINT (10), MPact (11), MPPI (12), and OPHID (13). Network visualization was performed in Cytoscape 2.8.1 (http://www.cytoscape.org/) (14).

1. Bader GD, Betel D, Hogue CWV (2003) BIND: The Biomolecular Interaction Network Database. *Nucleic Acids Res* 31:248–250.
2. Alfarano C, et al. (2005) The Biomolecular Interaction Network Database and related tools 2005 update. *Nucleic Acids Res* 33(Database issue):D418–D424.
3. Stark C, et al. (2006) BioGRID: A General Repository for Interaction Datasets. *Nucleic Acids Res* 34(Database issue):D535–D539.
4. Ruepp A, et al. (2010) CORUM: The Comprehensive Resource of Mammalian Protein Complexes—2009. *Nucleic Acids Res* 38(Database issue):D497–D501.
5. Salwinski L, et al. (2004) The Database of Interacting Proteins: 2004 update. *Nucleic Acids Res* 32(Database issue):D449–D451.
6. Peri S, et al. (2003) Development of human protein reference database as an initial platform for approaching systems biology in humans. *Genome Res* 13:2363–2371.
7. Mishra GR, et al. (2006) Human Protein Reference Database—2006 update. *Nucleic Acids Res* 34(Database issue):D411–D414.
8. Hermjakob H, et al. (2004) IntAct: An open source molecular interaction database. *Nucleic Acids Res* 32(Database issue):D452–D455.
9. Kerrien S, et al. (2007) IntAct—open source resource for molecular interaction data. *Nucleic Acids Res* 35(Database issue):D561–D565.
10. Chatr-aryamontri A, et al. (2007) MINT: The Molecular INTeraction database. *Nucleic Acids Res* 35(Database issue):D572–D574.
11. Güldener U, et al. (2006) MPact: The MIPS protein interaction resource on yeast. *Nucleic Acids Res* 34(Database issue):D436–D441.
12. Pagel P, et al. (2005) The MIPS mammalian protein–protein interaction database. *Bioinformatics* 21:832–834.
13. Brown KR, Jurisica I (2005) Online predicted human interaction database. *Bioinformatics* 21:2076–2082.
14. Smoot ME, Ono K, Ruscheinski J, Wang PL, Ideker T (2011) Cytoscape 2.8: New features for data integration and network visualization. *Bioinformatics* 27:431–432.

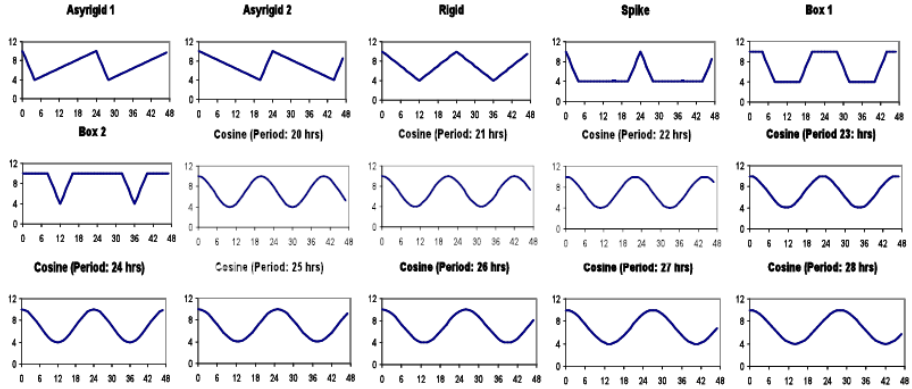

Fig. S1. HAYSTACK waveforms, displayed at 1-h resolution. These models represent the variety of shapes and periods used for HAYSTACK analysis. All base waveforms peak at time 0 (first time-point), but these models are progressively shifted by 1-h increments to achieve all possible phases. These waveforms are converted to lower resolution by removing intermediate points for analysis with 2-, 3-, or 4-h resolution data.

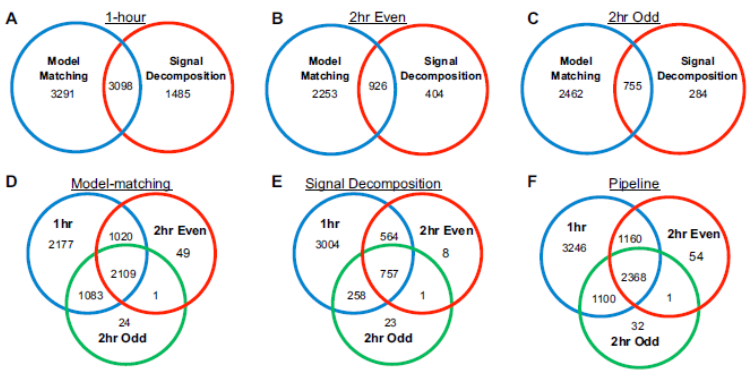

Fig. S2. Comparison of circadian calls for individual analytic methods and our pipeline. Two analytic methods as used in the pipeline, model matching and signal decomposition circadian calls from the same data are compared at 1-h (*A*), 2-h resolution with time points collected at even circadian times (2-h even; *B*), and 2-h resolution with time points collected at odd circadian times (2-h odd; *C*). The consistency of circadian calls between 1- and 2-h resolution was assessed for individual analytic methods and the overall pipeline using the three datasets presented in *A*–*C*: model matching (*D*), signal decomposition (*E*), and the pipeline (*F*).

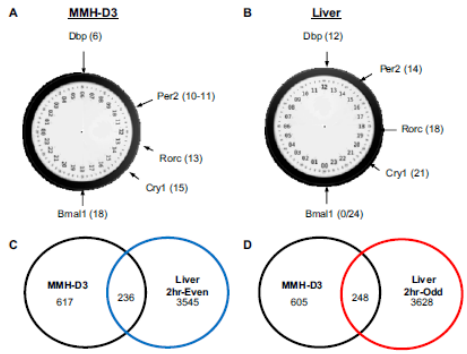

Fig. S3. Comparison of MMH-D3 to the Hughes WT liver dataset. (*A* and *B*) Phase differences of clock genes throughout the circadian (24-h) day in MMH-D3 (*A*) reflects that seen in the Hughes WT liver (*B*), indicating that the clock is intact. Because MMH-D3 hepatocytes do not receive systemic entrainment signals regarding external conditions, phase 0 was chosen as the start of time-course collection. MMH-D3 phases can be directly compared with those of the liver by adding 6 h to the MMH-D3 phase value. (*C* and *D*) Direct comparison of MMH-D3 and the Hughes WT liver dataset subsampled at 2-h resolution using our pipeline revealed that MMH-D3 displays a 28% concordance with the liver samples at even circadian times (*C*), and 29% compared with the liver samples at odd circadian times (*D*) (1).

1. Hughes ME, et al. (2009) Harmonics of circadian gene transcription in mammals. *PLoS Genet* 5:e1000442.

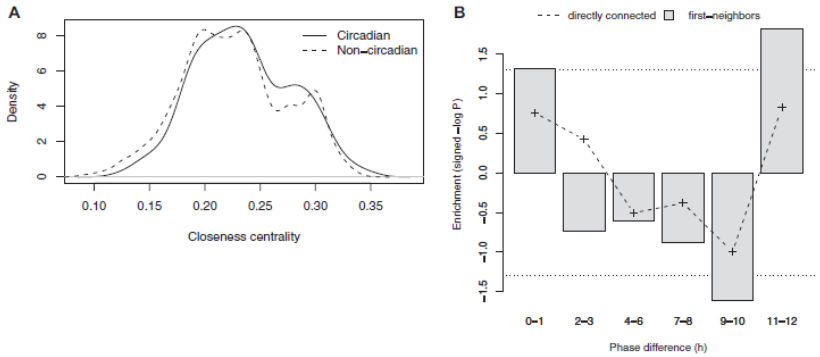

Fig. S4. PPI network statistics for circadian genes. (*A*) Circadian genes are central to the global PPI network. Smoothed densities of closeness centrality for both circadian and noncircadian nodes (Wilcoxon rank-sum test, $P = 0.017$). (*B*) Enrichments for each phase difference (in hours) among first neighbors of genes in the PPI network. *P* values represent the proportion of times that pair genes with the given phase difference were co-first neighbors at a higher frequency than seen at random across 1,000 permutations. The dashed line is the same proportion but between directly connected gene pairs only. The dotted lines represent the cutoff for <5% of permuted results having greater or lesser frequency.

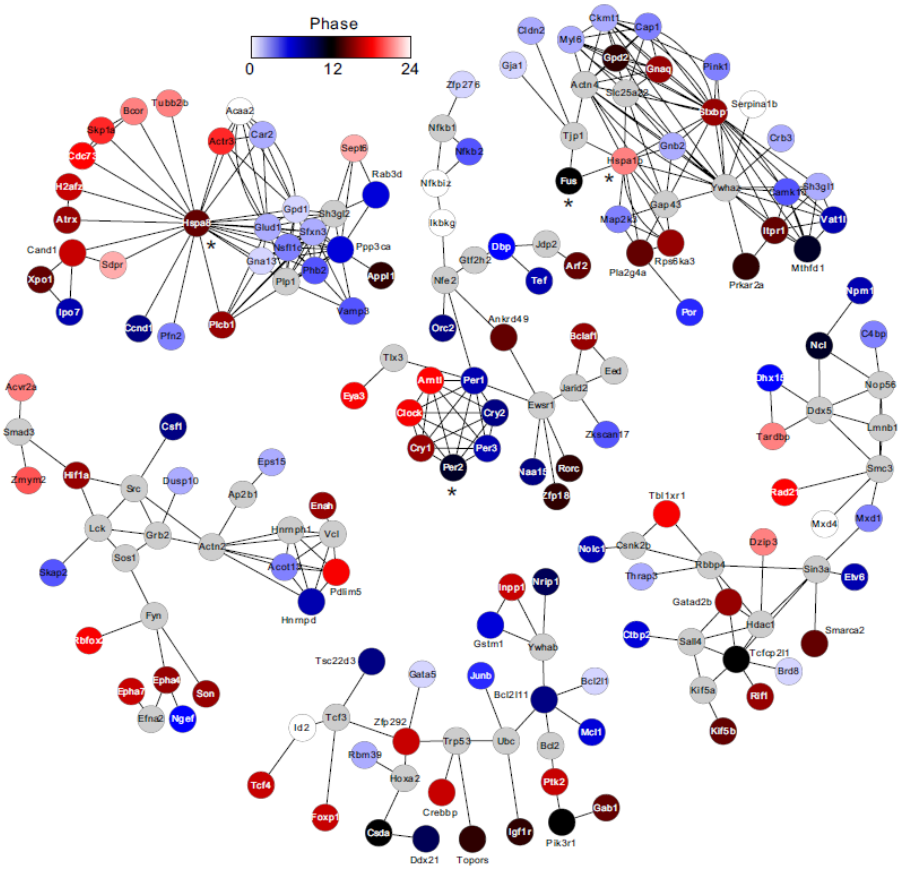

Fig. S5. Enlarged version of the MATISSE modules from Fig. 3C, with the addition of gene names and asterisks (*) marking the cycling genes that were also present in the 29 systemically driven circadian genes from Kornmann et al. (1).

1. Kommann B, Schaad O, Bujard H, Takahashi JS, Schibler U (2007) System-driven and oscillator-dependent circadian transcription in mice with a conditionally active liver clock. *PLoS Biol* 5:e34.

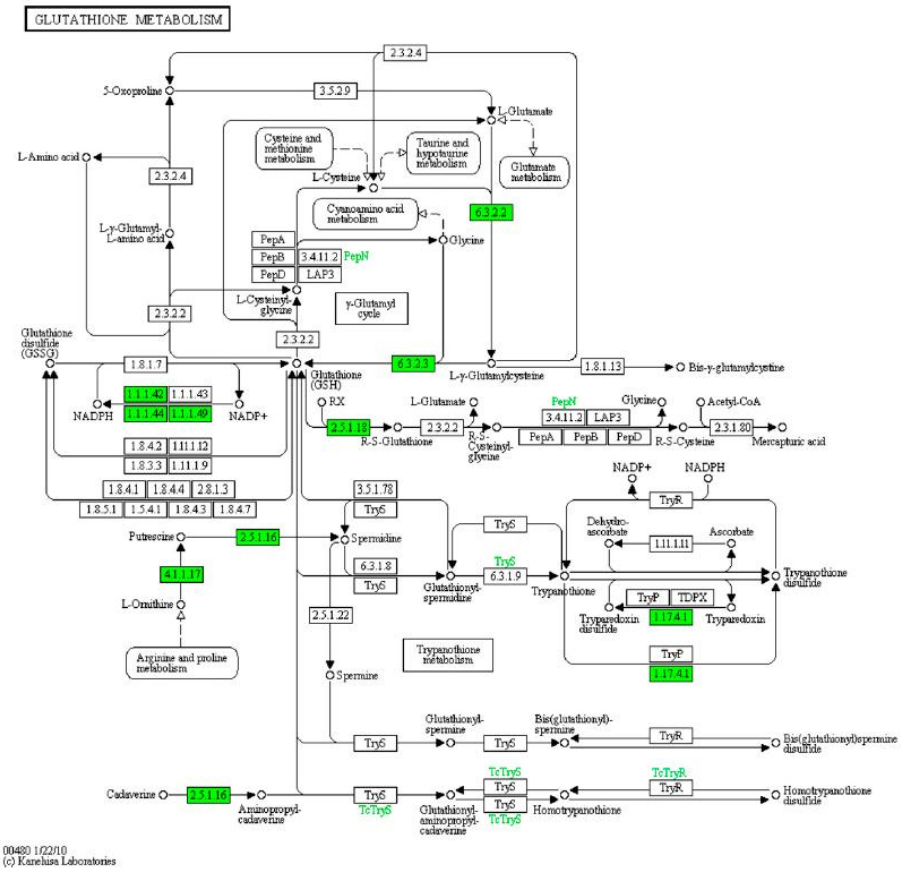

Fig. S6. MMH-D3 circadian list displays enrichment in the KEGG glutathione metabolism pathway. MMH-D3 circadian calls are highlighted in green and genes are as follows. 6.3.2.2: glutamate-cysteine ligase, catalytic subunit (Gclc); 6.3.2.3: glutathione synthetase (Gss); 2.5.1.18: GST, mu subunit 1 (Gstm1), GST, mu subunit 2 (Gstm2); 1.1.1.42: isocitrate dehydrogenase 1 (NADP+), soluble (Idh1); 1.1.1.44: phosphogluconate dehydrogenase (Pgd); 1.1.1.49: glucose-6-phosphate dehydrogenase, X-linked (G6pdx); 2.5.1.16: spermidine synthase (Srm); 4.1.1.17: ornithine decarboxlyase (Odc1); 1.17.4.1: ribonucleotide reductase M2 B (TP53 inducible; Rrm2b).

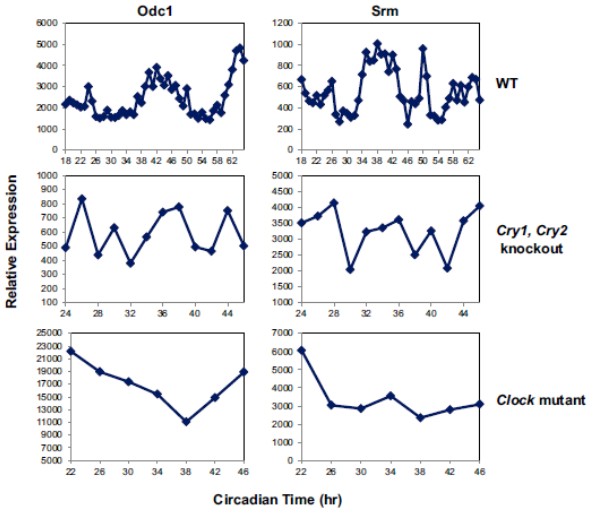

Fig. S7. Microarray traces for Odc1 and Srm in ad libitum-fed mice of the following genotypes: WT from the Hughes et al's (1) WT liver dataset (*A* and *B*), Miller et al.'s (2) *Clock* mutant dataset (*C* and *D*), and Vollmers et al.'s (3) *Cry1*, *Cry2* knockout dataset (*E* and *F*). Times expressed in hours of circadian time (CT).

1. Hughes ME, et al. (2009) Harmonics of circadian gene transcription in mammals. *PLoS Genet* 5:e1000442.
2. Miller BH, et al. (2007) Circadian and CLOCK-controlled regulation of the mouse transcriptome and cell proliferation. *Proc Natl Acad Sci USA* 104:3342–3347.
3. Vollmers C, et al. (2009) Time of feeding and the intrinsic circadian clock drive rhythms in hepatic gene expression. *Proc Natl Acad Sci USA* 106:21453–21458.

Table S1. Circadian transcripts identified in MMH-D3 hepatocytes by our bioinformatic pipeline

Table S1

Table S2. DAVID functional annotation clustering for GO terms and SwissProt keywords on the MMH-D3 circadian transcript list revealed enrichment in a wide range of biological processes and functions

Table S2

Enriched clusters display enrichment scores ≥1.3 (corresponds to a mean *P* value for included terms <0.05).

Table S3. KEGG pathways identified as enriched in circadian transcripts by DAVID pathway analysis

Table S3

Overrepresentation was determined by a combination *P* value and fold enrichment, where a term was significant with a $P < 0.05$ and had a fold enrichment ≥1.5.

Acknowledgements:

Chapter 3, in full, is a reprint of the article published in the journal *Proceedings of the National Academy of Sciences, USA* with the combining of captions with respective supplementary tables (Tables S1, Table S2, and Table S3) in the Chapter 3 appendices:

Atwood A, DeConde R, Wang SS, Mockler TC, Ideker T & SA Kay (2011) Cell-autonomous circadian clock of hepatocytes drives rhythms in transcription and polyamine synthesis. *Proc Natl Acad Sci U S A* 108:18560-18565.

The dissertation author was the primary investigator and author of this paper.

Appendix 1: Table S1

Table S1: Circadian transcripts identified in MMH-D3 hepatocytes by our bioinformatic pipeline.

	Signal Deocomposition			Model-Matching				Final Statistics and Annotations					
Transcript ID (Affymetrix probeset)	Fisher's G Test q-value	Period (hrs)	Phase	HAYSTACK Best Model	HAYSTACK Correlation	Period (hrs)	Phase	Phase (Final)	Gene Symbol	Description	GenBank	Entrez Gene	UniGene
1415721_a_at	0.019562699	21.8	10					10	Nat15	N-acetyltransferase 15 (GCN5-related, putative)	AK004750	74763	Mm.477486
1415724_a_at	0.001838832	25.5	20					20	Cdc42	cell division cycle 42 homolog (S. cerevisiae)	AV000235	12540	Mm.1022, Mm.447553, Mm.475151
1415772_at				cos_per_28_ph_08	0.726856189	28	8	8	Ncl	nucleolin	BF118393	17975	Mm.154378, Mm.474153
1415773_at				cos_per_28_ph_11	0.745251737	28	11	11	Ncl	nucleolin	BF118393	17975	Mm.154378, Mm.474153
1415776_at	0.030631652	25.3	6					6	Aldh3a2	aldehyde dehydrogenase family 3, subfamily A2	NM_007437	11671	Mm.398221
1415801_at				cos_per_28_ph_25	0.65047543	28	1	1	Gja1	gap junction protein, alpha 1	M63801	14609	Mm.378921, Mm.477216
1415843_at				cos_per_27_ph_02	0.650207355	27	2	2	Gbl	G protein beta subunit-like	NM_019988	56716	Mm.289516
1415899_at	0.003501032	30	29					5	Junb	Jun-B oncogene	NM_008416	16477	Mm.1167, Mm.470093
1415929_at	0.047506378	23.6	3					3	Map1lc3b	microtubule-associated protein 1 light chain 3 beta	AU080586	67443	Mm.28357
1415989_at	0.037419838	21.3	11					11	Vcam1	vascular cell adhesion molecule 1	BB250384	22329	Mm.440909, Mm.76649
1416039_x_at				box1_ph_05	0.6112894	24	5	5	Cyr61	cysteine rich protein 61	NM_010516	16007	Mm.1231
1416084_at	0.026898234	20.9	18					18	Zfand5	zinc finger, AN1-type domain 5	AA124553	22682	Mm.292405, Mm.379919
1416085_s_at	0.028541867	20.2	18					18	Zfand5	zinc finger, AN1-type domain 5	AA124553	22682	Mm.292405, Mm.379919
1416092_a_at				rigid_ph_15	0.628418972	24	15	15	Mtap4	microtubule-associated protein 4	BB000894	17758	Mm.217318, Mm.443428
1416112_at				spike_ph_05	0.614462166	24	5	5	Cox8a	cytochrome c oxidase, subunit VIIIa	NM_007750	12868	Mm.14022
1416131_s_at	0.018028218	30	13					13	Efr3a	EFR3 homolog A (S. cerevisiae)	BB188557	76740	Mm.260647
1416133_at	0.048733278	23.3	15					15	Efr3a	EFR3 homolog A (S. cerevisiae)	BB188557	76740	Mm.260647
1416145_at	0.003615541	28.2	6					6	Dhx15	DEAH (Asp-Glu-Ala-His) box polypeptide 15	BC003745	13204	Mm.993
1416166_a_at				cos_per_28_ph_19	0.722649462	28	19	19	Prdx4	peroxiredoxin 4	NM_016764	53381	Mm.247542
1416185_a_at	0.039036878	29.7	10					10	Adh5	alcohol dehydrogenase 5 (class III), chi polypeptide	NM_007410	11532	Mm.3874
1416188_at				cos_per_28_ph_20	0.62653475	28	20	20	Gm2a	GM2 ganglioside activator protein	BC004651	14667	Mm.287807

Table S1: Circadian transcripts (continued)

	Signal Deocomposition			Model-Matching				Final Statistics and Annotations					
Transcript ID (Affymetrix probeset)	Fisher's G Test q-value	Period (hrs)	Phase	HAYSTACK Best Model	HAYSTACK Correlation	Period (hrs)	Phase	Phase (Final)	Gene Symbol	Description	GenBank	Entrez Gene	UniGene
1416204_at				cos_per_27_ph_02	0.75785445	27	2	2	Gpd1	glycerol-3-phosphate dehydrogenase 1 (soluble)	BC019391	14555	Mm.252391
1416236_a_at				cos_per_26_ph_13	0.6178609	26	13	13	Mpzl2	myelin protein zero-like 2	BC015076	14012	Mm.33240
1416237_at	0.044895773	25.5	9					9	Mpzl2	myelin protein zero-like 2	BC015076	14012	Mm.33240
1416267_at				cos_per_28_ph_16	0.684348771	28	16	16	Scoc	short coiled-coil protein	NM_019708	56367	Mm.246911
1416297_s_at	0.030172394	23.3	4					4	Reg3b	regenerating islet-derived 3 beta	NM_011036	18489	Mm.2553
1416325_at				asyrigid2_ph_00	0.61399999	24	0	0	Crisp1	cysteine-rich secretory protein 1	NM_009638	11571	Mm.16781
1416328_a_at	0.008137639	26.1	1					1	Atp6v0e	ATPase, H+ transporting, lysosomal V0 subunit E	NM_025272	11974	Mm.22602
1416338_at	0.027512419	25.6	2					2	Sh3gl1	SH3-domain GRB2-like 1	NM_013664	20405	Mm.1773
1416360_at				box2_ph_17	0.609911313	24	17	17	Snx18	sorting nexin 18	AV344473	170625	Mm.33721
1416383_a_at				cos_per_25_ph_04	0.675480042	25	4	4	Pcx	pyruvate carboxylase	NM_008797	18563	Mm.1845
1416384_a_at	0.033759214	26	26					2	Cope	coatomer protein complex, subunit epsilon	NM_021538	59042	Mm.28668
1416411_at				cos_per_28_ph_24	0.648509986	28	0	0	Gstm2	glutathione S-transferase, mu 2	NM_008183	14863	Mm.440086
1416416_x_at	0.043130004	29.2	25	cos_per_27_ph_26	0.729375965	27	2	1	Gstm1	glutathione S-transferase, mu 1	NM_010358	14862	Mm.37199
1416447_at	0.016202741	26.8	18					18	Tmem30a	transmembrane protein 30A	BE986812	69981	Mm.355034
1416462_at	0.015637466	25.4	12					12	Caprin1	cell cycle associated protein 1	BE981338	53872	Mm.427589, Mm.469202
1416482_at				spike_ph_14	0.739532328	24	14	14	Ttc3	tetratricopeptide repeat domain 3	BB833716	22129	Mm.213408
1416496_at	0.029359784	29.4	23					23	Mrfap1	Morf4 family associated protein 1	BC010209	67568	Mm.332336, Mm.477721
1416502_a_at	0.035421703	27.7	0					0	Preb	prolactin regulatory element binding	NM_016703	50907	Mm.272414, Mm.477289
1416556_at	0.00224841	29.7	27					3	Tspan31	tetraspanin 31	NM_025982	67125	Mm.35650
1416649_at				cos_per_25_ph_03	0.682391298	25	3	3	Ambp	alpha 1 microglobulin/bikunin	NM_007443	11699	Mm.2197
1416654_at	0.043193383	29	22					22	Slc31a2	solute carrier family 31, member 2	NM_025286	20530	Mm.292539

Table S1: Circadian transcripts (continued)

	Signal Deocomposition			Model-Matching				Final Statistics and Annotations					
Transcript ID (Affymetrix probeset)	Fisher's G Test q-value	Period (hrs)	Phase	HAYSTACK Best Model	HAYSTACK Correlation	Period (hrs)	Phase	Phase (Final)	Gene Symbol	Description	GenBank	Entrez Gene	UniGene
1416659_at	0.046172379	25.5	12					12	Eif3a	eukaryotic translation initiation factor 3, subunit A	AW701127	13669	Mm.2238
1416673_at				cos_per_28_ph_24	0.710442615	28	0	0	Bace2	beta-site APP-cleaving enzyme 2	NM_019517	56175	Mm.97885
1416682_at				box2_ph_17	0.653957992	24	17	17	Ube3a	ubiquitin protein ligase E3A	AK018443	22215	Mm.9002
1416701_at	0.001838832	30	0					0	Rnd3	Rho family GTPase 3	BC009002	74194	Mm.46497
1416712_at	0.026839179	22	6					6	Pepd	peptidase D	NM_008820	18624	Mm.69751
1416730_at				cos_per_28_ph_08	0.623690591	28	8	8	Rcll	RNA terminal phosphate cyclase-like 1	BC004574	59028	Mm.28630
1416766_at	0.047133857	29.9	29					5	Moxc2	MOCO sulphurase C-terminal domain containing 2	NM_133684	67247	Mm.177724
1416770_at				cos_per_27_ph_02	0.84576641	27	2	2	Stk25	serine/threonine kinase 25 (yeast)	NM_021537	59041	Mm.28761
1416773_at	0.003123911	21.2	10	cos_per_21_ph_10	0.87292078	21	10	10	Wee1	WEE 1 homolog 1 (S. pombe)	NM_009516	22390	Mm.287173
1416774_at	0.019262207	21	11	cos_per_21_ph_11	0.819871231	21	11	11	Wee1	WEE 1 homolog 1 (S. pombe)	NM_009516	22390	Mm.287173
1416778_at				cos_per_28_ph_22	0.610138789	28	22	22	Sdpr	serum deprivation response	BE197945	20324	Mm.398690
1416779_at				cos_per_28_ph_22	0.63122582	28	22	22	Sdpr	serum deprivation response	BE197945	20324	Mm.398690
1416811_s_at				spike_ph_02	0.621215521	24	2	2	Ctla2a	cytotoxic T lymphocyte-associated protein 2 alpha	NM_007796	13024	Mm.30144
1416816_at	0.022895127	21.4	18					18	Nek7	NIMA (never in mitosis gene a)-related expressed kinase 7	NM_021605	59125	Mm.143817
1416823_a_at				cos_per_21_ph_14	0.730489669	21	14	14	Osbpl1a	oxysterol binding protein-like 1A	NM_020573	64291	Mm.259470, Mm.443224
1416880_at	0.012818239	20.4	7					7	Mcl1	myeloid cell leukemia sequence 1	BC003839	17210	Mm.1639
1416892_s_at	0.014197191	23.6	5					5	Fam107b	family with sequence similarity 107, member B	BC021353	66540	Mm.277864
1416925_at	0.016461376	24.8	13					13	Kpnb1	karyopherin (importin) beta 1	NM_008379	16211	Mm.251013
1416929_at				cos_per_26_ph_16	0.688913607	26	16	16	Rbm12	RNA binding motif protein 12	NM_029397	75710	Mm.27660, Mm.441281
1416933_at	0.001838832	27	5					5	Por	P450 (cytochrome) oxidoreductase	NM_008898	18984	Mm.3863
1416958_at	0.001838832	24.3	6	box1_ph_06	0.886754619	24	6	6	Nr1d2	nuclear receptor subfamily 1, group D, member 2	NM_011584	353187	Mm.26587
1416959_at	0.001838832	27	5	cos_per_26_ph_05	0.871547743	26	5	5	Nr1d2	nuclear receptor subfamily 1, group D, member 2	NM_011584	353187	Mm.26587

Table S1: Circadian transcripts (continued)

	Signal Decomposition			Model-Matching				Final Statistics and Annotations					
Transcript ID (Affymetrix probeset)	Fisher's G Test q-value	Period (hrs)	Phase	HAYSTACK Best Model	HAYSTACK Correlation	Period (hrs)	Phase	Phase (Final)	Gene Symbol	Description	GenBank	Entrez Gene	UniGene
1416984_at	0.01951333	24.6	2					2	Mrps18a	mitochondrial ribosomal protein S18A	NM_026768	68565	Mm.287443
1417030_at				box2_ph_17	0.639974668	24	17	17	Tmem206	transmembrane protein 206	NM_025864	66950	Mm.236300
1417031_at				asyrigid2_ph_11	0.633511854	24	11	11	Tmem206	transmembrane protein 206	NM_025864	66950	Mm.236300
1417040_a_at				cos_per_27_ph_01	0.695145222	27	1	1	Bok	BCL2-related ovarian killer protein	NM_016778	51800	Mm.3295
1417065_at				cos_per_28_ph_24	0.665194568	28	0	0	Egr1	early growth response 1	NM_007913	13653	Mm.181959
1417073_a_at				cos_per_28_ph_12	0.779879981	28	12	12	Qk	quaking	NM_021881	19817	Mm.384135, Mm.393248
1417089_a_at				cos_per_28_ph_25	0.633822929	28	1	1	Ckmt1	creatine kinase, mitochondrial 1, ubiquitous	NM_009897	12716	Mm.252145
1417108_at	0.019168853	27.1	1					1	Klc4	kinesin light chain 4	NM_029091	74764	Mm.279599
1417113_at	0.044057725	25.2	1					1	Gmcll	germ cell-less homolog 1 (Drosophila)	AF163665	23885	Mm.321452
1417122_at	0.04976808	21.6	19	asyrigid1_ph_22	0.707653662	24	22	19	Vav3	vav 3 oncogene	BC027242	57257	Mm.282257
1417135_at				box2_ph_15	0.630583425	24	15	15	Srpk2	serine/arginine-rich protein specific kinase 2	NM_009274	20817	Mm.288728
1417164_at	0.004822861	25.4	2	cos_per_25_ph_03	0.785866611	25	3	2	Dusp10	dual specificity phosphatase 10	NM_022019	63953	Mm.404024
1417179_at	0.001975425	27.1	0	cos_per_26_ph_01	0.855673905	26	1	0	Tspan5	tetraspanin 5	NM_019571	56224	Mm.31927
1417182_at	0.010207225	29.6	4					4	Dnaja2	DnaJ (Hsp40) homolog, subfamily A, member 2	C77509	56445	Mm.477493
1417183_at	0.031820157	26.4	7					7	Dnaja2	DnaJ (Hsp40) homolog, subfamily A, member 2	C77509	56445	Mm.477493
1417190_at	0.040690992	20.3	10					10	Nampt	nicotinamide phosphoribosyltransferase	AW989410	59027	Mm.202727
1417199_at	0.015681018	29.4	2					2	Tmem183a	transmembrane protein 183A	AK007779	57439	Mm.393140
1417215_at				asyrigid1_ph_23	0.724675794	24	23	23	Rab27b	RAB27b, member RAS oncogene family	BB121269	80718	Mm.246753
1417225_at				rigid_ph_04	0.617700395	24	4	4	Arl6ip5	ADP-ribosylation factor-like 6 interacting protein 5	NM_022992	65106	Mm.291014
1417232_at				cos_per_28_ph_26	0.631797198	28	2	2	Cldn2	claudin 2	NM_016675	12738	Mm.117068
1417272_at	0.006551085	22.9	4					4	Fam114a1	family with sequence similarity 114, member A1	NM_026667	68303	Mm.258545, Mm.477418
1417279_at				rigid_ph_15	0.644694169	24	15	15	Itpr1	inositol 1,4,5-triphosphate receptor 1	NM_010585	16438	Mm.227912

Table S1: Circadian transcripts (continued)

	Signal Deconposition			Model-Matching				Final Statistics and Annotations					
Transcript ID (Affymetrix probeset)	Fisher's G Test q-value	Period (hrs)	Phase	HAYSTACK Best Model	HAYSTACK Correlation	Period (hrs)	Phase	Phase (Final)	Gene Symbol	Description	GenBank	Entrez Gene	UniGene
1417290_at				cos_per_28_ph_24	0.66267253	28	0	0	Lrg1	leucine-rich alpha-2-glycoprotein 1	NM_029796	76905	Mm.348025
1417306_at	0.006209104	24.9	25					1	Tyk2	tyrosine kinase 2	NM_018793	54721	Mm.20249, Mm.450004
1417316_at	0.017130766	26	3					3	Them2	thioesterase superfamily member 2	NM_025790	66834	Mm.2125
1417370_at				cos_per_25_ph_04	0.693812783	25	4	4	Tff3	trefoil factor 3, intestinal	NM_011575	21786	Mm.4641
1417405_at	0.015683129	22.4	5					5	Stard3	START domain containing 3	NM_021547	59045	Mm.265546
1417420_at	0.040986717	22.6	11					11	Ccnd1	cyclin D1	NM_007631	12443	Mm.273049
1417421_at				cos_per_26_ph_01	0.668209947	26	1	1	S100a1	S100 calcium binding protein A1	BC005590	20193	Mm.24662
1417424_at	0.027742562	24.1	19					19	Ier3ip1	immediate early response 3 interacting protein 1	BE287896	66191	Mm.28593
1417461_at	0.048295211	29.7	27					3	Cap1	CAP, adenylate cyclase-associated protein 1 (yeast)	NM_007598	12331	Mm.8687
1417480_at				cos_per_25_ph_02	0.645019512	25	2	2	Fbxo9	f-box protein 9	NM_023605	71538	Mm.28584
1417517_at	0.033535292	29.8	11					11	Plagl2	pleiomorphic adenoma gene-like 2	NM_018807	54711	Mm.103199
1417519_at				cos_per_28_ph_12	0.643048745	28	12	12	Plagl2	pleiomorphic adenoma gene-like 2	NM_018807	54711	Mm.103199
1417602_at	0.001838832	24.1	10	rigid_ph_10	0.943734804	24	10	10	Per2	period homolog 2 (Drosophila)	AF035830	18627	Mm.218141
1417603_at	0.001838832	23	11					11	Per2	period homolog 2 (Drosophila)	AF035830	18627	Mm.218141
1417612_at	0.037477099	21.3	17					17	Ier5	immediate early response 5	BF147705	15939	Mm.12246
1417633_at				cos_per_28_ph_23	0.620445414	28	23	23	Sod3	superoxide dismutase 3, extracellular	NM_011435	20657	Mm.2407
1417689_a_at				cos_per_28_ph_27	0.681433887	28	3	3	Pdzk1ip1	PDZK1 interacting protein 1	BC013542	67182	Mm.30181
1417744_a_at	0.001838832	25.3	3					3	Ralb	v-ral simian leukemia viral oncogene homolog B (ras related)	BC006907	64143	Mm.27832
1417777_at				cos_per_28_ph_21	0.622123777	28	21	21	Ptgr1	prostaglandin reductase 1	BC014865	67103	Mm.34497
1417785_at	0.001838832	21.6	11					11	Pla1a	phospholipase A1 member A	NM_134102	85031	Mm.279805
1417802_at				cos_per_27_ph_25	0.669562651	27	1	1	1110032A04Rik	RIKEN cDNA 1110032A04 gene	AF365876	66183	Mm.45481
1417818_at	0.047473178	28.6	8					8	Wwtr1	WW domain containing transcription regulator 1	BC014727	97064	Mm.405029

Table S1: Circadian transcripts (continued)

	Signal Decomposition			Model-Matching				Final Statistics and Annotations					
Transcript ID (Affymetrix probeset)	Fisher's G Test q-value	Period (hrs)	Phase	HAYSTACK Best Model	HAYSTACK Correlation	Period (hrs)	Phase	Phase (Final)	Gene Symbol	Description	GenBank	Entrez Gene	UniGene
1417834_at	0.002133119	23.5	1					1	Synj2bp	synaptojanin 2 binding protein	NM_025292	24071	Mm.279603
1417846_at				box2_ph_06	0.639252225	24	6	6	Ulk2	Unc-51 like kinase 2 (C. elegans)	NM_013881	29869	Mm.162025
1417858_at				asyrigid1_ph_08	0.674237344	24	8	8	Rasal1	RAS protein activator like 1 (GAP1 like)	NM_013832	19415	Mm.41209
1417860_a_at				cos_per_28_ph_24	0.688607996	28	0	0	Spon2	spondin 2, extracellular matrix protein	NM_133903	100689	Mm.34694
1417877_at	0.021744521	25.1	2					2	Eepd1	endonuclease/exonuclease/phosphatase family domain containing 1	NM_026189	67484	Mm.112977
1417898_at	0.010431202	24.5	2					2	Sfxn3	sideroflexin 3	NM_053197	94280	Mm.36169
1417896_at				cos_per_28_ph_26	0.660183482	28	2	2	Tjp3	tight junction protein 3	NM_013769	27375	Mm.27984
1417959_at				spike_ph_01	0.654647052	24	1	1	Pdlim7	PDZ and LIM domain 7	NM_026131	67399	Mm.275648
1418024_at				asyrigid2_ph_09	0.644493139	24	9	9	Narg1	NMDA receptor-regulated gene 1	BG067031	74838	Mm.275281, Mm.392111
1418037_at				cos_per_25_ph_03	0.677616448	25	3	3	C4bp	complement component 4 binding protein	NM_007576	12269	Mm.306720
1418081_at	0.041835007	25.8	1					1	Dnajc30	DnaJ (Hsp40) homolog, subfamily C, member 30	NM_025362	66114	Mm.178012
1418089_at	0.013597156	25.8	3					3	Stx8	syntaxin 8	NM_018768	55943	Mm.3973
1418091_at	0.048078242	20.3	12					12	Tcfcp2l1	transcription factor CP2-like 1	NM_023755	81879	Mm.24621
1418113_at				cos_per_26_ph_03	0.63387709	26	3	3	Cyp2d10	cytochrome P450, family 2, subfamily d, polypeptide 10	BC010989	13101	Mm.174372
1418117_at				asyrigid2_ph_00	0.626013778	24	0	0	Ndufs4	NADH dehydrogenase (ubiquinone) Fe-S protein 4	NM_010887	17993	Mm.253142, Mm.399745
1418174_at	0.001838832	22.9	6	cos_per_24_ph_06	0.892158894	24	6	6	Dbp	D site albumin promoter binding protein	BC018323	13170	Mm.24222, Mm.378235
1418206_at	0.005989537	29.8	22					22	Sdf2l1	stromal cell-derived factor 2-like 1	NM_022324	64136	Mm.30222
1418209_a_at	0.018104112	20.3	3					3	Pfn2	profilin 2	NM_019410	18645	Mm.271744
1418219_at	0.027474156	24.8	2					2	Il15	interleukin 15	NM_008357	16168	Mm.4392
1418225_at				cos_per_28_ph_09	0.646307661	28	9	9	Orc2l	origin recognition complex, subunit 2-like (S. cerevisiae)	BB830976	18393	Mm.3411
1418226_at				cos_per_28_ph_09	0.631662602	28	9	9	Orc2l	origin recognition complex, subunit 2-like (S. cerevisiae)	BB830976	18393	Mm.3411
1418227_at				asyrigid2_ph_09	0.626633148	24	9	9	Orc2l	origin recognition complex, subunit 2-like (S. cerevisiae)	BB830976	18393	Mm.3411

Table S1: Circadian transcripts (continued)

	Signal Decomposition			Model-Matching				Final Statistics and Annotations					
Transcript ID (Affymetrix probeset)	Fisher's G Test q-value	Period (hrs)	Phase	HAYSTACK Best Model	HAYSTACK Correlation	Period (hrs)	Phase	Phase (Final)	Gene Symbol	Description	GenBank	Entrez Gene	UniGene
1418246_at				box2_ph_17	0.611363286	24	17	17	Rbm9	RNA binding motif protein 9	BG277926	93686	Mm.202774
1418282_x_at				asyrigid2_ph_00	0.630932036	24	0	0	Serpina1b	serine (or cysteine) peptidase inhibitor, clade A, member 1B	NM_009244	20701	Mm.439692, Mm.439693, Mm.458700
1418300_a_at	0.015530464	21.4	7					7	Mknk2	MAP kinase-interacting serine/threonine kinase 2	NM_021462	17347	Mm.42126, Mm.472174
1418312_at				rigid_ph_01	0.615014037	24	1	1	Zfp276	zinc finger protein (CZH2 type) 276	BB667131	57247	Mm.379084
1418332_a_at				box2_ph_16	0.667367094	24	16	16	Agtpbp1	ATP/GTP binding protein 1	NM_023328	67269	Mm.153008, Mm.212923
1418374_at				cos_per_28_ph_26	0.729758653	28	2	2	Fxyd3	FXYD domain-containing ion transport regulator 3	NM_008557	17178	Mm.263847
1418428_at				cos_per_28_ph_14	0.683676091	28	14	14	Kif5b	kinesin family member 5B	BI328541	16573	Mm.223744
1418429_at				cos_per_28_ph_15	0.826669019	28	15	15	Kif5b	kinesin family member 5B	BI328541	16573	Mm.223744
1418431_at				box1_ph_14	0.640558248	24	14	14	Kif5b	kinesin family member 5B	BI328541	16573	Mm.223744
1418443_at				rigid_ph_14	0.661459909	42	14	14	Xpo1	exportin 1, CRM1 homolog (yeast)	BC025628	103573	Mm.217547
1418469_at				cos_per_28_ph_10	0.64354495	28	10	10	Ntnp1	nuclear receptor interacting protein 1	NM_008735	268903	Mm.455873, Mm.74711
1418471_at				cos_per_28_ph_24	0.736611785	28	0	0	Pgf	placental growth factor	NM_008827	18654	Mm.4809
1418525_at				rigid_ph_17	0.659742771	24	17	17	Pcnl	pericentriolar material 1	NM_023662	18536	Mm.117896
1418659_at				box2_ph_17	0.65382889	24	17	17	Clock	circadian locomoter output cycles kaput	BB203106	12753	Mm.3552, Mm.392894
1418663_at				rigid_ph_14	0.649779429	24	14	14	Mpdz	multiple PDZ domain protein	AK019164	17475	Mm.153039
1418664_at				cos_per_27_ph_15	0.752296852	27	15	15	Mpdz	multiple PDZ domain protein	AK019164	17475	Mm.153039
1418696_at				cos_per_25_ph_03	0.674457055	25	3	3	Ttc36	tetratricopeptide repeat domain 36	NM_138951	192653	Mm.325487
1418704_at				cos_per_26_ph_02	0.704787616	26	2	2	S100a13	S100 calcium binding protein A13	NM_009113	20196	Mm.6523
1418709_at				cos_per_28_ph_24	0.683786414	28	0	0	Cox7a1	cytochrome c oxidase, subunit VIIa 1	AF087370	12865	Mm.423080
1418746_at				asyrigid1_ph_07	0.623192628	24	7	7	Pnkd	paroxysmal nonkinesiogenic dyskinesia	NM_019999	56695	Mm.384726
1418773_at	0.010016338	26.2	7					7	Fads3	fatty acid desaturase 3	BE652876	60527	Mm.253875

Table S1: Circadian transcripts (continued)

	Signal Decomposition			Model-Matching				Final Statistics and Annotations					
Transcript ID (Affymetrix probeset)	Fisher's G Test q-value	Period (hrs)	Phase	HAYSTACK Best Model	HAYSTACK Correlation	Period (hrs)	Phase	Phase (Final)	Gene Symbol	Description	GenBank	Entrez Gene	UniGene
1418777_at				cos_per_25_ph_05	0.691674274	25	5	5	Ccl25	chemokine (C-C motif) ligand 25	NM_009138	20300	Mm.7275
1418879_at	0.003452992	29.1	26					2	Fam110c	family with sequence similarity 110, member C	NM_027828	104943	Mm.248598
1418924_at	0.00376434	26.2	1					1	Rassf7	Ras association (RalGDS/AF-6) domain family (N-terminal) member 7	NM_025886	66985	Mm.21202
1418931_at	0.001838832	28.3	0					0	Reg4	regenerating islet-derived family, member 4	NM_026328	67709	Mm.46306
1418932_at				cos_per_24_ph_15	0.607185026	24	15	15	Nfil3	nuclear factor, interleukin 3, regulated	AY061760	18030	Mm.136604
1418947_at				cos_per_27_ph_03	0.708672692	27	3	3	Nek3	NIMA (never in mitosis gene a)-related expressed kinase 3	NM_011848	23954	Mm.41413
1418955_at				box2_ph_16	0.632067165	24	16	16	Zfp93	zinc finger protein 93	NM_009567	22755	Mm.459431
1418967_a_at				box2_ph_15	0.73838312	24	15	15	St7	suppression of tumorigenicity 7	NM_022332	64213	Mm.12051
1418976_s_at				cos_per_28_ph_27	0.6573664	28	3	3	Cideb	cell death-inducing DNA fragmentation factor, alpha subunit-like effector B	NM_009894	12684	Mm.180338, Mm.476914
1419012_at				rigid_ph_13	0.649459027	24	13	13	Zfpm2	zinc finger protein, multitype 2	NM_011766	22762	Mm.39496
1419022_a_at				spike_ph_06	0.626351788	24	6	6	Eno1	enolase 1, alpha non-neuron	NM_023119	13806	Mm.372357, Mm.372389, Mm.70666
1419042_at	0.034842482	21.4	0					0	Iigp1	interferon inducible GTPase 1	BM239828	60440	Mm.261140, Mm.468084
1419073_at	0.004588041	26.3	24	cos_per_26_ph_24	0.843533965	26	0	0	Tmeff2	transmembrane protein with EGF-like and two follistatin-like domains 2	NM_019790	56363	Mm.245154
1419086_at				cos_per_28_ph_26	0.624799657	28	2	2	Fgfbp1	fibroblast growth factor binding protein 1	U49641	14181	Mm.46053
1419093_at				cos_per_28_ph_22	0.807456697	28	22	22	Tdo2	tryptophan 2,3-dioxygenase	AI098840	56720	Mm.258622
1419124_at	0.034037313	22.9	15					15	Mfsd6	major facilitator superfamily domain containing 6	NM_133829	98682	Mm.475670
1419205_x_at				cos_per_28_ph_08	0.723901435	28	8	8	Gpatch4	G patch domain containing 4	NM_025663	66614	Mm.46029
1419252_at	0.001838832	29.9	2					2	Epsl5	epidermal growth factor receptor pathway substrate 15	BG067649	13858	Mm.318250
1419270_a_at				cos_per_27_ph_15	0.656608702	27	15	15	Dut	deoxyuridine triphosphatase	AF091101	110074	Mm.282499, Mm.471988
1419310_s_at	0.007919372	30	29					5	Rfxank	regulatory factor X-associated ankyrin-containing protein	L43164	19727	Mm.161167
1419404_s_at				box2_ph_17	0.66099447	24	17	17	Sinh1b	seven in absentia 1B	NM_009173	20438	Mm.37215

Table S1: Circadian transcripts (continued)

	Signal Decomposition			Model-Matching				Final Statistics and Annotations					
Transcript ID (Affymetrix probeset)	Fisher's G Test q-value	Period (hrs)	Phase	HAYSTACK Best Model	HAYSTACK Correlation	Period (hrs)	Phase	Phase (Final)	Gene Symbol	Description	GenBank	Entrez Gene	UniGene
1419458_at	0.011699693	26.5	4					4	Rgnef	Rho-guanine nucleotide exchange factor	BG069493	110596	Mm.252718
1419516_at	0.018051027	22.5	6					6	Fam50a	family with sequence similarity 50, member A	NM_138607	108160	Mm.4370
1419534_at				cos_per_24_ph_21	0.671685451	24	21	21	Olr1	oxidized low density lipoprotein (lectin-like) receptor 1	NM_138648	108078	Mm.293626
1419559_at				cos_per_26_ph_03	0.613663918	26	3	3	Cyp4f14	cytochrome P450, family 4, subfamily f, polypeptide 14	BC011228	64385	Mm.426027
1419574_at				cos_per_28_ph_15	0.703677393	28	15	15	Zfp292	zinc finger protein 292	NM_013889	30046	Mm.38193
1419575_s_at				rigid_ph_16	0.662784412	24	16	16	Zfp292	zinc finger protein 292	NM_013889	30046	Mm.38193
1419647_a_at	0.039882619	22.9	5					5	Ier3	immediate early response 3	NM_133662	15937	Mm.25613
1419654_at				rigid_ph_16	0.654000171	24	16	16	Tle3	transducin-like enhancer of split 3, homolog of Drosophila E(spl)	NM_009389	21887	Mm.24255, Mm.469199
1419752_at	0.005782739	29.5	4					4	Nfic1	nuclear transcription factor, X-box binding 1	AK013866	74164	Mm.247456, Mm.439181
1419754_at				rigid_ph_16	0.640880699	24	16	16	Myo5a	myosin VA	NM_010864	17918	Mm.3645
1419803_s_at				cos_per_26_ph_02	0.696597212	26	2	2	Ccdc12	coiled-coil domain containing 12	C76605	72654	Mm.249115
1419814_s_at				cos_per_26_ph_01	0.645846645	26	1	1	S100a1	S100 calcium binding protein A1	AI266795	20193	Mm.24662
1419819_s_at	0.045319471	20.2	19					19	Sec63	SEC63-like (S. cerevisiae)	AI649014	140740	Mm.214344
1420008_s_at				boxl_ph_05	0.658123833	24	5	5	Wwc1	WW, C2 and coiled-coil domain containing 1	AU017197	211652	Mm.31267
1420017_at				rigid_ph_04	0.683439091	24	4	4	Tspan8	tetraspanin 8	C76990	216350	Mm.22270
1420019_at				spike_ph_02	0.659053836	24	2	2	Tspan8	tetraspanin 8	C76990	216350	Mm.22270
1420093_s_at				boxl_ph_05	0.606862593	24	5	5	Hnrpdl	heterogeneous nuclear ribonucleoprotein D-like	AU015266	50926	Mm.389579, Mm.426680
1420380_at				rigid_ph_08	0.663804537	24	8	8	Ccl2	chemokine (C-C motif) ligand 2	AF065983	20296	Mm.290320
1420476_a_at	0.048596469	24.8	12					12	Napl1l	nucleosome assembly protein 1-like 1	BG064031	53605	Mm.290407
1420477_at	0.01417972	25.6	12					12	Napl1l	nucleosome assembly protein 1-like 1	BG064031	53605	Mm.290407
1420479_a_at	0.005247212	23.4	14					14	Napl1l	nucleosome assembly protein 1-like 1	BG064031	53605	Mm.290407
1420498_a_at				asyrigid2_ph_01	0.640128617	24	1	1	Pcyt2	phosphate cytidylyltransferase 2, ethanolamine	NM_024229	68671	Mm.21439

Table S1: Circadian transcripts (continued)

	Signal Deocomposition			Model-Matching				Final Statistics and Annotations					
Transcript ID (Affymetrix probeset)	Fisher's G Test q-value	Period (hrs)	Phase	HAYSTACK Best Model	HAYSTACK Correlation	Period (hrs)	Phase	Phase (Final)	Gene Symbol	Description	GenBank	Entrez Gene	UniGene
1420506_a_at	0.02477258	24.1	15					15	Stxbp1	syntaxin binding protein 1	AF326545	20910	Mm.278865
1420562_at				cos_per_28_ph_27	0.758534021	28	3	3	Slurp1	secreted Ly6/Plaur domain containing 1	NM_020519	57277	Mm.27630
1420603_s_at	0.014972275	20.6	16					16	Raetl a	retinoic acid early transcript 1, alpha	NM_009016	19368	Mm.458004
1420622_a_at				cos_per_28_ph_14	0.617285056	28	14	14	Hspa8	heat shock protein 8	BC006722	15481	Mm.290774, Mm.336743, Mm.351377, Mm.412745
1420650_at				rigid_ph_15	0.630965556	24	15	15	Zfhx3	zinc finger homeobox 3	NM_007496	11906	Mm.416972, Mm.477670
1420668_a_at				cos_per_28_ph_26	0.638192838	28	2	2	Yipf2	Yip1 domain family, member 2	NM_138303	74766	Mm.475712
1420727_a_at	0.035616433	27	23					23	Tmlhe	trimethyllysine hydroxylase, epsilon	AY033513	192289	Mm.394228
1420772_a_at				asyrigid2_ph_08	0.69474741	24	8	8	Tsc22d3	TSC22 domain family, member 3	NM_010286	14605	Mm.22216
1420774_a_at				cos_per_28_ph_23	0.631260807	28	23	23	4930583H14Rik	RIKEN cDNA 4930583H14 gene	NM_026358	67749	Mm.273339
1420847_a_at				cos_per_28_ph_26	0.623474855	28	2	2	Fgfr2	fibroblast growth factor receptor 2	NM_010207	14183	Mm.16340
1420876_a_at				rigid_ph_18	0.673133248	24	18	18	40427	septin 6	NM_019942	56526	Mm.260036
1420891_at	0.041969593	25.6	9					9	Wnt7b	wingless-related MMTV integration site 7B	W29605	22422	Mm.306946
1420892_at	0.005382121	26.9	7					7	Wnt7b	wingless-related MMTV integration site 7B	W29605	22422	Mm.306946
1420933_a_at				hoxl_ph_17	0.677728874	24	17	17	Eya3	eyes absent 3 homolog (Drosophila)	AI746570	14050	Mm.227733
1420948_s_at	0.012014813	24.1	15	rigid_ph_16	0.768358679	24	16	15	Atrx	alpha thalassemia/mental retardation syndrome X-linked homolog (human)	BB825830	22589	Mm.475674
1420951_a_at	0.048869406	23.7	15	rigid_ph_16	0.722226793	24	16	15	Son	Son DNA binding protein	BB701473	20658	Mm.328698, Mm.46401
1420956_at	0.041606434	29.1	13					13	Apc	adenomatosis polyposis coli	NM_007462	11789	Mm.384171
1420990_at	0.016062212	20.7	15					15	Chdl	chromodomain helicase DNA binding protein 1	NM_007690	12648	Mm.393794, Mm.8137
1420991_at	0.03922018	24.7	6					6	Ankrd1	ankyrin repeat domain 1 (cardiac muscle)	AK009959	107765	Mm.10279
1421022_x_at	0.045658634	24.9	21					21	Acyp1	acylphosphatase 1, erythrocyte (common) type	NM_025421	66204	Mm.311985
1421048_a_at	0.029695058	24.6	0					0	Ypel1	yippee-like 1 (Drosophila)	NM_023249	106369	Mm.237941

Table S1: Circadian transcripts (continued)

	Signal Deconvolution			Model-Matching				Final Statistics and Annotations					
Transcript ID (Affymetrix probeset)	Fisher's G Test q-value	Period (hrs)	Phase	HAYSTACK Best Model	HAYSTACK Correlation	Period (hrs)	Phase	Phase (Final)	Gene Symbol	Description	GenBank	Entrez Gene	UniGene
1421050_at				spike_ph_01	0.63053717	24	1	1	Vps25	vacuolar protein sorting 25 (yeast)	NM_026776	28084	Mm.301020
1421077_at	0.015875729	26	23					23	Sertad3	SERTA domain containing 3	BM124141	170742	Mm.200120
1421087_at	0.048431257	22.4	8					8	Per3	period homolog 3 (Drosophila)	NM_011067	18628	Mm.121361
1421102_a_at	0.00399222	27.6	3					3	Vamp3	vesicle-associated membrane protein 3	NM_009498	22319	Mm.273930
1421127_at				asyrigid2_ph_01	0.637117073	24	1	1	Tmem42	transmembrane protein 42	NM_025339	66079	Mm.347935
1421141_a_at				rigid_ph_16	0.709227177	24	16	16	Foxp1	forkhead box P1	BG962849	108655	Mm.234965, Mm.392313, Mm.461753
1421149_a_at				rigid_ph_16	0.653490268	24	16	16	Atn1	atrophin 1	NM_007881	13498	Mm.333380
1421252_a_at				rigid_ph_16	0.606942617	24	16	16	Mef2a	myocyte enhancer factor 2A	NM_013597	17258	Mm.132788, Mm.426509, Mm.466976
1421260_a_at				cos_per_28_ph_08	0.774190992	28	8	8	Srm	spermidine synthase	NM_009272	20810	Mm.10
1421392_a_at				cos_per_26_ph_04	0.782138647	26	4	4	Birc3	baculoviral IAP repeat-containing 3	NM_007464	11796	Mm.2026
1421491_a_at	0.012183793	20.5	20					20	Tmem49	transmembrane protein 49	NM_029478	75909	Mm.390394, Mm.477513
1421493_a_at				asyrigid2_ph_10	0.649095129	24	10	10	Rgs20	regulator of G-protein signaling 20	NM_021374	58175	Mm.103771
1421534_at				cos_per_28_ph_10	0.626180372	28	10	10	LOC14210	hypothetical LOC14210	NM_008016	14210	Mm.463873, Mm.477562
1421846_at	0.011153776	27.2	26					2	Wsb2	WD repeat and SOCS box-containing 2	BM730566	59043	Mm.28489
1421847_at	0.025044992	25.9	1					1	Wsb2	WD repeat and SOCS box-containing 2	BM730566	59043	Mm.28489
1421857_at				asyrigid1_ph_22	0.635894604	24	22	22	Adam17	a disintegrin and metallopeptidase domain 17	C76813	11491	Mm.27681
1421858_at	0.013916084	29.2	21					21	Adam17	a disintegrin and metallopeptidase domain 17	C76813	11491	Mm.27681
1421928_at				spike_ph_15	0.677402879	24	15	15	Epha4	Eph receptor A4	BB706548	13838	Mm.400747
1421946_at				cos_per_26_ph_00	0.60989748	26	0	0	Crp	C-reactive protein, pentraxin-related	NM_007768	12944	Mm.28767
1421977_at				asyrigid2_ph_14	0.634221725	24	14	14	Mmp19	matrix metallopeptidase 19	AF153199	58223	Mm.131266, Mm.24630
1422002_at				cos_per_27_ph_00	0.644633784	27	0	0	Mxd1	MAX dimerization protein 1	L38926	17119	Mm.279580

Table S1: Circadian transcripts (continued)

	Signal Decomposition			Model-Matching				Final Statistics and Annotations					
Transcript ID (Affymetrix probeset)	Fisher's G Test q-value	Period (hrs)	Phase	HAYSTACK Best Model	HAYSTACK Correlation	Period (hrs)	Phase	Phase (Final)	Gene Symbol	Description	GenBank	Entrez Gene	UniGene
1422041_at				cos_per_27_ph_03	0.6670237	27	3	3	Pilrb1	paired immunoglobin-like type 2 receptor beta 1	NM_133209	170741	Mm.347593
1422101_at				cos_per_26_ph_02	0.620829396	26	2	2	Tnfrsf23	tumor necrosis factor receptor superfamily, member 23	NM_024290	79201	Mm.290780
1422222_at				cos_per_21_ph_18	0.831277734	21	18	18	Ivl	involucrin	NM_008412	16447	Mm.207365
1422249_s_at				box2_ph_17	0.728656967	24	17	17	Zfa	zinc finger protein, autosomal	NM_009540	22639	Mm.390269
1422264_s_at				cos_per_28_ph_11	0.60913137	28	11	11	Klf9	Kruppel-like factor 9	NM_010638	16601	Mm.291595, Mm.392684
1422303_a_at				cos_per_28_ph_26	0.799922431	28	2	2	Tnfrsf18	tumor necrosis factor receptor superfamily, member 18	AF229434	21936	Mm.476937
1422399_a_at				asyrigid2_ph_09	0.621821242	24	9	9	Rab23	RAB23, member RAS oncogene family	NM_008999	19335	Mm.86744
1422433_s_at	0.00630283	27.1	22					22	Idh1	isocitrate dehydrogenase 1 (NADP+), soluble	NM_010497	15926	Mm.9925
1422492_at				cos_per_27_ph_14	0.672405928	27	14	14	Cpox	coproporphyrinogen oxidase	BG067254	12892	Mm.291519
1422493_at				cos_per_25_ph_14	0.651912496	25	14	14	Cpox	coproporphyrinogen oxidase	BG067254	12892	Mm.291519
1422504_at				cos_per_26_ph_17	0.659263138	26	17	17	Glrb	glycine receptor, beta subunit	NM_010298	14658	Mm.275639
1422524_at				cos_per_26_ph_03	0.685789676	26	3	3	Abcb6	ATP-binding cassette, sub-family B (MDR/TAP), member 6	NM_023732	74104	Mm.28663
1422528_a_at				rigid_ph_16	0.709423152	24	16	16	Zfp36l1	zinc finger protein 36, C3H type-like 1	M58566	12192	Mm.235132
1422538_at	0.00287282	26	3					3	Ext2	exostoses (multiple)-like 2	BM203810	58193	Mm.41739
1422614_s_at				cos_per_26_ph_02	0.696146747	26	2	2	Bloc1s1	biogenesis of lysosome-related organelles complex-1, subunit 1	NM_015740	14533	Mm.30118
1422678_at				cos_per_28_ph_04	0.780378495	28	4	4	Dgat2	diacylglycerol O-acyltransferase 2	AK002443	67800	Mm.180189, Mm.477728
1422733_at				asyrigid2_ph_00	0.651555959	24	0	0	Fjx1	four jointed box 1 (Drosophila)	AV230815	14221	Mm.29730
1422741_a_at				rigid_ph_15	0.665749085	24	15	15	Bbx	bobby sox homolog (Drosophila)	BF319769	70508	Mm.28940
1422743_at				box2_ph_16	0.659842658	24	16	16	Phka1	phosphorylase kinase alpha 1	NM_008832	18679	Mm.141197, Mm.212889, Mm.475669
1422747_at				cos_per_28_ph_19	0.672637806	28	19	19	Chek2	CHK2 checkpoint homolog (S. pombe)	NM_016681	50883	Mm.279308
1422748_at				cos_per_24_ph_15	0.608100967	24	15	15	Zeb2	zinc finger E-box binding homeobox 2	NM_015753	24136	Mm.440702

Table S1: Circadian transcripts (continued)

	Signal Decomposition			Model-Matching				Final Statistics and Annotations					
Transcript ID (Affymetrix probeset)	Fisher's G Test q-value	Period (hrs)	Phase	HAYSTACK Best Model	HAYSTACK Correlation	Period (hrs)	Phase	Phase (Final)	Gene Symbol	Description	GenBank	Entrez Gene	UniGene
1422761_at				box2_ph_17	0.634274997	24	17	17	Tbll xrl	transducin (beta)-like 1X-linked receptor 1	NM_030732	81004	Mm.202966, Mm.446265
1422821_s_at				cos_per_27_ph_05	0.663017138	27	5	5	Stard5	StAR-related lipid transfer (START) domain containing 5	BI076697	170460	Mm.357953
1422850_at				box1_ph_02	0.621632619	24	2	2	Pabpn1	poly(A) binding protein, nuclear 1	AV028400	54196	Mm.7723
1422861_s_at				cos_per_28_ph_16	0.668101501	28	16	16	Pdlim5	PDZ and LIM domain 5	NM_019808	56376	Mm.117709
1422878_at				cos_per_28_ph_04	0.798358418	28	4	4	Syt12	synaptotagmin XII	NM_134164	171180	Mm.262270
1422887_a_at	0.016688272	28.3	7					7	Ctbp2	C-terminal binding protein 2	NM_009980	13017	Mm.246240, Mm.389984
1422948_s_at				cos_per_27_ph_01	0.663125798	27	1	1	Hist1h3a	histone cluster 1, H3a	NM_013550	360198	Mm.221301
1422954_at				box2_ph_16	0.673962754	24	16	16	Zfp60	zinc finger protein 60	NM_009560	22718	Mm.348021, Mm.66913
1422979_at				cos_per_26_ph_15	0.611756617	26	15	15	Suv39h2	suppressor of variegation 3-9 homolog 2 (Drosophila)	NM_022724	64707	Mm.128273, Mm.441181
1422997_s_at	0.001838832	25.8	20					20	Acot2	acyl-CoA thioesterase 2	NM_134188	171210	Mm.371675
1423088_at	0.03478466	24.7	17					17	Tmod3	tropomodulin 3	AK017725	50875	Mm.38445
1423122_at				cos_per_28_ph_00	0.696252401	28	0	0	Avpi1	arginine vasopressin-induced 1	BI649826	69534	Mm.30060
1423149_at	0.001838832	29.5	19					19	Skp1a	S-phase kinase-associated protein 1A	AV347477	21402	Mm.42944
1423187_at	0.010477522	25.8	2					2	Gabarapl2	gamma-aminobutyric acid (GABA-A) receptor-associated protein-like 2	BF160931	93739	Mm.371666
1423199_at				rigid_ph_16	0.616856593	24	16	16	Brd3	bromodomain containing 3	BG072367	67382	Mm.28721
1423244_at				cos_per_26_ph_01	0.673038422	26	1	1	Cyp2c68	cytochrome P450, family 2, subfamily c, polypeptide 68	AI265721	433247	Mm.335660
1423250_a_at				spike_ph_08	0.644037581	24	8	8	Tgfb2	transforming growth factor, beta 2	BF144658	21808	Mm.18213
1423393_at	0.001838832	26.7	7					7	Clic4	chloride intracellular channel 4 (mitochondrial)	BB398988	29876	Mm.257765, Mm.473864
1423396_at	0.039842354	26.3	24					0	Agt	angiotensinogen (serpin peptidase inhibitor, clade A, member 8)	AK018763	11606	Mm.301626
1423421_at				spike_ph_14	0.633272798	24	14	14	Ankrd49	ankyrin repeat domain 49	BB233668	56503	Mm.272618
1423426_at				spike_ph_13	0.62558789	24	13	13	1300012G16Rik	RIKEN cDNA 1300012G16 gene	BB018522	71772	Mm.100065

Table S1: Circadian transcripts (continued)

	Signal Deocomposition			Model-Matching				Final Statistics and Annotations					
Transcript ID (Affymetrix probeset)	Fisher's G Test q-value	Period (hrs)	Phase	HAYSTACK Best Model	HAYSTACK Correlation	Period (hrs)	Phase	Phase (Final)	Gene Symbol	Description	GenBank	Entrez Gene	UniGene
1423433_at	0.020557759	23.1	17	rigid_ph_17	0.738832205	24	17	17	Trove2	TROVE domain family, member 2	BG069917	20822	Mm.40370
1423446_at				cos_per_25_ph_02	0.694785292	25	2	2	Dapk3	death-associated protein kinase 3	AI642212	13144	Mm.10294
1423585_at				boxl_ph_19	0.62616194	24	19	19	Polr2b	polymerase (RNA) II (DNA directed) polypeptide B	AI481026	231329	Mm.273217
1423608_at	0.020936258	29.5	25					1	Itm2a	integral membrane protein 2A	BI966443	16431	Mm.193
1423686_a_at	0.04317673	27.6	28					4	Prrl3	proline rich 13	BC016234	66151	Mm.393955
1423694_at	0.037033817	27.6	27					3	Kcnd10	potassium channel tetramerisation domain containing 10	BC006935	330171	Mm.238285, Mm.428824
1423722_at	0.004550951	20.5	1					1	Tmem49	transmembrane protein 49	BC004013	75909	Mm.390398, Mm.477513
1423723_s_at	0.029913438	29.4	21					21	Tardbp	TAR DNA binding protein	BC012873	230908	Mm.22453
1423765_at				cos_per_27_ph_01	0.675595522	27	1	1	Atdl1	ATH1, acid trehalase-like 1 (yeast)	BC023151	212974	Mm.260139
1423771_at				cos_per_28_ph_25	0.649350097	28	1	1	Prkcdbp	protein kinase C, delta binding protein	BC009660	109042	Mm.3124
1423776_s_at	0.004253787	28.9	26					2	Tbc1d22a	TBC1 domain family, member 22a	BC023106	223754	Mm.28904
1423858_a_at	0.036014278	22.4	22	rigid_ph_00	0.729225594	24	0	22	Hmgcs2	3-hydroxy-3-methylglutaryl-Coenzyme A synthase 2	BC014714	15360	Mm.289131
1423912_at	0.032120892	26.3	1					1	Aspscr1	alveolar soft part sarcoma chromosome region, candidate 1 (human)	BC022115	68938	Mm.294020
1423938_at				cos_per_27_ph_00	0.69020248	27	0	0	Llgl2	lethal giant larvae homolog 2 (Drosophila)	AY033650	217325	Mm.290450
1423959_at	0.004225148	20.2	2					2	Ropn1l	ropporin 1-like	AF305427	252967	Mm.436668
1424014_at				spike_ph_03	0.628741248	24	3	3	2900092E17Rik	RIKEN cDNA 2900092E17 gene	BC003932	67278	Mm.345385
1424054_at				cos_per_27_ph_01	0.623154863	27	1	1	Bbd2	BTB (POZ) domain containing 2	BC016566	208198	Mm.60720
1424064_at				cos_per_25_ph_02	0.68856001	25	2	2	Rabl6	RABL6, member RAS oncogene family	BC016408	76308	Mm.182563
1424067_at				rigid_ph_08	0.669049414	24	8	8	Icam1	intercellular adhesion molecule 1	BC008626	15894	Mm.435508
1424084_at				box2_ph_17	0.638191057	24	17	17	Rod1	ROD1 regulator of differentiation 1 (S. pombe)	BB519382	230257	Mm.331640, Mm.475882
1424090_at				cos_per_27_ph_03	0.688762144	27	3	3	Sdcbp2	syndecan binding protein (syntenin) 2	BC005556	228765	Mm.32068
1424103_at	0.023792511	23.8	3					3	Atg4b	autophagy-related 4B (yeast)	AV240631	66615	Mm.29087

Table S1: Circadian transcripts (continued)

	Signal Decomposition			Model-Matching				Final Statistics and Annotations					
Transcript ID (Affymetrix probeset)	Fisher's G Test q-value	Period (hrs)	Phase	HAYSTACK Best Model	HAYSTACK Correlation	Period (hrs)	Phase	Phase (Final)	Gene Symbol	Description	GenBank	Entrez Gene	UniGene
1424120_at	0.016615418	26.6	5					5	Rnf8	ring finger protein 8	BC021778	58230	Mm.305994
1424167_a_at				asyrigid2_ph_09	0.648083769	24	9	9	Pmm1	phosphomannomutase 1	BC006809	29858	Mm.18939
1424173_at	0.017858633	22.8	14	boxl_ph_14	0.739720517	24	14	14	Tmem48	transmembrane protein 48	BC021337	72787	Mm.28478
1424175_at	0.001838832	22.1	8	cos_per_22_ph_08	0.896967781	22	8	8	Tef	thyrotroph embryonic factor	BC017689	21685	Mm.270278
1424181_at				asyrigid1_ph_22	0.654979419	24	22	22	40427	septin 6	BC010489	56526	Mm.260036
1424193_at				cos_per_28_ph_08	0.687629244	28	8	8	Pwp2	PWP2 periodic tryptophan protein homolog (yeast)	AB041855	110816	Mm.103522
1424208_at	0.022498846	29.8	26	cos_per_27_ph_00	0.778073539	27	0	2	Ptger4	prostaglandin E receptor 4 (subtype EP4)	BC011193	19219	Mm.18509
1424239_at				boxl_ph_14	0.649852689	24	14	14	Fam65a	family with sequence similarity 65, member A	BC006820	75687	Mm.41261
1424251_a_at	0.005196583	28	2					2	Hnrpdl	heterogeneous nuclear ribonucleoprotein D-like	BC021374	50926	Mm.389579, Mm.426680
1424252_at	0.003436252	25.8	26	cos_per_26_ph_00	0.819281731	26	0	2	Hnrpdl	heterogeneous nuclear ribonucleoprotein D-like	BC021374	50926	Mm.389579, Mm.426680
1424261_at				asyrigid2_ph_23	0.651196167	24	23	23	Zfp672	zinc finger protein 672	BC003258	319475	Mm.72124
1424356_a_at				cos_per_28_ph_02	0.691188685	28	2	2	Metrnl	meteorin, glial cell differentiation regulator-like	BC024445	210029	Mm.153566
1424445_at				cos_per_28_ph_00	0.66203782	28	0	0	Tm4sf5	transmembrane 4 superfamily member 5	BC010782	75604	Mm.24400
1424452_at	0.023901306	24.8	3					3	Sltm	SAFB-like, transcription modulator	BC019992	66660	Mm.22379
1424457_at				spike_ph_01	0.690446135	24	1	1	Aplp3	amyloid beta (A4) precursor protein-binding, family B, member 3	BC024809	225372	Mm.89673
1424464_s_at				cos_per_28_ph_15	0.715491985	28	15	15	Mfsd6	major facilitator superfamily domain containing 6	BF225441	98682	Mm.475670
1424521_at	0.045581465	29.1	27					3	Zfand2b	zinc finger, AN1 type domain 2B	BC011495	68818	Mm.32646
1424573_at				cos_per_27_ph_14	0.701036529	27	14	14	Tmed5	transmembrane emp24 protein transport domain containing 5	BC020076	73130	Mm.363960, Mm.422969
1424600_at	0.035139309	23.4	6	asyrigid1_ph_09	0.756664842	24	9	6	Altp1	amiloride binding protein 1 (amine oxidase, copper-containing)	BC021880	76507	Mm.213898
1424607_a_at				asyrigid1_ph_06	0.674456025	24	6	6	100039204	predicted gene, 100039204	BM225255	100039204	
1424609_a_at				asyrigid1_ph_06	0.675483908	24	6	6	100039204	predicted gene, 100039204	BM225255	100039204	
1424643_at				asyrigid2_ph_09	0.641841527	24	9	9	Tcof1	Treacher Collins Franceschetti syndrome 1, homolog	U81030	21453	Mm.2215

Table S1: Circadian transcripts (continued)

	Signal Decomposition			Model-Matching				Final Statistics and Annotations					
Transcript ID (Affymetrix probeset)	Fisher's G Test q-value	Period (hrs)	Phase	HAYSTACK Best Model	HAYSTACK Correlation	Period (hrs)	Phase	Phase (Final)	Gene Symbol	Description	GenBank	Entrez Gene	UniGene
1424658_at				rigid_ph_16	0.660245016	24	16	16	Taok1	TAO kinase 1	BB151477	216965	Mm.340436
1424670_s_at	0.0115389	26.1	1					1	Zfyve21	zinc finger, FYVE domain containing 21	BC019521	68520	Mm.390497
1424672_at				cos_per_28_ph_14	0.614052516	28	14	14	Dmxl1	Dmx-like 1	BC020141	240283	Mm.257790
1424675_at				asyrigid2_ph_10	0.608453601	24	10	10	Slc39a6	solute carrier family 39 (metal ion transporter), member 6	BB825002	106957	Mm.21688
1424694_at	0.010510818	22.2	19					19	2010011I20Rik	RIKEN cDNA 2010011I20 gene	AK008190	67017	Mm.30013
1424695_at	0.009980088	22.4	19	cos_per_23_ph_19	0.779238973	23	19	19	2010011I20Rik	RIKEN cDNA 2010011I20 gene	AK008190	67017	Mm.30013
1424740_at	0.010775714	23	5					5	Creb3	cAMP responsive element binding protein 3	BG070002	12913	Mm.12407
1424752_x_at				box2_ph_17	0.621480297	24	17	17	Zfp71-rs1	zinc finger protein 71, related sequence	BC016248	235907	Mm.440123
1424768_at	0.009491432	23	16	rigid_ph_16	0.781851354	24	16	16	Cald1	caldesmon 1	BI248947	109624	Mm.308134
1424800_at	0.018817801	23.6	15					15	Enah	enabled homolog (Drosophila)	BQ044016	13800	Mm.389224, Mm.87759
1424806_s_at	0.014363698	26	2					2	Tmem214	transmembrane protein 214	BC027046	68796	Mm.205169
1424830_at	0.045020424	21.9	17	rigid_ph_16	0.733142926	24	16	17	Cenk	cyclin K	BC027297	12454	Mm.474441
1424906_at	0.044305865	26.1	22					22	Pqlc3	PQ loop repeat containing	BC025220	217430	Mm.379451
1424913_at				cos_per_28_ph_08	0.647702647	28	8	8	2310044G17Rik	RIKEN cDNA 2310044G17 gene	AK009800	217732	Mm.22337
1425099_a_at	0.001893038	22.9	18	cos_per_23_ph_18	0.840422928	23	18	18	Arntl	aryl hydrocarbon receptor nuclear translocator-like	BC011080	11865	Mm.440371
1425142_a_at	0.0122478	20.7	8					8	Hnrnpd	heterogeneous nuclear ribonucleoprotein D	BC011172	11991	Mm.150231
1425143_a_at	0.027419959	29.2	27					3	Ndufs1	NADH dehydrogenase (ubiquinone) Fe-S protein 1	BC006660	227197	Mm.290791, Mm.392955
1425177_at				asyrigid2_ph_02	0.69804512	24	2	2	Shmt1	serine hydroxymethyltransferase 1 (soluble)	AF237702	20425	Mm.364956
1425178_s_at				asyrigid2_ph_02	0.637739874	24	2	2	Shmt1	serine hydroxymethyltransferase 1 (soluble)	AF237702	20425	Mm.364956
1425276_at				rigid_ph_16	0.685327878	24	16	16	Fbn1	fibrosin	BB162362	14123	Mm.323505
1425281_a_at				cos_per_27_ph_09	0.62719668	27	9	9	Tsc22d3	TSC22 domain family, member 3	AF201289	14605	Mm.22216
1425299_s_at	0.036670536	27.9	1					1	0610038D11Rik	RIKEN cDNA 0610038D11 gene	BC019418	67674	Mm.318804, Mm.371597

Table S1: Circadian transcripts (continued)

	Signal Decomposition			Model-Matching				Final Statistics and Annotations					
Transcript ID (Affymetrix probeset)	Fisher's G Test q-value	Period (hrs)	Phase	HAYSTACK Best Model	HAYSTACK Correlation	Period (hrs)	Phase	Phase (Final)	Gene Symbol	Description	GenBank	Entrez Gene	UniGene
1425452_s_at				cos_per_27_ph_26	0.63861664	27	2	2	Fam84a	family with sequence similarity 84, member A	BC002154	105005	Mm.227253
1425456_a_at	0.043585302	28.7	3					3	Map2k3	mitogen-activated protein kinase kinase 3	AI481780	26397	Mm.18494
1425481_at				spike_ph_15	0.641745173	24	15	15	Cnot6l	CCR4-NOT transcription complex, subunit 6-like	BC018506	231464	Mm.283734, Mm.384746
1425483_at				cos_per_28_ph_02	0.825064451	28	2	2	LOC100044677	similar to thymus high mobility group box protein TOX	BB547854	100044677	
1425514_at	0.006643702	28.5	12	cos_per_25_ph_15	0.782418345	25	15	12	Pik3r1	phosphatidylinositol3-kinase, regulatory subunit, polypeptide 1 (p85 alpha)	M60651	18708	Mm.259333
1425525_a_at	0.01026701	25.6	1					1	P2rx4	purinergic receptor P2X, ligand-gated ion channel 4	AF089751	18438	Mm.290884, Mm.463383
1425547_a_at				cos_per_26_ph_02	0.726787514	26	2	2	Klc4	kinesin light chain 4	BC005746	74764	Mm.279599
1425560_a_at				cos_per_26_ph_02	0.745089959	26	2	2	S100a16	S100 calcium binding protein A16	BC020031	67860	Mm.331185
1425627_x_at				cos_per_26_ph_00	0.635035912	26	0	0	Gstm1	glutathione S-transferase, mu 1	J03952	14862	Mm.37199
1425631_at	0.025928362	29.9	21	cos_per_28_ph_21	0.829664752	28	21	21	Ppp1r3c	protein phosphatase 1, regulatory (inhibitor) subunit 3C	U89924	53412	Mm.24724
1425642_at	0.045224164	28.5	15	cos_per_26_ph_16	0.734327078	26	16	15	Cep290	centrosomal protein 290	BC004690	216274	Mm.229114
1425659_at				cos_per_28_ph_27	0.66265679	28	3	3	Tom1l2	target of myb1-like 2 (chicken)	BM226574	216810	Mm.218875
1425721_at	0.041443085	25.2	15	rigid_ph_16	0.714464937	24	16	15	Phip	pleckstrin homology domain interacting protein	BI737352	83946	Mm.221688
1425725_s_at	0.009586328	21.5	17					17	Ppp2r5c	protein phosphatase 2, regulatory subunit B (B56), gamma isoform	BF136532	26931	Mm.240396
1425792_a_at	0.001838832	22.1	13	cos_per_22_ph_13	0.881628995	22	13	13	Rorc	RAR-related orphan receptor gamma	AJ132394	19885	Mm.4372
1425835_a_at				cos_per_23_ph_15	0.656876113	23	15	15	Bbx	bobby sox homolog (Drosophila)	AF454944	70508	Mm.28940
1426022_a_at	0.022775055	26.8	1					1	Vill	villin-like	BC021808	22351	Mm.83817
1426051_a_at				cos_per_23_ph_05	0.614184231	23	5	5	Cenpb	centromere protein B	BC006628	12616	Mm.440169
1426060_at				asyrigid1_ph_06	0.699396615	24	6	6			BC007159		
1426095_a_at				cos_per_26_ph_02	0.609812042	26	2	2	Tnfrsf22	tumor necrosis factor receptor superfamily, member 22	AY046551	79202	Mm.261384
1426191_a_at				cos_per_28_ph_01	0.718971295	28	1	1	Bcl2l1	BCL2-like 1	U10100	12048	Mm.238213

Table S1: Circadian transcripts (continued)

	Signal Deconvolution			Model-Matching				Final Statistics and Annotations					
Transcript ID (Affymetrix probeset)	Fisher's G Test q-value	Period (hrs)	Phase	HAYSTACK Best Model	HAYSTACK Correlation	Period (hrs)	Phase	Phase (Final)	Gene Symbol	Description	GenBank	Entrez Gene	UniGene
1426218_at				cos_per_28_ph_20	0.638936003	28	20	20	Glcci1	glucocorticoid induced transcript 1	AA152997	170772	Mm.210787, Mm.458518
1426306_a_at				cos_per_28_ph_21	0.650306382	28	21	21	Maged2	melanoma antigen, family D, 2	AF319976	80884	Mm.22575
1426319_at				boxl_ph_04	0.635638994	24	4	4	Pdgfd	platelet-derived growth factor, D polypeptide	AF335583	71785	Mm.390122
1426334_a_at				asyrigid2_ph_09	0.665949848	24	9	9	Bcl2l11	BCL2-like 11 (apoptosis facilitator)	AF032460	12125	Mm.141083, Mm.453214
1426363_x_at				cos_per_28_ph_13	0.689456968	28	13	13	H2afy2	H2A histone family, member Y2	AW547431	404634	Mm.272870
1426368_at	0.018054891	22.4	19					19	Rin2	Ras and Rab interactor 2	AK014548	74030	Mm.433263, Mm.476860
1426383_at	0.001838832	24.9	9	cos_per_25_ph_09	0.851501795	25	9	9	Cry2	cryptochrome 2 (photolyase-like)	BF303057	12953	Mm.254181
1426392_a_at	0.002326786	25.2	19					19	Actr3	ARP3 actin-related protein 3 homolog (yeast)	BE372352	74117	Mm.183102
1426402_at	0.049896292	28.3	11					11	Syncrip	synaptotagmin binding, cytoplasmic RNA interacting protein	BB469322	56403	Mm.260545
1426419_at				rigid_ph_17	0.629543548	24	17	17	Rbm26	RNA binding motif protein 26	AK005802	74213	Mm.291542, Mm.474531, Mm.474826
1426461_at				cos_per_24_ph_04	0.608232262	24	4	4	Ugp2	UDP-glucose pyrophosphorylase 2	AI788759	216558	Mm.28877
1426464_at	0.001838832	24	4	cos_per_24_ph_04	0.867750792	24	4	4	Nr1d1	nuclear receptor subfamily 1, group D, member 1	W13191	217166	Mm.390397
1426487_a_at				cos_per_27_ph_15	0.685450631	27	15	15	Rbbp6	retinoblastoma binding protein 6	BB092954	19647	Mm.4480
1426501_a_at				boxl_ph_05	0.65078085	24	5	5	Tifa	TRAF-interacting protein with forkhead-associated domain	BB277065	211550	Mm.31852
1426502_s_at				asyrigid2_ph_01	0.743248413	24	1	1	Gpt	glutamic pyruvic transaminase, soluble	AK008086	76282	Mm.30130
1426504_a_at	0.025969991	25.5	2					2	Rnf121	ring finger protein 121	BI871826	75212	Mm.101141
1426513_at				cos_per_28_ph_10	0.639016531	28	10	10	Rbm28	RNA binding motif protein 28	BM228459	68272	Mm.40802
1426514_at				cos_per_21_ph_17	0.619911067	21	17	17	4631426J05Rik	RIKEN cDNA 4631426J05 gene	AK019474	77590	Mm.213582
1426565_at				rigid_ph_14	0.632328739	24	14	14	Igf1r	insulin-like growth factor I receptor	BE980124	16001	Mm.275742
1426583_at	0.034555079	29.1	14					14	Atf2	activating transcription factor 2	BM119623	11909	Mm.209903
1426601_at				asyrigid1_ph_09	0.75190052	24	9	9	Slc37a1	solute carrier family 37 (glycerol-3-phosphate transporter), member 1	AV376428	224674	Mm.311395

Table S1: Circadian transcripts (continued)

	SignalDecomposition			Model-Matching				Final Statistics and Annotations					
Transcript ID (Affymetrix probeset)	Fisher's G Test q-value	Period (hrs)	Phase	HAYSTACK Best Model	HAYSTACK Correlation	Period (hrs)	Phase	Phase (Final)	Gene Symbol	Description	GenBank	Entrez Gene	UniGene
1426622_a_at	0.049369186	26.5	25					1	Qpct	glutaminyl-peptide cyclotransferase (glutaminyl cyclase)	BB150720	70536	Mm.293870
1426631_at				cos_per_28_ph_08	0.712428737	28	8	8	Pus7	pseudouridylate synthase 7 homolog (S. cerevisiae)	BM199125	78697	Mm.58660
1426646_at				rigid_ph_03	0.612569771	24	3	3	9130011J15Rik	RIKEN cDNA 9130011J15 gene	AK018610	66818	Mm.22565
1426653_at				cos_per_20_ph_11	0.683049184	20	11	11	Mcm3	minichromosome maintenance deficient 3 (S. cerevisiae)	BI658327	17215	Mm.4502
1426706_s_at				cos_per_25_ph_14	0.634628768	25	14	14	Xylb	xylulokinase homolog (H. influenzae)	BB431728	102448	Mm.219497
1426736_at	0.022895207	28.6	13					13	Gspt1	G1 to S phase transition 1	AB003502	14852	Mm.325827
1426737_at				cos_per_28_ph_12	0.680923764	28	12	12	Gspt1	G1 to S phase transition 1	AB003502	14852	Mm.325827
1426754_x_at				rigid_ph_16	0.650434063	24	16	16	Ckap4	cytoskeleton-associated protein 4	BB312117	216197	Mm.334999
1426759_at	0.01311978	28.2	27					3	Map4k3	mitogen-activated protein kinase kinase kinase kinase 3	BF165548	225028	Mm.458168
1426775_s_at	0.005336887	26.2	1					1	Scamp1	secretory carrier membrane protein 1	BM115445	107767	Mm.201455
1426813_at				cos_per_28_ph_07	0.608445054	28	7	7	Ltv1	LTV1 homolog (S. cerevisiae)	U01139	353258	Mm.117581
1426863_at				cos_per_22_ph_01	0.703438714	22	1	1	Rbmx	RNA binding motif protein, X chromosome	BM123721	19655	Mm.28275
1426893_at				cos_per_25_ph_04	0.6484782	25	4	4	Fam102a	family with sequence similarity 102, member A	BC023470	98952	Mm.4065, Mm.472003
1426894_s_at	0.028525664	22.7	5	cos_per_24_ph_05	0.724494342	24	5	5	Fam102a	family with sequence similarity 102, member A	BC023470	98952	Mm.4065, Mm.472003
1426905_a_at	0.002111464	29	26					2	Dnajc10	DnaJ (Hsp40) homolog, subfamily C, member 10	AV114239	66861	Mm.21762
1426936_at				cos_per_27_ph_18	0.708767324	27	18	18	LOC215866	hypothetical protein LOC215866	BC002257	215866	
1426945_at	0.046772627	23.8	12					12	Ipo5	importin 5	AW536621	70572	Mm.221452, Mm.472208
1426946_at	0.023910531	28.6	9					9	Ipo5	importin 5	AW536621	70572	Mm.221452, Mm.472208
1426968_a_at	0.001838832	25.9	7					7	Rdh10	retinol dehydrogenase 10 (all-trans)	BG073496	98711	Mm.274376
1427033_at	0.0068098	28.7	2					2	Dnmbp	dynamin binding protein	BC025944	71972	Mm.159024
1427037_at				spike_ph_14	0.718507736	24	14	14	Eif4g1	eukaryotic translation initiation factor 4, gamma 1	BF227830	208643	Mm.260256
1427062_at				cos_per_22_ph_14	0.609963292	22	14	14	Rbbp8	retinoblastoma binding protein 8	BB167067	225182	Mm.154275

Table S1: Circadian transcripts (continued)

	Signal Deocomposition			Model-Matching				Final Statistics and Annotations					
Transcript ID (Affymetrix probeset)	Fisher's G Test q-value	Period (hrs)	Phase	HAYSTACK Best Model	HAYSTACK Correlation	Period (hrs)	Phase	Phase (Final)	Gene Symbol	Description	GenBank	Entrez Gene	UniGene
1427067_at				asyrigid2_ph_10	0.64629721	24	10	10	4933439F18Rik	RIKEN cDNA 4933439F18 gene	AJ404329	66771	Mm.29950, Mm.472990
1427068_x_at				cos_per_28_ph_11	0.642871434	28	11	11	4933439F18Rik	RIKEN cDNA 4933439F18 gene	AJ404329	66771	Mm.29950, Mm.472990
1427119_at				cos_per_28_ph_25	0.663186371	28	1	1	Spink4	serine peptidase inhibitor, Kazal type 4	AV066321	20731	Mm.25246
1427121_at				box1_ph_04	0.677354561	24	4	4	Fbxo4	F-box protein 4	BF455337	106052	Mm.234191
1427131_s_at				cos_per_27_ph_15	0.803140449	27	15	15	Lrrc58	leucine rich repeat containing 58	AV234245	320184	Mm.390882
1427151_at				cos_per_28_ph_14	0.622200663	28	14	14	Qsrl	glutamine and serine rich 1	BC021511	99003	Mm.274314
1427152_at				box2_ph_15	0.656688329	24	15	15	Qsrl	glutamine and serine rich 1	BC021511	99003	Mm.274314
1427163_at	0.024796721	29.5	8					8	Ubr2	ubiquitin protein ligase E3 component n-recognin 2	AI646734	224826	Mm.28234
1427261_at				box1_ph_05	0.705006753	24	5	5	Wwc1	WW, C2 and coiled-coil domain containing 1	BQ176786	211652	Mm.31267
1427270_a_at	0.013481656	22.6	2					2	Bsdc1	BSD domain containing 1	BF729638	100383	Mm.17918
1427296_at	0.036128917	27.3	9					9	Fam120a	family with sequence similarity 120, member A	BB553912	218236	Mm.426571
1427405_s_at				box2_ph_17	0.684272023	24	17	17	Rabl1fip5	RAB11 family interacting protein 5 (class I)	BF682225	52055	Mm.220334
1427410_at				cos_per_28_ph_02	0.628699814	28	2	2	Dleu2	deleted in lymphocytic leukemia, 2	BB812902	328425	Mm.32886, Mm.447100
1427411_s_at				cos_per_28_ph_02	0.620196499	28	2	2	Dleu2	deleted in lymphocytic leukemia, 2	BB812902	328425	Mm.32886, Mm.447100
1427457_a_at				rigid_ph_16	0.688884304	24	16	16	Bmp1	bone morphogenetic protein 1	BG248060	12153	Mm.27757
1427467_a_at	0.030205842	20.9	20					20	Rpgr	retinitis pigmentosa GTPase regulator	AJ238396	19893	Mm.247556
1427490_at				box2_ph_16	0.618706566	24	16	16	Abcb7	ATP-binding cassette, sub-family B (MDR/TAP), member 7	U43892	11306	Mm.426128
1427524_a_at				asyrigid2_ph_11	0.740225984	24	11	11	Mphosph8	M-phase phosphoprotein 8	BF168436	75339	Mm.152466, Mm.474486
1427531_a_at				cos_per_26_ph_01	0.72517712	26	1	1	Slc22a18	solute carrier family 22 (organic cation transporter), member 18	BF577497	18400	Mm.271740
1427568_a_at				cos_per_28_ph_20	0.687074307	28	20	20	Ift80	intraflagellar transport 80 homolog (Chlamydomonas)	BC013814	68259	Mm.477781
1427762_x_at				cos_per_25_ph_02	0.609364374	25	2	2	Hist1h2bp	histone cluster 1, H2bp	M25487	319188	Mm.264645
1427773_a_at	0.046677418	25.6	1					1	Rabac1	Rab acceptor 1 (prenylated)	L40934	14470	Mm.22473

Table S1: Circadian transcripts (continued)

	Signal Decomposition			Model-Matching				Final Statistics and Annotations					
Transcript ID (Affymetrix probeset)	Fisher's G Test q-value	Period (hrs)	Phase	HAYSTACK Best Model	HAYSTACK Correlation	Period (hrs)	Phase	Phase (Final)	Gene Symbol	Description	GenBank	Entrez Gene	UniGene
1427798_x_at				cos_per_28_ph_16	0.694215637	28	16	16			BF580235		
1427894_at	0.029577218	22.3	8					8	Vasn	vasorin	AK012169	246154	Mm.248337
1427971_at	0.046145235	22.1	17					17	Cdc73	cell division cycle 73, Paf1/RNA polymerase II complex component, homolog (S. cerevisiae)	BB622571	214498	Mm.389191, Mm.393505, Mm.398849
1428141_at	0.013690101	23.1	12	rigid_ph_13	0.765056511	24	13	12	Gga2	golgi associated, gamma adaptin ear containing, ARF binding protein 2	AK004632	74105	Mm.29619
1428146_s_at	0.049240684	29.5	25	cos_per_25_ph_02	0.713428032	52	2	1	Acaa2	acetyl-Coenzyme A acyltransferase 2 (mitochondrial3-oxoacyl-Coenzyme A thiolase)	AK002555	52538	Mm.245724
1428162_at				asyrigid1_ph_00	0.63507089	24	0	0	4933421E11Rik	RIKEN cDNA 4933421E11 gene	AK008209	321000	Mm.259638
1428167_a_at				cos_per_26_ph_17	0.695680211	26	17	17	Mpzl1	myelin protein zero-like 1	AK003513	68481	Mm.46438
1428170_at				cos_per_28_ph_13	0.612736338	28	13	13	Zfp180	zinc finger protein 180	AK009725	210135	Mm.32254
1428220_at				box2_ph_17	0.718161234	24	17	17	5730419I09Rik	RIKEN cDNA 5730419I09 gene	AK017577	74741	Mm.130260
1428234_at				cos_per_28_ph_16	0.731146341	28	16	16	Cpsf6	cleavage and polyadenylation specific factor 6	BB425379	432508	Mm.440510, Mm.440969, Mm.458589, Mm.476779
1428296_at	0.020403029	21.2	9					9	ENSMUSG00000074846	predicted gene, ENSMUSG00000074846	AV102258	100043714	
1428329_a_at				cos_per_28_ph_20	0.619600278	28	20	20	Ift80	intraflagellar transport 80 homolog (Chlamydomonas)	AK019542	68259	Mm.477781
1428373_at				cos_per_27_ph_01	0.655528972	27	1	1	Ipgk2	inositol hexaphosphate kinase 2	AK005166	76500	Mm.276336
1428428_at				cos_per_28_ph_04	0.626277759	28	4	4	Abhd11	abhydrolase domain containing 11	AK004244	68758	Mm.389700
1428443_a_at	0.017589507	26.5	2					2	Rap1gap	Rap1 GTPase-activating protein	AK005063	110351	Mm.180763
1428492_at				cos_per_28_ph_20	0.730211653	28	20	20	Gligr2	GLI pathogenesis-related 2	BM208214	384009	Mm.22213
1428512_at				box2_ph_15	0.641667166	24	15	15	Bhlhb9	basic helix-loop-helix domain containing, class B9	AK012577	70237	Mm.440847
1428562_at				cos_per_21_ph_02	0.722059193	21	2	2	2210403K04Rik	RIKEN cDNA 2210403K04 gene	AK008813	67098	Mm.458401
1428564_at				cos_per_28_ph_26	0.618124329	28	2	2	Zfp579	zinc finger protein 579	AK003337	68490	Mm.76400
1428584_a_at				cos_per_27_ph_01	0.707122918	27	1	1	Haghl	hydroxyacylglutathione hydrolase-like	AK012748	68977	Mm.29230

Table S1: Circadian transcripts (continued)

	Signal Decomposition			Model-Matching				Final Statistics and Annotations					
Transcript ID (Affymetrix probeset)	Fisher's G Test q-value	Period (hrs)	Phase	HAYSTACK Best Model	HAYSTACK Correlation	Period (hrs)	Phase	Phase (Final)	Gene Symbol	Description	GenBank	Entrez Gene	UniGene
1428630_x_at				cos_per_26_ph_01	0.677587911	26	1	1	Haghl	hydroxyacylglutathione hydrolase-like	AK021220	68977	Mm.29230
1428636_at	0.027378568	26.6	9					9	Steap2	six transmembrane epithelial antigen of prostate 2	AK015015	74051	Mm.274956, Mm.477119
1428639_at				asyrigid2_ph_09	0.681284086	24	9	9	Lin9	lin-9 homolog (C. elegans)	AK012271	72568	Mm.275044
1428649_at				box2_ph_15	0.650901635	24	15	15	Cand1	cullin associated and neddylation dissociated 1	AI510077	71902	Mm.203965
1428671_at				cos_per_26_ph_02	0.611347294	26	2	2	2200002D01Rik	RIKEN cDNA 2200002D01 gene	AK008617	72275	Mm.441142
1428732_at				asyrigid2_ph_00	0.61876485	24	0	0	1700008J07Rik	RIKEN cDNA 1700008J07 gene	AK005774	629159	Mm.256720
1428742_at	0.008638581	24.5	13					13	Fbxo45	F-box protein 45	AK011438	268882	Mm.256137
1428760_at	0.010482732	20.7	1					1	Snapc3	small nuclear RNA activating complex, polypeptide 3	AW537061	77634	Mm.271985
1428773_s_at	0.001838832	24.9	16	cos_per_25_ph_16	0.867458738	25	16	16	Bcor	BCL6 interacting corepressor	AK018370	71458	Mm.196328
1428777_at				rigid_ph_16	0.649962032	24	16	16	Spred1	sprouty protein with EVH-1 domain 1, related sequence	AK017680	114715	Mm.245890, Mm.392720, Mm.392726, Mm.397626
1428781_at				cos_per_28_ph_24	0.679106111	28	0	0	Dmkn	dermokine	BI452905	73712	Mm.30138
1428789_at	0.045319471	24.4	4					4	Ralgps2	Ral GEF with PH domain and SH3 binding motif 2	AK008856	78255	Mm.279007, Mm.28376
1428844_a_at				cos_per_28_ph_15	0.793034037	28	15	15	Bclaf1	BCL2-associated transcription factor 1	BI965039	72567	Mm.294783
1428849_at				rigid_ph_15	0.635452588	24	15	15	Rps6kb1	ribosomal protein S6 kinase, polypeptide 1	AI451506	72508	Mm.394280, Mm.446624
1428861_at	0.044792165	23.1	20					20	Filip1l	filamin A interacting protein 1-like	AK019472	78749	Mm.328360
1428870_at				cos_per_28_ph_08	0.708513942	28	8	8	Nolc1	nucleolar and coiled-body phosphoprotein 1	BM213850	70769	Mm.402190
1428873_a_at	0.033758531	22.4	15					15	Msl1	male-specific lethal 1 homolog (Drosophila)	AW495537	74026	Mm.258352
1428884_at	0.035152309	25.1	6					6	Tmem57	transmembrane protein 57	AK003528	66146	Mm.99798
1428894_at				cos_per_27_ph_02	0.829913976	27	2	2	1300018J18Rik	RIKEN cDNA 1300018J18 gene	AK005048	223776	Mm.44763, Mm.475235
1428898_at	0.026539069	27.4	1					1	Mon1a	MON1 homolog A (yeast)	AK013387	72825	Mm.38037
1428903_at	0.030702624	28.6	26					2	Dem1	defects in morphology 1 homolog (S. cerevisiae)	AK014134	73172	Mm.151436

Table S1: Circadian transcripts (continued)

	Signal Decomposition			Model-Matching				Final Statistics and Annotations					
Transcript ID (Affymetrix probeset)	Fisher's G Test q-value	Period (hrs)	Phase	HAYSTACK Best Model	HAYSTACK Correlation	Period (hrs)	Phase	Phase (Final)	Gene Symbol	Description	GenBank	Entrez Gene	UniGene
1428908_at	0.019138454	29.7	14					14	Rbm25	RNA binding motif protein 25	BG228787	67039	Mm.46005
1428938_at				rigid_ph_15	0.670053122	24	15	15	Gnaq	guanine nucleotide binding protein, alpha q polypeptide	W41916	14682	Mm.439701, Mm.441601
1428946_at				box2_ph_15	0.659238413	24	15	15	Uba6	ubiquitin-like modifier activating enzyme 6	BB417360	231380	Mm.34012, Mm.392216, Mm.393083, Mm.440954
1428967_at	0.042329881	24.2	13	rigid_ph_14	0.727231099	24	14	13	Igf1r	insulin-like growth factor I receptor	BB446952	16001	Mm.275742
1428968_at				spike_ph_14	0.658348421	24	14	14	Cep57	centrosomal protein 57	AW457682	74360	Mm.157212
1429006_x_at	0.007142068	27.5	22					22	2610110G12Rik	RIKEN cDNA 2610110G12 gene	AK011838	73242	Mm.273155
1429029_at				spike_ph_07	0.708121981	24	7	7	Sgms2	sphingomyelin synthase 2	AK016659	74442	Mm.273360
1429057_at				rigid_ph_15	0.633829825	24	15	15	Narg1l	NMDA receptor regulated 1-like	AK007755	66897	Mm.24425
1429060_at				rigid_ph_00	0.664517527	24	0	0	Malat1	metastasis associated lung adenocarcinoma transcript 1 (non-coding RNA)	AK020483	72289	Mm.298256
1429128_x_at				spike_ph_04	0.632797706	24	4	4	Nfkb2	nuclear factor of kappa light polypeptide gene enhancer in B-cells 2, p49/p100	BI466783	18034	Mm.102365
1429133_at				asyrigid2_ph_00	0.65892681	24	0	0	Nxnl2	nucleoredoxin-like 2	AK015847	75124	Mm.179243
1429169_at				cos_per_21_ph_01	0.609136802	21	1	1	Rbm3	RNA binding motif protein 3	AK011224	19652	Mm.128512, Mm.360569
1429190_at				rigid_ph_15	0.619803636	24	15	15	Arsb	arylsulfatase B	BI440651	11881	Mm.300178, Mm.472255
1429206_at				spike_ph_07	0.710216802	24	7	7	Rhobtb1	Rho-related BTB domain containing 1	AK014194	69288	Mm.26659
1429219_at				asyrigid1_ph_21	0.618882222	24	21	21	1200009F10Rik	RIKEN cDNA 1200009F10 gene	AK004670	67454	Mm.252843
1429227_x_at	0.049486629	22.8	13					13	Nap1l1	nucleosome assembly protein 1-like 1	AK007322	53605	Mm.290407
1429261_at				cos_per_28_ph_04	0.666886545	28	4	4	2210411K11Rik	RIKEN cDNA 2210411K11 gene	AW045964	664968	Mm.292837
1429294_at				rigid_ph_13	0.643430272	24	13	13	Trip13	thyroid hormone receptor interactor 13	AK010336	69716	Mm.275095
1429306_at				asyrigid2_ph_11	0.60949927	24	11	11	Lzic	leucine zipper and CTNNBIP1 domain containing	AK007657	69151	Mm.464434
1429326_at				cos_per_28_ph_19	0.61694168	28	19	19	Cenpl	centromere protein L	BB538449	70454	Mm.248212

Table S1: Circadian transcripts (continued)

	Signal Deconcomposition			Model-Matching				Final Statistics and Annotations					
Transcript ID (Affymetrix probeset)	Fisher's G Test q-value	Period (hrs)	Phase	HAYSTACK Best Model	HAYSTACK Correlation	Period (hrs)	Phase	Phase (Final)	Gene Symbol	Description	GenBank	Entrez Gene	UniGene
1429328_at	0.010526296	28.5	27					3	Nsflc	NSFL1 (p97) cofactor (p47)	BG922397	386649	Mm.419479
1429348_at	0.008826296	24.2	7					7	Sema3c	sema domain, immunoglobulin domain (Ig), short basic domain, secreted, (semaphorin) 3C	AK004119	20348	Mm.5071
1429373_x_at				box2_ph_17	0.623483722	24	17	17	Crtc2	CREB regulated transcription coactivator 2	AK014553	74343	Mm.35627
1429399_at	0.024303501	22.5	21					21	Rnfl25	ring finger protein 125	BB667823	67664	Mm.45980
1429413_at				spike_ph_05	0.677142997	24	5	5	Cpm	carboxypeptidase M	AK017670	70574	Mm.339332
1429417_at	0.021627238	23.1	19	rigid_ph_18	0.755521172	24	18	19	Chsy3	chondroitin sulfate synthase 3	AK019528	78923	Mm.477838, Mm.84007
1429434_at				spike_ph_19	0.615504138	24	19	19	Pik3ca	phosphatidylinositol3-kinase, catalytic, alpha polypeptide	BE647269	18706	Mm.260521, Mm.393204, Mm.394949
1429438_at				rigid_ph_16	0.656237772	24	16	16	Bcor	BCL6 interacting corepressor	AV318805	71458	Mm.196328
1429490_at				cos_per_28_ph_14	0.61358494	28	14	14	Rif1	Rap1 interacting factor 1 homolog (yeast)	AK018316	51869	Mm.254530
1429504_at				spike_ph_00	0.636008518	24	0	0	Rnpc3	RNA-binding region (RNP1, RRM) containing 3	BE134108	67225	Mm.316928
1429712_at	0.016688272	23.9	20					20	RP24-87L14.2	KRAB box and zinc finger, C2H2 type domain containing protein	AK005093	100125272	
1429764_at				cos_per_26_ph_02	0.695983705	26	2	2	Fam10b	family with sequence similarity 101, member B	BF101721	76566	Mm.34131
1429770_at				cos_per_28_ph_13	0.629672724	28	13	13	Pggt1b	protein geranylgeranyltransferase type I, beta subunit	BI107300	225467	Mm.262096, Mm.393044
1429792_at	0.001838832	29.2	4					4	9530048O09Rik	RIKEN cDNA 9530048O09 gene	BB398793	78611	Mm.446227
1429863_at	0.001838832	22	16					16	Lonrf3	LON peptidase N-terminal domain and ring finger 3	AK016522	74365	Mm.327654
1430051_at				cos_per_28_ph_27	0.72019468	28	3	3	4930486L24Rik	RIKEN cDNA 4930486L24 gene	AK015635	214639	Mm.19839
1430295_at				spike_ph_01	0.62972033	24	1	1	Gna13	guanine nucleotide binding protein, alpha 13	BG094302	14674	Mm.193925
1430367_at	0.005124604	25.1	25	cos_per_25_ph_00	0.803884543	25	0	1	Stambpl1	STAM binding protein like 1	BE331859	76630	Mm.130952
1430391_a_at				cos_per_28_ph_27	0.705161318	28	3	3	St8sia4	ST8 alpha-N-acetyl-neuraminide alpha-2,8-sialyltransferase 4	AK003690	20452	Mm.306228
1430527_a_at	0.041717871	29	28					4	Rnf167	ring finger protein 167	AK017523	70510	Mm.261818
1430553_at	0.012699878	27.7	25	cos_per_27_ph_26	0.802270324	27	2	1	Vsig1	V-set and immunoglobulin domain containing 1	AV268106	78789	Mm.244932

Table S1: Circadian transcripts (continued)

	Signal Deconvolution			Model-Matching				Final Statistics and Annotations					
Transcript ID (Affymetrix probeset)	Fisher's G Test q-value	Period (hrs)	Phase	HAYSTACK Best Model	HAYSTACK Correlation	Period (hrs)	Phase	Phase (Final)	Gene Symbol	Description	GenBank	Entrez Gene	UniGene
1430827_a_at				box2_ph_16	0.642907641	24	16	16	Ptk2	PTK2 protein tyrosine kinase 2	AV301702	14083	Mm.254494
1430963_at	0.008367627	26.4	3					3	Gcnt3	glucosaminyl (N-acetyl) transferase 3, mucin type	AK008762	72077	Mm.195555
1430997_at				asyrigid2_ph_11	0.674610453	24	11	11	Cd47	CD47 antigen (Rh-related antigen, integrin-associated signal transducer)	AI882525	16423	Mm.31752, Mm.390865
1431024_a_at				cos_per_28_ph_15	0.655459899	28	15	15	Arid4b	AT rich interactive domain 4B (RBP1-like)	AK020165	94246	Mm.439784
1431050_at	0.041727722	29	12	cos_per_27_ph_13	0.759658471	27	13	12	Rps6ka5	ribosomal protein S6 kinase, polypeptide 5	BE291900	73086	Mm.220417, Mm.392855
1431055_a_at	0.003524429	26.8	1					1	Snx10	sorting nexin 10	AK010399	71982	Mm.476868
1431101_a_at				asyrigid2_ph_01	0.639494772	24	1	1	Srd5a1	steroid 5 alpha-reductase 1	AK019597	78925	Mm.422833, Mm.451912
1431182_at				cos_per_21_ph_02	0.688589386	21	2	2	Hspa8	heat shock protein 8	AK004608	15481	Mm.290774, Mm.336743, Mm.351377, Mm.412745
1431183_at				box2_ph_17	0.637380053	24	17	17	1700066M21Rik	RIKEN cDNA 1700066M21 gene	AA109251	73467	Mm.263673, Mm.432181
1431212_a_at				cos_per_28_ph_08	0.620572412	28	8	8	Trmt6	tRNA methyltransferase 6 homolog (S. cerevisiae)	BG079674	66926	Mm.34199
1431320_a_at				cos_per_25_ph_16	0.690714871	25	16	16	Myo5a	myosin VA	AK002362	17918	Mm.3645
1431507_a_at	0.007927752	26.7	25					1	Synj2bp	synaptojanin 2 binding protein	AK008254	24071	Mm.279603
1431530_a_at				cos_per_25_ph_03	0.684886293	25	3	3	Tspan5	tetraspanin 5	AK015705	56224	Mm.31927
1431561_a_at				cos_per_28_ph_27	0.71362078	28	3	3	Dhx34	DEAH (Asp-Glu-Ala-His) box polypeptide 34	AK007461	71723	Mm.75259
1431744_a_at				cos_per_22_ph_16	0.628090379	22	16	16	Smap1	stromal membrane-associated protein 1	AK014888	98366	Mm.329963
1431768_a_at				cos_per_28_ph_10	0.609284996	28	10	10	Prmt3	protein arginine N-methyltransferase 3	AK008118	71974	Mm.33202, Mm.349442
1431929_a_at	0.020116282	26.5	7					7	Stxl7	syntaxin 17	AK014718	67727	Mm.171334
1431972_a_at				asyrigid2_ph_12	0.619897062	24	12	12	Gcap14	granule cell antiserum positive 14	AK005931	72972	Mm.27621
1432195_s_at	0.011002398	24	1					1	Ccnl2	cyclin L2	AK008585	56036	Mm.23492
1432416_a_at	0.02345327	29.5	8					8	Npm1	nucleophosmin 1	AK005498	18148	Mm.6343
1432418_a_at				cos_per_28_ph_26	0.701614946	28	2	2	Ckmt1	creatine kinase, mitochondrial 1, ubiquitous	AK018487	12716	Mm.252145

Table S1: Circadian transcripts (continued)

	Signal Deconvolution			Model-Matching				Final Statistics and Annotations					
Transcript ID (Affymetrix probeset)	Fisher's G Test q-value	Period (hrs)	Phase	HAYSTACK Best Model	HAYSTACK Correlation	Period (hrs)	Phase	Phase (Final)	Gene Symbol	Description	GenBank	Entrez Gene	UniGene
1432511_s_at				box2_ph_15	0.614585808	24	15	15	Cep27	centrosomal protein 27	AK007106	66296	Mm.221900
1433489_s_at				boxl_ph_04	0.633071281	24	4	4	Fgfr2	fibroblast growth factor receptor 2	BG873440	14183	Mm.16340
1433551_at	0.02335674	21.5	8	boxl_ph_05	0.768660277	24	5	8	Vat11	vesicle amine transport protein 1 homolog-like (T. californica)	AV173683	270097	Mm.334825
1433559_at	0.005354193	29.8	4					4	Slc45a4	solute carrier family 45, member 4	BB811412	106068	Mm.212813
1433574_at				asyrigid1_ph_07	0.617881854	24	7	7	Cdc37l1	cell division cycle 37 homolog (S. cerevisiae)-like 1	BE824561	67072	Mm.476835
1433633_at				asyrigid1_ph_21	0.613618661	24	21	21	Irf2bp2	interferon regulatory factor 2 binding protein 2	BB183385	270110	Mm.334918, Mm.470682
1433668_at	0.001838832	25.6	18					18	Pnrc1	proline-rich nuclear receptor coactivator 1	BI410130	108767	Mm.27769, Mm.48724
1433683_at	0.016622241	29.6	29					5	Rbm35b	RNA binding motif protein 35b	BF124648	77411	Mm.183003
1433691_at				cos_per_28_ph_22	0.834369524	28	22	22	Ppp1r3c	protein phosphatase 1, regulatory (inhibitor) subunit 3C	BQ176864	53412	Mm.24724
1433706_a_at	0.049602996	23	4					4	Ptpla d1	protein tyrosine phosphatase-like A domain containing 1	BG075943	57874	Mm.477769
1433717_at	0.028051454	27.5	23					23	D19Wsu162e	DNA segment, Chr 19, Wayne State University 162, expressed	BI903574	226178	Mm.329895
1433733_a_at	0.001838832	22.4	15	cos_per_23_ph_15	0.958762251	23	15	15	Cry1	cryptochrome 1 (photolyase-like)	BG069864	12952	Mm.26237
1433757_a_at				rigid_ph_00	0.681150851	24	0	0	Nisch	nischarin	BB025231	64652	Mm.298728
1433786_x_at				spike_ph_04	0.654671631	24	4	4	Serf2	small EDRK-rich factor 2	AI596986	378702	Mm.262252
1433802_at				boxl_ph_04	0.632433278	24	4	4	Tmem151a	transmembrane protein 151A	BM114677	381199	Mm.329663
1433823_at	0.035879641	24.3	16					16	Ptpdc1	protein tyrosine phosphatase domain containing 1	AV254040	218232	Mm.315089
1433872_at				box2_ph_17	0.688484759	24	17	17	Slc12a6	solute carrier family 12, member 6	BB143137	107723	Mm.477363
1433875_at	0.028842068	20	7					7	4732418C07Rik	RIKEN cDNA 4732418C07 gene	BG920372	230648	Mm.283565
1433932_x_at				cos_per_28_ph_23	0.612805536	28	23	23	C030046I01Rik	RIKEN cDNA C030046I01 gene	AW553381	109284	Mm.300416, Mm.395584
1433935_at				asyrigid1_ph_19	0.608280847	24	19	19	AU020206	expressed sequence AU020206	BI151331	101757	Mm.200422, Mm.394851
1433943_at	0.024556392	27.3	9					9	Itpr ip	inositol 1,4,5-triphosphate receptor interacting protein	BM207348	414801	Mm.29457
1434014_at				cos_per_24_ph_16	0.642724574	24	16	16	Atg4c	autophagy-related 4C (yeast)	BB291836	242557	Mm.277366

Table S1: Circadian transcripts (continued)

	Signal Deconvolution			Model-Matching				Final Statistics and Annotations					
Transcript ID (Affymetrix probeset)	Fisher's G Test q-value	Period (hrs)	Phase	HAYSTACK Best Model	HAYSTACK Correlation	Period (hrs)	Phase	Phase (Final)	Gene Symbol	Description	GenBank	Entrez Gene	UniGene
1434088_at	0.025258578	25.7	4					4	Zkscan17	zinc finger with KRAB and SCAN domains 17	BM119467	268417	Mm.239793
1434100_x_at				asyrigid1_ph_22	0.63763079	24	22	22			BB752359		
1434124_x_at	0.028996765	27.2	1					1	2400001E08Rik	RIKEN cDNA 2400001E08 gene	AV100071	66508	Mm.214841, Mm.30003, Mm.359278
1434149_at				rigid_ph_16	0.618550164	24	16	16	Tcf4	transcription factor 4	BB364520	21413	Mm.4269
1434175_s_at				box2_ph_17	0.677958891	24	17	17	Tecpr1	tectonin beta-propeller repeat containing 1	BB759101	70381	Mm.239412, Mm.458463
1434202_a_at				cos_per_20_ph_00	0.665045038	20	0	0	Fam107a	family with sequence similarity 107, member A	BF682848	268709	Mm.256058, Mm.472988
1434214_at	0.027914415	26.4	1	cos_per_26_ph_02	0.743445187	26	2	1	0910001L09Rik	RIKEN cDNA 0910001L09 gene	BI525016	66096	Mm.206901
1434215_at				rigid_ph_15	0.621825739	24	15	15	B230308N11Rik	RIKEN cDNA B230308N11 gene	AW554529	320060	Mm.278974, Mm.319516
1434236_at	0.018758272	26	18	rigid_ph_18	0.756166719	24	18	18	Zdhhc20	zinc finger, DHHC domain containing 20	BB667600	75965	Mm.29044
1434239_at				cos_per_28_ph_10	0.730248574	28	10	10	Rrp12	ribosomal RNA processing 12 homolog (S. cerevisiae)	AW554921	107094	Mm.276044
1434278_at				cos_per_28_ph_11	0.721183967	28	11	11	Mtm1	X-linked myotubular myopathy gene 1	BG976607	17772	Mm.274981, Mm.423278
1434279_at				cos_per_28_ph_11	0.766032915	28	11	11			BG976607		
1434280_at				cos_per_28_ph_11	0.738707189	28	11	11			BG976607		
1434298_at				cos_per_28_ph_14	0.651602857	28	14	14	Zeb2	zinc finger E-box binding homeobox 2	BQ174116	24136	Mm.440702
1434342_at				cos_per_28_ph_21	0.727275833	28	21	21	S100b	S100 protein, beta polypeptide, neural	BB316114	20203	Mm.235998
1434357_a_at				box1_ph_14	0.614120251	24	14	14	Kpnb1	karyopherin (importin) beta 1	AW544889	16211	Mm.251013
1434378_a_at	0.028428547	28	24	cos_per_26_ph_00	0.746393614	26	0	0			BG868949		
1434383_at	0.016921385	25.8	17					17	Pja2	praja 2, RING-H2 motif containing	BM114949	224938	Mm.41711
1434387_at	0.041443085	25.4	1					1	Itfg3	integrin alpha FG-GAP repeat containing 3	AV251853	106581	Mm.28844
1434391_at				spike_ph_00	0.618812964	24	0	0	AI503316	expressed sequence AI503316	BB200448	105860	Mm.426956, Mm.86589

Table S1: Circadian transcripts (continued)

	Signal Decomposition			Model-Matching				Final Statistics and Annotations					
Transcript ID (Affymetrix probeset)	Fisher's G Test q-value	Period (hrs)	Phase	HAYSTACK Best Model	HAYSTACK Correlation	Period (hrs)	Phase	Phase (Final)	Gene Symbol	Description	GenBank	Entrez Gene	UniGene
1434453_at	0.037487115	29.8	6					6	Polr3a	polymerase (RNA) III (DNA directed) polypeptide A	BB343487	218832	Mm.343610, Mm.395588, Mm.399136
1434456_at				cos_per_28_ph_08	0.612872137	28	8	8	Rundc3b	RUN domain containing 3B	BG075955	242819	Mm.332192
1434469_at	0.025592555	22.3	13					13	Otud4	OTU domain containing 4	BM238914	73945	Mm.34348
1434472_at	0.011851374	22.2	7					7	Dusp3	dual specificity phosphatase 3 (vaccinia virus phosphatase VH1-related)	AV287497	72349	Mm.196295, Mm.229761
1434478_at	0.019453109	27.1	26					2	Heca	headcase homolog (Drosophila)	BE447663	380629	Mm.276430, Mm.473073
1434491_a_at	0.013732756	24.9	17					17	Cox6c	cytochrome c oxidase, subunit VIc	AV111078	12864	Mm.548
1434500_at	0.00184127	27.7	1					1	Tsyh2	tweety homolog 2 (Drosophila)	BF585303	117160	Mm.271934, Mm.475167
1434568_at				asyrigid2_ph_00	0.609859201	24	0	0	Gtf3c6	general transcription factor IIIC, polypeptide 6, alpha	BG065425	67371	Mm.475662
1434581_at				box1_ph_04	0.646937497	24	4	4	2410066E13Rik	RIKEN cDNA 2410066E13 gene	BB167663	68235	Mm.233860
1434605_at	0.003958467	22.8	15	rigid_ph_15	0.821479523	24	15	15	Eif5b	eukaryotic translation initiation factor 5B	BM236870	226982	Mm.260943
1434642_at	0.020841129	25	3					3	Hsd17b11	hydroxysteroid (17-beta) dehydrogenase 11	BB546344	114664	Mm.46019
1434664_at				box2_ph_17	0.740718214	24	17	17	2410129H14Rik	RIKEN cDNA 2410129H14 gene	BI153133	76789	Mm.476849
1434687_at				box2_ph_16	0.687971556	24	16	16	C730026J16	hypothetical protein C730026J16	BE456566	331006	Mm.440158
1434792_at				cos_per_27_ph_00	0.614951241	27	0	0	2010320M18Rik	RIKEN cDNA 2010320M18 gene	BF531481	72093	Mm.271208
1434830_at				cos_per_26_ph_02	0.701842445	26	2	2	Mxd1	MAX dimerization protein 1	AV228517	17119	Mm.279580
1434851_s_at	0.028965696	27.2	1	asyrigid2_ph_01	0.78661694	24	1	1	Crb3	crumbs homolog 3 (Drosophila)	AU015319	224912	Mm.391027
1434875_a_at				cos_per_28_ph_17	0.672246113	28	17	17	Hmgn3	high mobility group nucleosomal binding domain 3	AV018952	94353	Mm.244426
1434880_at	0.012471813	22.7	8					8	Etv6	ets variant gene 6 (TEL oncogene)	BB667430	14011	Mm.269995
1434882_at				cos_per_23_ph_17	0.680489975	23	17	17	Mtdh	metadherin	AV083741	67154	Mm.130883
1434889_at	0.036526986	22.2	8					8	Plekha7	pleckstrin homology domain containing, family A member 7	BI905111	233765	Mm.3741
1434923_at	0.020856164	28.3	25					1	Cox19	COX19 cytochrome c oxidase assembly homolog (S. cerevisiae)	AV354536	68033	Mm.261064

Table S1: Circadian transcripts (continued)

	Signal Deocomposition			Model-Matching				Final Statistics and Annotations					
Transcript ID (Affymetrix probeset)	Fisher's G Test q-value	Period (hrs)	Phase	HAYSTACK Best Model	HAYSTACK Correlation	Period (hrs)	Phase	Phase (Final)	Gene Symbol	Description	GenBank	Entrez Gene	UniGene
1434957_at	0.038287677	28.1	6					6	Cdon	cell adhesion molecule-related/down-regulated by oncogenes	AW557006	57810	Mm.80509
1434958_at				cos_per_27_ph_12	0.635612738	27	12	12	Sacs	sacsin	BG075163	50720	Mm.440703, Mm.446687
1434975_x_at	0.049028155	27.1	23					23	4933439C20Rik	RIKEN cDNA 4933439C20 gene	AA673371	66776	Mm.247625, Mm.335641
1435041_at	0.033990816	23.2	2	rigid_ph_02	0.734748942	24	2	2	Myl6	myosin, light polypeptide 6, alkali, smooth muscle and non-muscle	BI108818	17904	Mm.337074
1435043_at	0.025366331	23.5	15					15	Plcb1	phospholipase C, beta 1	BB794831	18795	Mm.330607
1435058_x_at				cos_per_28_ph_16	0.673809441	28	16	16	Stxbp3a	syntaxin binding protein 3A	AI528529	20912	Mm.316894
1435079_at				cos_per_20_ph_02	0.611548145	20	2	2	Sfrs18	splicing factor, arginine/serine-rich 18	BB767442	66625	Mm.100117
1435114_at				cos_per_20_ph_11	0.645323498	20	11	11	Wdhd1	WD repeat and HMG-box DNA binding protein 1	C77437	218973	Mm.265615
1435167_at				cos_per_28_ph_14	0.669633427	28	14	14	Ranbp6	RAN binding protein 6	AW108431	240614	Mm.125503
1435170_at				cos_per_28_ph_06	0.649056413	28	6	6	Tsr2	TSR2, 20S rRNA accumulation, homolog (S. cerevisiae)	BQ177187	69499	Mm.475704, Mm.8142
1435181_at				box2_ph_17	0.62961076	24	17	17	Lin54	lin-54 homolog (C. elegans)	BG073348	231506	Mm.212568
1435209_at				rigid_ph_14	0.652931171	24	14	14	BC057079	cDNA sequence BC057079	AV270935	230393	Mm.287210
1435230_at				asyrigid2_ph_07	0.626141852	24	7	7	Ankrd12	ankyrin repeat domain 12	BB277613	106585	Mm.34706, Mm.441953
1435249_at	0.048741322	29.8	8					8	Btaf1	BTAF1 RNA polymerase II, B-TFIID transcription factor-associated, (Mot1 homolog, S. cerevisiae)	BG917504	107182	Mm.295062
1435267_at				asyrigid1_ph_06	0.745592488	24	6	6	A430108E01Rik	RIKEN cDNA A430108E01 gene	BB041868	384382	Mm.359054, Mm.414559, Mm.432328
1435327_at	0.00751356	28.6	12					12	Lpgat1	lysophosphatidylglycerol acyltransferase 1	BG071867	226856	Mm.277958
1435346_at				cos_per_28_ph_20	0.629901144	28	20	20	Ccdc82	coiled-coil domain containing 82	BE352816	66396	Mm.290620
1435353_a_at	0.039833422	27.1	25					1	Sfi1	Sfi1 homolog, spindle assembly associated (yeast)	BI454991	78887	Mm.320785
1435394_s_at	0.040864329	23.6	4					4	Rhoc	ras homolog gene family, member C	AI503490	11853	Mm.262
1435435_at	0.037293857	29.9	23					23	Cttnbp2	cortactin binding protein 2	BB357580	30785	Mm.224189
1435525_at				cos_per_27_ph_15	0.678619793	27	15	15	Kctd17	potassium channel tetramerisation domain containing 17	BI408602	72844	Mm.390816

Table S1: Circadian transcripts (continued)

	Signal Deconvolution			Model-Matching				Final Statistics and Annotations					
Transcript ID (Affymetrix probeset)	Fisher's G Test q-value	Period (hrs)	Phase	HAYSTACK Best Model	HAYSTACK Correlation	Period (hrs)	Phase	Phase (Final)	Gene Symbol	Description	GenBank	Entrez Gene	UniGene
1435534_a_at				cos_per_28_ph_13	0.666631302	28	13	13	OTTMUSG00000016825	predicted gene, OTTMUSG00000016825	BF228097	100043869	Mm.6932
1435562_at				box2_ph_15	0.631997863	24	15	15	Pdzd8	PDZ domain containing 8	BB795209	107368	Mm.268797, Mm.361919
1435565_at				rigid_ph_03	0.703355679	24	3	3			BM219187		
1435581_at				asyrigid2_ph_21	0.641875382	24	21	21	Bace2	beta-site APP-cleaving enzyme 2	BE947462	56175	Mm.97885
1435589_at				spike_ph_06	0.620598629	24	6	6	Ccdc85b	coiled-coil domain containing 85B	AV308222	240514	Mm.329657
1435598_at				cos_per_27_ph_00	0.651801776	27	0	0			BE996371		
1435635_at				cos_per_22_ph_17	0.685968334	22	17	17	Pcmtd1	protein-L-isoaspartate (D-aspartate) O-methyltransferase domain containing 1	BB549335	319263	Mm.21539
1435650_at				asyrigid1_ph_22	0.651599121	24	22	22	Hapln4	hyaluronan and proteoglycan link protein 4	BB082407	330790	Mm.152048
1435744_at				asyrigid2_ph_20	0.654954038	24	20	20	6720401G13Rik	RIKEN cDNA 6720401G13 gene	BG075556	103012	Mm.336056
1435795_at				cos_per_27_ph_13	0.68808873	27	13	13	Glb1	galactosidase, beta 1	BE956926	12091	Mm.290516, Mm.440489
1435800_a_at				cos_per_28_ph_12	0.667264804	28	12	12	Csda	cold shock domain protein A	BB779100	56449	Mm.458000
1435880_at	0.002807581	29.5	4					4	Ankrd50	ankyrin repeat domain 50	BM119343	99696	Mm.290587
1435891_x_at				cos_per_28_ph_14	0.620308689	28	14	14			BQ175465		
1435910_at	0.046370467	26.8	5					5	Fads3	fatty acid desaturase 3	BM235658	60527	Mm.253875
1436025_at				rigid_ph_16	0.628666902	24	16	16	Ccdc88a	coiled coil domain containing 88A	BB228331	108686	Mm.338284, Mm.441367
1436051_at				cos_per_26_ph_14	0.65917742	26	14	14	Myo5a	myosin VA	BQ174518	17918	Mm.3645
1436079_s_at				cos_per_25_ph_03	0.693612328	25	3	3	Vapb	vesicle-associated membrane protein, associated protein B and C	BB308907	56491	Mm.260456
1436081_a_at				rigid_ph_04	0.655750833	24	4	4	Zfp414	zinc finger protein 414	BE632205	328801	Mm.181488
1436103_at				asyrigid2_ph_00	0.640973095	24	0	0	Rab3ip	RAB3A interacting protein	AV235634	216363	Mm.336394
1436116_x_at				cos_per_28_ph_13	0.656375576	28	13	13	Appl1	adaptor protein, phosphotyrosine interaction, PH domain and leucine zipper containing 1	AI585782	72993	Mm.202322
1436183_at	0.003577619	29.8	6					6	9830115L13Rik	RIKEN cDNA 9830115L13 gene	BB757349	319257	Mm.25243, Mm.392230

Table S1: Circadian transcripts (continued)

	Signal Decomposition			Model-Matching				Final Statistics and Annotations					
Transcript ID (Affymetrix probeset)	Fisher's G Test q-value	Period (hrs)	Phase	HAYSTACK Best Model	HAYSTACK Correlation	Period (hrs)	Phase	Phase (Final)	Gene Symbol	Description	GenBank	Entrez Gene	UniGene
1436188_a_at				cos_per_28_ph_21	0.661597681	28	21	21	Ndrg4	N-myc downstream regulated gene 4	AI837704	234593	Mm.29846
1436200_at	0.008600905	22.5	15	rigid_ph_15	0.782732742	24	15	15	Lonrf3	LON peptidase N-terminal domain and ring finger 3	BE956940	74365	Mm.327654
1436209_at				asyrigid2_ph_10	0.621759719	24	10	10	Dnajc16	DnaJ (Hsp40) homolog, subfamily C, member 16	BB447500	214063	Mm.39102
1436215_at				cos_per_28_ph_03	0.641933227	28	3	3	Ipmk	inositol polyphosphate multikinase	BB081797	69718	Mm.245867
1436298_x_at				cos_per_28_ph_14	0.646605827	28	14	14	Paics	phosphoribosylaminoimidazole carboxylase, phosphoribosylaminoribosylaminoimidazole, succinocarboxamide synthetase	BB066556	67054	Mm.182981, Mm.431705
1436309_at	0.039865714	29.8	10	cos_per_28_ph_12	0.786490519	28	12	10	Neto2	neuropilin (NRP) and tolloid (TLL)-like 2	BB125651	74513	Mm.126079
1436310_at	0.024628545	25.5	11	asyrigid2_ph_09	0.759431773	24	9	11	Gemin5	gem (nuclear organelle) associated protein 5	BB824003	216766	Mm.275349
1436333_a_at	0.029015769	26	15	cos_per_26_ph_15	0.722900105	26	15	15	Synj1	synaptojanin 1	BM232846	104015	Mm.187079
1436334_at				rigid_ph_15	0.696055298	24	15	15	Synj1	synaptojanin 1	BM232846	104015	Mm.187079
1436365_at	0.001838832	29.7	2					2	Zbtb7c	zinc finger and BTB domain containing 7C	BG922355	207259	Mm.440160
1436394_at				cos_per_20_ph_11	0.711112408	20	11	11	Trim37	tripartite motif-containing 37	BG065227	68729	Mm.17436
1436456_at				box2_ph_17	0.658129455	24	17	17	Slc38a9	solute carrier family 38, member 9	BQ031896	268706	Mm.259799
1436505_at				spike_ph_14	0.607539519	24	14	14	Ppig	peptidyl-prolyl isomerase G (cyclophilin G)	BG069107	228005	Mm.11815, Mm.474951
1436507_at	0.001973115	29.2	29					5	Irak2	interleukin-1 receptor-associated kinase 2	AV241470	108960	Mm.152142
1436533_at				rigid_ph_16	0.712183553	24	16	16	Trove2	TROVE domain family, member 2	BQ176653	20822	Mm.40370
1436534_at				rigid_ph_16	0.710401987	24	16	16	Trove2	TROVE domain family, member 2	BQ176653	20822	Mm.40370
1436535_at	0.034396001	22.5	16	rigid_ph_16	0.745843303	24	16	16	Trove2	TROVE domain family, member 2	BQ176653	20822	Mm.40370
1436538_at				cos_per_28_ph_25	0.614382058	28	1	1	Ankrd37	ankyrin repeat domain 37	AV084342	654824	Mm.334517
1436540_at				rigid_ph_01	0.630437443	24	1	1			BQ031149		
1436570_at	0.029100187	25.2	8					8			BG143461		
1436665_a_at				asyrigid1_ph_21	0.646977043	24	21	21	Ltbp4	latent transforming growth factor beta binding protein 4	BB554226	108075	Mm.272251

Table S1: Circadian transcripts (continued)

	Signal Decomposition			Model-Matching				Final Statistics and Annotations					
Transcript ID (Affymetrix probeset)	Fisher's G Test q-value	Period (hrs)	Phase	HAYSTACK Best Model	HAYSTACK Correlation	Period (hrs)	Phase	Phase (Final)	Gene Symbol	Description	GenBank	Entrez Gene	UniGene
1436697_at	0.041577712	24.2	24					0			AV303202		
1436740_at				cos_per_22_ph_03	0.760441594	22	3	3	6820431F20Rik	RIKEN cDNA 6820431F20 gene	AI585679	381598	Mm.157360, Mm.359054, Mm.362165, Mm.440442
1436804_s_at				cos_per_27_ph_01	0.651910498	27	1	1	Scyl1	SCY1-like 1 (S. cerevisiae)	AU016501	78891	Mm.276063
1436826_at	0.006756526	29	14					14	Tmtc3	transmembrane and tetratricopeptide repeat containing 3	BM226072	237500	Mm.296805
1436895_at				box2_ph_16	0.622167328	24	16	16	Amp2	ArfGAP with RhoGAP domain, ankyrin repeat and PH domain 2	BB182934	212285	Mm.244403
1436925_at				rigid_ph_17	0.713088952	24	17	17	Foxn3	forkhead box N3	AV228812	71375	Mm.341972, Mm.392143
1436983_at				cos_per_22_ph_16	0.637413671	22	16	16	Crebbp	CREB binding protein	BG069466	12914	Mm.132238, Mm.392384
1436999_at	0.009236616	22	20					20	5033414K04Rik	RIKEN cDNA 5033414K04 gene	AI504908	98496	Mm.187470
1437044_a_at	0.001852906	28.6	26					2	Gba	glucosidase, beta, acid	BB241507	14466	Mm.5031
1437154_at				cos_per_28_ph_15	0.717957901	28	15	15	Cep170	centrosomal protein 170	BB667247	545389	Mm.269991
1437216_at				cos_per_25_ph_15	0.694692201	25	15	15	Cdc88a	coiled coil domain containing 88A	BB498608	108686	Mm.338284, Mm.441367
1437218_at				spike_ph_01	0.6458438	24	1	1	Fn1	fibronectin 1	BM234360	14268	Mm.193099
1437221_at				rigid_ph_16	0.630189098	24	16	16	Rrm2b	ribonucleotide reductase M2 B (TP53 inducible)	BB702377	382985	Mm.24738
1437285_at				cos_per_28_ph_16	0.649877697	28	16	16	1110020G09Rik	RIKEN cDNA 1110020G09 gene	BB277742	68646	Mm.244226, Mm.468219
1437342_x_at				spike_ph_03	0.651690057	24	3	3	Ptpg1ip	pituitary tumor-transforming 1 interacting protein	BB498753	108705	Mm.28853
1437357_at				box2_ph_15	0.627077051	24	15	15	Ythdc2	YTH domain containing 2	AI481820	240255	Mm.244482
1437372_at				cos_per_20_ph_02	0.61127136	20	2	2	Cpsf6	cleavage and polyadenylation specific factor 6	BB335087	432508	Mm.440510, Mm.440969, Mm.458589, Mm.476779
1437380_x_at	0.02561806	21.8	3					3	Pgd	phosphogluconate dehydrogenase	BB558114	110208	Mm.252080
1437394_at				boxl_ph_14	0.698302828	24	14	14	Agap1	ArfGAP with GTPase domain, ankyrin repeat and PH domain 1	BE983523	347722	Mm.291135
1437404_at				rigid_ph_16	0.659717583	24	16	16	Mast4	microtubule associated serine/threonine kinase family member 4	AI642422	328329	Mm.202606, Mm.447520

Table S1: Circadian transcripts (continued)

	Signal Decomposition			Model-Matching				Final Statistics and Annotations					
Transcript ID (Affymetrix probeset)	Fisher's G Test q-value	Period (hrs)	Phase	HAYSTACK Best Model	HAYSTACK Correlation	Period (hrs)	Phase	Phase (Final)	Gene Symbol	Description	GenBank	Entrez Gene	UniGene
1437417_s_at				cos_per_25_ph_16	0.677604155	25	16	16	LOC100045283	similar to Glypican 6	BB493031	100045283	
1437424_at				asymjoid2_ph_10	0.638087533	24	10	10	Syde2	synapse defective 1, Rho GTPase, homolog 2 (C. elegans)	BG069296	214804	Mm.268854
1437447_s_at				spike_ph_02	0.642168421	24	2	2	Ercc1	excision repair cross-complementing rodent repair deficiency, complementation group 1	BB815240	13870	Mm.280913
1437474_at				rigid_ph_15	0.620806236	24	15	15	Gatad2b	GATA zinc finger domain containing 2B	BB409476	229542	Mm.270999
1437476_at				rigid_ph_16	0.635201528	24	16	16	Rrm2b	ribonucleotide reductase M2 B (TP53 inducible)	BB470755	382985	Mm.24738
1437563_at				rigid_ph_15	0.633663047	24	15	15	Phf2011	PHD finger protein 20-like 1	BB667768	239510	Mm.267473
1437581_at				box2_ph_17	0.643628075	24	17	17	Zfp800	zinc finger protein 800	AW824355	627049	Mm.84441
1437708_x_at	0.003354082	24.2	4					4	Vamp3	vesicle-associated membrane protein 3	BB552111	22319	Mm.273930
1437711_x_at				cos_per_28_ph_12	0.625153444	28	12	12	Odc1	ornithine decarboxylase, structural 1	BB519474	18263	Mm.34102, Mm.472891
1437714_x_at				cos_per_28_ph_14	0.61843702	28	14	14	Usp14	ubiquitin specific peptidase 14	BB304409	59025	Mm.219648, Mm.329277, Mm.447089
1437716_x_at				cos_per_28_ph_20	0.618531242	28	20	20	Kif22	kinesin family member 22	BB251322	110033	Mm.286488
1437717_x_at	0.017239759	22	3	cos_per_22_ph_03	0.784664903	22	3	3	6820431F20Rik	RIKEN cDNA 6820431F20 gene	BB471300	381598	Mm.157360, Mm.359054, Mm.362165, Mm.440442
1437719_x_at	0.008701268	22.9	17					17	A230046K03Rik	RIKEN cDNA A230046K03 gene	BB387783	319277	Mm.278577
1437729_at				spike_ph_04	0.616677988	24	4	4	Rpl27a	ribosomal protein L27a	BG141806	26451	Mm.305750
1437811_x_at	0.024696658	29.3	20					20			AV312368		
1437846_x_at				cos_per_28_ph_25	0.707327319	28	1	1	Bace2	beta-site APP-cleaving enzyme 2	BB348062	56175	Mm.97885
1437850_a_at				cos_per_28_ph_14	0.65800906	28	14	14	Cnbp	cellular nucleic acid binding protein	AV299745	12785	Mm.290251, Mm.475181
1437892_at	0.022982597	23.1	2	rigid_ph_02	0.742420034	24	2	2	Zkscan3	zinc finger with KRAB and SCAN domains 3	BQ084812	72739	Mm.296071
1437894_at				rigid_ph_16	0.664444921	24	16	16	Prox1	prospero-related homeobox 1	BE994433	19130	Mm.132579, Mm.392678
1437921_x_at				rigid_ph_16	0.687794642	24	16	16	Zfp516	zinc finger protein 516	AW744723	329008	Mm.326526

Table S1: Circadian transcripts (continued)

	Signal Decomposition			Model-Matching				Final Statistics and Annotations					
Transcript ID (Affymetrix probeset)	Fisher's G Test q-value	Period (hrs)	Phase	HAYSTACK Best Model	HAYSTACK Correlation	Period (hrs)	Phase	Phase (Final)	Gene Symbol	Description	GenBank	Entrez Gene	UniGene
1437945_x_at	0.043139056	26.7	12					12	Nap1l1	nucleosome assembly protein 1-like 1	AA260459	53605	Mm.290407
1438015_at				cos_per_28_ph_09	0.675136486	28	9	9	Dkc1	dyskeratosis congenita 1, dyskerin homolog (human)	BG068512	245474	Mm.291062
1438016_at				cos_per_28_ph_09	0.701956685	28	9	9	Dkc1	dyskeratosis congenita 1, dyskerin homolog (human)	BG068512	245474	Mm.291062
1438049_at				asyrigid1_ph_06	0.758714056	24	6	6	A430108E01Rik	RIKEN cDNA A430108E01 gene	AW541326	384382	Mm.359054, Mm.414559, Mm.432328
1438081_at				cos_per_28_ph_12	0.709530467	28	12	12	Mcc	mutated in colorectal cancers	BB794635	328949	Mm.312511, Mm.427116
1438092_x_at				cos_per_28_ph_16	0.674094661	28	16	16	H2afz	H2A histone family, member Z	AV003424	51788	Mm.117541, Mm.372513, Mm.465508
1438117_x_at				spike_ph_04	0.621979823	24	4	4	Tmem41b	transmembrane protein 41B	BB508081	233724	Mm.43212, Mm.475196
1438177_x_at				rigid_ph_04	0.620215904	24	4	4	LOC100048085	similar to ectonucleoside triphosphate diphosphohydrolase 4	AV255351	100048085	
1438179_s_at	0.044948518	24.1	4					4	Elp2	elongation protein 2 homolog (S. cerevisiae)	BB188218	58523	Mm.25298
1438181_x_at				spike_ph_02	0.667588112	24	2	2	Tm2d2	TM2 domain containing 2	BB302809	69742	Mm.28626
1438208_at				cos_per_28_ph_25	0.635034349	28	1	1	Taok2	TAO kinase 2	BM198170	381921	Mm.259634
1438211_s_at	0.001838832	23.2	6	boxl_ph_06	0.883838607	24	6	6	Dbp	D site albumin promoter binding protein	BB550183	13170	Mm.24222, Mm.378235
1438285_at				cos_per_28_ph_08	0.608544645	28	8	8	2210015D19Rik	RIKEN cDNA 2210015D19 gene	BM245369	76508	Mm.260203
1438291_x_at				cos_per_28_ph_15	0.644603431	28	15	15	Rpl37	ribosomal protein L37	AV069169	67281	Mm.10474
1438303_at				spike_ph_08	0.764878421	24	8	8	Tgfb2	transforming growth factor, beta 2	AV246759	21808	Mm.18213
1438349_at				asyrigid1_ph_00	0.619575747	24	0	0	BC043476	cDNA sequence BC043476	BG069331	381067	Mm.254463
1438361_at				box2_ph_16	0.610738037	24	16	16	2310035C23Rik	RIKEN cDNA 2310035C23 gene	BB543289	227446	Mm.337339
1438362_x_at				box2_ph_17	0.665693354	24	17	17	2310035C23Rik	RIKEN cDNA 2310035C23 gene	BB543289	227446	Mm.337339
1438403_s_at				boxl_ph_02	0.615121024	24	2	2	Malat1	metastasis associated lung adenocarcinoma transcript 1 (non-coding RNA)	BF537798	72289	Mm.298256
1438413_at				rigid_ph_18	0.659607978	24	18	18	Senp7	SUMO1/sentrin specific peptidase 7	AV231698	66315	Mm.255784

Table S1: Circadian transcripts (continued)

	Signal Decomposition			Model-Matching				Final Statistics and Annotations					
Transcript ID (Affymetrix probeset)	Fisher's G Test q-value	Period (hrs)	Phase	HAYSTACK Best Model	HAYSTACK Correlation	Period (hrs)	Phase	Phase (Final)	Gene Symbol	Description	GenBank	Entrez Gene	UniGene
1438420_at				cos_per_21_ph_02	0.649989884	21	2	2	Rbm39	RNA binding motif protein 39	AV019076	170791	Mm.392436, Mm.436932
1438478_a_at	0.003042884	28.8	7					7	Ppp3ca	protein phosphatase 3, catalytic subunit, alpha isoform	AI313926	19055	Mm.331389
1438575_a_at	0.042676774	22.9	18	rigid_ph_17	0.737572119	24	17	18			BG143413		
1438633_x_at	0.002194658	26.4	18					18	Lasp1	LIM and SH3 protein 1	BB377636	16796	Mm.271967
1438645_x_at				cos_per_28_ph_25	0.641624704	28	1	1	Bace2	beta-site APP-cleaving enzyme 2	BB558905	56175	Mm.97885
1438712_at				cos_per_28_ph_04	0.615860869	28	4	4	Cept1	choline/ethanolaminephosphotransferase 1	AV372648	99712	Mm.14816
1438714_at				spike_ph_01	0.746893577	24	1	1			BB622498		
1438783_at	0.047333003	22.2	2					2			BB325257		
1438798_at				box2_ph_18	0.636831485	24	18	18	4931406P16Rik	RIKEN cDNA 4931406P16 gene	BB764190	233103	Mm.476734
1438938_x_at				spike_ph_04	0.613045219	24	4	4	Phb2	prohibitin 2	AV212294	12034	Mm.36241
1438968_x_at	0.034013257	28.8	28					4	Spint2	serine protease inhibitor, Kunitz type 2	AV058358	20733	Mm.295230
1439062_at	0.01064478	26.1	1					1	Klhdc3	kelch repeat and BTB (POZ) domain containing 3	BB264869	69149	Mm.25946
1439066_at				cos_per_28_ph_26	0.643308096	28	2	2	Angpt1	angiopoietin 1	BB453314	11600	Mm.309336
1439087_a_at	0.034328396	25.1	4					4	5830455E04Rik	RIKEN cDNA 5830455E04 gene	BB030508	109026	Mm.390323
1439109_at				cos_per_25_ph_02	0.63109704	25	2	2	Ccdc68	coiled-coil domain containing 68	AV378320	381175	Mm.266831
1439119_a_at				box2_ph_17	0.660259417	24	17	17	Fam120a	family with sequence similarity 120, member A	BB324206	218236	Mm.426571
1439153_at	0.031456306	21.3	6					6	Rnf144b	ring finger protein 144B	AV274826	218215	Mm.287609, Mm.461654
1439300_at	0.025331033	22.8	17	box2_ph_17	0.789607054	24	17	17	Chic1	cysteine-rich hydrophobic domain 1	BG065782	12212	Mm.42223
1439348_at	0.024537498	24.5	0	rigid_ph_00	0.759124357	24	0	0	S100a10	S100 calcium binding protein A10 (calpactin)	BB450829	20194	Mm.1
1439410_x_at	0.001973115	29.6	5					5	Slc25a39	solute carrier family 25, member 39	BI966363	68066	Mm.44226
1439450_x_at	0.0041899	24.6	16					16	A230046K03Rik	RIKEN cDNA A230046K03 gene	BB267264	319277	Mm.278577
1439453_x_at				cos_per_28_ph_25	0.607418793	28	1	1	Rnaseh2c	ribonuclease H2, subunit C	AV259141	68209	Mm.246200

Table S1: Circadian transcripts (continued)

	Signal Deconvolution			Model-Matching				Final Statistics and Annotations					
Transcript ID (Affymetrix probeset)	Fisher's G Test q-value	Period (hrs)	Phase	HAYSTACK Best Model	HAYSTACK Correlation	Period (hrs)	Phase	Phase (Final)	Gene Symbol	Description	GenBank	Entrez Gene	UniGene
1439477_at	0.049085368	23.1	1	rigid_ph_01	0.707534047	24	1	1	5430406J06Rik	RIKEN cDNA 5430406J06 gene	BB047737	73848	Mm.440651
1439516_at				cos_per_28_ph_09	0.735139265	28	9	9	2610201A13Rik	RIKEN cDNA 2610201A13 gene	AW488471	70434	Mm.432136
1439555_at				asyrigid2_ph_10	0.669011094	24	10	10	Rif	rearranged L-myc fusion sequence	BB704706	109263	Mm.215745
1439624_at				cos_per_26_ph_00	0.691114612	26	0	0	Ugt2b35	UDP glucuronosyltransferase 2 family, polypeptide B35	AA572504	243085	Mm.312095
1439651_at				boxl_ph_02	0.666781437	24	2	2			AV370006		
1439727_at				cos_per_27_ph_03	0.661557354	27	3	3	Clca6	chloride channel calcium activated 6	AV375098	99663	Mm.442050
1439824_at	0.004547142	29.4	18					18	Chm	choroideremia	BB263701	12662	Mm.257316
1439878_at				cos_per_20_ph_19	0.822365217	20	19	19	Ivl	involucrin	AV009441	16447	Mm.207365
1439942_at				cos_per_28_ph_07	0.666703448	28	7	7	Prep	prolyl endopeptidase	BM118423	19072	Mm.37294
1439965_at	0.003915719	22.5	18					18			BM593678		
1440005_at				spike_ph_17	0.635207181	24	17	17	Onecut2	one cut domain, family member 2	BB667396	225631	Mm.234723
1440125_at				box2_ph_17	0.629230402	24	17	17	A530054K11Rik	RIKEN cDNA A530054K11 gene	BG072966	212281	Mm.342918
1440153_at				cos_per_28_ph_11	0.623870743	28	11	11			AI854555		
1440198_at				cos_per_26_ph_11	0.646721479	26	11	11	Ankrd12	ankyrin repeat domain 12	AV346451	106585	Mm.34706, Mm.441953
1440454_at				cos_per_26_ph_03	0.655559294	26	3	3	Pion	pigeon homolog (Drosophila)	AV377136	212167	Mm.121705
1440482_at	0.015489089	24.6	13					13	Vps13a	vacuolar protein sorting 13A (yeast)	AV276280	271564	Mm.211963
1440559_at				cos_per_26_ph_03	0.673903971	26	3	3	Hmga2-ps1	high mobility group AT-hook 2, pseudogene 1	AV377334	15365	Mm.441435
1440734_at	0.008857911	22.8	17	rigid_ph_16	0.80996574	24	16	17	Ttbk2	tau tubulin kinase 2	BM200220	140810	Mm.275698
1440795_x_at	0.026761036	23.3	3					3	Rabep2	rabaptin, RAB GTPase binding effector protein 2	BB259371	70314	Mm.35467
1440894_at				cos_per_25_ph_15	0.654006946	25	15	15	Tmtc3	transmembrane and tetratricopeptide repeat containing 3	BE984574	237500	Mm.296805
1441722_at	0.030703244	23.2	2	rigid_ph_01	0.743415026	24	1	2			AI790499		
1441931_x_at				cos_per_25_ph_02	0.643543187	25	2	2	BB125219	expressed sequence BB125219	BB125219	105063	

Table S1: Circadian transcripts (continued)

	Signal Decomposition			Model-Matching				Final Statistics and Annotations					
Transcript ID (Affymetrix probeset)	Fisher's G Test q-value	Period (hrs)	Phase	HAYSTACK Best Model	HAYSTACK Correlation	Period (hrs)	Phase	Phase (Final)	Gene Symbol	Description	GenBank	Entrez Gene	UniGene
1441937_s_at				boxl_ph_03	0.616637393	24	3	3	LOC100047214	similar to PTEN induced putative kinase 1	AV371921	100047214	
1441986_at				spike_ph_00	0.700306016	24	0	0	Zcchc6	zinc finger, CCHC domain containing 6	BG067943	214290	Mm.233082
1442067_at				rigid_ph_01	0.672603026	24	1	1			BB468437		
1442073_at				cos_per_27_ph_16	0.618496279	27	16	16	Inpp1	inositol polyphosphate-1-phosphatase	BQ266693	16329	Mm.917
1442083_at	0.049691647	21.9	2					2	Rsrc2	arginine/serine-rich coiled-coil 2	BB036922	208606	Mm.276341
1442107_at				asyrigid1_ph_06	0.719026433	24	6	6	Flnb	filamin, beta	BM218614	286940	Mm.475646
1442169_at	0.015762024	28.7	9					9	Vldlr	very low density lipoprotein receptor	BG063333	22359	Mm.393599, Mm.4141
1442367_at				box2_ph_16	0.681496303	24	16	16	Atp1 1c	ATPase, class VI, type 11C	BB184010	320940	Mm.476917
1442753_at				spike_ph_01	0.60867414	24	1	1	Tnfaip8	tumor necrosis factor, alpha-induced protein 8	BF321807	106869	Mm.27740
1442886_at				cos_per_22_ph_02	0.694460101	22	2	2			BB667153		
1442939_at				box2_ph_15	0.723629253	24	15	15	Rif1	Rap1 interacting factor 1 homolog (yeast)	BG065807	51869	Mm.254530
1443086_at	0.043193383	22.7	1	rigid_ph_01	0.725077524	24	1	1	Alcam	activated leukocyte cell adhesion molecule	BB534113	11658	Mm.288282
1443612_at	0.022895127	29.4	17					17	Ano3	anoctamin 3	AW123199	228432	Mm.156043
1443819_x_at				asyrigid2_ph_00	0.706109854	24	0	0	Fis1	fission 1 (mitochondrial outer membrane) homolog (yeast)	BB379928	66437	Mm.25849
1443864_at				cos_per_20_ph_12	0.614904759	20	12	12	Dtl	denticleless homolog (Drosophila)	BG070404	76843	Mm.189102
1443867_at				cos_per_26_ph_12	0.611038427	26	12	12	Ankrd12	ankyrin repeat domain 12	BB320633	106585	Mm.34706, Mm.441953
1443877_a_at				box2_ph_16	0.712211123	24	16	16	Rapgef6	Rap guanine nucleotide exchange factor (GEF) 6	BB306768	192786	Mm.254404
1443878_at				cos_per_22_ph_16	0.644512399	22	16	16	Rapgef6	Rap guanine nucleotide exchange factor (GEF) 6	BB306768	192786	Mm.254404
1443952_at	0.008653558	27.4	23	cos_per_27_ph_22	0.844727939	27	22	23			BI525006		
1443986_at				cos_per_22_ph_18	0.630854722	22	18	18	Cdc73	cell division cycle 73, Paf1/RNA polymerase II complex component, homolog (S. cerevisiae)	BB211070	214498	Mm.389191, Mm.393505, Mm.398849
1444003_at				cos_per_28_ph_26	0.721488746	28	2	2	Neurl3	neuralized homolog 3 homolog (Drosophila)	AW610818	214854	Mm.389110

Table S1: Circadian transcripts (continued)

	Signal Decomposition			Model-Matching				Final Statistics and Annotations					
Transcript ID (Affymetrix probeset)	Fisher's G Test q-value	Period (hrs)	Phase	HAYSTACK Best Model	HAYSTACK Correlation	Period (hrs)	Phase	Phase (Final)	Gene Symbol	Description	GenBank	Entrez Gene	UniGene
1444262_at				cos_per_28_ph_25	0.653238102	28	1	1	1110017F19Rik	RIKEN cDNA 1110017F19 gene	AI506151	68528	Mm.441893
1444327_at				box2_ph_16	0.682455922	24	16	16	Ubr5	ubiquitin protein ligase E3 component n-recognin 5	BF224640	70790	Mm.275426, Mm.476840
1444402_at				box2_ph_15	0.67643434	24	15	15	Zc3h12c	zinc finger CCCH type containing 12C	BB383429	244871	Mm.295686, Mm.390172, Mm.413447
1444468_at				asyrigid2_ph_11	0.61110918	24	11	11	Paqr8	progestin and adipoQ receptor family member VIII	AV328983	74229	Mm.40780
1444565_at				asyrigid1_ph_06	0.674747286	24	6	6	BB166591	expressed sequence BB166591	BB136975	99458	Mm.436745
1444607_at				cos_per_28_ph_00	0.832112469	28	0	0			AI849219		
1444952_a_at				rigid_ph_16	0.672743775	24	16	16	Nucks1	nuclear casein kinase and cyclin-dependent kinase substrate 1	BB260383	98415	Mm.392848, Mm.436518, Mm.477777
1445081_at				box2_ph_17	0.670769001	24	17	17	A930041I02Rik	RIKEN cDNA A930041I02 gene	BB335888	320271	Mm.204836
1445322_x_at	0.017219612	23.4	1					1			BG063377		
1445534_at	0.045079943	23.8	1	rigid_ph_01	0.729952905	24	1	1	Flnb	filamin, beta	BM206272	286940	Mm.475646
1446075_at	0.021535382	23.2	1	boxl_ph_02	0.753251059	24	2	1			AV376107		
1446147_at				cos_per_22_ph_02	0.699767921	22	2	2	Rbm39	RNA binding motif protein 39	BB436856	170791	Mm.392436, Mm.436932
1446148_x_at				cos_per_22_ph_02	0.631931724	22	2	2	Rbm39	RNA binding motif protein 39	BB436856	170791	Mm.392436, Mm.436932
1446417_at				cos_per_21_ph_02	0.674621657	21	2	2			AW553625		
1447217_at				cos_per_26_ph_17	0.607059915	26	17	17	Uhrf2	ubiquitin-like, containing PHD and RING finger domains 2	BB292098	109113	Mm.313364
1447223_at				asyrigid1_ph_10	0.609198188	24	10	10			AW120584		
1447403_a_at				cos_per_28_ph_07	0.632524221	28	7	7	Zmynd19	zinc finger, MYND domain containing 19	AW125726	67187	Mm.296106
1447676_x_at				cos_per_26_ph_02	0.636323898	26	2	2	S100a16	S100 calcium binding protein A16	AV074236	67860	Mm.331185
1447774_x_at	0.044575126	24.1	19	cos_per_25_ph_18	0.721635104	25	18	19	5730469M10Rik	RIKEN cDNA 5730469M10 gene	AV332575	70564	Mm.27227
1447854_s_at				spike_ph_01	0.677849053	24	1	1	Hist2h2be	histone cluster 2, H2be	AV127319	319190	Mm.439791

Table S1: Circadian transcripts (continued)

	Signal Decomposition			Model-Matching				Final Statistics and Annotations					
Transcript ID (Affymetrix probeset)	Fisher's G Test q-value	Period (hrs)	Phase	HAYSTACK Best Model	HAYSTACK Correlation	Period (hrs)	Phase	Phase (Final)	Gene Symbol	Description	GenBank	Entrez Gene	UniGene
1447868_x_at				cos_per_28_ph_14	0.673326934	28	14	14	Glrx3	glutaredoxin 3	BB030680	30926	Mm.267692
1447899_x_at				spike_ph_04	0.61402272	24	4	4	Epcam	epithelial cell adhesion molecule	AV099587	17075	Mm.4259
1447904_s_at	0.041606434	28.9	27					3	Fnta	farnesyltransferase, CAAX box, alpha	AV313761	14272	Mm.3496
1447993_a_at				cos_per_21_ph_02	0.620233651	21	2	2	Snhg10	small nucleolar RNA host gene (non-protein coding) 10	AV043099	69434	Mm.380736
1448013_at				rigid_ph_16	0.632693322	24	16	16	Usp24	ubiquitin specific peptidase 24	AI196998	329908	Mm.234544, Mm.397646
1448154_at				cos_per_28_ph_20	0.658933293	28	20	20	Ndrg2	N-myc downstream regulated gene 2	NM_013864	29811	Mm.26722
1448161_a_at	0.021847985	21.1	5					5	Clcn4-2	chloride channel 4-2	NM_011334	12727	Mm.297883
1448182_a_at	0.046208662	20.1	8					8	Cd24a	CD24a antigen	NM_009846	12484	Mm.29742
1448183_a_at				rigid_ph_15	0.60888975	24	15	15	Hif1a	hypoxia inducible factor 1, alpha subunit	BB269715	15251	Mm.3879, Mm.446610
1448187_at				cos_per_20_ph_10	0.679722226	20	10	10	Pold1	polymerase (DNA directed), delta 1, catalytic subunit	BC009128	18971	Mm.16549
1448249_at	0.015875729	27.1	1					1	Gpd1	glycerol-3-phosphate dehydrogenase 1 (soluble)	BC019391	14555	Mm.252391
1448253_at	0.011557952	24.6	2					2	Glud1	glutamate dehydrogenase 1	NM_008133	14661	Mm.10600
1448270_at				cos_per_28_ph_10	0.664086302	28	10	10	Ddx21	DEAD (Asp-Glu-Ala-Asp) box polypeptide 21	BM246099	56200	Mm.413275
1448273_at				cos_per_25_ph_03	0.65880213	25	3	3	Gss	glutathione synthetase	NM_008180	14854	Mm.252316
1448276_at	0.001838832	23.9	9	cos_per_24_ph_08	0.948470719	24	8	9	Tspan4	tetraspanin 4	NM_053082	64540	Mm.259477
1448297_a_at				asyrigid1_ph_21	0.624715797	24	21	21	Trk2	tyrosine kinase, non-receptor, 2	NM_016788	51789	Mm.251115
1448330_at				asyrigid1_ph_07	0.651518292	24	7	7	Gstm1	glutathione S-transferase, mu 1	NM_010358	14862	Mm.37199
1448339_at	0.037208676	28.9	27					3	Tmem30a	transmembrane protein 30A	BE986812	69981	Mm.355084
1448354_at	0.036559494	23.8	15					15	G6pdx	glucose-6-phosphate dehydrogenase X-linked	NM_008062	14381	Mm.27210
1448377_at				cos_per_22_ph_09	0.617492856	22	9	9	Slpi	secretory leukocyte peptidase inhibitor	NM_011414	20568	Mm.371583
1448411_at				cos_per_28_ph_12	0.696304004	28	12	12	Wfsl	Wolfram syndrome 1 homolog (human)	NM_011716	22393	Mm.20916
1448418_s_at				rigid_ph_04	0.684754898	24	4	4	Wdr23	WD repeat domain 23	NM_133734	28199	Mm.11535

Table S1: Circadian transcripts (continued)

	Signal Decomposition			Model-Matching				Final Statistics and Annotations					
Transcript ID (Affymetrix probeset)	Fisher's G Test q-value	Period (hrs)	Phase	HAYSTACK Best Model	HAYSTACK Correlation	Period (hrs)	Phase	Phase (Final)	Gene Symbol	Description	GenBank	Entrez Gene	UniGene
1448425_at	0.013143798	24.3	13					13	Eif3a	eukaryotic translation initiation factor 3, subunit A	AW701127	13669	Mm.2238
1448436_a_at	0.017017781	23.9	5					5	Irf1	interferon regulatory factor 1	NM_008390	16362	Mm.105218
1448447_at	0.032713935	25.1	2					2	Vps28	vacuolar protein sorting 28 (yeast)	NM_025842	66914	Mm.30028
1448468_a_at				cos_per_28_ph_02	0.66963417	28	2	2	Kcnab1	potassium voltage-gated channel, shaker-related subfamily, beta member 1	AF033003	16497	Mm.316402
1448472_at				asyrigid2_ph_08	0.607975786	24	8	8	Vars	valyl-tRNA synthetase	AF087680	22321	Mm.28420
1448474_at	0.004388717	22.4	18					18	Nek7	NIMA (never in mitosis gene a)-related expressed kinase 7	NM_021605	59125	Mm.143817
1448490_at	0.011058767	27.9	26	cos_per_26_ph_01	0.808316857	26	1	2	Addc4	aarF domain containing kinase 4	NM_133770	76889	Mm.124728
1448500_a_at	0.028444631	24.9	0	cos_per_25_ph_01	0.713923432	25	1	0	Lime1	Lck interacting transmembrane adaptor 1	NM_023684	72699	Mm.440138
1448509_at				rigid_ph_05	0.632703304	24	5	5	Fam107b	family with sequence similarity 107, member B	BC021353	66540	Mm.277864
1448537_at	0.043355548	29.5	28					4	Ttc1	tetratricopeptide repeat domain 1	NM_133795	66827	Mm.271974
1448558_a_at				cos_per_27_ph_14	0.643504191	27	14	14	Pla2g4a	phospholipase A2, group IVA (cytosolic, calcium-dependent)	NM_008869	18783	Mm.4186
1448564_at	0.016624903	27	26					2	Cib1	calcium and integrin binding 1 (calmyrin)	BC003714	23991	Mm.30217
1448565_at	0.010878848	26.8	25					1	Ppp1r11	protein phosphatase 1, regulatory (inhibitor) subunit 11	NM_029632	76497	Mm.46176
1448639_a_at				cos_per_28_ph_09	0.637834387	28	9	9	Spata5	spermatogenesis associated 5	NM_021343	57815	Mm.172679
1448647_at				cos_per_28_ph_09	0.669343615	28	9	9	Man2a1	mannosidase 2, alpha 1	NM_008549	17158	Mm.2433
1448654_at	0.037429246	22.9	7					7	Mtch2	mitochondrial carrier homolog 2 (C. elegans)	BI872421	56428	Mm.28023
1448660_at				spike_ph_14	0.643962407	24	14	14	Arhgdig	Rho GDP dissociation inhibitor (GDI) gamma	NM_008113	14570	Mm.1383
1448664_a_at				asyrigid1_ph_23	0.609922821	24	23	23	Speg	SPEG complex locus	NM_007463	11790	Mm.275397
1448680_at				boxl_ph_04	0.646865217	24	4	4	Serpina1c	serine (or cysteine) peptidase inhibitor, clade A, member 1C	NM_009245	20702	Mm.439692, Mm.439694
1448694_at				asyrigid2_ph_01	0.77771497	24	1	1	Jun	Jun oncogene	NM_010591	16476	Mm.275071
1448698_at	0.011260493	23.3	9					9	Ccnd1	cyclin D1	NM_007631	12443	Mm.273049
1448724_at	0.043900598	24.6	5					5	Cish	cytokine inducible SH2-containing protein	NM_009895	12700	Mm.4592

Table S1: Circadian transcripts (continued)

	Signal Deconvolution			Model-Matching				Final Statistics and Annotations					
Transcript ID (Affymetrix probeset)	Fisher's G Test q-value	Period (hrs)	Phase	HAYSTACK Best Model	HAYSTACK Correlation	Period (hrs)	Phase	Phase (Final)	Gene Symbol	Description	GenBank	Entrez Gene	UniGene
1448752_at				cos_per_26_ph_02	0.626464229	26	2	2	Car2	carbonic anhydrase 2	NM_009801	12349	Mm.1186
1448767_s_at				cos_per_27_ph_26	0.709154241	27	2	2	Gjb1	gap junction protein, beta 1	BC026833	14618	Mm.21198
1448793_a_at	0.049264452	26.6	0	boxl_ph_04	0.709522454	24	4	0	Sdc4	syndecan 4	BC005679	20971	Mm.477724
1448794_s_at				boxl_ph_12	0.674286319	24	12	12	Dnajc2	DnaJ (Hsp40) homolog, subfamily C, member 2	BG067003	22791	Mm.266312
1448798_at				cos_per_28_ph_01	0.661178683	28	1	1	Eps8l3	EPS8-like 3	NM_133867	99662	Mm.108491
1448813_at				boxl_ph_05	0.613165261	24	5	5	Aadac	arylacetamide deacetylase (esterase)	NM_023383	67758	Mm.24547
1448814_at				cos_per_23_ph_14	0.6392535	23	14	14	Gab1	growth factor receptor bound protein 2-associated protein 1	NM_021356	14388	Mm.277409
1448820_a_at				cos_per_28_ph_11	0.687229681	28	11	11	Eif2s2	eukaryotic translation initiation factor 2, subunit 2 (beta)	AA985754	67204	Mm.377134, Mm.470088
1448838_at	0.043876725	26.7	13					13	Topors	topoisomerase I binding, arginine/serine-rich	NM_134097	106021	Mm.251548
1448843_at	0.002095072	27.6	14					14	Ssr1	signal sequence receptor, alpha	BG077348	107513	Mm.426670, Mm.476789
1448868_at				cos_per_27_ph_25	0.621085336	27	1	1	Scand1	SCAN domain-containing 1	NM_020255	19018	Mm.389346
1448914_a_at	0.008663369	24.7	9					9	Csf1	colony stimulating factor 1 (macrophage)	BM233698	12977	Mm.795
1448959_at	0.010507916	27.6	1					1	Ndufs4	NADH dehydrogenase (ubiquinone) Fe-S protein 4	NM_010887	17993	Mm.253142, Mm.399745
1448967_at	0.007142068	20.9	2					2	Nipsnap3a	nipsnap homolog 3A (C. elegans)	NM_025623	66536	Mm.38244
1448978_at	0.002218381	23.5	6	boxl_ph_05	0.823176325	24	5	6	Ngef	neuronal guanine nucleotide exchange factor	NM_019867	53972	Mm.435439
1449014_at				cos_per_28_ph_14	0.613036736	28	14	14	Lactb	lactamase, beta	NM_030717	80907	Mm.157882
1449039_a_at	0.017590842	24.8	5					5	Hnrpdl	heterogeneous nuclear ribonucleoprotein D-like	NM_016690	50926	Mm.389579, Mm.426680
1449065_at	0.001838832	24.9	20					20	Acot1	acyl-CoA thioesterase 1	NM_012006	26897	Mm.1978
1449083_at				cos_per_25_ph_03	0.671208744	25	3	3	Ccdc91	coiled-coil domain containing 91	AA067702	67015	Mm.209774
1449120_a_at				cos_per_27_ph_15	0.706250247	27	15	15	Pcm1	pericentriolar material 1	NM_023662	18536	Mm.117896
1449155_at	0.009212524	23.8	5	cos_per_25_ph_04	0.770408024	25	4	5	Polr3g	polymerase (RNA) III (DNA directed) polypeptide G	NM_026190	67486	Mm.279781
1449164_at				cos_per_28_ph_24	0.620642625	28	0	0	Cd68	CD68 antigen	BC021637	12514	Mm.15819

Table S1: Circadian transcripts (continued)

	Signal Decomposition			Model-Matching				Final Statistics and Annotations					
Transcript ID (Affymetrix probeset)	Fisher's G Test q-value	Period (hrs)	Phase	HAYSTACK Best Model	HAYSTACK Correlation	Period (hrs)	Phase	Phase (Final)	Gene Symbol	Description	GenBank	Entrez Gene	UniGene
1449248_at				asyrigid1_ph_10	0.643819039	24	10	10	Clcn2	chloride channel 2	NM_009900	12724	Mm.177761
1449259_at				asyrigid1_ph_07	0.710585477	24	7	7	Rab3d	RAB3D, member RAS oncogene family	BB349707	19340	Mm.260157
1449292_at				spike_ph_14	0.613219469	24	14	14	Rb1cc1	RB1-inducible coiled-coil 1	BE570980	12421	Mm.293811
1449314_at	0.030563069	25.3	9					9	Zfpn2	zinc finger protein, multitype 2	NM_011766	22762	Mm.39496
1449328_at				rigid_ph_15	0.671479605	24	15	15	Ly75	lymphocyte antigen 75	NM_013825	17076	Mm.2074
1449351_s_at	0.030994505	22.2	22					22	Pdgfc	platelet-derived growth factor, C polypeptide	NM_019971	54635	Mm.331089
1449357_at	0.01499321	26.2	24					0	2310030G06Rik	RIKEN cDNA 2310030G06 gene	NM_025865	66952	Mm.273375
1449746_s_at	0.047879716	23.3	1	box1_ph_01	0.692146158	24	1	1	Krr1	KRR1, small subunit (SSU) processome component, homolog (yeast)	AU020154	52705	Mm.34606
1449851_at	0.003826558	25.3	8	cos_per_25_ph_08	0.812420558	25	8	8	Per1	period homolog 1 (Drosophila)	AF022992	18626	Mm.7373
1449891_a_at				asyrigid2_ph_09	0.683090549	24	9	9	Dcbld2	discoidin, CUB and LCCL domain containing 2	NM_028523	73379	Mm.373589
1449910_at				box2_ph_17	0.704278439	24	17	17	2210418O10Rik	RIKEN cDNA 2210418O10 gene	NM_029813	76958	Mm.379980, Mm.436749
1450047_at				rigid_ph_14	0.696506277	24	14	14	Hs6st2	heparan sulfate 6-O-sulfotransferase 2	AW536432	50786	Mm.252561
1450099_a_at	0.003666544	29.8	25					1	Gba	glucosidase, beta, acid	NM_008094	14466	Mm.5031
1450125_at				cos_per_28_ph_01	0.711249278	28	1	1	Gata5	GATA binding protein 5	BB447551	14464	Mm.388880
1450184_s_at	0.001838832	22.3	8	cos_per_23_ph_08	0.948291135	23	8	8	Tef	thyrotroph embryonic factor	NM_017376	21685	Mm.270278
1450187_a_at	0.008785544	21.6	4					4	Galt	galactose-1-phosphate uridyl transferase	NM_016658	14430	Mm.439669
1450259_a_at				box2_ph_16	0.610267691	24	16	16	Stat5a	signal transducer and activator of transcription 5A	U36502	20850	Mm.277403
1450400_at				rigid_ph_15	0.645810958	24	15	15	Tgsl	trimethylguanosine synthase homolog (S. cerevisiae)	BM233196	116940	Mm.171323
1450452_a_at	0.026449091	27.2	27					3	Narfl	nuclear prelamin A recognition factor-like	NM_026238	67563	Mm.24201
1450505_a_at	0.024556518	27.8	26					2	Fam134b	family with sequence similarity 134, member B	NM_025459	66270	Mm.25311
1450561_a_at	0.002421866	27.2	27					3	Surf1	surfeit gene 1	NM_013677	20930	Mm.347512
1450623_at	0.044299417	27.6	26					2	Gnb2	guanine nucleotide binding protein (G protein), beta 2	NM_010312	14693	Mm.30141

Table S1: Circadian transcripts (continued)

	Signal Decomposition			Model-Matching				Final Statistics and Annotations					
Transcript ID (Affymetrix probeset)	Fisher's G Test q-value	Period (hrs)	Phase	HAYSTACK Best Model	HAYSTACK Correlation	Period (hrs)	Phase	Phase (Final)	Gene Symbol	Description	GenBank	Entrez Gene	UniGene
1450728_at				asyrigid2_ph_00	0.671125218	24	0	0	Fjx1	four jointed box 1 (Drosophila)	AV230815	14221	Mm.29730
1450762_s_at				box2_ph_17	0.622126406	24	17	17	Zfp191	zinc finger protein 191	BF780333	59057	Mm.417427
1450769_s_at				asyrigid1_ph_11	0.674960288	24	11	11	Stard5	StAR-related lipid transfer (START) domain containing 5	BI076697	170460	Mm.357953
1450786_x_at	0.007261848	23.9	17					17	Pdlim5	PDZ and LIM domain 5	NM_019808	56376	Mm.117709
1450902_at				spike_ph_15	0.659425446	24	15	15	Brd3	bromodomain containing 3	BG072367	67982	Mm.28721
1450908_at				rigid_ph_16	0.624669974	24	16	16	Rad23b	RAD23b homolog (S. cerevisiae)	BF138887	19359	Mm.196846
1450922_a_at				asyrigid2_ph_08	0.683911716	24	8	8	Tgfb2	transforming growth factor, beta 2	BF144658	21808	Mm.18213
1450923_at				asyrigid2_ph_08	0.697727432	24	8	8	Tgfb2	transforming growth factor, beta 2	BF144658	21808	Mm.18213
1450958_at				cos_per_28_ph_00	0.827132804	28	0	0	Tm4sf1	transmembrane 4 superfamily member 1	BQ177170	17112	Mm.856
1451004_at	0.020025235	21.2	21					21	Acvr2a	activin receptor IIA	BB818297	11480	Mm.314338
1451016_at				cos_per_28_ph_08	0.610218412	28	8	8	Ifrd2	interferon-related developmental regulator 2	BB540964	15983	Mm.215335
1451047_at	0.007142068	29.9	26					2	Itm2a	integral membrane protein 2A	BI966443	16431	Mm.193
1451063_at	0.027415168	29	15					15	Stxbp4	syntaxin binding protein 4	BB771462	20913	Mm.207203, Mm.390411
1451123_at				cos_per_20_ph_13	0.632160837	20	13	13	C330016O10Rik	RIKEN cDNA C330016O10 gene	BC006740	212706	Mm.41760
1451156_s_at				rigid_ph_15	0.660798216	24	15	15	Vldlr	very low density lipoprotein receptor	BB628702	22359	Mm.393599, Mm.4141
1451201_s_at	0.006165429	24.7	4					4	Rnh1	ribonuclease/angiogenin inhibitor 1	BC010331	107702	Mm.279485
1451285_at	0.024517933	24	12	cos_per_25_ph_13	0.740445682	25	13	12	Fus	fusion, derived from t(12;16) malignant liposarcoma (human)	AF224264	233908	Mm.277680
1451286_s_at	0.045258535	23.5	12	box2_ph_14	0.731587794	24	14	12	Fus	fusion, derived from t(12;16) malignant liposarcoma (human)	AF224264	233908	Mm.277680
1451307_at				asyrigid1_ph_06	0.695623888	24	6	6	Mrpl14	mitochondrial ribosomal protein L14	BC027021	68463	Mm.379158
1451335_at	0.047704253	24.7	3	cos_per_25_ph_04	0.712990813	25	4	3	Phc3	phoenta-specific 8	AF263458	231507	Mm.34609
1451340_at	0.020944089	29.8	5					5	Arid5a	AT rich interactive domain 5A (MRF1-like)	BC027152	214855	Mm.34316
1451412_a_at	0.033371397	25	1					1	Ift20	intraflagellar transport 20 homolog (Chlamydomonas)	AY082613	55978	Mm.358671

Table S1: Circadian transcripts (continued)

	Signal Deconvolution			Model-Matching				Final Statistics and Annotations					
Transcript ID (Affymetrix probeset)	Fisher's G Test q-value	Period (hrs)	Phase	HAYSTACK Best Model	HAYSTACK Correlation	Period (hrs)	Phase	Phase (Final)	Gene Symbol	Description	GenBank	Entrez Gene	UniGene
1451450_at	0.018045504	22.5	18					18	2010011I20Rik	RIKEN cDNA 2010011I20 gene	AK008190	67017	Mm.30013
1451464_at				rigid_ph_15	0.627681404	24	15	15	Mfap3	microfibrillar-associated protein 3	BI661422	216760	Mm.30501
1451501_a_at				asyrigid2_ph_00	0.639273303	24	0	0	Ghr	growth hormone receptor	BC024375	14600	Mm.3986
1451513_x_at				asyrigid2_ph_01	0.62834091	24	1	1	Serpina1b	serine (or cysteine) peptidase inhibitor, clade A, member 1B	BC012874	20701	Mm.439692, Mm.439693, Mm.458700
1451539_at	0.037170686	21.8	18					18	Baiap2l1	BAI1-associated protein 2-like 1	BC015459	66898	Mm.18814
1451560_at				spike_ph_16	0.637963691	24	16	16	Prrl2	proline rich 12	AW045856	233210	Mm.219137
1451643_a_at	0.021513378	23.9	2					2	Rab4b	RAB4B, member RAS oncogene family	BC007147	19342	Mm.262447
1451671_at	0.021631076	23.7	3					3	Gorasp1	golgi reassembly stacking protein 1	AV094567	74498	Mm.104789
1451678_at	0.001838832	24	3	cos_per_24_ph_03	0.840512792	24	3	3	Narf	nuclear prelamin A recognition factor	BI452475	67608	Mm.291832
1451680_at				cos_per_25_ph_03	0.6642135	25	3	3	Srsx1	sulfiredoxin 1 homolog (S. cerevisiae)	BC011325	76650	Mm.218639
1451714_a_at	0.001982816	26.2	3					3	Map2k3	mitogen-activated protein kinase kinase 3	AI481780	26397	Mm.18494
1451723_at				box2_ph_15	0.658567936	24	15	15	Cnot6l	CCR4-NOT transcription complex, subunit 6-like	BC018506	231464	Mm.28374, Mm.384746
1451822_a_at				rigid_ph_02	0.607853134	24	2	2	Scrn2	secernin 2	BC021346	217140	Mm.46189
1451854_a_at				spike_ph_07	0.639625695	24	7	7	Shroom3	shroom family member 3	AF199422	27428	Mm.46014
1451920_a_at				spike_ph_14	0.660967044	24	14	14	Rfc1	replication factor C (activator 1) 1	M88489	19687	Mm.148877
1451928_a_at				rigid_ph_14	0.6150199	24	14	14	Rad18	RAD18 homolog (S. cerevisiae)	BC011120	58186	Mm.103812
1451935_a_at	0.024311295	30	30					6	Spint2	serine protease inhibitor, Kunitz type 2	AF099020	20733	Mm.295230
1451967_x_at				cos_per_28_ph_13	0.651893538	28	13	13	Kpnb1	karyopherin (importin) beta 1	BC004096	16211	Mm.251013
1451991_at				spike_ph_16	0.669859176	24	16	16	Epha7	Eph receptor A7	BC026153	13841	Mm.257266
1452050_at				box1_ph_04	0.634069082	24	4	4	Camkk1d	calcium/calmodulin-dependent protein kinase 1D	BG071931	227541	Mm.191949
1452067_at				asyrigid1_ph_21	0.638289691	24	21	21	Naaa	N-acylethanolamine acid amidase	BI106821	67111	Mm.28890

Table S1: Circadian transcripts (continued)

	Signal Deconvolution			Model-Matching				Final Statistics and Annotations					
Transcript ID (Affymetrix probeset)	Fisher's G Test q-value	Period (hrs)	Phase	HAYSTACK Best Model	HAYSTACK Correlation	Period (hrs)	Phase	Phase (Final)	Gene Symbol	Description	GenBank	Entrez Gene	UniGene
1452119_at				cos_per_27_ph_12	0.718420383	27	12	12	Rrp1b	ribosomal RNA processing 1 homolog B (S. cerevisiae)	BG293527	72462	Mm.102761
1452125_at	0.003843313	22.9	2	rigid_ph_01	0.822846317	24	1	2	Thrap3	thyroid hormone receptor associated protein 3	BG075035	230753	Mm.236211, Mm.29813
1452132_at				cos_per_28_ph_26	0.619980071	28	2	2	Tlcd1	TLC domain containing 1	BE951033	68385	Mm.390375
1452146_a_at	0.005670513	29.5	20					20	Cox15	COX15 homolog, cytochrome c oxidase assembly protein (yeast)	BC021498	226139	Mm.248237
1452181_at				spike_ph_15	0.655335906	24	15	15	Ckap4	cytoskeleton-associated protein 4	BB312117	216197	Mm.334999
1452190_at				asyrigid1_ph_20	0.658292774	24	20	20	Prcp	prolylcarboxypeptidase (angiotensinase C)	AK011112	72461	Mm.389969
1452200_at	0.003988321	24.7	6					6	Cdkn2aipnl	CDKN2A interacting protein N-terminal like	BF100837	52626	Mm.289456
1452233_at	0.043840998	29.8	9					9	Abcc1	ATP-binding cassette, sub-family C (CFTR/MRP), member 1	BG071908	17250	Mm.196634
1452239_at				asyrigid2_ph_20	0.774652875	24	20	20	Gt(ROSA)26Sor	gene trap ROSA 26, Philippe Soriano	U83174	14910	Mm.280950
1452252_at				cos_per_28_ph_10	0.693377541	28	10	10	Utp20	UTP20, small subunit (SSU) processome component, homolog (yeast)	BC005522	70683	Mm.29631
1452258_at				spike_ph_15	0.628481969	24	15	15	Phf20	PHD finger protein 20	BB308157	228829	Mm.427078
1452264_at				cos_per_28_ph_03	0.658188065	28	3	3	Tenc1	tensin like C1 domain-containing phosphatase	BI408679	209039	Mm.29389
1452278_a_at				box2_ph_16	0.66700235	24	16	16	Hace1	HECT domain and ankyrin repeat containing, E3 ubiquitin protein ligase 1	BG923448	209462	Mm.34916, Mm.458633
1452318_a_at				cos_per_28_ph_21	0.623096033	28	21	21	Hspa1b	heat shock protein 1B	M12573	15511	Mm.372314
1452328_s_at				rigid_ph_16	0.697312178	24	16	16	Pja2	praja 2, RING-H2 motif containing	BF160731	224938	Mm.41711
1452333_at				rigid_ph_14	0.637324145	24	14	14	Smarca2	SWI/SNF related, matrix associated, actin dependent regulator of chromatin, subfamily a, member 2	BM230202	67155	Mm.477499
1452350_at				spike_ph_01	0.639752198	24	1	1	Brd8	bromodomain containing 8	BM219644	78656	Mm.411740, Mm.45602
1452351_at				rigid_ph_16	0.647975291	24	16	16	C030027K23Rik	RIKEN cDNA C030027K23 gene	BC025847	77419	Mm.379357
1452378_at				spike_ph_01	0.610634963	24	1	1	Malat1	metastasis associated lung adenocarcinoma transcript 1 (non-coding RNA)	AW012617	72289	Mm.298256
1452383_at				spike_ph_15	0.631335455	24	15	15	Rps6ka3	ribosomal protein S6 kinase polypeptide 3	BE376079	110651	Mm.328476
1452411_at				asyrigid1_ph_10	0.696184259	24	10	10	Lrrc1	leucine rich repeat containing 1	BG966295	214345	Mm.28534, Mm.442042

Table S1: Circadian transcripts (continued)

	Signal Decomposition			Model-Matching				Final Statistics and Annotations					
Transcript ID (Affymetrix probeset)	Fisher's G Test q-value	Period (hrs)	Phase	HAYSTACK Best Model	HAYSTACK Correlation	Period (hrs)	Phase	Phase (Final)	Gene Symbol	Description	GenBank	Entrez Gene	UniGene
1452586_at				asyrigid2_ph_01	0.641455287	24	1	1	Anapc13	anaphase promoting complex subunit 13	BM122700	69010	Mm.2000
1452631_at				box2_ph_16	0.733108467	24	16	16	Rufy2	RUN and FYVE domain-containing 2	AI852705	70432	Mm.234587, Mm.274784
1452679_at				cos_per_28_ph_21	0.615552241	28	21	21	Tubb2b	tubulin, beta 2B	AA986082	73710	Mm.379227, Mm.472121
1452690_at				rigid_ph_16	0.613542976	24	16	16	Khsrp	KH-type splicing regulatory protein	BQ174458	16549	Mm.34296
1452741_s_at				spike_ph_13	0.678517067	24	13	13	Gpd2	glycerol phosphate dehydrogenase 2, mitochondrial	BQ175968	14571	Mm.3711, Mm.441211
1452778_x_at	0.036410733	25	12					12	Nap1l1	nucleosome assembly protein 1-like 1	AK004633	53605	Mm.290407
1452803_at				cos_per_28_ph_21	0.718644902	28	21	21	Glipr2	GLI pathogenesis-related 2	BM208214	384009	Mm.22213
1452829_at				cos_per_26_ph_12	0.687467063	26	12	12	Cad	carbamoyl-phosphate synthetase 2, aspartate transcarbamylase, and dihydroorotase	AK010453	69719	Mm.305535
1452830_s_at	0.014821184	27.1	12	cos_per_27_ph_12	0.778903336	27	12	12	Cad	carbamoyl-phosphate synthetase 2, aspartate transcarbamylase, and dihydroorotase	AK010453	69719	Mm.305535
1452867_at	0.043723144	26.7	0					0	Col4a3bp	collagen, type IV, alpha 3 (Goodpasture antigen) binding protein	AK020301	68018	Mm.24125, Mm.392062
1452896_at	0.026607805	26.2	24					0	Gt3	gene trap locus 3	AK011217	14894	Mm.2080
1452902_at				cos_per_23_ph_07	0.630940656	23	7	7	Dhrs13	dehydrogenase/reductase (SDR family) member 13	AK011939	70451	Mm.390342
1452907_at				asyrigid1_ph_21	0.614969091	24	21	21	Galc	galactosylceramidase	AK010101	14420	Mm.5120
1452910_at				asyrigid1_ph_21	0.70355229	24	21	21	Bcor	BCL6 interacting corepressor	AK018370	71458	Mm.196328
1452915_at	0.0496385	22.8	13					13	Prkar2a	protein kinase, cAMP dependent regulatory, type II alpha	AK004336	19087	Mm.253102
1452970_at	0.01601578	20.2	20					20	Zmym2	zinc finger, MYM-type 2	AK017929	76007	Mm.31417, Mm.450404
1452982_at				cos_per_26_ph_13	0.648414147	26	13	13	Igf1r	insulin-like growth factor 1 receptor	BB446952	16001	Mm.275742
1452992_at				spike_ph_01	0.611132459	24	1	1	Cdc26	cell division cycle 26	AK008199	66440	Mm.109930
1453004_at	0.00573898	22.6	5					5	Slc22a23	solute carrier family 22, member 23	BM234253	73102	Mm.23932
1453009_at				asyrigid1_ph_07	0.692413173	24	7	7	Cpm	carboxypeptidase M	AK004327	70574	Mm.339332
1453012_at				asyrigid2_ph_11	0.6197628	24	11	11	Tsc22d2	TSC22 domain family, member 2	AK017449	72033	Mm.218409

Table S1: Circadian transcripts (continued)

	Signal Decomposition			Model-Matching				Final Statistics and Annotations					
Transcript ID (Affymetrix probeset)	Fisher's G Test q-value	Period (hrs)	Phase	HAYSTACK Best Model	HAYSTACK Correlation	Period (hrs)	Phase	Phase (Final)	Gene Symbol	Description	GenBank	Entrez Gene	UniGene
1453119_at				box2_ph_16	0.661055392	24	16	16	Otud1	OTU domain containing 1	BB530087	71198	Mm.83981
1453134_at				box2_ph_17	0.643473366	24	17	17	Pik3ca	phosphatidylinositol3-kinase, catalytic, alpha polypeptide	BE647269	18706	Mm.260521, Mm.393204, Mm.394949
1453139_at				cos_per_28_ph_17	0.683701262	28	17	17	Nudt12	nudix (nucleoside diphosphate linked moiety X)-type motif 12	AK018117	67993	Mm.36507
1453175_at				box2_ph_15	0.633527209	24	15	15	Zbtb25	zinc finger and BTB domain containing 25	AK013374	109929	Mm.402165, Mm.41880
1453207_at	0.012766465	24.6	1					1	2900053A13Rik	RIKEN cDNA 2900053A13 gene	BE865083	554362	Mm.254898
1453232_at				spike_ph_01	0.687695308	24	1	1	Calr3	calreticulin 3	AK006582	73316	Mm.196315
1453233_s_at				cos_per_26_ph_25	0.647333702	26	1	1	Calr3	calreticulin 3	AK006582	73316	Mm.196315
1453300_at	0.040727464	30	30					6	Slc35d2	solute carrier family 35, member D2	AK017526	70484	Mm.133731
1453332_at				asyrigid1_ph_01	0.700809565	24	1	1	2410002O22Rik	RIKEN cDNA 2410002O22 gene	AK012141	66975	Mm.272541, Mm.477893
1453341_a_at				cos_per_28_ph_05	0.714987644	28	5	5	Tmem202	transmembrane protein 202	AK008510	73893	Mm.216135
1453345_at				cos_per_28_ph_01	0.611493901	28	1	1	Npal1	NIPA-like domain containing 1	AK014427	70701	Mm.38884
1453412_a_at	0.014821184	20.5	12					12	Sec14l1	SEC14-like 1 (S. cerevisiae)	BI652727	74136	Mm.272312, Mm.474931
1453468_at				box2_ph_17	0.635268996	24	17	17	Cep290	centrosomal protein 290	AV312369	216274	Mm.229114
1453475_at				spike_ph_03	0.677668882	24	3	3	4930445K14Rik	RIKEN cDNA 4930445K14 gene	BM123601	74886	Mm.469954
1453596_at	0.033382836	24.2	0	rigid_ph_01	0.735000016	24	1	0	Id2	inhibitor of DNA binding 2	AK013239	15902	Mm.34871, Mm.476766
1453605_s_at				cos_per_27_ph_02	0.635951474	27	2	2	Cdc91	coiled-coil domain containing 91	AK007017	67015	Mm.209774
1453727_at				rigid_ph_17	0.623403331	24	17	17	Esf1	ESF1, nucleolar pre-rRNA processing protein, homolog (S. cerevisiae)	BB612598	66580	Mm.21228
1453740_a_at	0.011888639	26.3	25					1	Ccnl2	cyclin L2	BI112766	56036	Mm.23492
1453783_at	0.020131738	23.7	16	rigid_ph_16	0.763902389	24	16	16	6330411E07Rik	RIKEN cDNA 6330411E07 gene	BE864772	70733	Mm.404138
1453826_at				cos_per_28_ph_10	0.677256821	28	10	10	Pard3b	par-3 partitioning defective 3 homolog B (C. elegans)	BQ179596	72823	Mm.35153, Mm.441881
1453988_a_at	0.020131738	24.9	13					13	Ide	insulin degrading enzyme	AK014703	15925	Mm.28366

Table S1: Circadian transcripts (continued)

	Signal Decomposition			Model-Matching				Final Statistics and Annotations					
Transcript ID (Affymetrix probeset)	Fisher's G Test q-value	Period (hrs)	Phase	HAYSTACK Best Model	HAYSTACK Correlation	Period (hrs)	Phase	Phase (Final)	Gene Symbol	Description	GenBank	Entrez Gene	UniGene
1454043_a_at				cos_per_28_ph_08	0.702660951	28	8	8	Kcnabl	potassium voltage-gated channel, shaker-related subfamily, beta member 1	AK015412	16497	Mm.316402
1454149_a_at	0.009924613	22.9	2					2	Ccnl2	cyclin L2	AK008585	56036	Mm.23492
1454211_a_at				spike_ph_06	0.63272927	24	6	6	Shroom3	shroom family member 3	AK003320	27428	Mm.46014
1454625_at				cos_per_28_ph_16	0.658272067	28	16	16	Phf6	PHD finger protein 6	BG073473	70998	Mm.26870
1454659_at				cos_per_28_ph_10	0.701260825	28	10	10	Dctd	dCMP deaminase	BG069699	320685	Mm.121549
1454665_at				asyrigid1_ph_21	0.65593255	42	21	21	Irf2bp2	interferon regulatory factor 2 binding protein 2	BB183385	270110	Mm.334918, Mm.470682
1454675_at				boxl_ph_22	0.712058627	24	22	22	Thra	thyroid hormone receptor alpha	BI076689	21833	Mm.265917, Mm.442648
1454690_at				asyrigid2_ph_00	0.611453543	24	0	0	Ikbkg	inhibitor of kappaB kinase gamma	BB147462	16151	Mm.12967
1454701_at				cos_per_25_ph_16	0.632400594	25	16	16	4930503L19Rik	RIKEN cDNA 4930503L19 gene	AI450962	269033	Mm.87470
1454717_at	0.043437564	29.3	3					3	Ankrd27	ankyrin repeat domain 27 (VPS9 domain)	BB401190	245886	Mm.272620
1454729_at				cos_per_28_ph_24	0.763474624	28	0	0	Tmem108	transmembrane protein 108	BB293313	81907	Mm.384704
1454825_at				cos_per_26_ph_02	0.632634921	26	2	2	1110014N23Rik	RIKEN cDNA 1110014N23 gene	BI412086	68505	Mm.227361
1454878_at				asyrigid1_ph_21	0.630070604	24	21	21	Dzip3	DAZ interacting protein 3, zinc finger	BM936291	224170	Mm.275138
1454887_at	0.038298805	26	7					7	Pak2	p21 (CDKN1A)-activated kinase 2	AW537308	224105	Mm.234204
1454901_at				cos_per_20_ph_18	0.63819124	20	18	18	Ypel2	yippee-like 2 (Drosophila)	BG069663	77864	Mm.191894
1454930_at				asyrigid2_ph_13	0.674494669	24	13	13	Fam168a	family with sequence similarity 168, member A	BB699417	319604	Mm.260362
1454955_at	0.009833212	26.9	8					8	Ipo7	importin 7	BG922298	233726	Mm.476899
1455033_at	0.026761036	27.5	26					2	Fam102b	family with sequence similarity 102, member B	BB325849	329739	Mm.69013
1455049_at				boxl_ph_14	0.611534832	24	14	14	Igsf3	immunoglobulin superfamily, member 3	BB484576	78908	Mm.257997, Mm.396180, Mm.458336
1455057_at				cos_per_28_ph_10	0.64556444	28	10	10	Gmps	guanine monophosphate synthetase	AV308908	229363	Mm.331051, Mm.394565, Mm.441120

Table S1: Circadian transcripts (continued)

	Signal Decomposition			Model-Matching				Final Statistics and Annotations					
Transcript ID (Affymetrix probeset)	Fisher's G Test q-value	Period (hrs)	Phase	HAYSTACK Best Model	HAYSTACK Correlation	Period (hrs)	Phase	Phase (Final)	Gene Symbol	Description	GenBank	Entrez Gene	UniGene
1455061_a_at	0.049858696	27	24					0	Acaa2	acetyl-Coenzyme A acyltransferase 2 (mitochondrial 3-oxoacyl-Coenzyme A thiolase)	BB718075	52538	Mm.245724
1455063_at				spike_ph_01	0.626349748	24	1	1	Fam82a1	family with sequence similarity 82, member A1	AW061290	381110	Mm.293063
1455091_at				asyrigid2_ph_09	0.677058155	24	9	9	3222402P14Rik	RIKEN cDNA 3222402P14 gene	AI642021	235542	Mm.335386
1455104_at	0.048568798	28.1	27	cos_per_27_ph_00	0.768335317	27	0	3	Mxd1	MAX dimerization protein 1	AV228517	17119	Mm.279580
1455115_a_at	0.009712895	26.7	2					2	Crb3	crumbs homolog 3 (Drosophila)	AU015319	224912	Mm.391027
1455173_at				cos_per_28_ph_11	0.666868898	28	11	11	Gspt1	G1 to S phase transition 1	AW537663	14852	Mm.325827
1455177_at				box2_ph_14	0.679723168	24	14	14	Abi1	Abelson helper integration site 1	BQ175532	52906	Mm.253280
1455197_at				cos_per_28_ph_09	0.616431599	28	9	9	Rnd1	Rho family GTPase 1	BE852181	223881	Mm.274010
1455198_a_at				cos_per_28_ph_01	0.747478781	28	1	1	Ppp2r3a	protein phosphatase 2 (formerly 2A), regulatory subunit B'', alpha	BB550312	19054	Mm.271249
1455236_x_at				spike_ph_05	0.676635092	24	5	5	Serf2	small EDRK-rich factor 2	BB704811	378702	Mm.262252
1455237_at				cos_per_28_ph_08	0.610942475	28	8	8	Usp36	ubiquitin specific peptidase 36	BB006147	72344	Mm.232293
1455238_at	0.046172379	22.7	19	cos_per_25_ph_17	0.708390555	25	17	19	Mum1l1	melanoma associated antigen (mutated) 1-like 1	BB103233	245631	Mm.131001
1455279_at				cos_per_28_ph_26	0.635270252	28	2	2	Gm1060	gene model 1060, (NCBI)	BG070552	381738	Mm.389604, Mm.458839
1455298_at	0.011047457	22.1	18					18	Leo1	Leo1, Paf1/RNA polymerase II complex component, homolog (S. cerevisiae)	BG065311	235497	Mm.41508
1455372_at				box2_ph_14	0.633255636	24	14	14	Cpeb3	cytoplasmic polyadenylation element binding protein 3	BB770826	208922	Mm.391176
1455385_at	0.016047923	29.2	5					5	Sh3glb1	SH3-domain GRB2-like B1 (endophilin)	AV005520	54673	Mm.271775, Mm.440295, Mm.474936
1455387_at				rigid_ph_14	0.649007154	24	14	14	Nufip2	nuclear fragile X mental retardation protein interacting protein 2	AV112972	68564	Mm.428996
1455398_at				rigid_ph_14	0.69608748	24	14	14	Lrrc8c	leucine rich repeat containing 8 family, member C	BB333759	100604	Mm.319847, Mm.392291
1455445_at				cos_per_28_ph_25	0.780832593	28	1	1	Cbln3	cerebellin 3 precursor protein	BB800230	56410	Mm.97163
1455454_at				box1_ph_05	0.6205431	24	5	5	Akr1c19	aldo-keto reductase family 1, member C19	BG073853	432720	Mm.22832
1455459_at				box2_ph_16	0.612132528	24	16	16	Prdm15	PR domain containing 15	BB213846	114604	Mm.328741

Table S1: Circadian transcripts (continued)

	Signal Deconvolution			Model-Matching				Final Statistics and Annotations					
Transcript ID (Affymetrix probeset)	Fisher's G Test q-value	Period (hrs)	Phase	HAYSTACK Best Model	HAYSTACK Correlation	Period (hrs)	Phase	Phase (Final)	Gene Symbol	Description	GenBank	Entrez Gene	UniGene
1455477_x_at				cos_per_28_ph_26	0.637146436	28	2	2	Pdzk1ip1	PDZK1 interacting protein 1	AA396586	67182	Mm.30181
1455488_at				box1_ph_13	0.615576002	24	13	13	6230416J20Rik	RIKEN cDNA 6230416J20 gene	BB827546	230376	Mm.74730
1455496_at	0.018317151	26.6	11	cos_per_26_ph_12	0.754022892	26	12	11	Pfas	phosphoribosylformylglycinamidine synthase (FGAR amidotransferase)	AV306055	237823	Mm.340288
1455566_x_at				cos_per_28_ph_26	0.667385334	28	2	2	2810022L02Rik	RIKEN cDNA 2810022L02 gene	AV337975	67198	Mm.159989
1455581_x_at	0.01348048	21.5	3					3	Samd9l	sterile alpha motif domain containing 9-like	BQ175154	209086	Mm.196013
1455608_at				asytrigid2_ph_09	0.713924641	24	9	9	Sclt1	sodium channel and clathrin linker 1	BB700774	67161	Mm.331001
1455665_at				cos_per_28_ph_10	0.63@62515	28	10	10	Lonrf1	LON peptidase N-terminal domain and ring finger 1	BB705689	244421	Mm.324032
1455687_at				cos_per_27_ph_04	0.625450115	27	4	4	Ick	intestinal cell kinase	BB376918	56542	Mm.288719
1455709_at				spike_ph_00	0.610914377	24	0	0	Tspan8	tetraspanin 8	BM211929	216350	Mm.22270
1455711_at				spike_ph_00	0.650498776	24	0	0	Dtx4	deltex 4 homolog (Drosophila)	AW122183	207521	Mm.247@5, Mm.477187
1455751_at				rigid_ph_16	0.623323611	24	16	16	Cand1	cullin associated and neddylation dissociated 1	BB770361	71902	Mm.203965
1455775_at				box2_ph_17	0.64882451	24	17	17			AW988196		
1455787_x_at				cos_per_28_ph_17	0.626538857	28	17	17	Mimpp1	multiple inositol polyphosphate histidine phosphatase 1	AV339366	17930	Mm.255116
1455795_at				cos_per_25_ph_16	0.610693204	25	16	16	Dse	dermatan sulfate epimerase	BM207218	212898	Mm.34557
1455817_x_at				cos_per_25_ph_17	0.612319374	25	17	17	Zxdb	zinc finger, X-linked, duplicated B	AI661029	668166	Mm.426145
1455872_at				cos_per_28_ph_26	0.678026369	28	2	2	Fam167a	family with sequence similarity 167, member A	BB151460	219148	Mm.37882
1455908_a_at				cos_per_27_ph_16	0.808564731	27	16	16	Scpep1	serine carboxypeptidase 1	AV102733	74617	Mm.34126
1455927_x_at				spike_ph_03	0.673815787	24	3	3	Nsmce1	non-SMC element 1 homolog (S. cerevisiae)	AV216677	67711	Mm.4467
1455938_x_at				cos_per_28_ph_18	0.694439997	28	18	18	Rad21	RAD21 homolog (S. pombe)	AV025454	19357	Mm.182628, Mm.470496
1455959_s_at	0.032215727	25.2	21					21	Gclc	glutamate-cysteine ligase, catalytic subunit	AW825835	14629	Mm.89888
1455960_at				rigid_ph_16	0.646034697	24	16	16	Megf9	multiple EGF-like-domains 9	BB483642	230316	Mm.251188
1455964_at				rigid_ph_15	0.653579467	24	15	15	Crkrs	CDC2-related kinase, arginine/serine-rich	BB795494	69131	Mm.260516

Table S1: Circadian transcripts (continued)

	SignalDecomposition			Model-Matching				Final Statistics and Annotations					
Transcript ID (Affymetrix probeset)	Fisher's G Test q-value	Period (hrs)	Phase	HAYSTACK Best Model	HAYSTACK Correlation	Period (hrs)	Phase	Phase (Final)	Gene Symbol	Description	GenBank	Entrez Gene	UniGene
1456032_x_at				cos_per_28_ph_16	0.75232116	28	16	16	H2afz	H2A histone family, member Z	AV215230	51788	Mm.117541, Mm.372513, Mm.465508
1456063_at				cos_per_27_ph_11	0.630506726	27	11	11	Fam120c	family with sequence similarity 120, member C	BM237456	207375	Mm.391339
1456070_at				cos_per_28_ph_12	0.640268016	28	12	12	Ptprg	protein tyrosine phosphatase, receptor type, G	AI507538	19270	Mm.431266
1456117_at				cos_per_28_ph_07	0.745878008	28	7	7	Rrp1b	ribosomal RNA processing 1 homolog B (S. cerevisiae)	AV228374	72462	Mm.102761
1456152_at				cos_per_28_ph_01	0.710206277	28	1	1	Paqr5	progestin and adipoQ receptor family member V	BB744177	74090	Mm.273267
1456201_at	0.030589843	23	2					2	4632427E13Rik	RIKEN cDNA 4632427E13 gene	BB464034	666737	Mm.292102, Mm.473620, Mm.476428
1456216_at	0.044948518	23.2	0					0			BM239982		
1456229_at	0.043113119	27.3	24					0	Hoxb3	homeo box B3	BG073383	15410	Mm.342481
1456244_x_at				cos_per_28_ph_14	0.611840439	28	14	14	Glrx3	glutaredoxin 3	BB458835	30926	Mm.267692
1456245_x_at	0.002852185	25.3	4					4	Vamp3	vesicle-associated membrane protein 3	BB531498	22319	Mm.273980
1456273_x_at	0.007802073	27	13					13	Tpmt	thiopurine methyltransferase	BB744467	22017	Mm.10169
1456284_at	0.013478656	29.8	4					4	Tmem171	transmembrane protein 171	BB701775	380863	Mm.28264
1456309_x_at				spike_ph_04	0.622865221	24	4	4	Lasp1	LIM and SH3 protein 1	BG146595	16796	Mm.271967
1456396_at				cos_per_28_ph_10	0.628215725	28	10	10			BG064541		
1456415_at				cos_per_24_ph_18	0.688630799	24	18	18	Zfp451	zinc finger protein 451	BI083675	98403	Mm.289103, Mm.440137
1456419_at				spike_ph_14	0.630983928	24	14	14	5730455P16Rik	RIKEN cDNA 5730455P16 gene	BI108098	70591	Mm.86860
1456420_at				rigid_ph_15	0.678883235	24	15	15	Arid4a	AT rich interactive domain 4A (RBP1-like)	BB667227	238247	Mm.241601
1456495_x_at				box2_ph_15	0.62748493	24	15	15	Osbpl6	oxysterol binding protein-like 6	BG070848	99031	Mm.240435
1456505_at				rigid_ph_15	0.633106167	24	15	15	Braf	Braf transforming gene	BB332976	109880	Mm.245513, Mm.477773
1456577_x_at				cos_per_28_ph_14	0.765175614	28	14	14	Pitrm1	pitrilysin metallepetidase 1	AV304625	69617	Mm.41933
1456586_x_at	0.038890813	24.7	3					3	Mvp	major vault protein	BB139464	78388	Mm.228797

Table S1: Circadian transcripts (continued)

	Signal Deconvolution			Model-Matching				Final Statistics and Annotations					
Transcript ID (Affymetrix probeset)	Fisher's G Test q-value	Period (hrs)	Phase	HAYSTACK Best Model	HAYSTACK Correlation	Period (hrs)	Phase	Phase (Final)	Gene Symbol	Description	GenBank	Entrez Gene	UniGene
1456603_at				cos_per_24_ph_04	0.62590614	24	4	4	Fam101b	family with sequence similarity 101, member B	BG070087	76566	Mm.34131
1456624_at	0.033035704	25.7	15	rigid_ph_16	0.756376664	24	16	15	Wipi1	WD repeat domain, phosphoinositide interacting 1	BI251603	52639	Mm.35817
1456651_a_at	0.022494968	25.1	15	rigid_ph_16	0.752369292	24	16	15	Tpr	translocated promoter region	BG067858	108989	Mm.174256
1456653_a_at	0.001838832	24.4	11	cos_per_24_ph_12	0.871009099	24	12	11	Mthfd1l	methylenetetrahydrofolate dehydrogenase (NADP+ dependent) 1-like	AV095209	270685	Mm.184752
1456712_at				rigid_ph_19	0.665650167	24	19	19	Lcor	ligand dependent nuclear receptor corepressor-like	AV231984	209707	Mm.451765, Mm.71498
1456741_s_at				cos_per_28_ph_25	0.618322253	28	1	1	Gpm6a	glycoprotein m6a	BB348674	234267	Mm.241700
1456743_x_at	0.01129986	28.6	18					18	Mort1l2	mortality factor 4 like 2	BB068032	56397	Mm.27218
1456811_at	0.002323819	23.7	19	boxl_ph_19	0.843138705	24	19	19	Cxxc4	CXXC finger 4	AV307265	319478	Mm.442744, Mm.457442
1456869_at				cos_per_27_ph_00	0.682795404	27	0	0	Zfp787	zinc finger protein 787	AI462089	67109	Mm.3254
1456871_a_at	0.031262421	21.3	12					12	Phf2011	PHD finger protein 20-like 1	BE956921	239510	Mm.267473
1457086_at	0.005358179	28	26					2	D930028M14Rik	RIKEN cDNA D930028M14 gene	AW123201	434147	Mm.59171
1457097_at				asyrigid2_ph_04	0.637406762	24	4	4	Skap2	src family associated phosphoprotein 2	BB212597	54453	Mm.221479, Mm.392558
1457271_at				cos_per_26_ph_15	0.695848642	26	15	15	Gm1311	gene model 1311, (NCBI)	AI326975	229697	Mm.476749
1457306_at	0.00599398	21	9	cos_per_23_ph_08	0.783365911	23	8	9			C86690		
1457404_at	0.049369186	24.2	24	rigid_ph_01	0.709045764	24	1	0	Nfkbiz	nuclear factor of kappa light polypeptide gene enhancer in B-cells inhibitor, zeta	BM240058	80859	Mm.247272
1457473_at				rigid_ph_16	0.612905223	24	16	16	Chd1	chromodomain helicase DNA binding protein 1	AI851787	12648	Mm.393794, Mm.8137
1457588_at	0.01279249	21.8	2	cos_per_22_ph_02	0.801885807	22	2	2	C76213	expressed sequence C76213	C76213	97124	Mm.379457
1457824_at	0.038276675	21.4	2	cos_per_22_ph_02	0.74355411	22	2	2	Plscr1	phospholipid scramblase 1	AI504076	22038	Mm.421956, Mm.441702
1457867_at	0.044661765	28.6	27	cos_per_26_ph_02	0.7333759	26	2	3	Sgpp2	sphingosine-1-phosphate phosphotase 2	BB360745	433323	Mm.276248, Mm.406972
1458284_at				spike_ph_04	0.664098132	24	4	4	Prbp1	polypyrimidine tract binding protein 1	BM195499	19205	Mm.265610, Mm.472059
1458370_at				rigid_ph_14	0.63622238	24	14	14	Bmp2k	BMP2 inducible kinase	BM234405	140780	Mm.281490, Mm.436797, Mm.460821

Table S1: Circadian transcripts (continued)

	Signal Decomposition			Model-Matching				Final Statistics and Annotations					
Transcript ID (Affymetrix probeset)	Fisher's G Test q-value	Period (hrs)	Phase	HAYSTACK Best Model	HAYSTACK Correlation	Period (hrs)	Phase	Phase (Final)	Gene Symbol	Description	GenBank	Entrez Gene	UniGene
1458541_at				cos_per_20_ph_00	0.614720479	20	0	0	Dctn4	dynactin 4	BB125218	67665	Mm.272801
1458643_at				box1_ph_04	0.608220986	24	4	4	Dtx1	deltex 1 homolog (Drosophila)	AI551217	14357	Mm.1645
1459766_x_at				spike_ph_04	0.610422233	24	4	4	Sf1	splicing factor 1	BB055869	22668	Mm.256422
1459850_x_at				asyrigid1_ph_21	0.635764162	24	21	21	Glrb	glycine receptor, beta subunit	BB345174	14658	Mm.275639
1460182_at	0.00764263	26.5	26					2	Snx4	sorting nexin 4	NM_080557	69150	Mm.28196, Mm.396285
1460196_at				cos_per_28_ph_26	0.621572439	28	2	2	Cbr1	carbonyl reductase 1	NM_007620	12408	Mm.26940
1460203_at				cos_per_25_ph_14	0.631382571	25	14	14	Itpr1	inositol 1,4,5-triphosphate receptor 1	NM_010585	16438	Mm.227912
1460220_a_at	0.00590407 1	23.6	9					9	Csf1	colony stimulating factor 1 (macrophage)	BM233698	12977	Mm.795
1460228_at				asyrigid2_ph_01	0.626417977	24	1	1	Usf2	upstream transcription factor 2	AW537576	22282	Mm.322453, Mm.466352
1460239_at				cos_per_28_ph_25	0.76603211	28	1	1	Tspan13	tetraspanin 13	BB807707	66109	Mm.254663
1460295_s_at				box2_ph_16	0.698072874	24	16	16	Il6st	interleukin 6 signal transducer	AA717838	16195	Mm.4364
1460314_s_at				asyrigid2_ph_00	0.666751069	24	0	0	Hist2h3c1	histone cluster 2, H3c1	NM_019469	15077	Mm.383293, Mm.422680
1460325_at				rigid_ph_16	0.651923255	24	16	16	Pum1	pumilio 1 (Drosophila)	BB837171	80912	Mm.440206
1460344_at	0.023459596	24	16					16	Pbxip1	pre-B-cell leukemia transcription factor interacting protein 1	AV220340	229534	Mm.65906
1460428_at	0.044879667	20.1	8					8	Ankrd13a	ankyrin repeat domain 13a	BC008286	68420	Mm.275554
1460445_at				box1_ph_13	0.632894863	24	13	13	Sfrs2ip	splicing factor, arginine/serine-rich 2, interacting protein	AK012092	72193	Mm.324474, Mm.472183
1460447_at				cos_per_28_ph_08	0.623061172	28	8	8	Pus7l	pseudouridylate synthase 7 homolog (S. cerevisiae)-like	AK019372	78895	Mm.34344
1460459_at				cos_per_28_ph_00	0.728119667	28	0	0	Paqr5	progestin and adipoQ receptor family member V	AK002481	74090	Mm.273267
1460486_at	0.018218873	23.1	17					17	Rabgap1	RAB GTPase activating protein 1	BB486322	227800	Mm.383192
1460614_at	0.045665128	21.7	16	rigid_ph_15	0.716770782	24	15	16	Mier3	mesoderm induction early response 1, family member 3	BB530158	218613	Mm.31012
1460674_at	0.039253886	22.5	8					8	Paqr7	progestin and adipoQ receptor family member VII	BC022922	71904	Mm.142343

Table S1: Circadian transcripts (continued)

	Signal Deconvolution			Model-Matching				Final Statistics and Annotations					
Transcript ID (Affymetrix probeset)	Fisher's G Test q-value	Period (hrs)	Phase	HAYSTACK Best Model	HAYSTACK Correlation	Period (hrs)	Phase	Phase (Final)	Gene Symbol	Description	GenBank	Entrez Gene	UniGene
1460708_s_at	0.014169778	23.4	22					22	Cdc42	cell division cycle 42 homolog (S. cerevisiae)	AV000235	12540	Mm.1022, Mm.447553, Mm.475151
1460728_s_at				cos_per_26_ph_01	0.640989033	26	1	1	Ing4	inhibitor of growth family, member 4	BB042583	28019	Mm.262547, Mm.347910
AFFX-PyruCarbMur/L09192_3_at	0.039499412	22.9	5	cos_per_24_ph_05	0.704731966	24	5	5	Pcx	pyruvate carboxylase	AFFX-PYRUCARBMUR/L09192_3	18563	Mm.1845
AFFX-PyruCarbMur/L09192_5_at			asyrigid1_ph_09	0.673712231	24	9	9	Pcx	pyruvate carboxylase	AFFX-PYRUCARBMUR/L09192_5	18563	Mm.1845 Mm.1845	Mm.1845
AFFX-PyruCarbMur/L09192_MA_at			cos_per_25_ph_04	0.613558007	25	4	4	Pcx	pyruvate carboxylase	AFFX-PYRUCARBMUR/L09192_MA	18563		
AFFX-PyruCarbMur/L09192_MB_at			asyrigid1_ph_10	0.619025035	24	10	10	Pcx	pyruvate carboxylase	AFFX-PYRUCARBMUR/L09192_MB	18563		

Appendix 2: Table S2

Table S2: DAVID Functional Annotation Clustering for gene ontology terms and Swiss-Prot keywords on the MMH-D3 circadian transcript list revealed enrichment in a wide range of biological processes and functions. Enriched clusters display enrichment scores ≥1.3 (corresponds to a mean *P*-value for included terms <0.05).

Annotation Cluster 1	**Enrichment Score: 4.7892089039752594**	**Description: rhythmic process**		
Category	**Term**	**# Genes**	***P*-value**	**Fold Enrichment**
SP_PIR_KEYWORDS	biological rhythms	9	2.9607E-06	9.00
GOTERM_BP_FAT	GO:0048511 (rhythmic process)	17	7.3159E-06	3.84
GOTERM_BP_FAT	GO:0007623 (circadian rhythm)	9	1.9802E-04	5.38
Annotation Cluster 2	**Enrichment Score: 3.772954821403953**	**Description: regulation of transcription**		
Category	**Term**	**# Genes**	***P*-value**	**Fold Enrichment**
SP_PIR_KEYWORDS	nucleus	253	2.8475E-09	1.40
GOTERM_BP_FAT	GO:0006350 (transcription)	124	4.1293E-07	1.55
SP_PIR_KEYWORDS	transcription regulation	113	3.8637E-06	1.54
SP_PIR_KEYWORDS	Transcription	125	5.6793E-06	1.48
GOTERM_BP_FAT	GO:0045449 (regulation of transcription)	142	8.9124E-06	1.41
GOTERM_MF_FAT	GO:0003677 (DNA binding)	112	2.1207E-04	1.39
SP_PIR_KEYWORDS	dna-binding	91	2.1419E-03	1.36
GOTERM_MF_FAT	GO:0030528 (transcription regulator activity)	72	1.2347E-02	1.32
GOTERM_BP_FAT	GO:0051252 (regulation of RNA metabolic process)	80	6.8215E-02	1.19
GOTERM_BP_FAT	GO:0006355 (regulation of transcription, DNA-dependent)	76	1.3450E-01	1.15
GOTERM_MF_FAT	GO:0003700 (transcription factor activity)	40	2.6573E-01	1.14
Annotation Cluster 3	**Enrichment Score: 3.4881163699919275**	**Description: cation binding**		
Category	**Term**	**# Genes**	***P*-value**	**Fold Enrichment**
GOTERM_MF_FAT	GO:0008270 (zinc ion binding)	135	1.3700E-05	1.42
GOTERM_MF_FAT	GO:0046914 (transition metal ion binding)	157	6.6413E-05	1.33
SP_PIR_KEYWORDS	zinc	124	1.5829E-04	1.38
GOTERM_MF_FAT	GO:0043167 (ion binding)	217	3.5074E-04	1.22
SP_PIR_KEYWORDS	zinc-finger	84	3.8781E-04	1.47
GOTERM_MF_FAT	GO:0043169 (cation binding)	211	1.1043E-03	1.20
GOTERM_MF_FAT	GO:0046872 (metal ion binding)	208	1.6427E-03	1.19
SP_PIR_KEYWORDS	metal-binding	157	3.5024E-03	1.23

Table S2: DAVID Functional Annotation Clustering (continued)

Annotation Cluster 4	**Enrichment Score: 2.784165262100181**	**Description: protein transport**		
Category	**Term**	**# Genes**	***P*-value**	**Fold Enrichment**
GOTERM_BP_FAT	GO:0015031 (protein transport)	54	2.1240E-05	1.84
GOTERM_BP_FAT	GO:0045184 (establishment of protein localization)	54	2.5996E-05	1.82
GOTERM_BP_FAT	GO:0008104 (protein localization)	57	1.4902E-04	1.68
SP_PIR_KEYWORDS	protein transport	40	3.7178E-04	1.82
GOTERM_BP_FAT	GO:0046907 (intracellular transport)	34	2.1277E-03	1.75
GOTERM_BP_FAT	GO:0006605 (protein targeting)	15	2.7067E-03	2.50
GOTERM_BP_FAT	GO:0006886 (intracellular protein transport)	22	1.3624E-02	1.76
GOTERM_BP_FAT	GO:0034613 (cellular protein localization)	23	1.6752E-02	1.70
GOTERM_BP_FAT	GO:0070727 (cellular macromolecule localization)	23	1.8013E-02	1.69
SP_PIR_KEYWORDS	Transport	83	1.9881E-01	1.11
Annotation Cluster 5	**Enrichment Score: 2.711853762047121**	**Description: proteolysis**		
Category	**Term**	**# Genes**	***P*-value**	**Fold Enrichment**
SP_PIR_KEYWORDS	ubl conjugation pathway	42	2.5786E-04	1.82
GOTERM_BP_FAT	GO:0051603 (proteolysis involved in cellular protein catabolic process)	42	6.1156E-04	1.74
GOTERM_BP_FAT	GO:0044257 (cellular protein catabolic process)	42	6.8584E-04	1.73
GOTERM_BP_FAT	GO:0043632 (modification-dependent macromolecule catabolic process)	40	8.2333E-04	1.74
GOTERM_BP_FAT	GO:0019941 (modification-dependent protein catabolic process)	40	8.2333E-04	1.74
GOTERM_BP_FAT	GO:0030163 (protein catabolic process)	42	1.3252E-03	1.67
SP_PIR_KEYWORDS	Ligase	26	3.0414E-03	1.88
GOTERM_BP_FAT	GO:0044265 (cellular macromolecule catabolic process)	43	4.0267E-03	1.56
GOTERM_BP_FAT	GO:0009057 (macromolecule catabolic process)	43	1.3135E-02	1.46
GOTERM_BP_FAT	GO:0006508 (proteolysis)	59	4.8703E-02	1.26
Annotation Cluster 6	**Enrichment Score: 2.3691398352165955**	**Description: cytoskeletal protein binding**		
Category	**Term**	**# Genes**	***P*-value**	**Fold Enrichment**
GOTERM_MF_FAT	GO:0015631 (tubulin binding)	12	5.8296E-04	3.49
GOTERM_MF_FAT	GO:0008017 (microtubule binding)	10	1.5769E-03	3.62
GOTERM_MF_FAT	GO:0008092 (cytoskeletal protein binding)	26	8.4946E-02	1.39

Table S2: DAVID Functional Annotation Clustering (continued)

Annotation Cluster 7	**Enrichment Score: 2.1611620483694693**	**Description: phosphorylation**		
Category	**Term**	**# Genes**	***P*-value**	**Fold Enrichment**
GOTERM_MF_FAT	GO:0000166 (nucleotide binding)	136	5.1512E-05	1.38
GOTERM_BP_FAT	GO:0006793 (phosphorus metabolic process)	61	5.6916E-04	1.56
GOTERM_BP_FAT	GO:0006796 (phosphate metabolic process)	61	5.6916E-04	1.56
GOTERM_BP_FAT	GO:0006468 (protein amino acid phosphorylation)	47	1.1895E-03	1.63
GOTERM_BP_FAT	GO:0016310 (phosphorylation)	50	2.4442E-03	1.54
GOTERM_MF_FAT	GO:0004672 (protein kinase activity)	42	3.3523E-03	1.59
GOTERM_MF_FAT	GO:0032555 (purine ribonucleotide binding)	103	7.9701E-03	1.27
GOTERM_MF_FAT	GO:0032553 (ribonucleotide binding)	103	7.9701E-03	1.27
GOTERM_MF_FAT	GO:0017076 (purine nucleotide binding)	106	9.7416E-03	1.25
SP_PIR_KEYWORDS	nucleotide-binding	98	1.2137E-02	1.26
GOTERM_MF_FAT	GO:0001882 (nucleoside binding)	89	1.5142E-02	1.26
GOTERM_MF_FAT	GO:0032559 (adenyl ribonucleotide binding)	84	1.5910E-02	1.27
GOTERM_MF_FAT	GO:0005524 (ATP binding)	83	1.6729E-02	1.27
GOTERM_MF_FAT	GO:0001883 (purine nucleoside binding)	88	1.8049E-02	1.25
SP_PIR_KEYWORDS	kinase	47	1.9218E-02	1.40
GOTERM_MF_FAT	GO:0030554 (adenyl nucleotide binding)	87	1.9759E-02	1.25
GOTERM_MF_FAT	GO:0004674 (protein serine/threonine kinase activity)	29	2.6877E-02	1.52
SP_PIR_KEYWORDS	atp-binding	76	3.7401E-02	1.24
SP_PIR_KEYWORDS	transferase	81	3.9133E-02	1.23
SP_PIR_KEYWORDS	serine/threonine-protein kinase	27	4.5062E-02	1.48
Annotation Cluster 8	**Enrichment Score: 2.0431620391140064**	**Description: negative regulation of transcription**		
Category	**Term**	**# Genes**	***P*-value**	**Fold Enrichment**
GOTERM_MF_FAT	GO:0003714 (transcription corepressor activity)	12	3.6220E-04	3.68
GOTERM_MF_FAT	GO:0003712 (transcription cofactor activity)	18	3.2967E-03	2.21
GOTERM_MF_FAT	GO:0016564 (transcription repressor activity)	20	3.3420E-03	2.09
GOTERM_BP_FAT	GO:0045934 (negative regulation of nucleobase, nucleoside, nucleotide and nucleic acid metabolic process)	31	4.0181E-03	1.73
GOTERM_BP_FAT	GO:0051172 (negative regulation of nitrogen compound metabolic process)	31	4.6389E-03	1.71
GOTERM_BP_FAT	GO:0016481 (negative regulation of transcription)	29	5.6390E-03	1.73
GOTERM_MF_FAT	GO:0008134 (transcription factor binding)	24	5.9748E-03	1.84
GOTERM_BP_FAT	GO:0010605 (negative regulation of macromolecule metabolic process)	36	7.9128E-03	1.57
GOTERM_BP_FAT	GO:0010629 (negative regulation of gene expression)	30	1.1120E-02	1.62

Table S2: DAVID Functional Annotation Clustering (continued)

Category	**Term**	**# Genes**	***P*-value**	**Fold Enrichment**
GOTERM_BP_FAT	GO:0010558 (negative regulation of macromolecule biosynthetic process)	30	1.4281E-02	1.59
GOTERM_BP_FAT	GO:0031327 (negative regulation of cellular biosynthetic process)	30	2.0067E-02	1.54
GOTERM_BP_FAT	GO:0009890 (negative regulation of biosynthetic process)	30	2.2340E-02	1.53
GOTERM_BP_FAT	GO:0051253 (negative regulation of RNA metabolic process)	23	2.4143E-02	1.64
GOTERM_BP_FAT	GO:0000122 (negative regulation of transcription from RNA polymerase II promoter)	18	3.2698E-02	1.72
GOTERM_BP_FAT	GO:0045892 (negative regulation of transcription, DNA-dependent)	22	3.9379E-02	1.58
GOTERM_BP_FAT	GO:0006357 (regulation of transcription from RNA polymerase II promoter)	38	4.6464E-02	1.37
Annotation Cluster 9	**Enrichment Score: 1.7989554500645537**	**Description: regulation of phosphorylation**		
Category	**Term**	**# Genes**	***P*-value**	**Fold Enrichment**
GOTERM_BP_FAT	GO:0042325 (regulation of phosphorylation)	27	6.7192E-04	2.06
GOTERM_BP_FAT	GO:0051174 (regulation of phosphorus metabolic process)	27	1.1730E-03	1.99
GOTERM_BP_FAT	GO:0019220 (regulation of phosphate metabolic process)	27	1.1730E-03	1.99
GOTERM_BP_FAT	GO:0033674 (positive regulation of kinase activity)	15	2.1871E-03	2.55
GOTERM_BP_FAT	GO:0051347 (positive regulation of transferase activity)	15	3.1064E-03	2.46
GOTERM_BP_FAT	GO:0001932 (regulation of protein amino acid phosphorylation)	14	3.1656E-03	2.56
GOTERM_BP_FAT	GO:0031399 (regulation of protein modification process)	17	3.2308E-03	2.28
GOTERM_BP_FAT	GO:0032268 (regulation of cellular protein metabolic process)	24	4.1322E-03	1.90
GOTERM_BP_FAT	GO:0043549 (regulation of kinase activity)	18	6.1671E-03	2.07
GOTERM_BP_FAT	GO:0051338 (regulation of transferase activity)	18	8.7184E-03	2.00
GOTERM_BP_FAT	GO:0045860 (positive regulation of protein kinase activity)	13	1.0183E-02	2.32
GOTERM_BP_FAT	GO:0045859 (regulation of protein kinase activity)	16	2.1298E-02	1.90
GOTERM_BP_FAT	GO:0043085 (positive regulation of catalytic activity)	19	4.8932E-02	1.61
GOTERM_BP_FAT	GO:0044093 (positive regulation of molecular function)	21	6.2135E-02	1.52
GOTERM_BP_FAT	GO:0032147 (activation of protein kinase activity)	5	1.9716E-01	2.17
GOTERM_BP_FAT	GO:0043406 (positive regulation of MAP kinase activity)	5	2.7551E-01	1.88
GOTERM_BP_FAT	GO:0043405 (regulation of MAP kinase activity)	6	3.2897E-01	1.58
GOTERM_BP_FAT	GO:0000165 (MAPKKK cascade)	6	5.8952E-01	1.16
GOTERM_BP_FAT	GO:0000187 (activation of MAPK activity)	3	6.6617E-01	1.33

Table S2: DAVID Functional Annotation Clustering (continued)

Annotation Cluster 10	**Enrichment Score: 1.782145589497685**	**Descritption: response to DNA damage**		
Category	**Term**	**# Genes**	***P*-value**	**Fold Enrichment**
GOTERM_BP_FAT	GO:0006974 (response to DNA damage stimulus)	27	5.8494E-04	2.08
GOTERM_BP_FAT	GO:0033554 (cellular response to stress)	33	1.4417E-03	1.81
GOTERM_BP_FAT	GO:0006259 (DNA metabolic process)	30	1.5539E-02	1.58
GOTERM_BP_FAT	GO:0006281 (DNA repair)	18	2.3428E-02	1.79
SP_PIR_KEYWORDS	DNA damage	13	2.1388E-01	1.41
Category	**Term**	**# Genes**	***P*-value**	**Fold Enrichment**
SP_PIR_KEYWORDS	dna repair	11	3.0888E-01	1.34
Annotation Cluster 11	**Enrichment Score: 1.7054170653947816**	**Description: protein dimerization**		
Category	**Term**	**# Genes**	***P*-value**	**Fold Enrichment**
GOTERM_MF_FAT	GO:0046983 (protein dimerization activity)	26	1.1671E-02	1.69
GOTERM_MF_FAT	GO:0042802 (identical protein binding)	22	2.2578E-02	1.67
GOTERM_MF_FAT	GO:0042803 (protein homodimerization activity)	16	2.9036E-02	1.83
Annotation Cluster 12	**Enrichment Score: 1.6203842725366808**	**Description: sexual reproduction process**		
Category	**Term**	**# Genes**	***P*-value**	**Fold Enrichment**
GOTERM_BP_FAT	GO:0048511 (rhythmic process)	17	7.3159E-06	3.84
GOTERM_BP_FAT	GO:0008406 (gonad development)	12	1.9612E-03	3.02
GOTERM_BP_FAT	GO:0007548 (sex differentiation)	14	5.8460E-03	2.38
GOTERM_BP_FAT	GO:0048608 (reproductive structure development)	14	5.8460E-03	2.38
GOTERM_BP_FAT	GO:0045137 (development of primary sexual characteristics)	12	7.1655E-03	2.55
GOTERM_BP_FAT	GO:0003006 (reproductive developmental process)	22	8.5082E-03	1.84
GOTERM_BP_FAT	GO:0008584 (male gonad development)	6	2.9815E-02	3.40
GOTERM_BP_FAT	GO:0046661 (male sex differentiation)	7	4.2623E-02	2.72
GOTERM_BP_FAT	GO:0019953 (sexual reproduction)	26	4.4431E-02	1.49
GOTERM_BP_FAT	GO:0022602 (ovulation cycle process)	6	5.9440E-02	2.83
GOTERM_BP_FAT	GO:0042698 (ovulation cycle)	6	6.4006E-02	2.77
GOTERM_BP_FAT	GO:0046660 (female sex differentiation)	7	6.7966E-02	2.42
GOTERM_BP_FAT	GO:0008585 (female gonad development)	6	8.9676E-02	2.51
GOTERM_BP_FAT	GO:0046546 (development of primary male sexual characteristics)	6	8.9676E-02	2.51
GOTERM_BP_FAT	GO:0048610 (reproductive cellular process)	13	9.2037E-02	1.66
GOTERM_BP_FAT	GO:0046545 (development of primary female sexual characteristics)	6	1.1349E-01	2.33
GOTERM_BP_FAT	GO:0009566 (fertilization)	5	4.1980E-01	1.52

Table S2: DAVID Functional Annotation Clustering (continued)

Category	**Term**	**# Genes**	***P*-value**	**Fold Enrichment**
GOTERM_BP_FAT	GO:0001541 (ovarian follicle development)	3	4.4237E-01	2.01
Annotation Cluster 13	**Enrichment Score: 1.6045462866664049**	**Description: multicellular organism reproduction**		
Category	**Term**	**# Genes**	***P*-value**	**Fold Enrichment**
GOTERM_BP_FAT	GO:0003006 (reproductive developmental process)	22	8.5082E-03	1.84
GOTERM_BP_FAT	GO:0048609 (reproductive process in a multicellular organism)	30	1.0868E-02	1.62
GOTERM_BP_FAT	GO:0032504 (multicellular organism reproduction)	30	1.0868E-02	1.62
GOTERM_BP_FAT	GO:0007276 (gamete generation)	24	2.6668E-02	1.60
GOTERM_BP_FAT	GO:0019953 (sexual reproduction)	26	4.4431E-02	1.49
GOTERM_BP_FAT	GO:0007283 (spermatogenesis)	18	7.0172E-02	1.56
GOTERM_BP_FAT	GO:0048232 (male gamete generation)	18	7.0172E-02	1.56
Annotation Cluster 14	**Enrichment Score: 1.591149145739853**	**Description: nuclear transport**		
Category	**Term**	**# Genes**	***P*-value**	**Fold Enrichment**
GOTERM_BP_FAT	GO:0006605 (protein targeting)	15	2.7067E-03	2.50
GOTERM_BP_FAT	GO:0006606 (protein import into nucleus)	9	3.4341E-03	3.56
GOTERM_BP_FAT	GO:0051170 (nuclear import)	9	4.2835E-03	3.43
GOTERM_BP_FAT	GO:0034504 (protein localization in nucleus)	9	5.8498E-03	3.27
GOTERM_BP_FAT	GO:0017038 (protein import)	10	1.1385E-02	2.70
GOTERM_BP_FAT	GO:0006886 (intracellular protein transport)	22	1.3624E-02	1.76
GOTERM_BP_FAT	GO:0034613 (cellular protein localization)	23	1.6752E-02	1.70
GOTERM_BP_FAT	GO:0070727 (cellular macromolecule localization)	23	1.8013E-02	1.69
GOTERM_BP_FAT	GO:0000059 (protein import into nucleus, docking)	4	2.7713E-02	5.90
GOTERM_BP_FAT	GO:0006913 (nucleocytoplasmic transport)	10	2.9077E-02	2.31
GOTERM_BP_FAT	GO:0033365 (protein localization in organelle)	10	3.0823E-02	2.28
GOTERM_BP_FAT	GO:0051169 (nuclear transport)	10	3.2642E-02	2.26
GOTERM_CC_FAT	GO:0005643 (nuclear pore)	6	1.1039E-01	2.35
GOTERM_CC_FAT	GO:0046930 (pore complex)	6	2.0717E-01	1.90
GOTERM_MF_FAT	GO:0008565 (protein transporter activity)	5	3.4928E-01	1.67
GOTERM_CC_FAT	GO:0005635 (nuclear envelope)	8	4.9297E-01	1.21

Table S2: DAVID Functional Annotation Clustering (continued)

Annotation Cluster 15	**Enrichment Score: 1.566947544697898**	**Description: chromatin**		
Category	**Term**	**# Genes**	***P*-value**	**Fold Enrichment**
GOTERM_CC_FAT	GO:0000785 (chromatin)	17	2.0827E-03	2.38
GOTERM_BP_FAT	GO:0006333 (chromatin assembly or disassembly)	13	3.6782E-03	2.64
GOTERM_CC_FAT	GO:0044427 (chromosomal part)	24	1.0838E-02	1.74
GOTERM_CC_FAT	GO:0005694 (chromosome)	27	1.2969E-02	1.65
GOTERM_BP_FAT	GO:0051276 (chromosome organization)	28	2.7006E-02	1.53
GOTERM_BP_FAT	GO:0006325 (chromatin organization)	23	2.7868E-02	1.62
SP_PIR_KEYWORDS	chromosomal protein	12	5.9613E-02	1.85
GOTERM_BP_FAT	GO:0016568 (chromatin modification)	13	3.8004E-01	1.22
SP_PIR_KEYWORDS	chromatin regulator	11	4.3018E-01	1.20
Annotation Cluster 16	**Enrichment Score: 1.4889353961860838**	**Description: carbohydrate biosynthetic process**		
Category	**Term**	**# Genes**	***P*-value**	**Fold Enrichment**
GOTERM_BP_FAT	GO:0046364 (monosaccharide biosynthetic process)	7	2.3059E-03	5.00
GOTERM_BP_FAT	GO:0046165 (alcohol biosynthetic process)	7	5.7922E-03	4.19
GOTERM_BP_FAT	GO:0034637 (cellular carbohydrate biosynthetic process)	8	1.2513E-02	3.16
GOTERM_BP_FAT	GO:0019318 (hexose metabolic process)	15	2.0808E-02	1.96
GOTERM_BP_FAT	GO:0019319 (hexose biosynthetic process)	5	2.4404E-02	4.43
GOTERM_BP_FAT	GO:0005996 (monosaccharide metabolic process)	16	2.6278E-02	1.85
GOTERM_BP_FAT	GO:0016051 (carbohydrate biosynthetic process)	8	8.0424E-02	2.13
GOTERM_BP_FAT	GO:0006006 (glucose metabolic process)	11	1.0132E-01	1.74
GOTERM_BP_FAT	GO:0006094 (gluconeogenesis)	3	2.2740E-01	3.32
GOTERM_BP_FAT	GO:0006090 (pyruvate metabolic process)	3	3.1221E-01	2.66
Annotation Cluster 17	**Enrichment Score: 1.4842262048069976**	**Description: chromatin assembly**		
Category	**Term**	**# Genes**	***P*-value**	**Fold Enrichment**
GOTERM_CC_FAT	GO:0000785 (chromatin)	17	2.0827E-03	2.38
GOTERM_BP_FAT	GO:0006333 (chromatin assembly or disassembly)	13	3.6782E-03	2.64
GOTERM_BP_FAT	GO:0034622 (cellular macromolecular complex assembly)	20	4.4250E-03	2.04
GOTERM_BP_FAT	GO:0034621 (cellular macromolecular complex subunit organization)	21	7.6824E-03	1.90
GOTERM_BP_FAT	GO:0065003 (macromolecular complex assembly)	26	1.0604E-02	1.70
GOTERM_BP_FAT	GO:0043933 (macromolecular complex subunit organization)	27	1.5406E-02	1.63
GOTERM_BP_FAT	GO:0006325 (chromatin organization)	23	2.7868E-02	1.62
Category	**Term**	**# Genes**	***P*-value**	**Fold**

Table S2: DAVID Functional Annotation Clustering (continued)

				Enrichment
GOTERM_BP_FAT	GO:0006334 (nucleosome assembly)	8	4.5974E-02	2.43
GOTERM_BP_FAT	GO:0031497 (chromatin assembly)	8	5.1929E-02	2.36
GOTERM_BP_FAT	GO:0043623 (cellular protein complex assembly)	10	5.5011E-02	2.05
GOTERM_BP_FAT	GO:0034728 (nucleosome organization)	8	5.5080E-02	2.33
GOTERM_BP_FAT	GO:0065004 (protein-DNA complex assembly)	8	5.5080E-02	2.33
SP_PIR_KEYWORDS	nucleosome core	6	5.6548E-02	2.86
SP_PIR_KEYWORDS	chromosomal protein	12	5.9613E-02	1.85
GOTERM_BP_FAT	GO:0006461 (protein complex assembly)	16	8.9752E-02	1.56
GOTERM_BP_FAT	GO:0070271 (protein complex biogenesis)	16	8.9752E-02	1.56
GOTERM_CC_FAT	GO:0000786 (nucleosome)	6	1.2891E-01	2.24
GOTERM_BP_FAT	GO:0006323 (DNA packaging)	8	1.7111E-01	1.75
GOTERM_CC_FAT	GO:0032993 (protein-DNA complex)	6	2.2283E-01	1.85
Annotation Cluster 18	**Enrichment Score: 1.4105517394608398**	**Description: vasculature development**		
Category	**Term**	**# Genes**	***P*-value**	**Fold Enrichment**
GOTERM_BP_FAT	GO:0048514 (blood vessel morphogenesis)	17	1.7483E-02	1.90
GOTERM_BP_FAT	GO:0001944 (vasculature development)	20	1.8540E-02	1.77
GOTERM_BP_FAT	GO:0001568 (blood vessel development)	19	2.7897E-02	1.72
GOTERM_BP_FAT	GO:0001525 (angiogenesis)	9	2.5207E-01	1.50
Annotation Cluster 19	**Enrichment Score: 1.3814054754821377**	**Description: RNA metabolic process**		
Category	**Term**	**# Genes**	***P*-value**	**Fold Enrichment**
SP_PIR_KEYWORDS	rna-binding	41	5.2359E-04	1.78
GOTERM_BP_FAT	GO:0016071 (mRNA metabolic process)	21	5.5792E-02	1.54
SP_PIR_KEYWORDS	mrna processing	18	6.6375E-02	1.58
SP_PIR_KEYWORDS	mrna splicing	15	7.2039E-02	1.65
GOTERM_BP_FAT	GO:0006397 (mRNA processing)	18	8.6174E-02	1.52
GOTERM_BP_FAT	GO:0006396 (RNA processing)	27	8.9875E-02	1.37
GOTERM_BP_FAT	GO:0008380 (RNA splicing)	13	1.9770E-01	1.43

Appendix 3: Table S3

Table S3: KEGG pathways identified as enriched in circadian transcripts by DAVID pathway analysis. Over-representation was determined by a combination P-value and fold enrichment, where a term was significant with a P <0.05 and had a fold enrichment >1.5.

Pathway	**# Genes**	***P*-value**	**Fold Enrichment**
Circadian rhythm	8	5.90E-07	13.2
Glutathione metabolism	10	5.60E-04	4.1
Renal cell carcinoma	11	1.30E-03	3.4
mTOR signaling pathway	9	3.20E-03	3.6
Pathways in cancer	27	4.10E-03	1.8
MAPK signaling pathway	23	5.60E-03	1.9
Pancreatic cancer	10	5.80E-03	3
Chronic myeloid leukemia	10	8.30E-03	2.8
Prostate cancer	11	8.60E-03	2.6
ErbB signaling pathway	10	1.90E-02	2.5
Apoptosis	10	1.90E-02	2.5
Wnt signaling pathway	14	2.10E-02	2
Focal adhesion	17	2.10E-02	1.8
Colorectal cancer	9	4.60E-02	2.2
Acute myeloid leukemia	7	4.80E-02	2.6

Chapter 4: Conclusion

Section 4.1: Summary of findings

Circadian rhythms pervade mammalian physiology and behavior, yet we know little about how they are regulated by the circadian clock. In fact, many questions still remain regarding the clock itself, how it responds to external environmental changes, much less how overt rhythms in behavior and physiology are achieved. The studies presented in Chapter 2 and Chapter 3 extend our knowledge of mammalian circadian networks involved in input, output, and the clock, itself.

In Chapter 2, to identify for novel clock genes and genes involved in circadian input, we performed a genome-wide siRNA screen, which identified hundreds of novel genes whose KD alters clock function (1). These siRNA hits represent candidate novel clock components or input genes. To validate hits from this screen, the sensitivity clock modifier (siRNA screen hit) impact on circadian function and known clock gene expression were assessed. Similar to known clock genes, many of these clock modifiers displayed dose-dependent effects on clock function and clock gene expression. These dose-dependent effects on clock gene transcription suggest that many of the clock modifiers impact clock function through transcriptional regulation. In particular, knockdown of most clock modifiers resulted in a reduction of the level of REV-ERBα (NR1D1) and DBP transcripts, which are regulated by E-box mediated transcription (BMAL1/CLOCK mediated), implying that E-box mediated transcription represents a vulnerable node of regulation within the

mammalian clock. To suggest how the clock modifiers interact with clock genes on a physical, proteomic level, an expanded gene clock network was constructed using PPIs for the known clock genes and novel clock modifiers. This network centered on known clock genes and displayed a high level of connections between known clock genes and novel clock modifiers. While some clock modifiers directly interact with known clock genes, many clock modifiers interact with clock genes at one degree of separation—the clock modifier physically interacts with a bridging molecule (common interactor) which interacts with a known clock gene. These interactions can not only suggest mechanisms by which clock modifiers affect the clock but implicate common interactors in clock function as well. For example, TP53 (gene encoding p53)—a tumor suppressor gene that is mutated or deleted in many cancers—had not been associated with the circadian clock. Yet, through its interactions described in this PPI network, it may provide a mechanism between clock disruption and increased incidence of cancer (2).

Moreover, DAVID Pathway Analysis revealed multiple cellular pathways over-represented in list of novel clock modifiers, including folate metabolism, hedgehog signaling, cell cycle, and insulin signaling. Components of these pathways have previously been found to be transcriptionally regulated by the circadian clock. These examples of individual pathways which are both regulated by the clock and impinge upon clock function exposes how the circadian clock and cellular pathways are intertwined and emphasizes the importance of understanding circadian regulation to understand the regulation of cellular processes. Thus, our siRNA screen expands

the composition of circadian networks to include these novel clock modifiers as well as enhance the significance of the circadian clock for broader biological inquiry.

In Chapter 3, we focused on cell-autonomous circadian output regulation in our hepatocyte model system: the MMH-D3 cell line. The respective roles of systemic and cell-autonomous regulation in governing rhythms of gene expression in peripheral tissues, like the liver, remained to be characterized. Through gene expression profiling in MMH-D3 and bioinformatic analyses, we established MMH-D3 as a circadian cell-based model system and revealed that cell-autonomous circadian regulation can drive rhythmic gene expression and oscillations in polyamine synthesis.

Using a bioinformatic pipeline that combines multiple algorithms, we identified 1,130 circadian expressed transcripts in MMH-D3 hepatocytes, indicating that the cell-autonomous clock can drive a substantial number of rhythms. This refutes the conclusion that few rhythms can be driven by cell-autonomous circadian regulation in immortalized cell line by Hughes et al., based on their analsyis of the U2-OS and NIH3T3 (immortalized mouse fibroblast) cell lines (3). The MMH-D3 circadian transcript list displays substantial overlap with those called in Hughes et al.'s *in vivo* liver dataset analyzed in parallel with the same bioinformatics pipeline at the same resolution (2-hour) (29% overlap), implying maintenance of hepatic circadian regulatory networks in MMH-D3 hepatocytes (3).

Using a global mouse PPI network, we assessed the how these transcripts may be organized into circadian regulatory networks. Within this network, MMH-D3

circadian genes were more centrally located than non-circadian genes, consistent with the expanded clock network generated in Chapter 2 and further indicating a high level of interconnectedness between the circadian system and broader biology. Circadian genes also display phasic relationships of distribution, such that co- and anti-phasic genes are in closest proximity to each other. These relationships may indicate competitive relationships, such as seen in the associate loops of the clock. In the RRE loop, ROR activators and REV-ERB repressors compete for RRE binding sites, resulting in rhythmic transcription of target genes. Co- and anti-phasic relationships of proximity suggest that competition like this may represent a broader theme of circadian regulation, extending beyond the clock itself.

NIH DAVID pathway analysis revealed enrichment of multiple cellular pathways with circadian transcripts, including multiple cancer pathways, glutathione metabolism, mTOR signaling, and MAPK signaling. Further inspection of the glutathione metabolism pathway, revealed transcriptional rhythms in the first two enzymes of the polyamine biosynthesis module: ornithine decarboxylase (Odc1) and spermidine synthase (Srm). ODC1 represents the rate limiting enzyme of polyamine biosynthesis and SRM is the succeeding enzyme within the pathway. Transcriptional rhythms in Odc1 and Srm are also found in WT liver but not observed in arrhythmic mice (*Clock* mutant or *Cry1, Cry2* knockout). Furthermore, a circadian rhythm was detected in the product of SRM, spermidine, indicating circadian rhythms in enzymatic activity. As Srm and Odc1 transcriptional rhythms are coordinated and ODC1—the rate limiting enzyme—precedes SRM in the pathway, circadian

oscillations of spermidine reflect the activity rhythms of both enzymes. Since polyamines levels correlate with cell proliferation and they are essential for initiation of liver regeneration, cell autonomous circadian regulation of polyamine biosynthesis suggests a novel mechanism by which the clock gates initiation of liver regeneration.

Section 4.2: Future studies

The studies presented in Chapters 2 and 3 extended our knowledge of the components and revealed the influence and interconnectedness of cell-autonomous circadian regulatory networks to broader biological functions (i.e. cell cycle, folate metabolism, hedgehog signaling, insulin signaling, and polyamine synthesis). This interconnectedness both in terms of clock output and regulation of the clock emphasizes the importance of understanding how the clock interacts with these cellular pathways. Moreover, our studies have illustrated a continued significance and need for cell-based circadian studies. *In vivo* circadian regulation is highly complex and composed of both systemic regulation, including orchestrating signals from the SCN, communication from various peripheral tissues, behavior, and cell-autonomous regulation. Our study presented in Chapter 3 revealed that the cell autonomous clock can drive rhythms of many transcripts and at least one significant cellular function. Likewise, while U2-OS does not contain many circadian regulated transcripts, it does contain a robust clock and can be successfully used as in the siRNA screen to refine our knowledge of the clock and how it receives input information. The clock modifier gene list and MMH-D3 circadian transcript list provide candidates for further

characterization of circadian input and output networks as well as elucidation of novel gears of the clock.

Further investigation is required to characterize how these genes are organized into circadian regulatory networks. As the MMH-D3 circadian list represents transcripts under circadian regulation, it should be used to construct circadian output networks. However, the clock modifiers identified in the siRNA screen may represent either novel clock components or input genes. To categorize these clock modifiers, bioinformatics analysis as well as genetic and biochemical investigation is required. Some insight will be gained by analysis of microarray gene expression time-courses for circadian transcripts, such as the MMH-D3 circadian transcript list. Circadian transcripts are under transcriptional regulation by the clock and are more likely to be involved in the clockwork itself than input. After categorizing the clock modifiers as either candidate input or clock genes, we can proceed to address the central questions in each of these networks.

Section 4.2.1: Characterizing new gears of the clock

To expand the clockwork, the mechanisms by which candidate clock genes (clock modifiers that are under circadian transcriptional regulation) impact known clock gene expression must be elucidated. How do these candidate genes interact with known clock genes? How do they contribute to the topology of the clock? What regulatory mechanisms are employed? This would include defining the direct targets of clock modifier gene regulation, such as metabolic substrates, and target genes for

transcriptional regulation and phosphorylation. By leveraging the mammalian bioinformatic databases for ChIP-chip, PPI, and kinase phosphorylation targets, regulatory mechanisms connecting clock modifiers and the known clock genes can be proposed and tested using genetic and molecular perturbations. The validation studies in Chapter 2 suggested that multiple clock modifiers affected E-box mediated transcription (CLOCK/BMAL1 mediated transcription). In defining the connections between clock modifiers and known clock genes, we would address whether interactions between clock modifiers and a specific known clock gene or mode of regulation was over-represented. Thus, we would address if E-box mediated transcription represents a regulatory bottleneck in the clock. Second, our current understanding of the clock largely centers on negative feedback loops that produce 24-hour cycles of transcriptional regulation. Are novel clock genes also organized into loops? Competitive interactions by clock modifiers on each other or bridging molecules indicated by bioninformatic databases (PPI, kineome, ChiP-Seq) may suggest a negative feedback loop, especially if they are cyclically expressed anti-phasic to one another. Similarly, transcription factor clock modifiers that act through the same transcription factor binding sites may imply a node with multiple regulatory events, some of which may represent the positive and other the negative arm of a loop structure. The hypotheses formed based on these annotations will then be tested in terms of genetic effects of the clock modifiers on the known clock genes and clock function as well as detailed assessment of the mechanism of action using molecular biology techniques to identify the key domains and targets. Lastly, the mechanism by

which novel clock genes regulate circadian targets must be defined. In Chapter 2, KD of individual clock modifiers produced dose-dependent transcriptional effects on known clock genes in many cases, suggesting that transcription may be a significant mode of regulation for many clock modifiers. Genetic perturbations, chemical inhibitors, and ChIP for individual clock modifiers will allow for the characterization of whether regulation occurs at the transcriptional levels and the location of the transcription factor binding sites within clock gene regulatory sequences.

Section 4.2.2: Revealing input networks

For circadian input networks, characterization non-light induced input networks will reveal how the cell-autonomous clock is entrained by systemic circadian signals, such as hormones, neural impulses, metabolites, and behavior (2). For example, restricting feeding to daylight hours can invert the hepatic clock in mice (4, 5), but the specific molecules and signaling events by which this is achieved remain unclear. Insulin has been suggested to play a role in hepatic circadian input, which is supported by the findings in Chapter 2 that components of the insulin signaling pathway are over-represented in the clock modifier gene list (4-6). Yet, a mechanistic description of which components interact with the circadian clock is necessary to determine if this pathway is directly involved in circadian input networks. Clock modifiers not under circadian transcriptional control provide strong candidates for input networks and represent seed genes for elucidating the architecture and composition of these networks. First, the mechanism by which the clock modifiers

affect circadian clock function should be determined using genetic and molecular perturbations. The validations studies in Chapter 2 illustrated that many of the clock modifiers produce dose dependent effects on clock function and clock gene expression, suggesting that they may impact the clock gene network at a transcriptional level—a hypothesis that must be examined using mutant forms of individual clock modifiers to measure the effects on clock gene expression. In the Chapter 2 validation studies, many of the clock modifiers tested appeared to impact E-box mediated transcriptional targets. Once the nature of the regulatory relationships between clock modifiers and known clock genes are understood, the vulnerability of E-box mediated transcription in the clock network topology can be assessed. Once this first level of nodes within the input networks are characterized, these nodes can be used to trace these networks back to upstream genes and regulatory events within the networks, eventually revealing the signaling molecules ultimately received from the extracellular environment. To begin this process, the interactions of the clock modifiers at a protein and functional level should be assessed, using the expanded clock PPI network (Figure 15) and clock modifier enriched functional pathways (cell cycle, folate metabolism, hedgehog signaling, and insulin signaling) (Figure 16, Figure 17). By applying the information in these analyses and the siRNA screen data available through BioGPS, questions—such as "Can the components upstream of the clock modifiers in these pathways also impact circadian function?" and "Do they produce the same effects on clock genes expression as knockdown of the clock modifier itself?"—can be addressed. Answering these questions will enable continued

characterization of the components and regulatory of circadian input networks and entrainment signals, which will suggest methods to strengthen and coordinate circadian synchronization throughout the body to reduce circadian dysfunction in jetlag and shiftwork syndrome.

Section 4.2.3: Constructing output networks

Lastly, our findings in Chapter 3 point to a significant role for the cell-autonomous clock in regulating output in hepatocytes. Due to the tissue-specificity of rhythmic transcripts *in vivo*, similar analyses must be undertaken in other cell types in order to characterize the role of the cell autonomous clock in other tissues, such as adipocytes, muscle cells, and various immune cell lineages. However, we have learned from MMH-D3 hepatocytes that the cell-autonomous liver clock can drive many transcriptional rhythms and regulates polyamine biosynthesis. While evidence suggests that regulation of the circadian polyamine biosynthetic enzymes ornithine decarboxylase (Odc1) and spermidine synthase (Srm) occurs directly through E-box mediated transcription, this remains to be demonstrated. To do so would include evidence of direct physical interaction between BMAL1/CLOCK with the E-boxes in Odc1 and Srm regulatory regions in MMH-D3 hepatocytes (ChIP experiments) as well as demonstration that these E-boxes are required for rhythmic transcription using transfected promoter:luciferase constructs (luciferase reporter assays). Two forms of these constructs would be prepared for each gene, one with the WT E-box sequence and one with the E-box sequence mutated. If the E-box is required for rhythmic

transcription at that promoter, bioluminescent rhythms should be detected in the WT promoter construct but ablated in the mutant promoter construct. Moreover, these experiments should be repeated in primary hepatocytes as well as ultimately confirmed *in vivo* to confirm our findings from MMH-D3 hepatocytes.

At this point, the architecture of output networks is not well understood. Two possibilities have been proposed in the field: that circadian output is either through (a) limited networks, in which few regulatory nodes exist between clock components the terminal physiology, or (b) extensive networks, in which multiple regulatory nodes exist between clock components and the resultant physiology and may resemble a signaling cascade. While examples of the former type of regulation exist (7-10), leaders in the field espouse the latter hypothesis for the majority of circadian output regulation (11, 12). Ulitizing bioinformatics analyses—such as co-expression analysis—and resources (PPI, ChIP-chip, and genetic databases), interactions and regulatory relationships for the MMH-D3 circadian transcripts can be proposed and the transcripts organized into a regulatory output network. Connections within this network can be experimentally tested to reveal the architecture of cell-autonomous circadian transcriptional output networks in hepatocytes. This hepatocyte output network can then be used as a model to assist in the characterization of cell-autonomous output networks in other cell types, such as adipocytes, muscle cells, and lung epithelium.

Finally, while we have expanded our knowledge of cell-autonomous regulatory networks—particularly in characterizing a role for the hepatocyte clock in polyamine

synthesis—circadian regulation *in vivo* is complex. Cell-autonomous and systemic circadian regulation likely both contribute to circadian regulation within a tissue (i.e. liver). We have established that the cell-autonomous clock can drive transcriptional rhythms and play a role in functional regulation, but we have yet to understand how cell-autonomous and systemic regulation are integrated *in vivo*.

Section 4.3: Significance

Characterization of the circadian networks that comprise the clock, input transmittance and output regulation will elucidate the mechanisms by which the circadian clock governs overt rhythms in behavior and physiology as well as explicate how circadian dysfunction contributes to major human health problems, such as jetlag, shift work syndrome, mood disorders, heart disease, cancer, and metabolic syndrome. By understanding how the circadian clock is intertwined with regulation of cellular processes underlying these conditions, we can develop novel preventative and therapeutic measures to combat them. For example, through characterizing circadian input networks, we elucidate the mechanisms by which entrainment to the external environment and synchronization between tissues occurs, and can they develop measures to reduce jetlag and improve efficiency of resynchronization. Or, by understanding how the amplitude of clock rhythms are controlled within the clock itself, we may be able to modulate amplitude of clock rhythms and reduce sleep fragmentation in individuals, which would improve quality of life experienced especially by the elderly. Moreover, circadian dysfunction is associated with

increased the risk for many human diseases, including cancer, heart disease, obesity and type 2 diabetes; yet, we do not understand exactly how the circadian clock relates to the cell cycle, lipid homeostasis, glucose homeostasis, and metabolism. By understanding the networks by which the circadian clock is intertwined with these physiological processes, we can not only reveal the mechanisms by which circadian dysfunction relates to human disease but develop methods to intervene and improve human health outcomes.

Section 4.4: Chapter 4 references

1. Zhang EE, Liu AC, Hirota T, Miraglia LJ, Welch G, Pongsawakul PY, Liu X, Atwood A, Huss,Jon W.,,III, Janes J, Su AI, Hogenesch JB & Kay SA (2009) A genome-wide RNAi screen for modifiers of the circadian clock in human cells. *Cell* 139: 199-210.

2. Hastings MH, Reddy AB & Maywood ES (2003) A clockwork web: Circadian timing in brain and periphery, in health and disease. *Nature Reviews Neuroscience* 4: 649-661.

3. Hughes ME, DiTacchio L, Hayes KR, Vollmers C, Pulivarthy S, Baggs JE, Panda S & Hogenesch JB (2009) Harmonics of circadian gene transcription in mammals. *PLoS Genet* 5: e1000442.

4. Damiola F, Le Minh N, Preitner N, Kornmann B, Fleury-Olela F & Schibler U (2000) Restricted feeding uncouples circadian oscillators in peripheral tissues from the central pacemaker in the suprachiasmatic nucleus. *Genes Dev* 14: 2950-2961.

5. Hara R, Wan K, Wakamatsu H, Aida R, Moriya T, Akiyama M & Shibata S (2001) Restricted feeding entrains liver clock without participation of the suprachiasmatic nucleus. *Genes Cells* 6: 269-278.

6. Zhang EE & Kay SA (2010) Clocks not winding down: Unravelling circadian networks. *Nat Rev Mol Cell Biol* 11: 764-776.

7. Gachon F, Olela FF, Schaad O, Descombes P & Schibler U (2006) The circadian PAR-domain basic leucine zipper transcription factors DBP, TEF, and HLF modulate

basal and inducible xenobiotic detoxification RID A-9289-2010. *Cell Metabolism* 4: 25-36.

8. Guillaumond F, Grechez-Cassiau A, Subramaniam M, Brangolo S, Peteri-Bruenback B, Staels B, Fievet C, Spelsberg TC, Delaunay F & Teboul M (2010) Kruppel-like factor KLF10 is a link between the circadian clock and metabolism in liver. *Mol Cell Biol* 30: 3059-3070.

9. Lavery D, Lopez-Molina L, Margueron R, Fleury-Olela F, Conquet F, Schibler U & Bonfils C (1999) Circadian expression of the steroid 15 alpha-hydroxylase (Cyp2a4) and coumarin 7-hydroxylase (Cyp2a5) genes in mouse liver is regulated by the PAR leucine zipper transcription factor DBP. *Mol Cell Biol* 19: 6488-6499.

10. Le Martelot G, Claudel T, Gatfield D, Schaad O, Kornmann B, Lo Sasso G, Moschetta A & Schibler U (2009) REV-ERB alpha participates in circadian SREBP signaling and bile acid homeostasis. *Plos Biology* 7: e1000181.

11. Ueda HR, Hayashi S, Chen WB, Sano M, Machida M, Shigeyoshi Y, Iino M & Hashimoto S (2005) System-level identification of transcriptional circuits underlying mammalian circadian clocks. *Nat Genet* 37: 187-192.

12. Ueda HR, Chen WB, Adachi A, Wakamatsu H, Hayashi S, Takasugi T, Nagano M, Nakahama K, Suzuki Y, Sugano S, Iino M, Shigeyoshi Y & Hashimoto S (2002) A transcription factor response element for gene expression during circadian night. *Nature* 418: 534-539.